The development of radiolabelled peripheral benzodiazepine receptor ligands for imaging cancer and neurodegenerative disorders

Taryn P. Homes
University of Wollongong

The Development of Radiolabelled Peripheral Benzodiazepine Receptor Ligands for Imaging Cancer and Neurodegenerative Disorders

Taryn P Homes

B. Med. Chem. Hons.

A thesis submitted in fulfilment of the requirements

for the award of the degree

Doctor of Philosophy

from

University of Wollongong

Department of Chemistry

December 2007

Certification

I, Taryn P. Homes, declare that this thesis, submitted in fulfilment of the requirements for the award of Doctor of Philosophy, in the Department of Chemistry, University of Wollongong, is wholly my own work unless otherwise referenced or acknowledged. The document has not been submitted for qualifications at any other academic institute.

Taryn P. Homes

December 2007

Acknowledgements

I would like to express my deepest thanks to the following people…

My supervisors **Dr Andrew Katsifis** (ANSTO) and **Assoc. Prof. Paul Keller** (UOW) for their time and guidance, and for giving me the opportunity to complete a PhD

AINSE for the partial funding of the project and conference funds

Filomena Mattner for teaching me all the pharmacological methods used in this project

Tien Pham for teaching me how to radiolabel

Xiang Liu and **Thomas Bourdier** for their help with metabolite studies

Tim Jackson and **John Howse** for their QC work

The radiopharmaceuticals group at ANSTO, including the **pharmacology group** for helping with animal studies

The Keller Group for their help and support with presentations

The **UOW Department of Chemistry technical staff** for running mass specs

Office buddies **Mark Ashford**, **Mitchell Quinlivan,** and **Pam Sumner** for making my PhD a lot of fun, and for their help with writing my thesis

Mum, Dad, Steve, Jared, my best friend **Cathy**, and **Vinh,** for being so proud of me

My fiancé **Brad Angel** for his love and support

List of Abbreviations

^{13}C NMR	Carbon Nuclear Magnetic Resonance
^{1}H NMR	Proton Nuclear Magnetic Resonance
ACN	Acetonitrile
AcOH	Acetic Acid
AIBN	Azobisisobutyronitrile
ANT	Adenine Nucleotide Translocase
Ar	Aryl
bs	Broad singlet
CAT	Chloramine-T
CBR	Central Benzodiazepine Receptor
CI	Chemical Ionisation
CNS	Central Nervous System
DBI	Diazepam Binding Inhibitor
DCM	Dichloromethane
dd	Doublet of doublets
ddd	Doublet of doublets of doublets
DEPT	Distortionless Enhancement by Polarisation Transfer
DMF	Dimethylformamide
DMSO	Dimethylsulfoxide
dt	Doublet of triplets
EAE	Experimental Autoimmune Encephalomyelitis
EI	Electron Impact

ES	Electrospray
FDG	Fluorodeoxyglucose
GABA	Gamma-aminobutyric Acid
GIT	Gastrointestinal Tract
h	Hour
HPLC	High Performance Liquid Chromatography
HRMS	High Resolution Mass Spectrometry
Hz	Hertz
IC_{50}	Inhibition Constant at 50%
ID/g	Injected dose per gram
IMM	Inner mitochondrial membrane
LE	Lupus Erythmatosus
M	Molar
m	Multiplet
MBq	Megabequerel
min	Minute
mL	Millilitre
mmol	Milli mol
mp.	Melting Point
MS	Mass Spectometry
m/z	Mass/charge ratio
NBS	*N*-Bromosuccinimide
OMM	Outer mitochondrial membrane
PBR	Peripheral Benzodiazepine Receptor
PE	Petroleum Ether

PET	Positron Emission Tomography
PPA	Polyphosphoric Acid
q	Quartet
qC	Quaternary Carbon
RCY	Radiochemical Yield
RT	Room Temperature
s	Singlet
SAR	Structure-Activity Relationship
SPECT	Single Photon Emission Computed Tomography
StAR	Steroidogenic acute regulatory protein
t	Triplet
TFA	Trifluoroacetic Acid
THF	Tetrahydrofuran
TLC	Thin Layer Chromatography
Tris	Tris(Hydroxymethyl)aminomethane
UV	Ultraviolet
VDAC	Voltage Dependent Anion Channel

Publications/Presentations

Publications

- **Homes, T.P**., Keller, P.A., Katsifis, A., Mattner, F. (2006); Synthesis and in vitro binding of *N,N*-dialkyl-2-phenylindol-3-ylglyoxylamides for the peripheral benzodiazepine binding sites; Bioorganic and Medicinal Chemistry; 14; 3938-3946
- **Homes, T.P**. Mattner, F. Keller, P.A, Katsifis, A. (2007); Synthesis and in vivo evaluation of a novel [^{123}I] indolglyoxylamide for the Peripheral Benzodiazepine Binding Sites; Journal of Labelled Compounds and Radiopharmaceuticals; 50; S307
- **Homes, T.P**., Mattner, F., Keller, P.A., Katsifis, A. In vivo evaluation of ^{123}I- *N,N*-diethyl-[5-chloro-2-(4-iodophenyl)indol-3-yl]glyoxylamide for the peripheral benzodiazepine binding sites. To be submitted to Nuclear Medicine and Biology.

Oral Presentations

- **Homes, T.P.**, Keller, P.A., Katsifis, A. Synthesis and peripheral and central benzodiazepine receptor binding affinity of *N,N*-dialkyl-2-phenylindol-3-ylglyoxylamides. RACI Young Chemist's Symposium, 3rd July 2005, University of Sydney
- **Homes, T.P.**, Keller, P.A., Katsifis, A., Mattner, F. Development of radiolabelled peripheral benzodiazepine receptor ligands. University of Wollongong Department of Chemistry Annual Conference. 24-25th October, 2005, ANU Kialoa coastal campus.

Poster Presentations

- **Homes, T.P**., Keller, P.A., Katsifis, A., Mattner, F. (2006); Synthesis and evaluation of *N,N*-dialkyl-2-phenylindol-3-ylglyoxylamides for the study of peripheral benzodiazepine binding sites; 4th France – Australia Symposium on Nuclear Medicine, Melbourne
- **Homes, T.P**., Mattner, F., Keller, P.A., Katsifis, A. (2007); Synthesis and in vivo evaluation of a novel [^{123}I] indolglyoxylamide for the peripheral benzodiazepine binding sites; 17th International Symposium on Radiopharmaceutical Science, 29th April-3rd May, Aachen, Germany

Abstract

Three classes of compounds were chosen for investigation to find a high affinity and selective iodinated peripheral benzodiazepine receptor (PBR) ligand; indol-3-ylglyoxylamides, pyrazolopyrimidines, and pyridopyrrolooxazepines and pyrrolobenzoxazepines. These compounds were chosen from a literature search for their high PBR affinity and selectivity, ease of synthesis, and the potential for radioiodination.

Fifteen new halogenated *N,N*-dialkylindol-3-ylglyoxylamides were synthesised and tested for their PBR and central benzodiazepine receptor (CBR) affinity. The compounds IC_{50} values for the PBR ranged from 7.8 – 618 nM, and a structure activity relationship (SAR) was determined. Brominated compounds had higher binding affinities than their iodinated analogues, and indoles with a chloro substituent on position 5 had higher binding affinities than the non-chlorinated compounds. The optimum alkyl chain length was found to be two carbons. The highest affinity iodinated ligand, with a PBR IC_{50} of 8.2 nM, was radiolabelled with ^{123}I in 55-60% radiochemical yield and evaluated *in vivo* in Sprague-Dawley rats. Biodistribution studies revealed high uptake of the radiotracer in organs known to contain PBR, such as the kidneys, adrenals, heart, liver and lungs. Drug competition studies showed that the PBR drugs PK11195 and Ro5-4864, when injected into the rat 5 min prior to injection of the radiotracer, significantly decreased uptake of radiotracer into those organs. The CBR drug, flumazenil, did not decrease the uptake of the radiotracer. Metabolite studies showed that the radiotracer was > 95% intact in the heart, kidneys, adrenals, and brain after 3 h and was 65% intact in the plasma. This compound is the first radiolabelled

PBR ligand of this class, and is an excellent candidate for future studies and may lead to a clinically useful imaging agent.

Three pyrazolopyrimidines were synthesised, with lengths of the alkyl chains being methyl, ethyl, or propyl groups. The highest affinity ligand, with the propyl groups, displayed an IC_{50} of 7.9 nM, however, only the compound with ethyl groups displaying an IC_{50} of 11.7 nM was radiolabelled with ^{123}I in 95% radiochemical yield, and evaluated *in vivo* in rats. This compound showed high uptake into organs known to contain PBR, and also showed an interesting result in which pre-administration of Ro5-4864 did not cause any significant decrease of uptake of radiotracer in the kidney or heart, however PK11195 did cause of significant decrease in these organs. This compound provides the first radioiodinated PBR ligand of this class.

Two pyrrolopyridooxazepines and two pyrrolobenzoxazepines were synthesised and tested. One of the compounds was found to be inactive, while the others had moderate PBR IC_{50} values of 24-39 nM. The moderate binding affinity for these compounds would unlikely lead to a successful imaging agent.

Table of Contents

List of Figures

List of Schemes

List of Tables

1 Introduction

1.1 Peripheral Benzodiazepine Receptors

Benzodiazepines are drugs used clinically for the treatment of anxiety, convulsions, and insomnia.[1] In the mammalian body, some benzodiazepines including diazepam, bind to two types of receptors, the central benzodiazepine receptor (CBR) and the peripheral benzodiazepine receptor (PBR). The therapeutic effects of benzodiazepines are mediated through the former (CBR), which are located within the neurons of the central nervous system. The PBR was discovered in 1977 when it was found that the benzodiazepine, diazepam, not only bound in the central nervous system, but also in the kidneys, liver and lungs, resulting in the name peripheral benzodiazepine receptor.[2] PBRs were later found in many other peripheral organs, and also in glial cells of the brain.[3] While the structure and function of the CBR is well known, the PBR is not well understood and the exact function of this receptor is not known. They differ in their pharmacology, tissue distribution, subcellular location, and effector mechanism, which is summarised in Table 1.1.[4]

The PBR is sometimes referred to as the mitochondrial benzodiazepine receptor (MBR) due to its predominant localisation in the mitochondria. Other names include the mitochondrial diazepam binding inhibitor receptor, ω3 receptor, or p-sites. Most recently, groups of PBR researchers have a new proposed nomenclature of the PBR, defining the name ‘translocator protein (18 kDa)’, the abbreviation ‘TSPO’, and the specific nomenclature ‘mitochondrial translocator protein (18 kDa)’ and ‘nuclear translocator protein (18 kDa)’.[5]

Table 1.1 Difference between PBR and CBR.[4]

Please see print copy for Table 1.1

1.2 Molecular Structure of the PBR

The peripheral benzodiazepine receptor is a component of a heteromeric complex made up of at least three subunits, including an isoquinoline binding subunit of molecular mass 18 kDa (the PBR itself), a voltage-dependent anion channel (VDAC) (32 kDa), and an adenine nucleotide translocase (ANT) (30 kDa) (Figure 1.1).[6] The 18 kDa protein consisting of 169 amino acids has been purified and the cDNA encoding the receptor has been cloned from the rat,[7] human,[8] bovine[9] and mouse species.[10] Among these species, the 18 kDa protein shows approximately 80% amino acid conservation.[11] The gene for the protein has been cloned and characterised from the rat and human.[12,13]

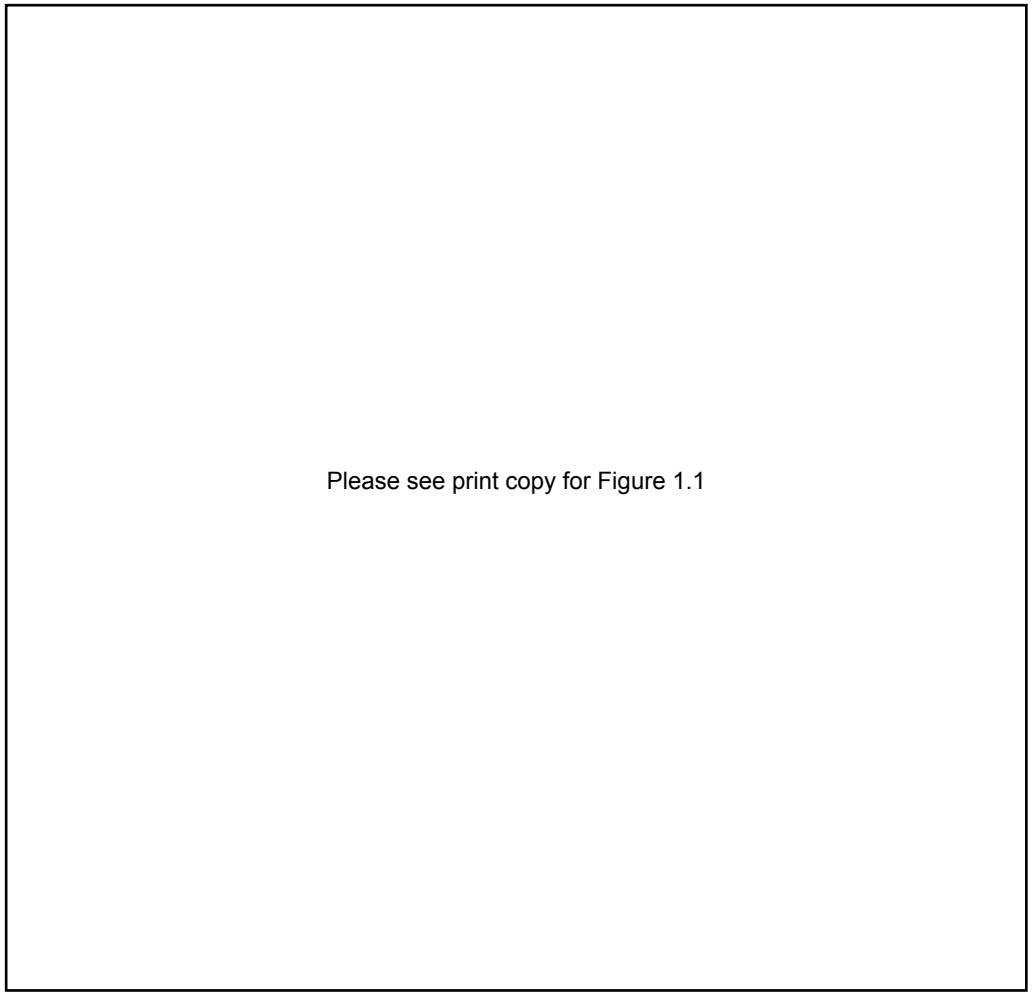

Figure 1.1 A schematic diagram of the structure of the PBR complex in the mitochondria. VDAC: voltage dependent anion channel, ANT: adenine nucleotide translocase.[5]

The protein is highly hydrophobic and rich in tryptophan, and has a positive charge with a pI of 9.6. A single PBR binding site consists of 5 hydrophobic transmembrane segments (5 alpha helices) connected with hydrophilic loops, with the N-terminus of the protein located inside the mitochondria, and the C-terminus exposed to the cytoplasm.[14,15] A single PBR molecule is the minimal functional unit for cholesterol and

drug ligand binding. However, PBR polymers bind PBR ligands with higher affinity than monomers.[16,17] PBR polymers are formed *in vivo* and *in vitro* in response to reactive oxygen species (ROS).[18] These polymers are 18 kDa PBR monomers linked through dityrosine formation. Clusters of 4-6 PBR molecules are found *in vivo*.

An unknown protein of 10 kDa has also been reported which may also be associated with PBR.[19] More recently, a new cytoplasmic protein of 240 kDa, named PRAX-1 (peripheral benzodiazepine receptor associated protein-1) has been shown to interact with the PBR in 1:2 PRAX-1: PBR stoichiometry.[20] PRAX-1, however, is only found in the brain and thymus, not in steroidogenic tissues, and the function of this protein is not known.

Two other cytosolic protein partners of PBR are the steroidogenic acute regulatory protein (StAR), and PBR and protein kinase A associated protein (PAP7), which are involved in cholesterol transport[21,22] and will be described in more detail in section 1.6.2.

1.3 Cellular and Tissue Location of the PBR

The PBR is expressed in endocrine organs such as the adrenal cortex, testis, prostate, ovary, uterus, mammary gland, thyroid and pineal gland, and the posterior pituitary gland.[23] The PBR is also found in the heart,[24] liver,[25] lungs and the kidneys,[26] especially in the distal convoluted tubules and in the ascending loop of Henle.[27] Although called the peripheral benzodiazepine receptor, the PBR is also localised in small concentrations in glial cells of the brain.[28] The PBR is also expressed in blood platelets, red blood cells and all subsets of leukocytes.[29,30]

The PBR is mainly located in the outer mitochondrial membrane,[31] but has also been found in other subcellular locations, including the plasma membrane of red blood cells, which lack mitochondria.[32,33] Other locations include the plasma membrane of:

- Biliary epithelial cells in liver[34]
- Leydig cells in testes[35]
- Heart[36]
- Adrenal cortex[37], and also:
- Nuclear fractions of normal and cancerous human liver tissues[38]
- Nucleus of human breast tumour[39]

The PBR is not only present in mammals, but is also present in potatoes,[40] *Arabidopsis thaliana*,[41] and insects,[42] supporting the hypothesis that it is a highly conserved receptor system during evolution. Deleting the PBR gene in mice resulted in death of the mice at an embryonic stage, suggesting that PBR has a critical role.[43]

1.4 Endogenous Ligands for the PBR

The endogenous ligand for the PBR is not known, however possibilities have been suggested, including the diazepam binding inhibitor (DBI), an 11 kDa protein of 86 amino acids[4,44] which was found first to inhibit the binding of diazepam to CBRs, and was later found to have the same affinity (μM range) for the PBR.[45] It is preferentially localised in the periphery of mitochondria and was detected in tissues which had a high concentration of PBR. Two fragments of DBI, called octadecaneuropeptide (ODN; DBI_{33-50}) and triakontatetraneuropeptide (TTN; DBI_{17-50}) were tested for their ability to stimulate mitochondrial pregnenolone formation and displace PBR drug ligands. Only TTN was shown to have PBR affinity (IC_{50} = 6 μM) and increased pregnenolone formation.[45,46,47]

Porphyrins (protoporphyrin IX **[1]**, mesoporphyrin IX, deuteroporphyrin IX, hemin **[2]**) have high nanomolar binding affinity (K_i = 14.5 - 40.6 nM) for PBR and have therefore been suggested as endogenous ligands (Figure 1.2).[48] Protoporphryin IX **[1]** was found to have the highest affinity (K_i = 14.5 nM) of the porphyrins. PBR also binds cholesterol **[3]** with nanomolar affinity (K_d = 6 nM) at the cholesterol binding site in the carboxyl-terminus of PBR. (Figure 1.2).[16,17]

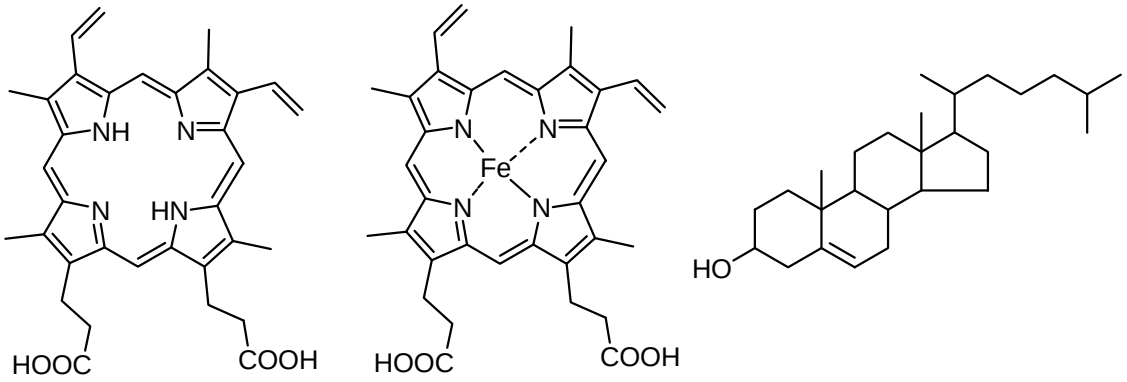

Protoporphyrin IX **[1]** Heme **[2]** Cholesterol **[3]**

Figure 1.2 Possible endogenous PBR ligands.

Another proposed endogenous ligand is a protein of 16 kDa called anthralin, which was found to inhibit the specific binding of Ro5-4864 to PBR, but also inhibited the binding of nitrendipine to the dihydropyridine Ca^{2+} channel.[49]

1.5 Synthetic PBR Ligands

There are many reported high affinity PBR ligands of different chemical classes, such as PK11195 **[4]** and PK14105 **[5]**,[50,51] isoquinoline carboxamides; Ro5-4864 **[6]**,[52] a benzodiazepine; Alpidem **[7]**,[53] an imidazopyridine; FGIN-1-27 **[8]**,[54] a 2-aryl-3-indoleacetamide; NF182 **[9]**,[55,56] a pyrrolobenzoxazepine, and SSR180575 **[10]**,[57] a pyridazinoindole derivative (Figure 1.3). PK11195 and Ro5-4864 radiolabelled with ^{3}H are most commonly used in displacement studies to determine the affinities of other compounds for the PBR.

It was initially suggested that isoquinoline carboxamides such as PK11195 bound to the 18 kDa protein of the PBR complex, while benzodiazepines such as Ro5-4864 required some association with the VDAC.[58] Garnier *et al*. hypothesised that the benzodiazepine binding site is partly situated on the 18 kDa protein and partly on the VDAC.[58] A later study found that mitochondria prepared from the 18 kDa protein producing cells devoid of either VDAC or ANT exhibited both isoquinoline carboxamide and benzodiazepine binding sites.[59] They hypothesised that the 18 kDa protein contains both the isoquinoline carboxamide and benzodiazepine binding sites.

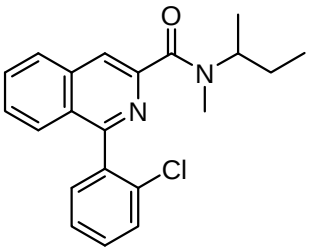

PK 11195 **[4]**

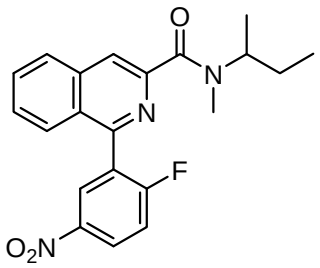

PK 14105 **[5]**

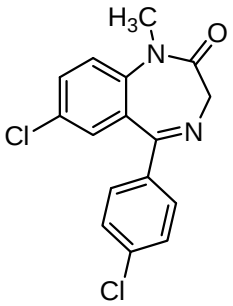

Ro5-4864 **[6]**

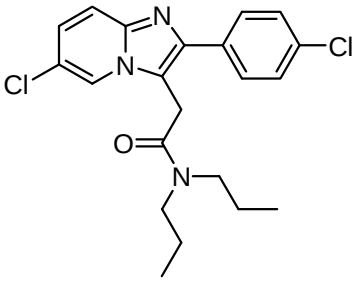

Alpidem **[7]**

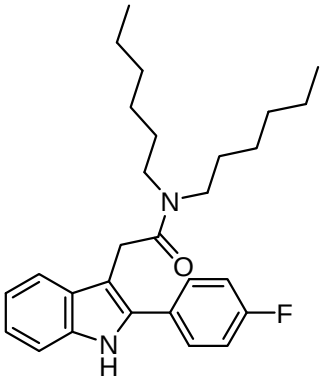

FGIN-1-27 **[8]**

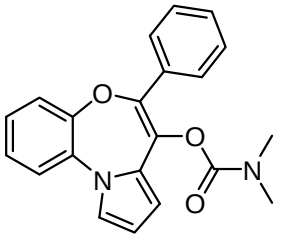

NF 182 **[9]**

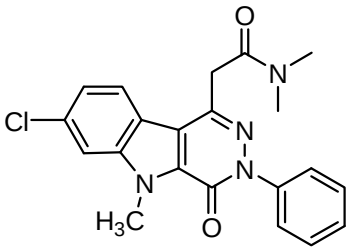

SSR180575 **[10]**

Figure 1.3 Synthetic PBR ligands.

1.6 Possible Functions of the PBR

1.6.1 Cellular Respiration

The mitochondrial location of the PBR led to studies involving the effect of PBR ligands on mitochondrial respiration.[60,61] In 1989, Hirsch *et al*. described an inhibition of the respiratory control ratio due to PBR ligand binding. In 1992, Zisterer *et al*. found that PBR ligands only affect respiration at high concentrations, and suggested that the results of the previous study were due to non-specific effects of PBR ligands and were not mediated through PBR.[62]

The proposed association of PBR with VDAC provides a likely mechanism by which PBR can inhibit cellular respiration by influencing the transport of metabolites through the mitochondrial membrane. One study performed on heart mitoplast preparations revealed the inhibition of at least two large conductance channels with nanomolar concentrations of Ro5-4864 and PK11195.[63]

1.6.2 Steroid and Bile Acid Biosynthesis

PBRs have been found on the outer mitochondrial membrane of steroid producing cells such as Leydig cells in the testes, granulosa cells in the ovaries, cortical cells of the adrenals, glial cells in the brain, and also in the placenta, suggesting a role in steroidogenesis. It has been observed that various PBR ligands stimulate the biosynthesis of steroids.[64] The first step in steroidogenesis occurs in the inner mitochondrial membrane and is the conversion of cholesterol into pregnenolone, catalysed by the enzyme, side chain cleavage cytochrome P450 (CYP11A1) (Figure

1.4). The rate-limiting step of steroidogenesis is the transport of intracellular cholesterol from the outer to the inner mitochondrial membrane.

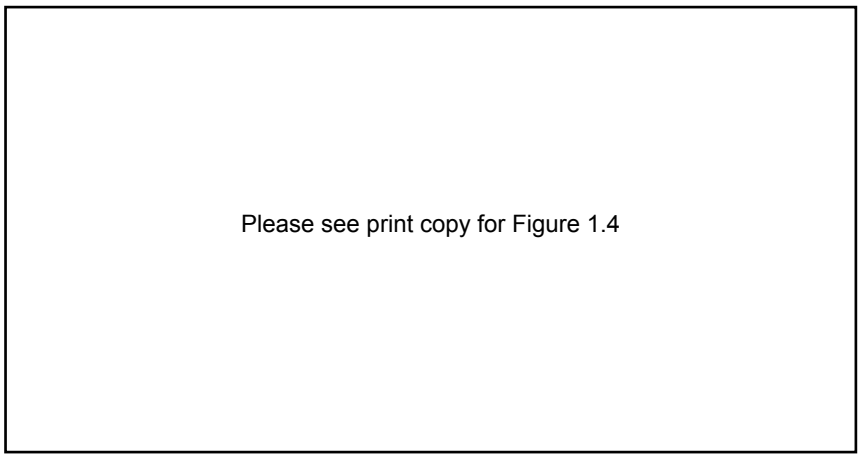

Figure 1.4 The mechanism of steroid and bile acid biosynthesis in the mitochondria of steroid producing cells and hepatic cells respectively.[16]

Results have demonstrated that PBR ligands stimulate pregnenolone formation by inducing the transport of cholesterol into the inner mitochondrial membrane. By disrupting the PBR gene in the Leydig cells of the testes *in vitro*, steroidogenesis was stopped, as there was no cholesterol transport.[65] Steroidogenesis was revived by replacing the gene with cDNA encoding the gene. The PBR binds cholesterol with nanomolar affinity at the cholesterol binding site in the carboxyl-terminus of PBR.[16] Using molecular dynamics simulations, a model of the receptor was generated and it was shown that a PBR could accommodate a cholesterol molecule and possibly function as a channel. However, it is more likely that the PBR acts as a cholesterol transporter or exchanger, as channels need a cholesterol gradient between the cytosol and the mitochondria which does not exist *in vivo*.

The PBR is found in considerable amounts in the hepatic cells of the liver, which is the site of bile acid biosynthesis.[16] Bile acids are made from cholesterol by two pathways, the classical pathway, which occurs in the endoplasmic reticulum, or the alternative pathway, which takes place in the mitochondria. In the alternative pathway, cholesterol is converted to 27-hydroxycholesterol by the enzyme cytochrome P450 27 hydroxylase (CYP27A1) (Figure 1.4).[16]

Like steroidogenesis, cholesterol transport to the inner mitochondrial membrane is the rate-limiting step of bile acid biosynthesis in the mitochondria of hepatic cells[66] and this transport is activated by PBR ligands.[67] Hydroxylation of cholesterol is modulated by PBR ligands.[68,16]

It has been proposed that in both steroid and bile acid synthesis, steroidogenic acute regulatory protein (StAR) binds cholesterol in the cytosol and carries it to the PBR (Figure 1.5). PAP7 interaction with protein kinase A (PKA) facilitates the phosphorylation of StAR by PKA.[22] PAP7 binds to the PBR, and cholesterol is transferred from StAR to PBR. Upon DBI binding to PBR, cholesterol is transferred to the inner mitochondrial membrane where it is converted to pregnenolone or 27-hydroxycholesterol by cytochrome P450. Recently, it has been suggested that presence of PBR is required for import of StAR into the mitochondria, and that StAR and PBR act together to transfer cholesterol into mitochondria.[69]

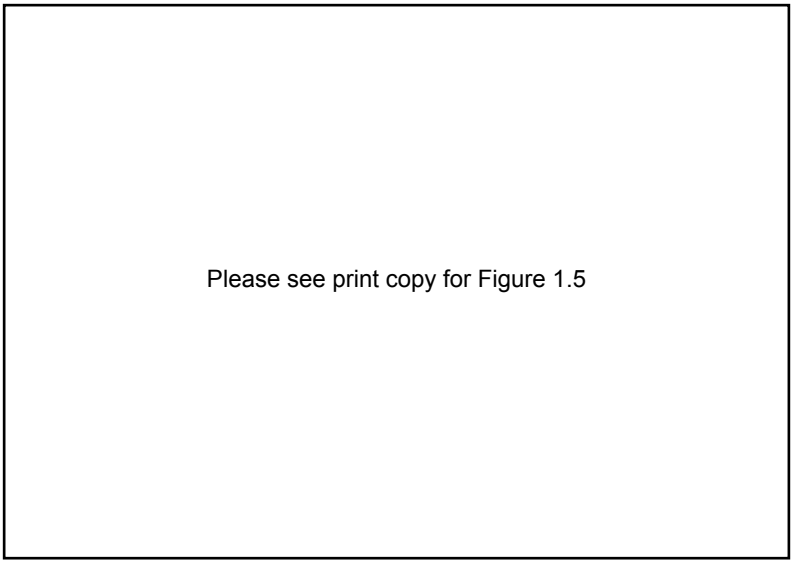

Figure 1.5 Hypothetical model for cholesterol transport into mitochondria.[17]

OMM = outer mitochondrial membrane, IMM = inner mitochondrial membrane

1.6.3 Modulation of Apoptosis

The PBR is found in all blood leukocyte subsets, mainly in monocytes and polymorphonuclear cells. A study has shown a strong correlation between expression of PBR and the ability of hematopoietic cells to resist oxygen radical damage and therefore cell death.[30] In some cell types, the expression level of the PBR compared to the Bcl-2 proto-oncogene showed high similarity. One function of Bcl-2 is the decrease in the production of reactive oxygen species (ROS).

1.6.4 Cellular Proliferation and Differentiation

Many studies have investigated the effect of PBR ligands on the cellular activity in different cell types. An inhibition of cellular proliferation with PBR drugs was shown in

mouse thymoma cells,[70] B16 melanoma cells,[71] MCF-7 breast cancer cells,[72] rat C6 glioma and mouse neuro-2A neuroblastoma cells,[73] and V79 Chinese hamster lung cells.[74] The inhibitions were concentration dependant, but micromolar concentrations of these drugs with nanomolar affinity were needed, therefore it cannot be concluded that these results are due to a specific interaction of the PBR drugs with the PBR. Recently, the inhibition of mitochondrial F_1F_0-ATPase by PK11195 was observed.[75] Inhibition of this enzyme causes apoptosis or cell growth arrest. The data indicated that cellular responses commonly attributed to modulation of PBR, are likely a direct result of mitochondrial F_1F_0-ATPase inhibition. Antiproliferation effects of PBR drugs were similar with SP2 hybridoma and NCTC epithelial cell cultures, which do not have PBR.[73]

A low concentration (10 nM) of PK 11195 stimulated growth rate and DNA synthesis in Swiss 3T3 and C6 glioma cells.[76] Other cellular changes caused by micromolar concentrations of PBR ligands include induction of differentiation of Friend erythroleukemia cells,[52,77] stimulation of phospholipid methylation of C6 astrocytoma cells,[78] induction of ornithine decarboxylase and inhibition of neurite outgrowth in PC12 cells,[79] and elevated expression of the c-fos proto-oncogene following exposure of PC12 cells to nerve growth factor.[80] Increased mitochondrial proliferation and morphological changes due to PK11195 and Ro5-4864 were observed in glioma cells.[81] Melanin synthesis in B16/C3 mouse melanoma cells was induced by high PBR affinity benzodiazepines, and was less effective with lower affinity drugs, however, micromolar concentrations were still needed.[82]

1.6.5 Immune Responses

PBRs are present on immune cells, such as monocytes, granulocytes, B lymphocytes, NK cells and T lymphocytes. Knowledge of the presence of PBRs on immune cells prompted studies involving PBR and immunomodulation. An early study discovered that the agonist PBR ligand Ro5-4864 induced the chemotaxis of human monocytes, while the (partial) PBR antagonist PK11195 did not.[83] This benzodiazepine-induced chemotaxis is impaired in monocytes from patients with generalised anxiety.[84]

Cytokines such as interleukin-1 (IL-1), tumour necrosis factor alpha (TNF-α), interleukin-6 (IL-6), granulocyte/macrophage-colony-stimulating factor (GM-CSF) and interleukin 8 (IL-8), are important mediators of the inflammatory response. The PBR ligand Ro5-4864 showed an immunosuppressive property, inhibiting the production of IL-1, IL-6 and TNF by macrophages, induced by bacterial lipopolysaccharide (LPS).[85]

A process called oxidative burst occurs in activated macrophages, producing a number of reactive oxygen species that are toxic to microorganisms. One such reactive oxygen intermediate is the superoxide anion, O_2^-. PBR ligands Ro5-4864 and diazepam have been shown to enhance arachidonic acid-induced superoxide anion production in a mouse macrophage cell line.[86] It was suggested that the effects are mediated specifically through the PBR.

1.7 The PBR under Pathological Conditions

1.7.1 Neurodegenerative Disorders

In healthy brain tissue, the PBR is localised primarily in glial cells, but a neuronal expression has also been reported in the olfactory bulb, choroid plexus and along the ependymal linings of the ventricles.[87] Patients with Huntington's disease,[88] multiple sclerosis,[89] or Alzeimer's disease[90] have been shown to have an increased PBR density in lesioned brain areas, whereas diminished platelet PBR density has been detected in Parkinson's disease[91] and Alzeimer's disease.[92] A lower PBR density in T-lymphocytes was found in Parkinson's disease patients as compared with healthy controls.[93]

Microglia are specialised immune cells in the central nervous system (CNS) that act as macrophages, removing damaged cells and foreign invaders. Microglia are usually 'resting', but become 'activated' in neuronal injuries or disease. When activated, they increase the number of PBR.[94] In normal brain tissue, binding of PK11195 is minimal, however, when microglia are activated, *in vivo* binding increases significantly. Activated glia are isolated cells which do not spread diffusely beyond the site of activation, therefore neuronal injury can be localised by the visualisation of activated microglia.

1.7.2 Inflammation and Autoimmune Diseases

Lupus erythmatosus (LE) is an autoimmune disease characterised by a butterfly-shaped rash over the face, centred over the nose. Using Mrl/Lpr mice which develop

inflammation pathologies similar to human LE, it was found that PBR ligands show a protective effect against the formation of skin lesions of LE. Skin lesions were reduced by 40-60% following treatment with PK11195, Ro5-4864 and SSR180575. Some other symptoms of LE are pulmonary inflammation and alveolitis, which are a major cause of death in patients with LE. By treating the same mouse model with the same PBR ligands, a significant beneficial decrease in these symptoms was observed.[95,96] The results of these two recent studies show that not only do PBR ligands have potential therapeutic use for skin disorders involving inflammation, but also potential for PBR to be used as a biomarker of pulmonary lesions.

1.7.3 Cancer

An increased PBR expression has been observed in certain cancers, including ovarian, hepatic, colon and endometrial carcinomas, adenocarcinomas, and glioma.[38,97-100] Even higher levels of PBR density are observed in aggressive human breast cancer cell lines and metastatic human breast tumours.[97,101,102] Recent studies have suggested a close correlation between the expression of PBR and the progression of breast cancer, shown by PBR gene amplification in an aggressive breast cancer cell line, but not in non-aggressive breast cancer cell lines.[101] This gene amplification may be an important indicator of breast cancer progression.[101] The PBR in the breast cancer cell lines and in glioblastoma biopsies were localised in the nucleus of the cells and it is thought the transport of cholesterol into the nucleus may regulate cell proliferation. A recent study showed that decreased PBR expression in aggressive human mammary carcinoma cells was associated with cell cycle arrest at G2 phase, decreased cell proliferation, and increased protein levels of the cyclin-dependent kinase inhibitor $p21^{WAF/C1P1}$.[103] In colorectal and prostate carcinomas, PBR levels were higher in the tumour than in non-

tumour tissues, whereas in adrenocortical tumours and hepatomas, PBR levels were lower than non-tumour tissues, suggesting that PBR overexpression is limited to certain cancers.[104]

The use of PBR as a prognostic marker of colorectal cancer and glioma has also been studied.[105,106] These studies found that PBR expression correlated positively with tumour malignancy grade and negatively with patient survival, indicating that prognosis of certain cancers can be made by monitoring PBR expression. The diagnosis of cancer has also been studied with radiolabelled PBR ligands using positron emission tomography (PET). The therapeutic use of PBR ligands for cancer has been tested both indirectly (as conjugates with known anticancer drugs) and directly (by itself). PBR ligands therefore have potential in the diagnosis, prognosis, and therapy of several types of cancer.

1.8 Peripheral Benzodiazepine Receptor Ligands

1.8.1 Benzodiazepines

Benzodiazepines were the first class of compound found to bind selectively to PBR over the CBR. A large series of benzodiazepine structures were tested for their PBR affinity and the first selective PBR ligand, Ro5-4864 **[6]**, was found by adding only a chlorine atom on the 4′ position of the phenyl group of diazepam **[11]** (Figure 1.6).[52,70]

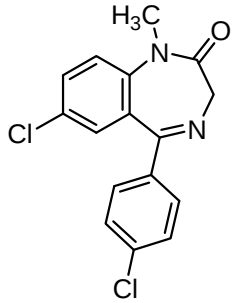

Ro5-4864 **[6]**
PBR IC_{50} = 6 nM
CBR IC_{50} = 5000 nM

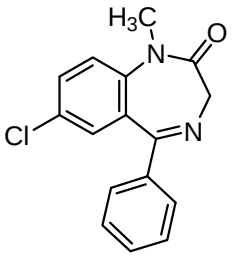

Diazepam **[11]**
PBR IC_{50} = 79 nM
CBR IC_{50} = 6 nM

Figure 1.6 Structure of Ro5-4864 **[6]** and diazepam **[11]**.

1.8.2 Isoquinoline Carboxamides

In 1983, Le Fur *et al*. found that isoquinoline carboxamides bound with high affinity to the PBR, whilst having no affinity for the CBR.[50] PK11195 **[4]**, an isoquinoline carboxamide, is one of the most widely used and studied PBR ligands. Under UV irradiation, a photoaffinity probe similar to PK11195 **[4]**, called PK14105 **[5]**, covalently links with the 18 kDa PBR protein,[51] enabling the protein to be purified (Figure 1.3).[107]

The mapping of the PBR binding site by conformationally restrained derivatives of PK11195 **[4]** was achieved using a synthetic-computational approach.[108] Twenty-nine derivatives of PK11195 were synthesised, most of which showed PBR affinities in the nanomolar range. Further studies including the synthesis of 20 new PK11195 derivatives resulted in a compound with nanomolar affinity similar to that shown by PK11195.[109]

1.8.3 Imidazopyridines and Imidazopyridazines

Imidazo[1,2-*a*]pyridine-3-acetamides **[12]**, such as alpidem **[7]** and zolpidem **[13]**, (Figure 1.7) were first described as potent anticonvulsant drugs,[110] and later, as ligands of the peripheral and central benzodiazepine receptor respectively,[53,111] with the former found to have selectivity for the PBR only.

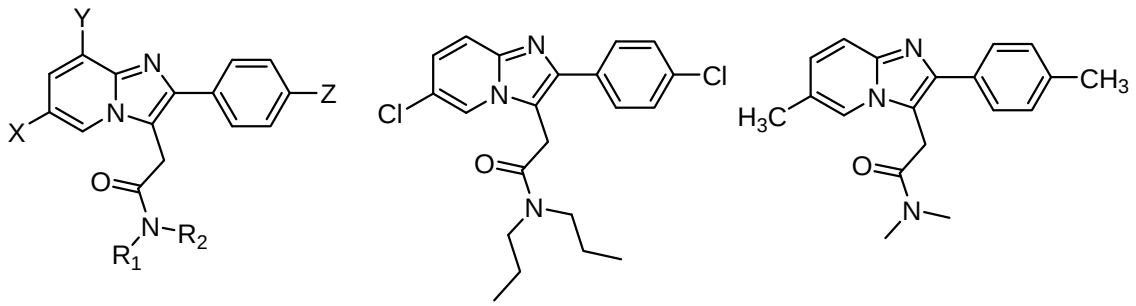

[12]

Alpidem **[7]**
PBR IC_{50} = 1 nM
CBR IC_{50} = 7 nM

Zolpidem **[13]**
PBR IC_{50} = 1036 nM
CBR IC_{50} = 26 nM

Figure 1.7 Imidazo[1,2-*a*]pyridine-3-acetamides **[12]**, alpidem **[7]** and zolpidem **[13]**.

In a search for new PBR ligands with improved affinity and selectivity, analogues of alpidem **[7]** were designed and synthesised investigating the substitution on positions X, Y and Z on **[12]**, and the importance of the carbon chain length between the heterocyclic nucleus and the amide function.[112,113] The *N*,*N*-dialkyl-(2-phenylimidazo[1,2-*a*]pyridinyl-3-yl)acetamides **[12]** had high affinity and selectivity for PBR, however, exchanging the acetamide moiety with an ester functionality resulted in total loss of affinity to PBR. The 6,8-disubstituted derivatives showed 1000-fold higher selectivity for PBR over CBR.

Three imidazo[1,2-*a*]pyridine-3-acetamide derivatives, CB 34 **[14]**, CB 50 **[15]** and CB 54 **[16]** (Figure 1.8), were found to be potent and selective agonists of the PBR, and stimulated steroidogenesis in the brain and the periphery.[114]

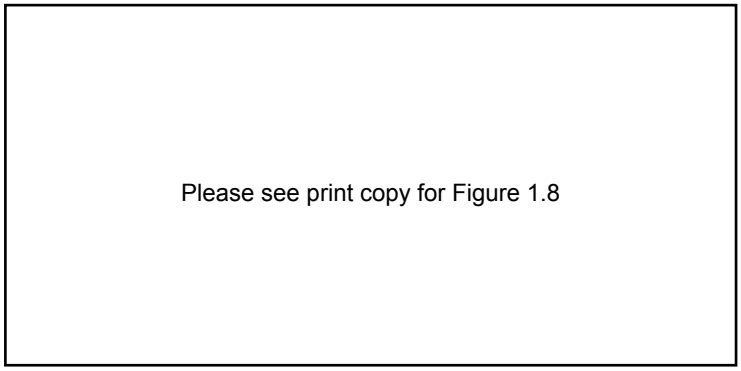

Figure 1.8 General structure of imidazo[1,2-*a*]pyridine-3-acetamides **[14]-[16]**.[114]

Several imidazo[1,2-*b*]pyridazines which differ in just one nitrogen from imidazo[1,2-*a*]pyridines, are also potent and selective PBR ligands.[115,116]

1.8.4 Pyrazolopyrimidines

The imidazopyridine heterocycle of alpidem **[7]** was modified to a pyrazolopyrimidine to create a new highly potent and selective class of PBR ligands, 2-arylpyrazolo[1,5-*a*]-pyrimidin-3-yl acetamides **[17]** (Figure 1.9).[117,118]

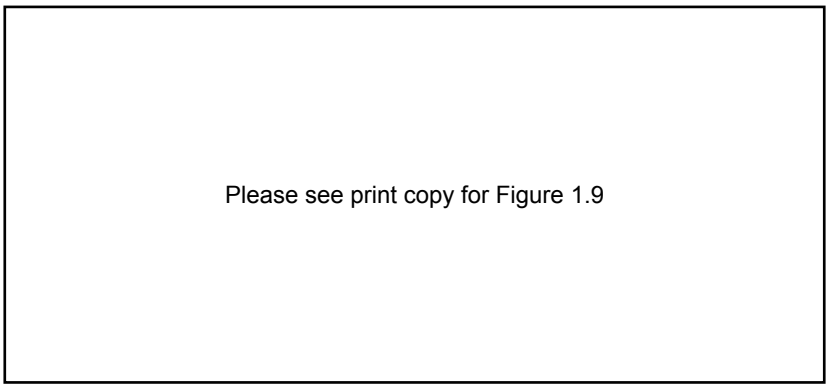

Figure 1.9 General structure of 2-arylpyrazolo[1,5-*a*]pyrimidin-3-yl acetamides **[17]**.[117]

1.8.5 Pyrrolobenzothiazepines, pyrrolobenzoxazepines and pyridopyrrolooxazepines

With the aim of discovering high affinity CBR ligands, it was found that several 6-(*p*-methoxyphenyl)pyrrolo[2,1-*d*][1,5]benzothiazepines **[18]** (Figure 1.10) had nanomolar affinity for PBR.[119] Further investigation found the 6,7 double bond and the 6-aryl substitution to be important for PBR binding.[120] A structure activity relationship (SAR) study and some molecular modelling on 42 6-arylpyrrolo[2,1-*d*][1,5]benzothiazepine derivatives **[18]** determined the structural features which improved affinity.[120] This then lead to the synthesis and testing of various pyrrolobenzoxazepines **[19]**,[121] pyridopyrrolooxazepines **[20]**,[56] and further pyrrolobenzothiazepines **[18]**,[122,123] (Figure 1.10) with PBR IC_{50} values in the nanomolar range.

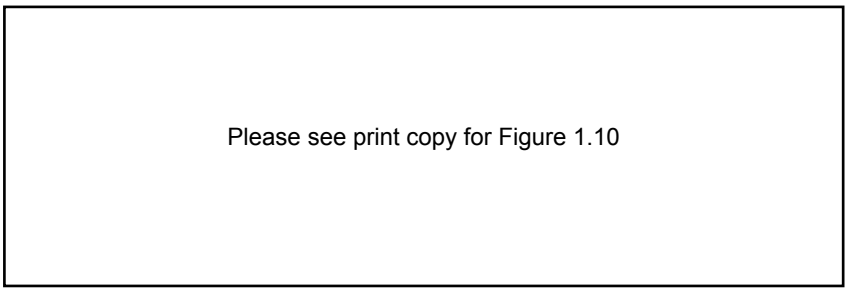

Figure 1.10 Potent PBR ligands: pyrrolobenzothiazepines **[18]**, pyrrolobenzoxazepines **[19]**, and pyridopyrrolooxazepines **[20]**.[119-123]

1.8.6 Aryloxyanilides

Recently, various high affinity PBR ligands have been designed and synthesised based on aryloxyanilide derivatives.[124] The aryloxyanilide derivatives were derived from opening of the diazepine ring of Ro5-4864 (Figure 1.11). Opening this diazepine ring

allows for increased flexibility in the structure, and by modifying groups Ar^1, Ar^2, R^1, X^1 and Y, the affinity (IC_{50}) for PBR was optimised.

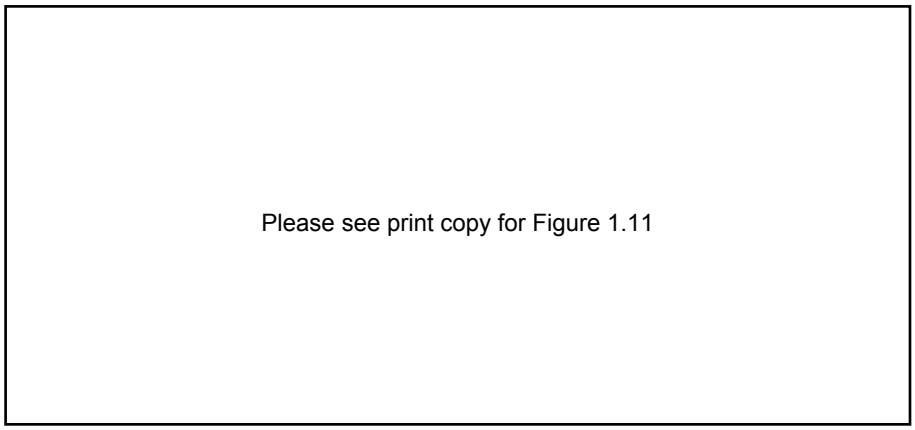

Figure 1.11 Opening of the diazepine ring of Ro5-4864 leading to new PBR ligands based on aryloxyanilide derivatives **[21]**.[124]

Two aryloxyanilide derivatives, DAA1106 **[22]** and DAA1097 **[23]** (Figure 1.12), have received much attention due to their high PBR affinity and selectivity with IC_{50} values for the inhibition of [^{3}H]PK11195 binding to crude mitochondrial preparations of rat whole brain being 0.28 and 0.92 nM, respectively. Okuyama *et al*. have examined the neuropharmacological profile of the two PBR agonists.[125] Both ligands had anxiolytic effects in laboratory animals, thought to be mediated by the indirect modulation of $GABA_A$ gating chloride channel by neurosteroids, produced by PBR induced mitochondrial steroidogenesis.

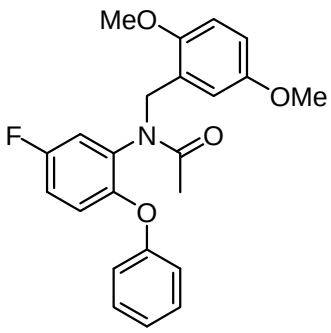

DAA1106 **[22]**

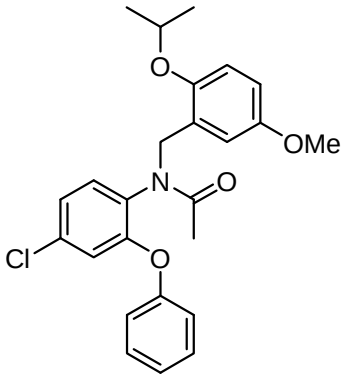

DAA1097 **[23]**

Figure 1.12 Structures of DAA1106 **[22]** and DAA1097 **[23]**.

1.8.7 2-Aryl-3-indoleacetamides (FGIN series)

In 1992, a class of potent and specific ligands for the PBR was discovered, based on the structure of the imidazopyridines, alpidem **[7]** and zolpidem **[13]** (Figure 1.7), but without the nitrogen atom at the ring fusion position. The derivatives synthesised were 2-aryl-3-indoleacetamides **[24]** (Figure 1.13), collectively known as FGIN-1.[126,127] These were the first compounds found to increase steroidogenesis as well as having high affinity and selectivity for PBR.[54] The most promising of these derivatives, FGIN-1-27 **[8]**, has a fluorine atom on the phenyl ring attached to the indole and a dihexyl group attached to the amide. FGIN-1-27 **[8]** has a K_i value of 4.4 nM, and was the most effective FGIN-1 at enhancing pregnenolone synthesis *in vitro*, however, *in vivo*, it was not as efficient. By adding 1,2,4 benzenetricarboxylic acid onto the indole nitrogen, the compound (FGIN-1-44 **[25]**, Figure 1.13) was more soluble in the blood therefore had higher bioavailability and the *in vivo* potency was increased.[128] It was found that FGIN-1-44 **[25]** was being hydrolysed *in vivo* to FGIN-1-27 **[8]**, which in turn was stimulating the PBR.

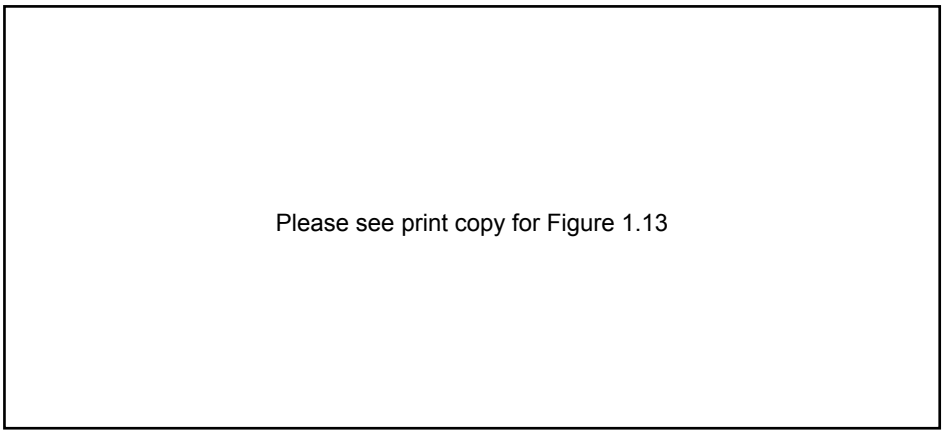

Figure 1.13 The basic structure of 2-aryl-3-indoleacetamides (FGIN-1) **[24]**, and FGIN-1-44 **[25]**.[126-128]

FGIN-1 **[24]** compounds, especially FGIN-1-27 **[8]** and FGIN-1-44 **[25]**, elicited anxiolytic, antiamnestic, anticonvulsant, and antidepressant effects in rats and mice.[54] The compounds bind to PBR and increase the production of neurosteroids which act on the $GABA_A$ receptor to elicit the responses observed.

A series of benzofuran analogues of FGIN-1-27 **[8]** were evaluated for PBR affinity, and found to be equally potent and selective as **[8]**.[129] Guillon *et al*. evaluated new 3-aryl-3-pyrrol-1-ylpropanamides, analogues of FGIN-1 **[24]**, with the indole ring replaced with a pyrrole ring (Figure 1.14).[130]

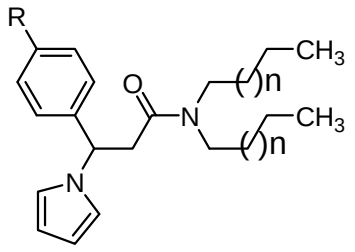

[26]

R = H, F, Cl, CH_3, CH_3O
n = 1, 2, 3

Figure 1.14 General structure of 3-aryl-3-pyrrol-1-ylpropanamides, analogues of FGIN-1 **[24]**.[130]

The analogues were found to have sedative properties in mice, but no anxiolytic effect. The most active compounds were the compounds with the most similar structure to FGIN-1-27 **[8]**, with a dihexylamide moiety, and with *para*-substituted F or Cl on the aryl group. Therefore, replacing the indole ring with a pyrrole ring led to compounds with sedative activity, but no anxiolytic activity.

1.8.8 Phenylindol-3-ylglyxoxylamides

Recently, an exciting new class of potent and selective PBR ligands, the *N*,*N*-dialkyl-2-phenylindol-3-ylglyoxylamide derivatives **[27]**, have been found by restraining the conformation of FGIN-1 **[24]** by replacing the methylene group with a carbonyl group.[131] The structure of these indolylglyoxylamides which have been synthesised and evaluated for PBR and CBR binding is shown in Figure 1.15. These FGIN-1 analogues showed affinities for PBR at least 1 order of magnitude higher than the respective FGIN-1 compounds. The high affinity compounds were also shown to stimulate pregnenolone production in rat C6 glioma cells. Three of these compounds increased pregnenolone production by more than 145% when compared to controls.

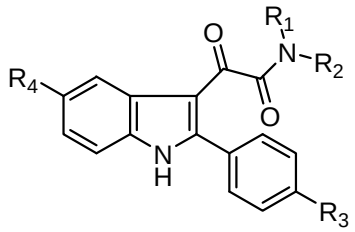

[27]

Figure 1.15 Structure of *N*,*N*-dialkyl-2-phenylindol-3-ylglyoxyamides **[27]**.

1.9 Radiopharmaceutical Chemistry

Radiolabelled PBR ligands would be useful not only in learning more about the ligand binding sites of the receptor complex, but also in the diagnosis of various neurodegenerative diseases and cancers using non-invasive external imaging. The general aspects of radiopharmaceutical chemistry will be briefly reviewed, followed by some applications of radiolabelled PBR ligands.

1.9.1 Radionuclides

Radionuclides are isotopes that are unstable and undergo radioactive decay to achieve stability. When the radionuclides undergo radioactive decay, they eject small nuclear fragments and/or electromagnetic radiation. Radioactive decay can be in the form of:

- Alpha radiation - the emission of helium nuclei,
- Beta radiation - the emission of a positron or an electron, and
- Gamma radiation - the emission of gamma rays (photons).

Gamma rays have greater penetrating ability than α or β particles, therefore can be externally detected by gamma detectors. Some commonly used radionuclides are ^{3}H, ^{11}C, ^{13}N, ^{15}O, ^{18}F, ^{123}I, ^{99m}Tc, and ^{131}I.

Carbon, nitrogen and oxygen are the most chemically appealing radionuclides as they can be directly substituted into biological compounds to study processes in the body.[132] However, due to the short half lives of these radionuclides they are not always practical in radiopharmaceutical development. This fact leads to the use of radionuclides such as fluorine and iodine, which have longer half lives. Since these halogens are not usually

present in biological compounds or pharmaceuticals, they must be incorporated into the target compound so that its overall interaction with the biological system is not changed dramatically. Examples of groups that can be substituted with ^{18}F are H and OH, and ^{123}I can replace OH and CH_3. A significant number of molecular radiopharmaceuticals in use today are based on ^{18}F and ^{123}I.[133]

1.9.2 Radiopharmaceuticals

Radiopharmaceuticals are drugs composed of a radionuclide attached to a chemical substance for specific localisation in distinct regions and tissues in the body for diagnosis or treatment of disease.[134] The radiopharmaceutical can be injected into the body and the gamma rays emitted can be detected by the non-invasive imaging techniques, positron emission tomography (PET) and single photon emission computed tomography (SPECT). An efficient diagnostic radiopharmaceutical should have high uptake soon after injection, but radioactivity should wash out quickly after imaging to reduce the dose to the patients and carers. A therapeutic radiopharmaceutical emits beta particles which are intended to destroy diseased tissue. The ionising radiation of the beta particles disrupts vital cell processes resulting in cell death.[135] Another important feature of the beta particle is that its path length is only 0.5 mm, so the radiation induced damage is limited to the target tissue. Different radionuclides may be used for diagnosis and therapy, for example, ^{123}I is used in SPECT imaging, ^{18}F is used in PET, and ^{131}I is used for therapy. Table 1.2 shows the half-life, decay mode, and use of selected radionuclides. ^{123}I decays by electron capture, a type of nuclear reaction in which an orbital electron collapses into the nucleus and combines with a proton to produce a neutron and a neutrino.[134] The nucleus that has captured the orbital electron can emit a

gamma ray. ^{131}I emits gamma photons and high energy beta particles making it useful for therapy. If radiopharmaceuticals incorporating the radionuclide ^{123}I are effective in the diagnostic study of cancer, then substitution with the therapeutic radionuclide ^{131}I could be potentially employed in therapy. This would prove useful in cancer treatment if the radiopharmaceutical containing ^{131}I is selectively taken up by the tumour in high concentration ratios to destroy the diseased tissue. The radiopharmaceutical should have high uptake in the tumour and metastases, but low uptake in other tissues. An efficient therapeutic radiopharmaceutical should remain in the tumour for a prolonged period of time, but have fast washout from other tissues.

Table 1.2 Radionuclides and their uses.[136]

Please see print copy for Table 1.2

1.9.3 Radiation Detection

Diagnostic imaging involves the detection and spatial mapping of the radiation emitted by a radiopharmaceutical. The most common nuclear medicine studies image the distribution of a radiopharmaceutical in the body with a scintillation or gamma camera.

A scintillation camera consists of a detector head and a display console. The detector head is made up of a sodium iodide crystal, which absorbs the γ-rays and emits the absorbed energy as flashes of light. A coupled photomultiplier tube converts the light flashes to electronic pulses which undergo position and energy analysis to produce a projectional or planar image.[133] Emission computed tomography (ECT) is a technique which aims to give an improved 3D representation of the target tissue. There are two types of ECT that have been developed, PET and SPECT.

In PET imaging, positrons (β^+, positively charged electrons) are emitted from a positron-emitting radionuclide such as ^{11}C, ^{13}N, ^{15}O and ^{18}F, and travel a few millimetres until they collide with an electron. This causes annihilation of both particles, with the creation of two 511 keV γ-rays travelling at 180°. Gamma detectors on opposite sides of the positron source detect the pair of γ-rays in coincidence. There are many detectors in a PET camera, which are arranged in a circle around the body, as shown in Figure 1.16.[133] Most commercial PET cameras use bismuth germanate detectors instead of sodium iodide crystals, because of superior performance.[134]

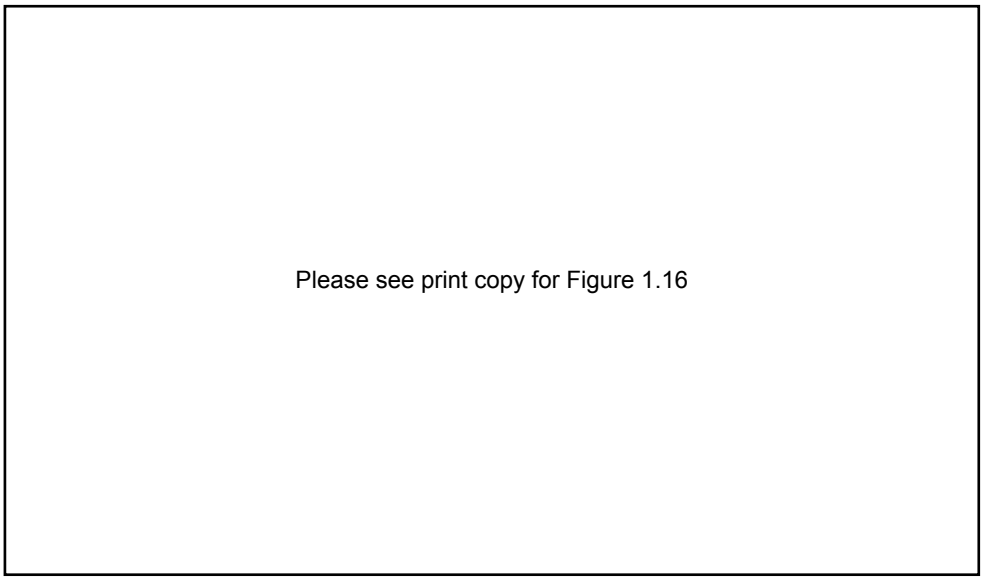

Figure 1.16 PET detector and brain images obtained with a SPECT camera.[134]

SPECT uses a gamma scintillation camera to detect gamma rays emitted from radionuclides such as ^{123}I and ^{99m}Tc. A computer is used to reconstruct transverse (cross section), sagittal (longitudinal) or coronal (frontal) images (Figure 1.16).[134] PET cameras are more sensitive than SPECT cameras and the radioisotopes used with PET have shorter half-lives.

PET and SPECT are powerful tools for the non-invasive study of physiological, biochemical and pharmacological functions at the molecular level in living beings. During the last two decades numerous biochemical processes have been probed in neuroscience, oncology and cardiology using radiolabelled metabolic tracers such as 2-[^{18}F]-fluorodeoxyglucose, radiolabelled amino acids[137] and nucleotides, receptor ligands, fatty acids, enzyme inhibitors, DNA probes and immuno-conjugates.[138]

Of enormous significance is the ability of these techniques to detect and measure functional receptors and binding sites at sub-nanomolar concentrations. As a consequence, monitoring the changes in receptor concentration or binding sites may provide significant insights into the aetiology and progress of diseases at the molecular level. In addition to high specificity and selectivity, a radiolabelled ligand should display other essential properties including high specific activity, low non-specific binding, slow metabolism, receptor saturability, blood brain barrier permeability and safety for human use.

1.10 Radiolabelled PBR Ligands

Many PBR ligands have been radiolabelled with positron emitting radioisotopes ^{3}H, ^{11}C, and ^{18}F. DAA1106 **[22]** has been radiolabelled with ^{18}F, ^{11}C and ^{3}H.[139-143] Two ^{18}F analogues of DAA1106 were synthesised, [^{18}F]FMDAA1106 **[28]** and [^{18}F]FEDAAA1106 **[29]**, one with a $OCH_2{}^{18}F$ group and one with a $OCH_2CH_2{}^{18}F$, both bioisosteres of the OCH_3 group of DAA1106 **[22]** (Figure 1.17). [^{18}F]FEDAA1106 **[29]** binding to PBR in living human brain was quantified.[144]

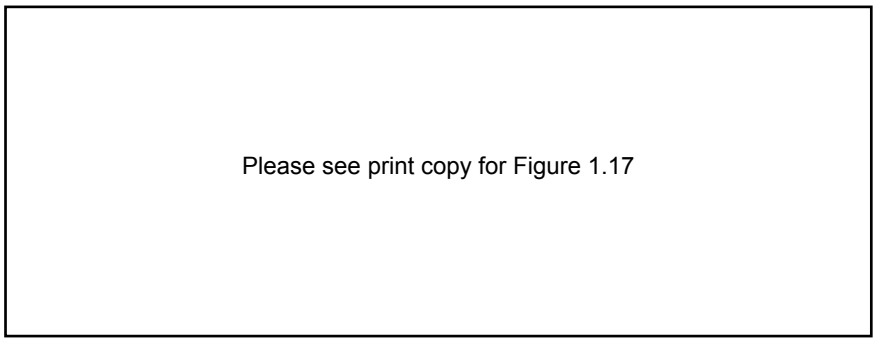

Figure 1.17 DAA1106 radiolabelled with ^{18}F.

Three quinoline-carboxamide derivatives similar to PK11195 were radiolabelled with ^{11}C and evaluated for *in vivo* PET imaging of neurodegeneration.[145] [^{11}C]VC195 **[30]** had *in vivo* behaviour similar to that of [^{11}C]PK11195 **[31]** (Figure 1.18).

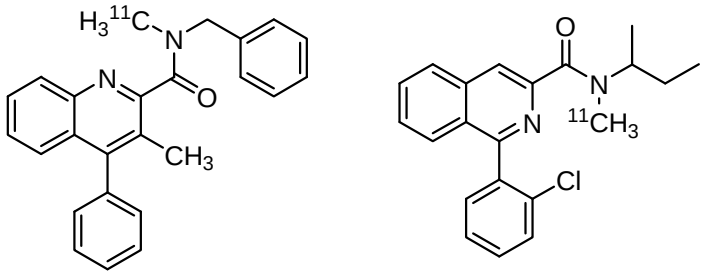

[^{11}C]VC195 **[30]** [^{11}C]PK11195 **[31]**

Figure 1.18 [^{11}C]PK11195 **[31]** and PK11195 derivative, [^{11}C]VC195 **[30]**.

The only pyrazolopyrimidine PBR ligand to be labelled has been PET radioligand [^{11}C]DPA-713 **[32]**, (Figure 1.19) which has been used in *in vivo* studies in baboons and indicated selective binding to PBR.[146,147]

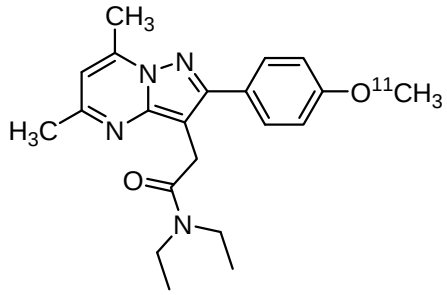

[32]

Figure 1.19 Carbon-11 radiolabelled pyrazolopyrimidine, [^{11}C]DPA-713 **[32]**.

Using PET and SPECT, radiolabelled PBR ligands can be used to visualise 'activated' microglia, and therefore the areas of neuronal damage or disease. This can be used to monitor the progression of the disease in the brain.[148] [^{11}C]PK11195 **[31]** has been used in PET studies for the *in vivo* imaging of activated microglia in multiple sclerosis,[149] Alzeimer's disease,[90] and following herpes encephalitis.[150] In the study of patients with Alzeimer's, high [^{11}C]PK11195 signals showed the most atrophic changes within the following year. This suggests that an *in vivo* measure of activated microglia predicts disease activity. A patient that showed minimal cognitive impairment showed increased [^{11}C]PK11195 binding in areas of the brain similar to patients with Alzeimer's.[90] Interestingly, within 23 months of the PET scan, the areas with high binding underwent atrophic changes, with no change in the cognitive performance. This suggests that pathological processes can occur years before the actual symptoms of the disease and before clinical diagnosis.

1.10.1 Iodine-123 Radiolabelled PBR Ligands

The short half life of positron emitting radioisotopes restricts the use of tracers labelled with these radioisotopes to a limited number of PET centres. A specific PBR ligand incorporating a longer-lived radionuclide such as ^{123}I may have greater clinical potential for imaging cancer or neurodegeneration using widely available SPECT cameras. PK11195 was radiolabelled with ^{123}I for mapping PBR in the heart,[151] and used to assess neuroinflammation and microglial activation in patients with Alzeimer's disease.[152] Other PBR ligands which have been radiolabelled with ^{123}I include [^{123}I]iodozolpidem **[33]**,[153] [^{123}I]imidazo[1,2-*a*]pyridines **[34]-[36]**,[113] and [^{123}I]iodoimidazo[1,2-*b*]pyridazines **[37]** and **[38]** (Figure 1.20).[154]

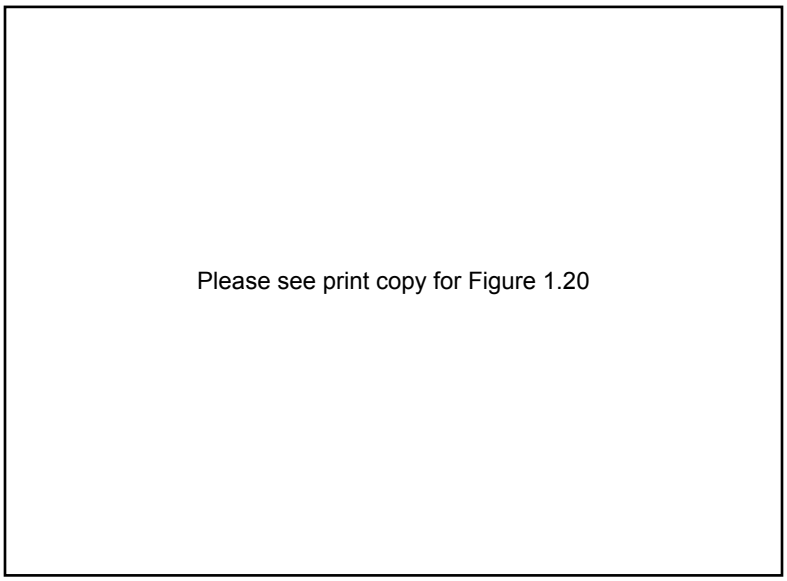

Figure 1.20 ^{123}I radiolabelled PBR ligands.[113,153,154]

[^{123}I]CLINDE **[35]** was evaluated in two animal tumour models, Babl/c nude mice implanted with A375 human melanoma cells, and Fischer rats implanted with rat

mammary adenocarcinoma.[155] *In vivo* imaging in the Fischer rats indicated significant contrast in the tumours compared to normal tissue. Further studies evaluated [^{123}I]CLINDE in CNS inflammation of experimental autoimmune encephalomyelitis (EAE). Uptake of [^{123}I]CLINDE was enhanced in the CNS of all rats exhibiting EAE when compared to controls, hence [^{123}I]CLINDE is a potential SPECT marker for imaging of CNS inflammation.[156]

1.11 Project Aims

The aim of this project was to develop highly potent (PBR IC_{50} <10 nM) and selective (CBR IC_{50} > 1000 nM) ligands for the peripheral benzodiazepine receptor, which could be radiolabelled with the radioisotope ^{123}I for SPECT imaging. As there are very few ^{123}I labelled PBR ligands, new ligands with improved *in vivo* properties and specific binding are required. Radiolabelling of PBR ligands will allow the study of the PBR *in vivo* using the radiolabelled ligands in biodistribution studies, competition studies, stability studies and SPECT imaging in normal animals, and in animals with tumours. Different classes of PBR ligands may bind to different areas on the PBR complex, and therefore another aim was to help elucidate the location of binding of PBR ligands. Synthesising compounds of varying structural classes could provide PBR ligands with different *in vivo* characteristics. Specifically, three different classes of compounds were investigated; the *N,N*-dialkyl-2-phenylindol-3-yl-glyoxylamides **[27]**, the 2-arylpyrazolo[1,5-*a*]pyrimidin-3-yl acetamides **[39]**, and pyrrolobenzo- and pyridopyrrolo- oxazepines **[40]** (Figure 1.21).

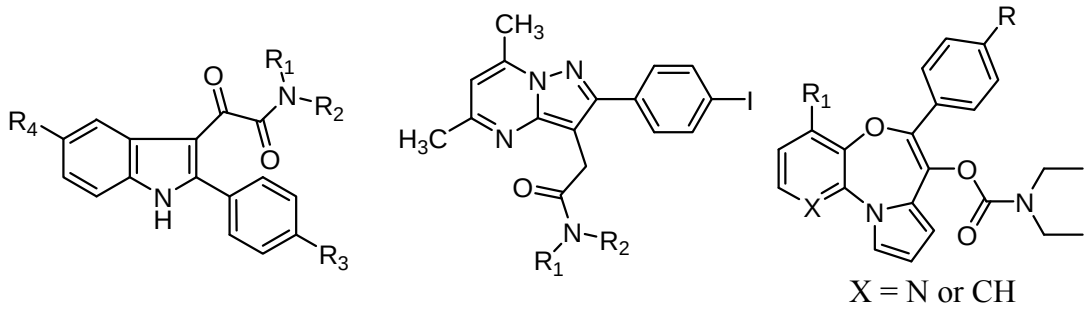

[27] **[39]** **[40]**

Figure 1.21 Proposed compound classes for synthesis and investigation.

The projects aims were to:

- To prepare iodinated compounds from the three different classes of PBR ligands.
- Perform *in vitro* binding studies to determine affinity of derivatives for PBR and CBR, and provide an SAR.
- Radiolabel high affinity and selective compounds with ^{123}I.
- Perform *in vivo* biodistribution studies in rats
- Perform *in vivo* competition studies
- Perform *in vivo* stability studies of radiotracers

Chapter 2 will discuss the synthesis of the *N*,*N*-dialkyl-2-phenylindol-3-yl-glyoxylamides; Chapter 3, the 2-arylpyrazolo[1,5-*a*]pyrimidin-3-yl acetamides; and Chapter 4, the pyrrolobenzo- and pyridopyrrolo- oxazepines. Chapter 5 will discuss the radiolabelling and the pharmacological studies.

2 Synthesis of *N,N*-Dialkyl-2-phenylindol-3-yl-glyoxylamides

2.1 *N,N*-Dialkyl-2-phenylindol-3-ylglyoxylamides for the PBR

The first class of iodinated compounds chosen for SAR investigation, with the aim of finding a high PBR affinity compound for potential radiolabelling with ^{123}I, were the recently developed *N,N*-dialkyl-2-phenylindol-3-ylglyoxylamides **[27]** (Figure 2.1).[131] The reported compounds, with functional modifications at positions R_1 to R_4, were found to be highly potent and selective PBR ligands.[131] Among these compounds were those with flexible or branched alkyl chains and cyclic amides, a methyl group, halogens (chlorine, fluorine) or hydrogen atom at R_3, and a chlorine or hydrogen atom at R_4. The PBR binding affinities of selected compounds are shown in Figure 2.2.

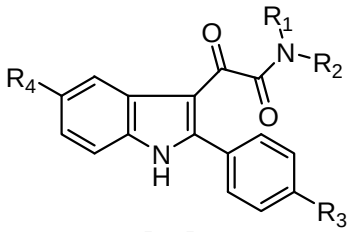

[27]

Figure 2.1 Structure of *N,N*-dialkyl-2-phenylindol-3-ylglyoxylamides.

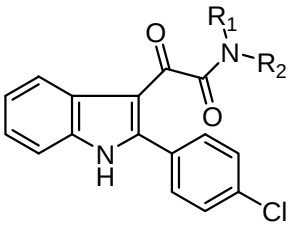

K_i (nM) for PBR
4.65 (R_1 and R_2 = propyl)
1.00 (R_1 and R_2 = butyl)
0.55 (R_1 and R_2 = hexyl)

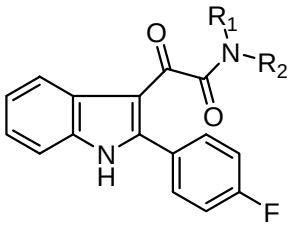

K_i (nM) for PBR
4.28 (R_1 and R_2 = propyl)
2.40 (R_1 and R_2 = butyl)
0.37 (R_1 and R_2 = hexyl)

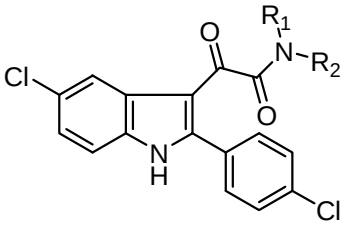

K_i (nM) for PBR
0.62 (R_1 and R_2 = propyl)
1.90 (R_1 and R_2 = butyl)
5.80 (R_1 and R_2 = hexyl)

Figure 2.2 Structures and PBR binding affinities for several *N*,*N*-dialkyl-2-phenylindol-3-ylglyoxylamides.

These compounds with a fluorine or chlorine atom on the *para* position of the phenyl group were found to be potent PBR ligands (Figure 2.2).[131] We thought that by changing the fluoro or chloro to an iodo, the affinity and selectivity for the PBR would not be affected, leading to high affinity iodinated analogues for potential radioiodination. The synthetic scheme allows flexibility as many derivatives can be made by changing the length of the alkyl chains at the last step.

2.2 Target Compounds

The target compounds include 15 new iodinated and brominated *N*,*N*-dialkyl-2-phenylindol-3-ylglyoxylamides. Although the aim was to find high PBR affinity iodinated ligands, brominated analogues were also synthesised, as they are used for the preparation of organotin derivatives for radiolabeling each compound with ^{123}I, and also provide a more extensive SAR. The target compounds therefore differ in their alkyl chains lengths, chlorine substitution on the indole, or the position of halogens on the phenyl ring (Figure 2.3).

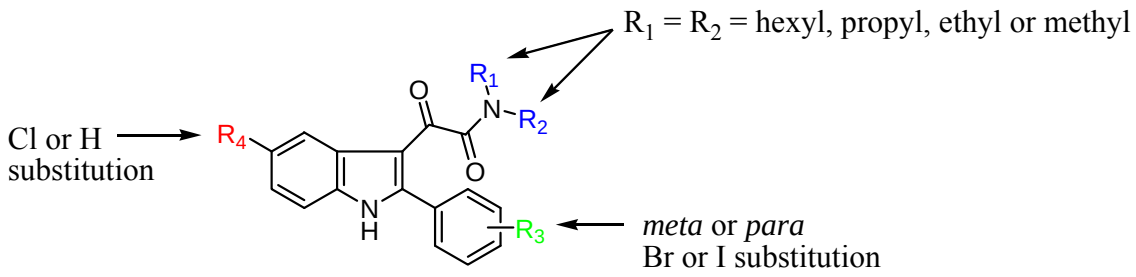

Figure 2.3 Possible variations for the target indol-3-ylglyoxylamides.

An additional target **[41]** was chosen to provide an iodinated compound, placing iodine onto the alkyl side chain, and fluorine on the phenyl ring at R_3 (Figure 2.4).

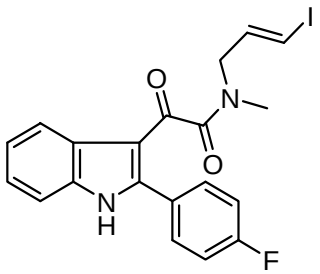

[41]

Figure 2.4 Iodinated target compound with the iodine on the alkyl chain.

2.3 General Synthetic Strategy

The general strategy for the synthesis of the target compounds was similar to that previously reported,[131] and is shown in Scheme 2.1. Reaction of a phenylhydrazine with an acetophenone gives a phenylhydrazone, which through Fischer indole synthesis undergoes acid catalysed rearrangement with the elimination of ammonia, producing the indole skeleton.[157] 2-Phenylindoles can be acylated with oxalyl chloride to give the corresponding indol-3-ylglyoxyl chloride. This is a key intermediate in the synthesis which can then undergo an S_N2 reaction with an array of dialkylamines to give the final *N*,*N*-dialkyl-2-phenylindol-3-ylglyoxylamides.

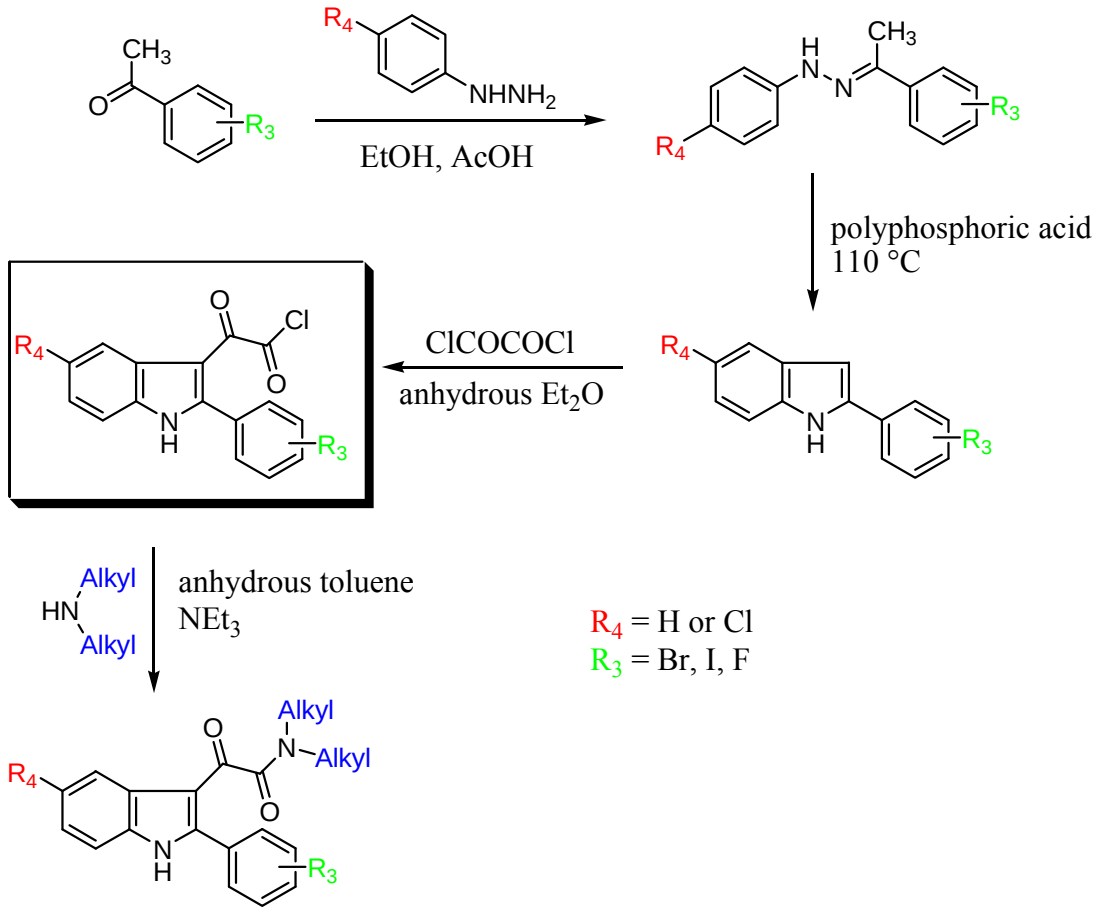

Scheme 2.1 General synthesis of *N*,*N*-dialkyl-2-phenylindol-3-ylglyoxylamides.

2.4 Synthesis of 5-Chloroindol-3-ylglyoxylamide Analogues

2.4.1 Synthesis of Glyoxylyl Chloride Intermediates

The synthetic strategy of the [5-chloro-2-(4-halophenyl)indol-3-yl]glyoxylyl chlorides **[46]** and **[47]** utilises standard Fischer indole chemistry, and is summarised in Scheme 2.2. Surprisingly, the intermediates **[42]-[47]** have not been previously reported. Therefore, reaction of 4-chlorophenylhydrazine hydrochloride with either 4-iodoacetophenone or 4-bromoacetophenone in ethanol at reflux with a catalytic amount of AcOH afforded the phenylhydrazones **[42]** and **[43]** in 54% and 75% yield, respectively. In a typical example, ^{1}H NMR analysis of **[42]** revealed a methyl peak at δ 2.21, a broad NH peak at δ 7.34, and four doublets corresponding to the eight protons of the two phenyl groups. Mass spectra of **[42]** displayed ^{35}Cl M^{+}, and ^{37}Cl M^{+} peaks at 370 and 372. The hydrazones **[42]** and **[43]** were cyclised using polyphosphoric acid at 110 °C to afford indoles **[44]** and **[45]** in 56% and 69% yields, respectively. The ^{1}H NMR spectra of **[44]** revealed the disappearance of the methyl peak of the hydrazone, and the appearance of a singlet at δ 6.92 assigned to H3 of the indole. It also included a doublet of doublets at δ 7.10 assigned to H6 of the indole, coupled to H7 (8.6 Hz) and H4 (2.0 Hz), a doublet at δ 7.39 assigned to H7, coupled to H6, and a doublet at δ 7.57 assigned to H4, coupled to H6.

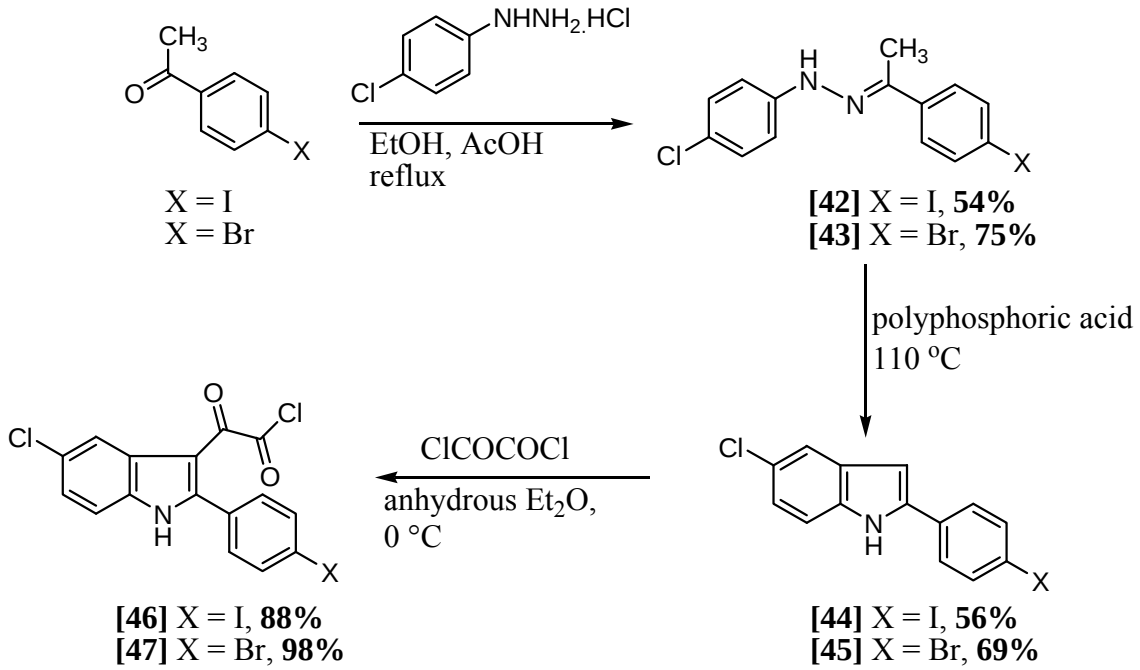

Scheme 2.2 Synthesis of [5-chloro-2-(4-halophenyl)indol-3-yl]glyoxylyl chlorides **[46]** and **[47]**.

The glyoxylyl chloride key intermediates **[46]** and **[47]** were synthesised in 88% and 98% yield by dropwise addition of oxalyl chloride to a partially dissolved mixture of indole, **[44]** and **[45]**, in anhydrous diethyl ether at 0 °C. The ^{1}H NMR spectra of crude **[46]** and **[47]** revealed the absence of the H3 proton peak of the indole. As the acid chlorides were relatively unstable, they were used directly in the subsequent amination reactions without further purification.

2.4.2 Synthesis of *N,N*-Dialkyl-[5-chloro-2-(4-halophenyl)indol-3-yl]glyoxylamides

In a typical amination reaction, dihexylamine was added to the acid chloride **[46]** in anhydrous toluene at 0 °C in the presence of triethylamine. The reaction was stirred at room temperature for 24 h, followed by column chromatography and recrystallisation to afford the glyoxylamide **[48]** in 30% yield. Amination of the acid chloride **[46]** with other dialkylamines afforded compounds **[49]-[51]** (Scheme 2.3). The reactions and outcomes for this series of analogues are summarised in Table 2.1.

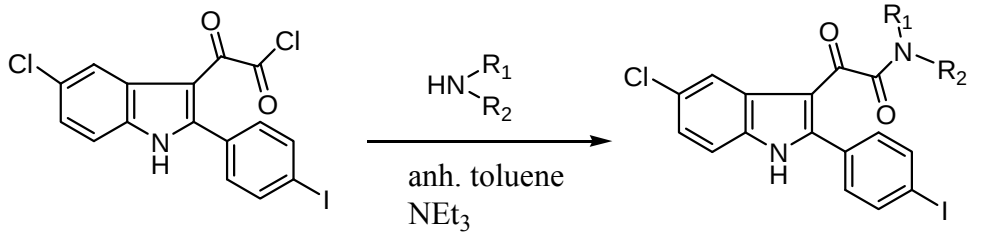

[46]

[48] R_1 and R_2 = hexyl
[49] R_1 and R_2 = propyl
[50] R_1 and R_2 = ethyl
[51] R_1 and R_2 = methyl

Scheme 2.3 Amination of [5-chloro-2-(4-iodophenyl)indol-3-yl]glyoxylyl chloride **[46]**.

Table 2.1 Reaction and purification conditions and yields for compounds **[48]-[51]**.

Amine Reagent	Product	Reaction time (h)	Recrystallisation solvent	Yield (%)
dihexylamine	**[48]**	24	EtOAc: petroleum ether (PE) 1:9	30
di-*n*-propylamine	**[49]**	7	PE (triturated)	57
diethylamine	**[50]**	19	EtOAc: PE 1:1	36
dimethylamine	**[51]**	1	EtOAc: PE 3:7	10

Key ^{1}H and ^{13}C NMR assignments for the target compounds **[48]-[51]** are summarised in Table 2.2. Typically, the two identical alkyl groups were seen as non-equivalent, and therefore two sets of peaks were observed for each CH_2 or CH_3. This may arise from resonance interaction between the lone pair of electrons on nitrogen and the carbonyl group, which interferes with free rotation around the C-N bond. The rate of rotation is slowed to the point that it takes longer than an NMR transition.[158] The low resolution mass spectra for the amides usually showed a weak molecular peak, and a base peak arising from α-cleavage of the amide.

Table 2.2 ^{1}H and ^{13}C NMR alkyl chain peak assignments for compounds **[48]-[51]**.

^{1}H NMR peaks					**^{13}C NMR peaks**
Cpd	**CH_3**	**CH_2**	**NCH_2**	**NCH_3**	
[48]	0.75 (t) 0.88 (t)	1.00 – 1.46 (m, $8CH_2$)	2.95 – 3.08 (m, $2NCH_2$)		15.4 and 15.6 (CH_3) 23.5 and 23.7 (CH_2) 27.2 and 27.9 (CH_2) 28.1 and 29.3 (CH_2) 32.3 and 32.8 (CH_2) 45.4 and 48.9 (NCH_2)
[49]	0.69 (t) 0.78 (t)	1.12 – 1.28 (m) 1.40 – 1.50 (m)	2.95 (t) 3.01 (t)		12.5 and 13.1 (CH_3) 21.6 and 22.8 (CH_2) 47.4 and 50.8 (NCH_2)
[50]	0.83 (t) 1.02 (t)		3.07 (q) 3.15 (q)		12.5 and 14.1 (CH_3) 38.5 and 42.2 (NCH_2)
[51]				2.45 (s) 2.79 (s)	33.7 and 37.4 (NCH_3)

Three amides **[52]-[54]** with bromo substituents attached to the phenyl ring were prepared in 32-59% yield from the acid chloride intermediate **[47]** by reaction with the

corresponding dialkylamine in toluene and triethylamine (Scheme 2.4). The reaction / purification conditions and yields are summarised in Table 2.3.

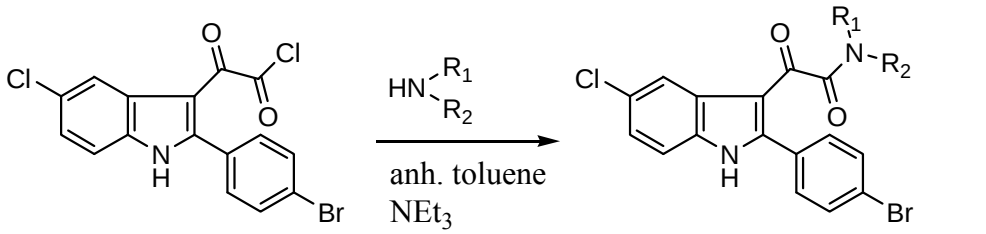

[47]

[52] R_1 and R_2 = hexyl
[53] R_1 and R_2 = propyl
[54] R_1 and R_2 = ethyl

Scheme 2.4 Amination of [5-chloro-2-(4-bromophenyl)indol-3-yl]glyoxylyl chloride **[47]**.

Table 2.3 Reaction and purification conditions and yields for compounds **[52]-[54]**.

Amine Reagent	**Product**	**Reaction time (h)**	**Recrystallisation solvent**	**Yield (%)**
dihexylamine	**[52]**	7	EtOAc / PE 1:9	32
di-*n*-propylamine	**[53]**	24	diethyl ether / PE	53
diethylamine	**[54]**	18	EtOAc: PE 1:1	59

The yields of amides **[48]-[54]** were not optimised, and the varying yields were most likely due to the variable purity of the acid chlorides used in the reaction. The low yield of **[51]** could be due to the short 1 h reaction time and/or due to using dimethylamine in water. Although it was bubbled into the reaction mixture through NaOH pellets, water could have entered the reaction and hydrolysed the acid chloride. This yield would probably be improved considerably if dimethylamine in THF (2M) was used.

The ^{1}H and ^{13}C NMR spectra of the iodinated indol-3-ylglyoxylamides **[48]-[51]** compared to the brominated **[52]-[54]** shared similarities in the indole moiety summarised in Figure 2.5.

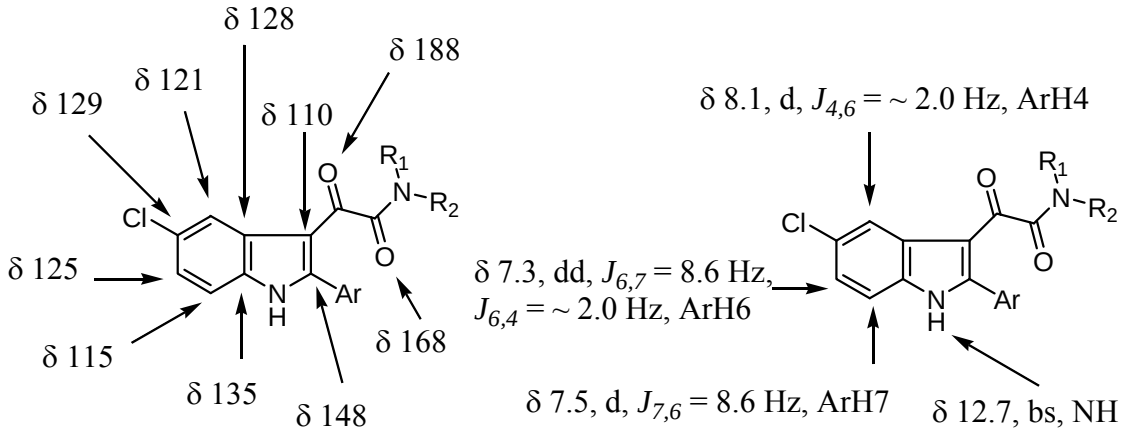

Figure 2.5 ^{1}H and ^{13}C NMR spectra similarities in the indole moiety for indol-3-ylglyoxylamides **[48]-[54]**.

2.5 Synthesis of Indol-3-ylglyoxylamide Analogues

2.5.1 Synthesis of Glyoxylyl Chloride Intermediates

The synthesis of non-chlorinated glyoxylyl chlorides are summarised in Scheme 2.5. Although the indoles **[59]** and **[60]** have been reported, the corresponding indol-3-ylglyoxylchlorides **[61]** and **[62]**, and the subsequent amides have not been previously published.

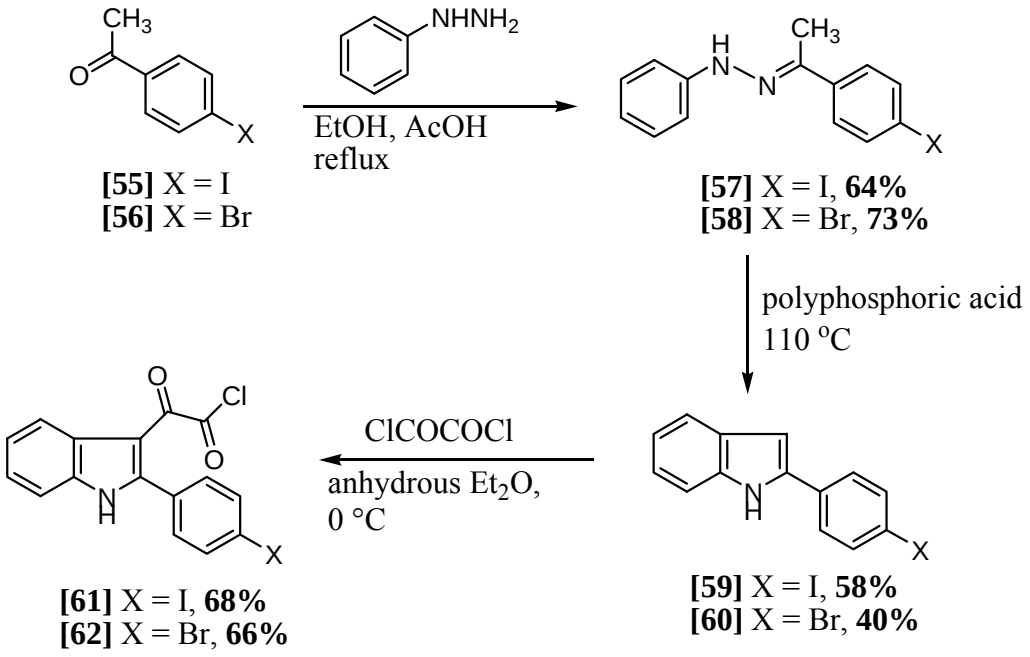

[55] X = I
[56] X = Br

[57] X = I, **64%**
[58] X = Br, **73%**

[59] X = I, **58%**
[60] X = Br, **40%**

[61] X = I, **68%**
[62] X = Br, **66%**

Scheme 2.5 Synthesis of non-chlorinated glyoxylyl chlorides.

The first attempt at the synthesis of 2-(4-iodophenyl)indole **[59]** involved heating 4-iodoacetophenone and phenylhydrazine in polyphosphoric acid (PPA), resulting in a 20% yield. Alternatively, using a two step method, involving the synthesis of the phenylhydrazone **[57]** in 64% yield, followed by cyclisation in 58% yield, the overall yield of indole **[59]** was 37%, which was comparable to that reported.[159]

4-Bromoacetophenone phenylhydrazone **[58]** was synthesised in 73% yield by heating 4-bromoacetophenone and phenylhydrazine in ethanol, with a catalytic amount of glacial AcOH, an improvement on that which did not use AcOH, giving a 44% yield.[160] ^{1}H NMR analysis of **[58]** was not identical to that reported in the literature, although the melting points were similar. The ^{1}H NMR spectra of **[58]** displayed a singlet at δ 2.20, integrating to three protons, assigned to the methyl group. The two doublets, each integrating to two protons, corresponded to the two sets of equivalent protons of the 4-

bromophenyl group. A doublet and two triplets correspond to the other 5 protons of the other phenyl group. The phenylhydrazone **[58]** was then heated to 110 °C in PPA to form the indole **[60]** in 40% yield.

A higher overall yield of indole **[60]** (58% as apposed to 29%) was achieved by heating 4-bromoacetophenone and phenylhydrazine in PPA at 110 °C (Scheme 2.6). The indole **[60]** was spectroscopically identical to that reported in the literature.[161]

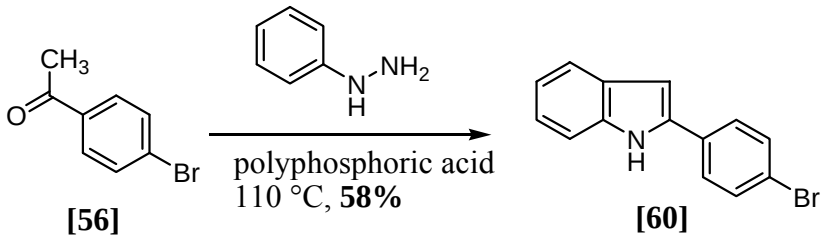

[56] **[60]**

Scheme 2.6 Synthesis of 2-(4-bromophenyl)indole **[60]** via the Fischer indole synthesis.

The glyoxylyl chlorides **[61]** and **[62]** were synthesised in 68% and 66% yields, respectively, by reaction of the indoles **[59]** and **[60]** with oxalyl chloride in anhydrous diethyl ether. The product, which precipitated out of solution, was filtered, washed with ether, and used directly for the next reaction. The ^{1}H NMR spectra of **[61]** and **[62]** showed the disappearance of the indole H3 peak, as expected. The two newly formed carbonyls appeared at δ 168 and 185 in the ^{13}C NMR spectra of **[61]**.

2.5.2 Amination of [2-(4-Halophenyl)indol-3-yl]glyoxylyl Chlorides

Amination of **[61]** was achieved by nucleophilic substitution with dihexylamine, di-*n*-propylamine, diethylamine or dimethylamine to afford **[63]**, **[64]**, **[65]** and **[66]** respectively, and amination of **[62]** with dihexylamine gave **[67]** (Scheme 2.7). The reactions took place in anhydrous toluene at room temperature in the presence of triethylamine, and gave yields between 5 - 46%. The reaction and purification conditions and yields are summarised in Table 2.4.

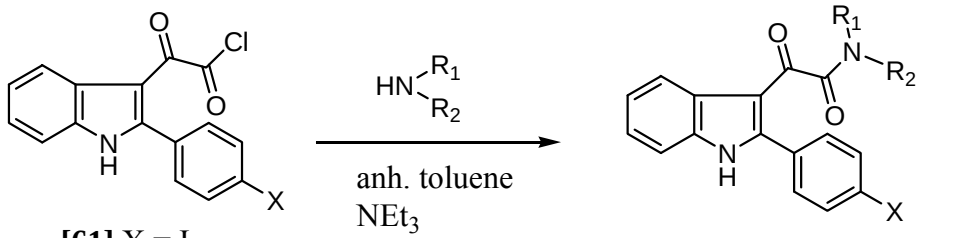

[61] X = I
[62] X = Br

For X = I **[63]** R_1 and R_2 = hexyl
[64] R_1 and R_2 = propyl
[65] R_1 and R_2 = ethyl
[66] R_1 and R_2 = methyl
For X = Br **[67]** R_1 and R_2 = hexyl

Scheme 2.7 Amination of [2-(4-halophenyl)indol-3-yl]glyoxylyl chlorides **[61]-[62]**.

Table 2.4 Reaction and purification conditions and yields for compounds **[63]-[67]**.

Amine Reagent	Product	Reaction time (h)	Recrystallisation solvent	Yield (%)
dihexylamine	**[63]**	18	EtOH / H_2O	32
di-*n*-propylamine	**[64]**	20	EtOAc: PE 3:7	22
diethylamine	**[65]**	3	EtOAc: PE 1:1	40
dimethylamine	**[66]**	1	EtOAc: PE 1:1	5
dihexylamine	**[67]**	24	EtOH / H_2O	46

The ^{1}H and ^{13}C NMR spectra of **[63]-[67]** displayed similarities in the indole region (Figure 2.6) and all compounds showed similar alkyl group peaks to the 5-chloroindol-3-ylglyoxylamides **[48]-[54]**.

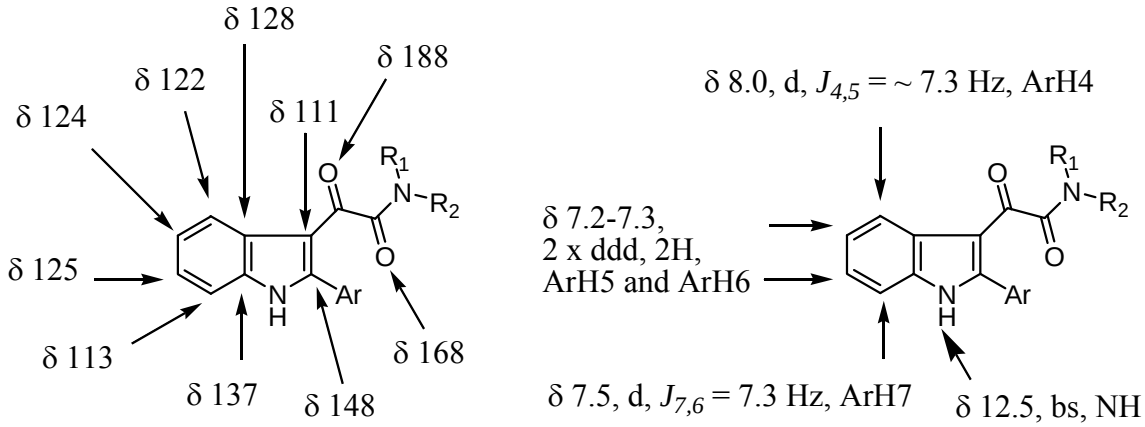

Figure 2.6 ^{1}H and ^{13}C NMR spectra similarities in the indole moiety for indol-3-ylglyoxylamides **[63]-[67]**.

2.6 Synthesis of *meta*-Substituted Indol-3-ylglyoxylamide Analogues

All the previous target compounds have had a bromo or iodo substituent in the *para* position of the phenyl group. To study the effect of a different substitution pattern on PBR affinity, two new derivatives containing a *meta* bromo or iodo substituted phenyl group were prepared. As 3-iodoacetophenone was not commercially available, the synthesis started with the 3-bromoacetophenone. The target bromo compound **[71]** was made, which was then stannylated with a trimethylstannyl group to form compound **[72]**. The trimethylstannyl group was substituted for iodine, to give target compound **[73]**. The complete synthesis is shown in Scheme 2.8.

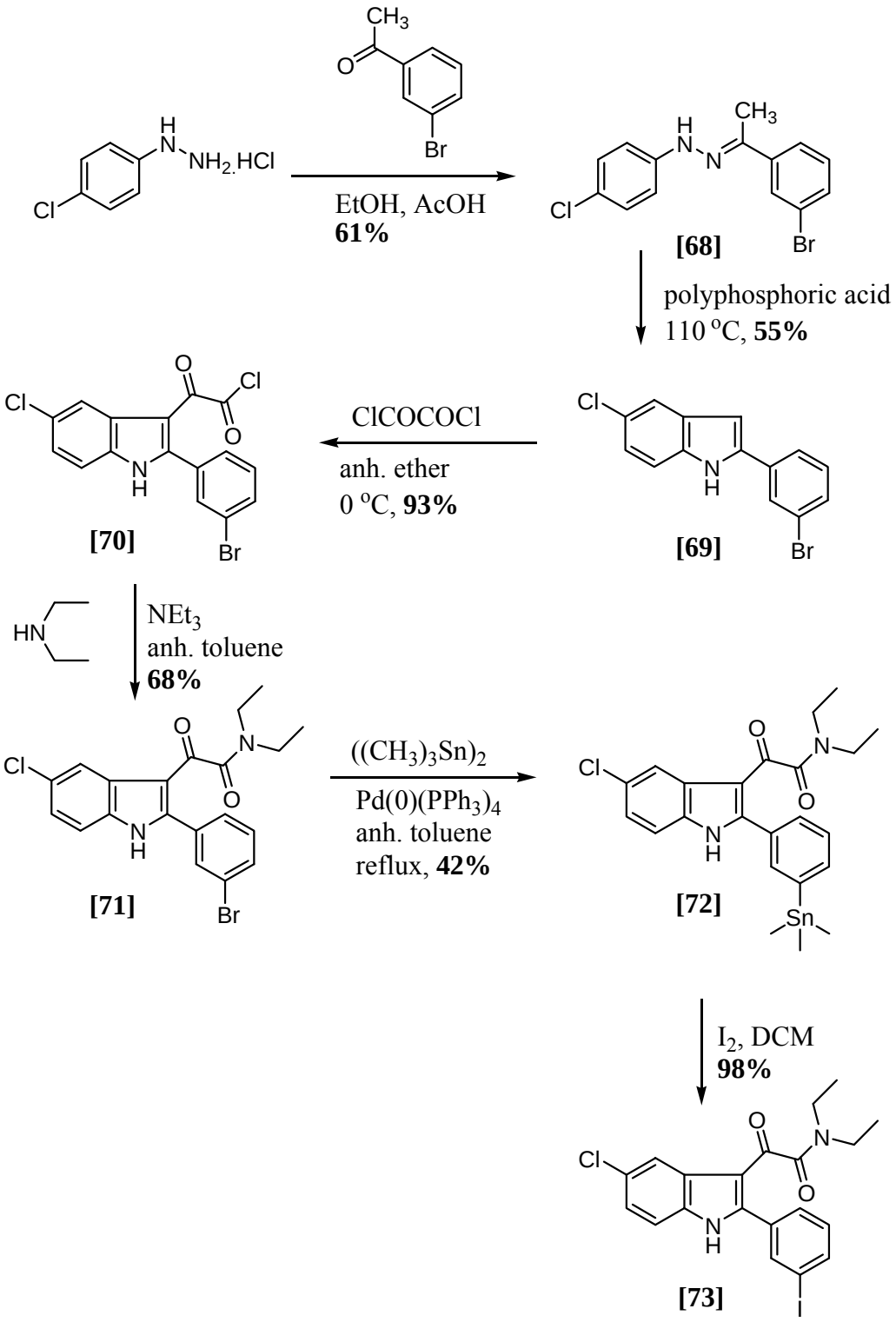

Scheme 2.8 Synthesis of *N,N*-diethyl-[5-chloro-2-(3-iodophenyl)indol-3-yl]glyoxylamide **[73]**.

The phenylhydrazone **[68]** was synthesised in 61% yield by the AcOH catalysed reaction of 4-chlorophenylhydrazine hydrochloride and 3-bromoacetophenone. ^{1}H NMR analysis revealed a singlet at δ 2.24 assigned to the methyl group; and two doublets (δ 7.48 and 7.66) a triplet (δ 7.34), and a singlet (δ 7.92) in the aromatic region of the spectra, a typical *meta* substitution pattern. A multiplet at δ 7.20-7.28 was assigned to the 4 aromatic protons of the 4-chlorophenyl group. The indole **[69]** was formed by cyclisation of **[68]** in PPA in 55% yield, confirmed by the loss of the methyl group peak in the ^{1}H NMR spectra. The indole was acylated with oxalyl chloride to give **[70]** in 93% yield, which was subsequently aminated with diethylamine in 68% yield to form the final bromo compound **[71]**. ^{1}H NMR spectra of **[71]** showed the addition of two CH_3 triplets (δ 0.84 and 1.04) and two NCH_2 quartets (δ 3.07 and 3.18) corresponding to the new diethylamide moiety. The bromo analogue **[71]** was stannylated with hexamethylditin, catalysed by palladium tetrakistriphenylphosphine in anhydrous toluene at reflux, to give the trimethylstannane **[72]** in 42% yield. ^{1}H NMR spectra analysis of **[72]** displayed a singlet at δ 0.36 integrating to the nine protons of the trimethyltin group. The mass spectra of **[72]** displayed M-1 peaks at *m/z* 521, 519, 518, 517, 516, 515, 514, and 513, corresponding to the combined isotope peaks of Sn[1] and Cl. The stannane **[72]** was iodinated in 98% yield by an iododestannylation reaction using I_2 in DCM to give **[73]**. The ^{1}H NMR spectra of **[73]** revealed the disappearance of the singlet of the trimethyltin group. Mass spectrometry (ES^-) revealed a base peak at *m/z* 479 assigned to the M-1 molecular peak.

[1] Tin has 7 isotopes of intensity larger than 1% (116, 117, 118, 119, 120, 122, and 124). ^{120}Sn and ^{118}Sn are the most abundant, with 24.2 and 32.6% abundance.

2.7 Synthesis of 2-(4-Fluorophenyl)indol-3-ylglyoxylamide Analogue

The synthetic scheme for target compound **[41]**, with the iodo attached to an alkyl chain, is summarised in Scheme 2.9. 2-(4-Fluorophenyl)indole **[74]** was prepared in 56% yield by reaction of 4-fluoroacetophenone and phenylhydrazine in PPA at 100-110 °C, and was spectroscopically identical to that recorded in the literature.[162] The indole **[74]** was acylated with oxalyl chloride in 60% yield to give **[75]**, followed by amination using *N*-methylpropargyl amine in 56% yield to give **[76]**. The ^{1}H NMR spectra revealed rotamers of **[76]** in a 1:1.8 ratio, displaying singlets at δ 2.56 and δ 2.87 assigned to the NCH_3 group, and doublets at δ 3.87 and δ 4.08 assigned to the NCH_2 group. Doublet of doublets at δ 3.26 and δ 3.36 were assigned to the alkyne CH. Characteristic ^{1}H-^{19}F and ^{13}C-^{19}F heteronuclear coupling was observed in the aromatic regions of the ^{1}H and ^{13}C NMR of **[74]-[76]**.

Compound **[76]** was tested for PBR binding affinity (see Section 2.8) before continuing on with the synthetic scheme, and it was found to have lower binding affinity than expected. Therefore, the synthesis of **[41]** was not continued. The next step would have involved radical reaction hydrostannylation of the alkyne, to form the vinyl stannane **[77]**. Reaction of the stannane with iodine or $Na^{123}I$ would have formed the iodinated or radioiodinated target compound **[41]**.

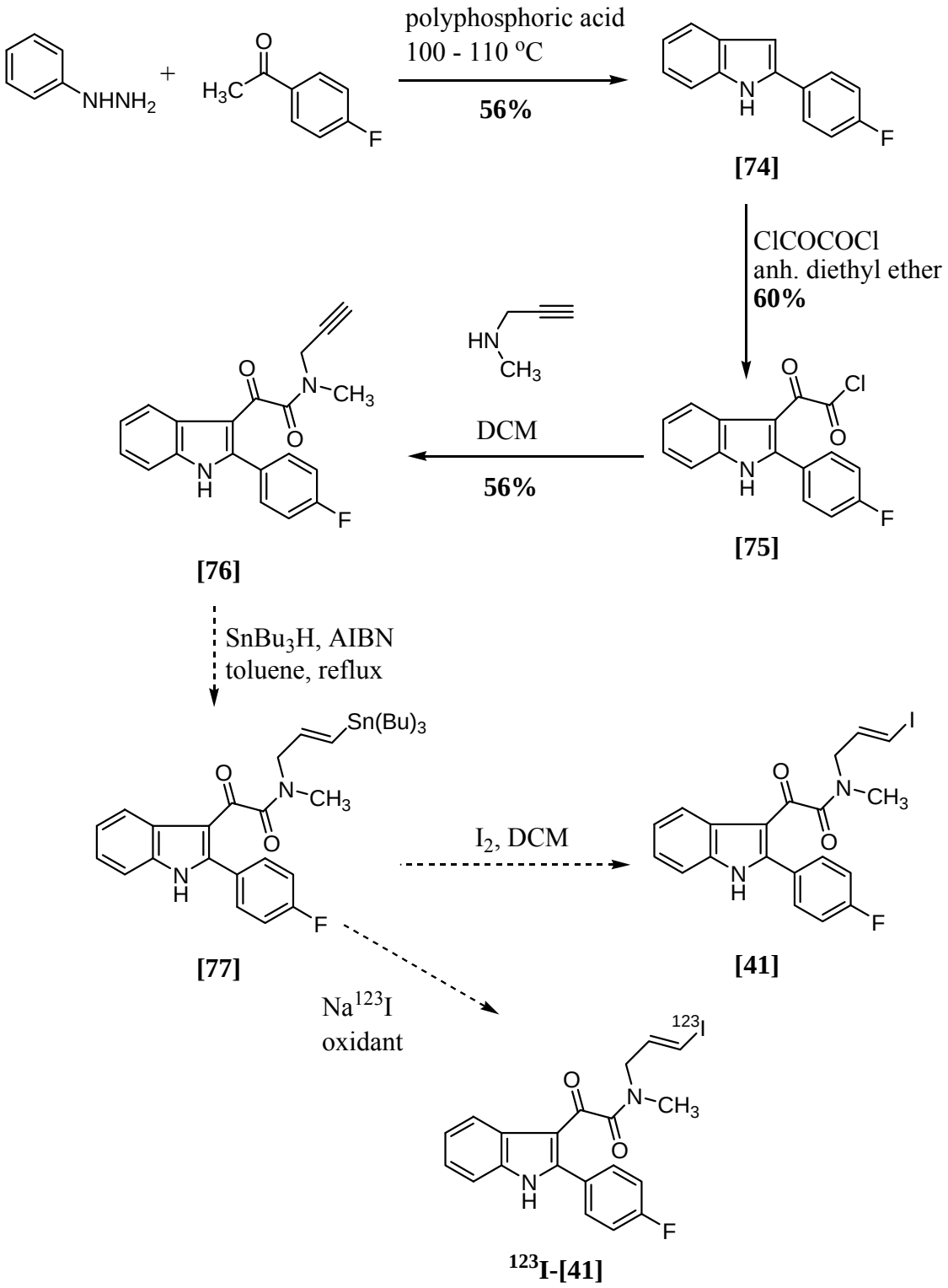

Scheme 2.9 Proposed synthetic scheme for the synthesis of *N*-((*E*)-3-iodoallyl-*N*-methyl-2-(4-fluorophenyl)indol-3-ylglyoxylamide **[41]**.

2.8 *In Vitro* Binding of *N,N*-Dialkyl-2-phenylindol-3-ylglyoxylamides

The *in vitro* binding affinities (IC_{50}) for all compounds for the PBR were determined by measuring the displacement of [^{3}H]PK11195 bound to rat kidney mitochondrial membranes.[163] To determine the selectivity of the compounds for PBR versus CBR, CBR binding affinities were determined using [^{3}H]flumazenil on rat cortical membranes. The average disintegrations per minute (dpm) were calculated for each concentration of test compound, non-specific binding, total binding and total activity, and entered into a computer program called Kell Radioligand. The program used a non-linear least squares fitting method to fit the data to a sigmoid curve, which could then be used to estimate the IC_{50} value. Figure 2.7 is an example of the fitted sigmoid curve the program generates. The IC_{50} values for the compounds are shown in Table 2.5.

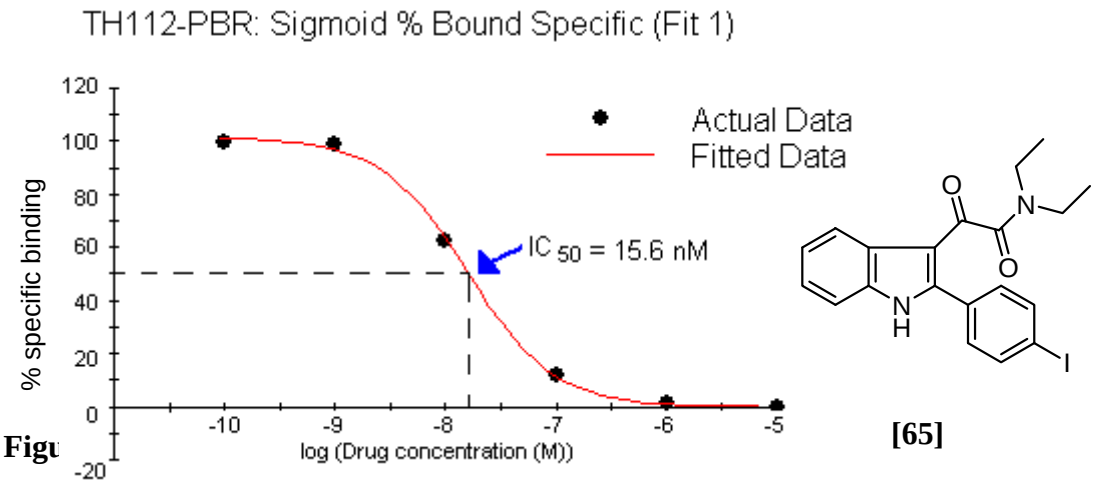

Figu **[65]**

[65].

Table 2.5 PBR and CBR binding affinities (IC_{50}) of halogenated indolglyoxylamides.

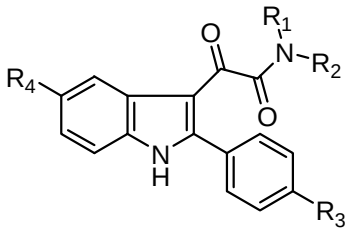

Compd	R_1	R_2	R_3	R_4	Log *P*	PBR IC_{50} (nM) [a]	CBR IC_{50} (nM) [b]
[48]	hexyl	hexyl	4-I	Cl	> 6	169 ± 35	18786 ± 1634
[49]	propyl	propyl	4-I	Cl	4.71 ± 0.19	37.4 ± 6.1	16156 ± 579
[50]	ethyl	ethyl	4-I	Cl	4.00 ± 0.16	8.23 ± 2.2	15652 ± 45
[51]	methyl	methyl	4-I	Cl	3.36 ± 0.13	17.5 ± 4.3	10146 ± 1967
[63]	hexyl	hexyl	4-I	H	> 6	115 ± 22	13803 ± 137
[64]	propyl	propyl	4-I	H	4.00 ± 0.16	43.6 ± 1.8	14662 ± 127
[65]	ethyl	ethyl	4-I	H	3.27 ± 0.13	19.1 ± 2.5	13197 ± 2975
[66]	methyl	methyl	4-I	H	2.69 ± 0.11	618 ± 39	5939 ± 815
[52]	hexyl	hexyl	4-Br	Cl	> 6	138 ± 35	13115 ± 3212
[53]	propyl	propyl	4-Br	Cl	4.56 ± 0.18	16.7 ± 4.7	10463 ± 2817
[54]	ethyl	ethyl	4-Br	Cl	3.89 ± 0.15	7.86 ± 1.2	11045 ± 1909
[67]	hexyl	hexyl	4-Br	H	> 6	54.7 ± 22.6	16348 ± 716
[71]	ethyl	ethyl	3-Br	Cl	3.95 ± 0.12	14.5 ± 6.8	> 5000
[73]	ethyl	ethyl	3-I	Cl	4.08 ± 0.13	15.4 ± 5.6	> 3000
[76]	methyl	CH_2CCH	4-F	H	2.34 ± 0.07	139 ± 38	> 5000
PK11195						3.7 ± 1.2	> 1000

(a) The concentration of tested compounds that inhibited [^{3}H]PK11195 binding to rat kidney mitochondrial membranes (IC_{50}) by 50% was determined with six concentrations of the test compounds, each performed in triplicate. (b) The concentration of tested compounds that inhibited [^{3}H]flumazenil binding to rat cortex (IC_{50}) by 50% was determined with six concentrations of the test compounds, each performed in triplicate. IC_{50} values are the average of three determinations.

The compounds examined displayed a medium to high affinity for the PBR, ranging from 7.86 nM to 618 nM. All compounds had high selectivity for PBR over CBR, with most CBR IC_{50} > 5000 nM. The effects of chemical modification to groups R_1 to R_4 on the binding to PBR was studied, including the length of the alkyl chains (R_1 and R_2), the presence of a chloro substituent on position 5 of the indole (R_4), and halogen substitution (bromo or iodo) on the phenyl ring (R_3). The most potent ligands for the PBR were compounds **[50]** and **[54]**, both displaying IC_{50} of <10 nM. Decreasing the length of the alkyl chains from hexyl to propyl to ethyl, increased the binding affinity for the PBR. However, compounds with R_1 and R_2 as methyl groups had a lower affinity than the compounds with ethyl groups. The compounds with a bromo substituent on R_3, **[52]-[54]** and **[67]**, had higher PBR affinities than their respective iodo analogues **[48]-[50]**, and **[63]**. This suggests that the smaller the halogen on R_3, the better the binding affinity. Although no direct comparison can be made, compounds reported previously[131] with smaller halogen (fluoro and chloro) substituents on R_3 appeared to have a higher PBR binding affinity than compounds presented here. It was reported that the optimum alkyl chain length (R_1 and R_2) for these compounds without a chloro substituent on R_4 were hexyl groups, whereas with the chloro substituent, the optimum length was propyl.[131] In this work it was found that brominated and iodinated compounds with hexyl groups had the lowest affinities, with and without a chloro substituent. It was also found that affinities increased with the addition of a chloro substituent in compounds containing propyl, ethyl or methyl groups. Compounds **[63]** and **[67]** containing hexyl groups showed higher PBR affinity than compounds **[48]** and **[52]** with a chloro group in the R_4. This suggests that it is more difficult to accommodate the sterically more demanding hexyl groups on molecules with R_4 = Cl than in compounds with R_4 = H, bearing propyl, ethyl or methyl groups, suggesting different molecular orientations are

possible. Compounds **[71]** and **[73]** differed from the other compounds by having bromine and iodine respectively on the *meta* position of the phenyl ring. Compounds **[71]** and **[73]** had PBR binding affinities of 15.4 and 14.5 nM, respectively, lower than that of *para*-substituted analogues **[50]** and **[54]** (8.23 and 7.86 nM, respectively), suggesting that *para*-substitution is preferred for PBR binding. The *para*-fluorinated analogue **[76]** had two different groups on the amide, a methyl and a propargyl ($CH_2C{\equiv}CH$) group. Compound **[76]** displayed a PBR IC_{50} of 139 nM. This suggested that for compounds with a smaller halogen on position R_3, longer alkyl chains are needed to fill the binding pocket.

2.9 Lipophilicity Estimations

The lipophilicity of each compound was examined by determination of the log $P_{7.5}$ value using a HPLC method.[164] The lipophilicities were determined by comparing HPLC retention times of test compounds with retention times of standards having known log *P* values. All compounds were subjected to lipophilicity measurements to gauge blood brain barrier permeability. The log *P* values are shown in Table 2.5. As expected the presence of bulky alkyl groups (R_1 and R_2) greatly influenced the overall lipophilicity of the molecules resulting in compounds with hexyl groups **[48]**, **[63]**, **[52]**, and **[67]** having log *P* values greater than 6 and molecules with propyl groups **[49]**, **[64]**, **[53]** greater than 4. In addition, incorporating a chloro substituent on R_4 increased the log *P* values from 3.27 in **[65]** and 2.69 in **[66]** to 4.00 in **[50]** and 3.36 in **[51]** respectively. Iodinated compounds had higher log *P* values than their brominated analogues. The presence of small alkyl groups such as ethyl and methyl in the R_1 and R_2 positions and hydrogen in the R_4 positions can deliver compounds with log *P* values

between 2 and 4. Compounds with log *P* of between 3 and 4 showed high PBR affinity, while compounds with log *P* greater than 6 or less than 3, showed lower affinities.

2.10 Comparison with Similar New Indolylglyoxylamides

Subsequent to the publication of the results of the present study,[165] another series of these ligands were synthesised by others, with the aim of radiolabelling with ^{123}I or ^{18}F for SPECT and PET imaging respectively.[166] The effect of different halogens (F, Cl, I) in different positions (*ortho*, *meta*, *para*) on the phenyl ring was investigated. Compounds with fluorinated or iodinated pyridine groups on position 2 of the indole were also synthesised and tested for PBR affinity (Table 2.6). The binding affinity results showed that increasing the size of the halogen from fluorine to chlorine to iodine, decreased the PBR binding affinity. This agrees with our results, which showed that bromo substituted compounds had higher affinities than the larger iodo substituted derivatives. The results also agreed that when a large iodine was placed on the phenyl ring, binding affinity increased with the decreasing size of the alkyl chains (hexyl < butyl < ethyl). It was found that the *meta*-iodo substituted compounds displayed higher binding affinity than *para* and *ortho* substituted compounds. Replacement of the 3'-iodophenyl group (Entry 9) with a 6-iodo-2-pyridinyl moiety (Entry 16) did not significantly improve the binding affinity.

Table 2.6 PBR K_i values of similar new indolylgloxylamides.[166]

Please see print copy for Table 2.6

2.11 Conclusion

Fifteen new halogenated *N*,*N*-dialkyl-2-phenylindol-3-ylglyoxylamides were synthesised and an SAR was undertaken. The SAR was based on the most likely 3D structures of the compounds and key differences correlated with the measured binding affinities. The length of the alkyl group for optimal PBR binding affinity was the ethyl group, with binding affinity decreasing from ethyl to propyl to hexyl. The brominated compounds had higher PBR affinity than their iodo analogues, and a chloro on position 5 of the indole was also beneficial for PBR binding. *Para*-substitution was preferred over *meta*-substitution of a bromo or iodo substituent on the phenyl ring. Most of the compounds showed high affinity and selectivity for PBR, proving this class of compounds to be appropriate for potential radiolabelling with ^{123}I. In Chapter 5, the radiolabelling of the most potent compound, **[50]**, will be discussed, along with the *in vivo* evaluation of the radioiodinated compound in rats.

3 Synthesis of 2-Arylpyrazolo[1,5-*a*]-pyrimidin-3-yl Acetamides

3.1 2-Arylpyrazolo[1,5-*a*]pyrimidin-3-yl Acetamides

The second class of iodinated compounds chosen for SAR investigation, with the aim of finding a high affinity compound for potential radiolabelling with ^{123}I, was the previously developed 2-arylpyrazolo[1,5-*a*]pyrimidin-3-yl acetamides **[17]**.[117,118] The reported compounds, with structures similar to alpidem **[7]**, were found to be potent and selective PBR ligands. The structure of alpidem and the basic structure of the derivatives are shown in Figure 3.1.

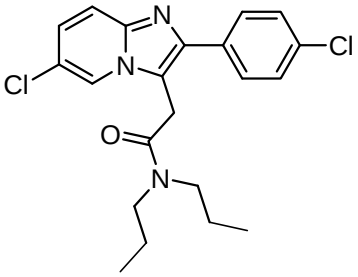

alpidem **[7]**

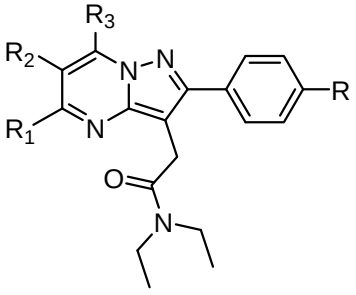

[17]

Figure 3.1 Basic structure of alpidem **[7]** and 2-arylpyrazolo[1,5-*a*]pyrimidin-3-yl acetamide derivatives **[17]**.

Previous studies have shown that modification of the R, R_1, R_2 and R_3 functionalities lead to compounds displaying high affinity and selectivity for PBR, with the highest affinity compound **[78]** having a K_i of 0.8 nM (Table 3.1).[117] The substituents on the pyrimidine group appeared to be important in selectivity of PBR over CBR, with methyl

moieties at both R_1 and R_3 favouring PBR over CBR binding. Some of the high affinity ligands were tested for steroid biosynthesis in C6 glioma rat cells, and were found to increase pregnenolone production, however, there was no correlation between PBR affinity and steroidogenic activity. More recently, the synthesis and binding studies of 2-phenylpyrazolo[1,5-*a*]pyrimidin-3-yl acetamides (Figure 3.2) have been reported, with focus being placed on differing substituents at the 3-position.[118]

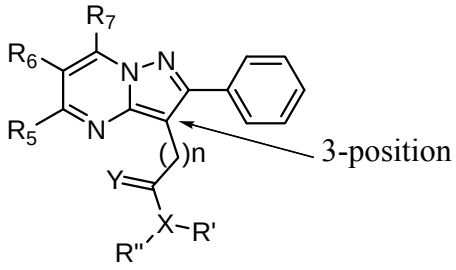

Figure 3.2 Structure of 2-phenylpyrazolo[1,5-*a*]pyrimidinyl-3-yl acetamides.

Alkyl chain length on the amide nitrogen was important for binding affinity, with compound **[81]** possessing *n*-propyl groups, showing higher binding affinities than compounds **[79]**, **[80]**, and **[82]** with methyl, ethyl, or butyl groups respectively (Table 3.1). Compounds with branched alkyl chains, such as compound **[83]** with isopropyl groups were found to be unfavourable. Dialkyl substitution was preferred over monosubstitution. Compound **[84]**, with an ethyl and a phenyl group on the amide gave an excellent binding affinity of 0.8 nM. Removal of the linker between the amide and the pyrazole group resulted in loss of affinity, whilst changing the acetamide to a thioacetamide only slightly reduced the affinity.

Table 3.1 PBR binding affinities of selected 2-arylpyrazolo[1,5-*a*]pyrimidinyl-3-yl acetamides.[117,118]

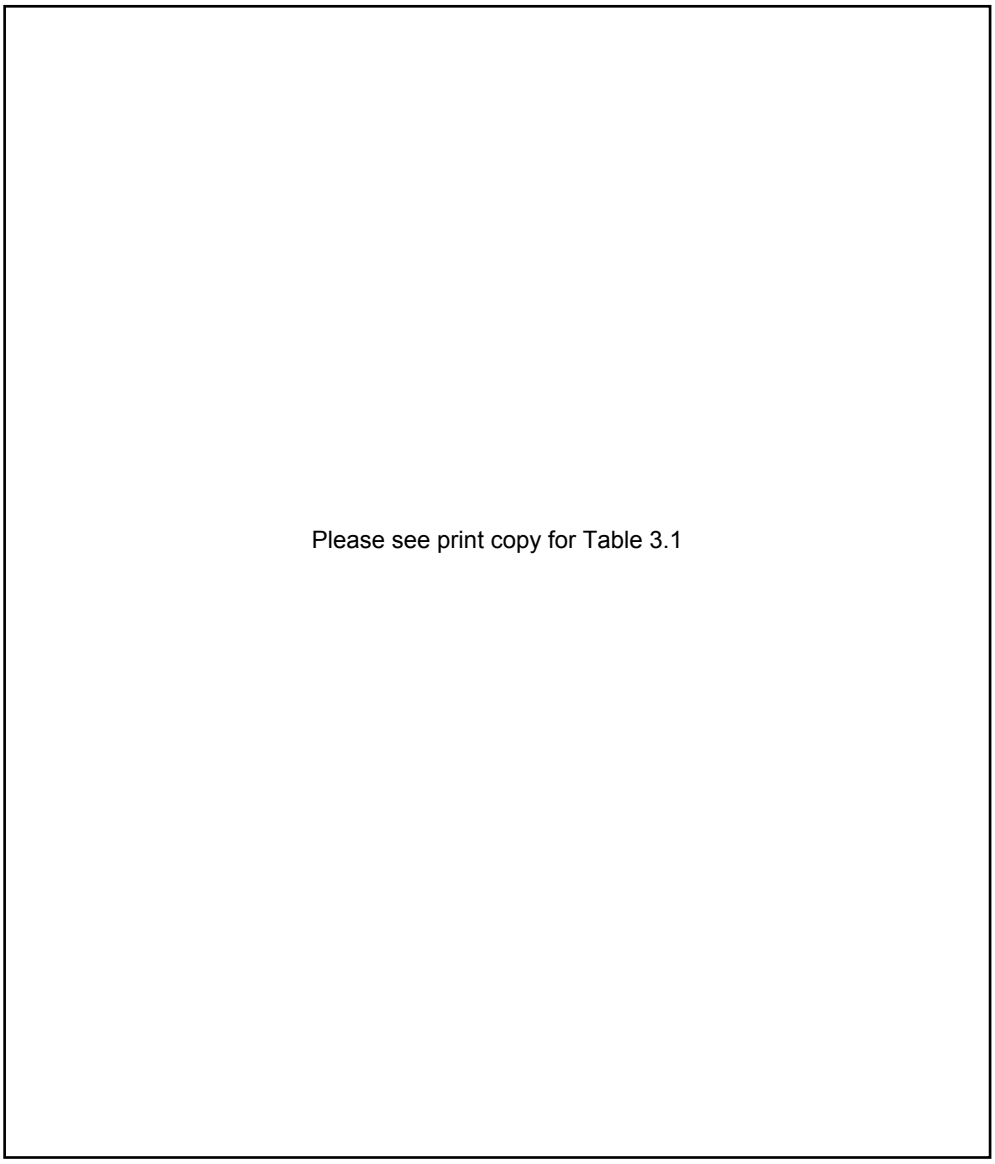

3.2 Rationale

The 2-arylpyrazolo[1,5-*a*]pyrimidinyl-3-yl acetamides have high affinity and selectivity for PBR. There have been no reported iodinated analogues and none of these compounds have been previously radiolabelled with ^{123}I. One aim of this project was to synthesise potent and selective iodinated compounds for PBR for possible radiolabelling with ^{123}I. Comparing structures in Table 3.1, it was observed that the binding affinity for PBR was higher for the compound with the larger halogen on position R (2.4 nM for chlorine **[85]**, as apposed to 9.2 nM for fluorine **[86]**). Based on this observation, it was thought by increasing the size of the halogen to an iodine atom, affinity for the PBR would be improved. Compound **[87]**, with a methoxy substituent on position R, had a PBR K_i of 4.7 nM, suggesting that the PBR will be able to accommodate an iodine atom in position R, as an iodine atom is roughly the same size as a methoxy group. Hence, the synthesis of new iodinated 2-arylpyrazolo[1,5-*a*]pyrimidinyl-3-yl acetamides was attempted.

3.3 General Synthetic Strategy

The synthesis of 2-phenylpyrazolo[1,5-*a*]pyrimidinyl-3-yl acetamides has been reported in the literature,[117] however no iodinated compounds were synthesised. The general synthetic scheme for the synthesis of new iodinated compounds is shown in Scheme 3.1.

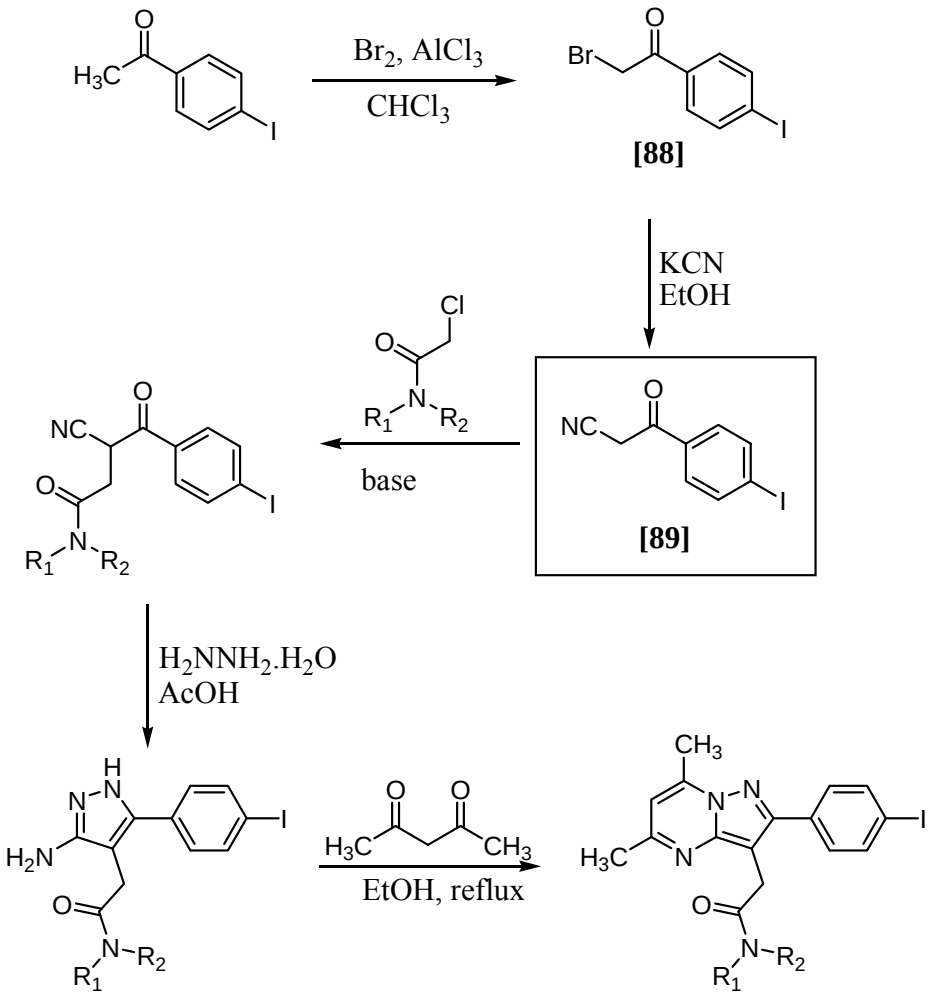

Scheme 3.1 General synthetic scheme for synthesis of 2-arylpyrazolo[1,5-*a*]pyrimidin-3-ylacetamides.

The target compounds have an iodine atom placed on the phenyl ring, and different lengths of alkyl chains on the amide. In order to find the optimum alkyl chain length for PBR binding, target molecules for this chapter include dimethyl- **[90]**, diethyl- **[91]** and dipropyl- **[92]** acetamides (Figure 3.3).

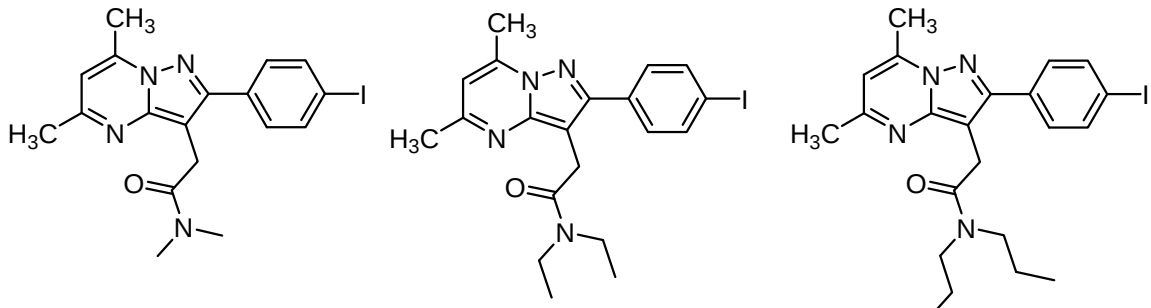

[90] **[91]** **[92]**

Figure 3.3 Target iodinated 2-arylpyrazolo[1,5-*a*]pyrimidin-3-yl acetamides.

4-Iodobenzoylacetonitrile **[89]** can easily be prepared via bromination of 4-iodoacetophenone, followed by cyanide displacement upon the known phenacyl bromide **[88]**. A base added to the benzoylacetonitrile **[89]** deprotonates the activated methylene group, which when reacted with different 2-chloroacetamides gives the corresponding butanamides through an S_N2 reaction. Subsequent reaction with hydrazine hydrate in acid results in cyclisation to form the 3-aminopyrazole ring. Condensation of the 3-aminopyrazole with the dielectrophile, pentane-2,4-dione gives the target pyrazolo[1,5-*a*]pyrimidines.

3.4 Synthesis of 4-Iodobenzoylacetonitrile Intermediate

The one-step synthesis of 4-iodobenzoylacetonitrile **[89]** from 4-iodobenzoylchloride has been described in a yield of only 20%.[167] To improve on this outcome, the synthesis of **[89]** was achieved in two steps from the commercially available 4-iodoacetophenone (Scheme 3.2). Bromination of 4-iodoacetophenone using bromine and $AlCl_3$ in $CHCl_3$ gave **[88]** in 82% yield, compared to the reported 76%.[168] Nucleophilic substitution with

KCN gave the benzoylacetonitrile **[89]** in quantitative yield, and was spectroscopically identical to that reported.[167]

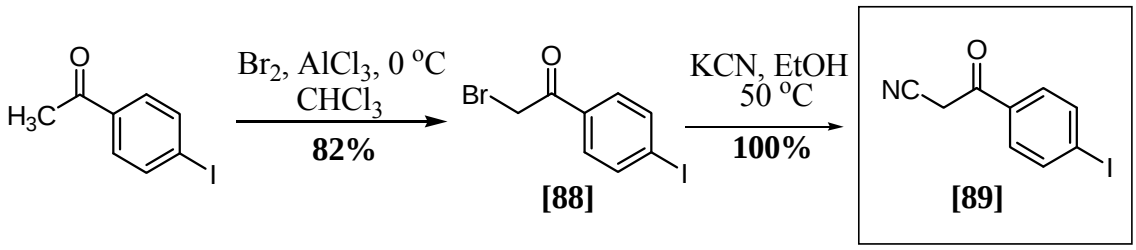

Scheme 3.2 Synthesis of key intermediate 4-iodobenzoylacetonitrile **[89]**.

The reagents, 2-chloro-*N*,*N*-di-*n*-propylacetamide **[93]**, and 2-chloro-*N*,*N*-di-*n*-butylacetamide **[94]**, used for reaction with **[89]** to produce the corresponding butanamides, were not commercially available, thus were synthesised in 69% and 39% yield by literature procedure from di-*n*-propylamine or di-*n*-butylamine and chloroacetyl chloride in 20% NaOH and 1,2-dichloroethane at -5 °C.[169]

3.5 Synthesis of Iodinated *N*,*N*-Dialkylbutanamides

The subsequent step in the overall synthetic scheme was the synthesis of the new butanamides **[95]-[98]** from the key intermediate **[89]**. Previously published yields for the synthesis of similar butanamides, using NaOH as the base, were low (~15%) due to the production of tars which then required extensive purification to isolate the purified products.[117] The synthesis of butanamides **[95]-[98]** using potassium carbonate with a phase transfer catalyst, gave higher yields than that obtained for similar butanamides in the literature. Therefore, reaction of 4-iodobenzoylacetonitrile **[89]** and the appropriate 2-chloro-*N*,*N*-dialkylacetamide, in the presence of the tetrabutylammonium iodide (TBAI), K_2CO_3 and KI, in anhydrous DMF yielded the butanamides **[95]-[98]** in 57-

69% yield (Scheme 3.3). In this reaction, a proton is abstracted from the weak CH acid. This deprotonation occurs on the surface of the K_2CO_3.[170] The TBAI provides a source of lipophilic cations which can undergo ion exchange to produce a lipophilic ion pair in order to bring the anion into the organic phase for reaction.[171]

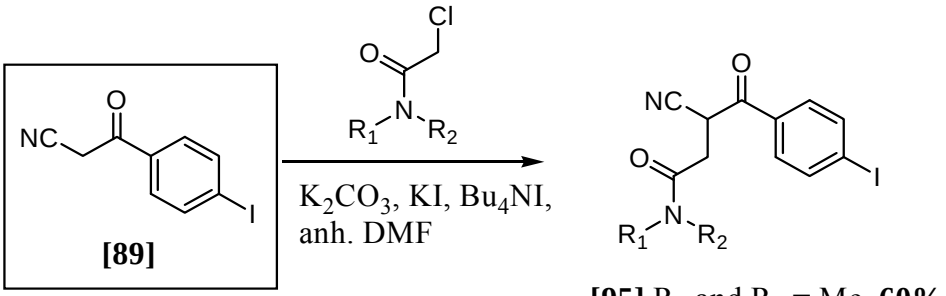

[95] R_1 and R_2 = Me, **60%**
[96] R_1 and R_2 = Et, **57%**
[97] R_1 and R_2 = Pr, **69%**
[98] R_1 and R_2 = Bu, **59%**

Scheme 3.3 Synthesis of butanamides **[95]-[98]**.

The butanamides **[95]-[98]** contain a stereogenic carbon, and hence the adjacent methylene protons are diastereotopic (Figure 3.4). Therefore in the ^{1}H NMR spectra, two signals for the two diastereotopic protons, and another signal for the proton on the chiral carbon are observed. The ^{1}H NMR spectra of **[95]** showed a doublet of doublets at δ 4.91 with *J* values of 9.4 and 4.3 Hz assigned to H_A (Figure 3.4). Signals at δ 2.90 (*J* = 16.4, 4.2 Hz) and δ 3.40 (*J* = 16.4, 9.4 Hz) were assigned to the diastereotopic protons H_B and H_C. The coupling constant of 16.4 Hz is characteristic of geminal (two bond) coupling (J_{BC}). The ^{1}H NMR also showed doublets at δ 7.76 and 7.89, typical of a *para*-substituted phenyl group, and singlets at δ 2.92 and 3.07 corresponding to the methyl groups on the amide nitrogen. Similarities between the butanamides **[95]-[98]** in their ^{1}H NMR spectrum assignments are shown in Figure 3.4.

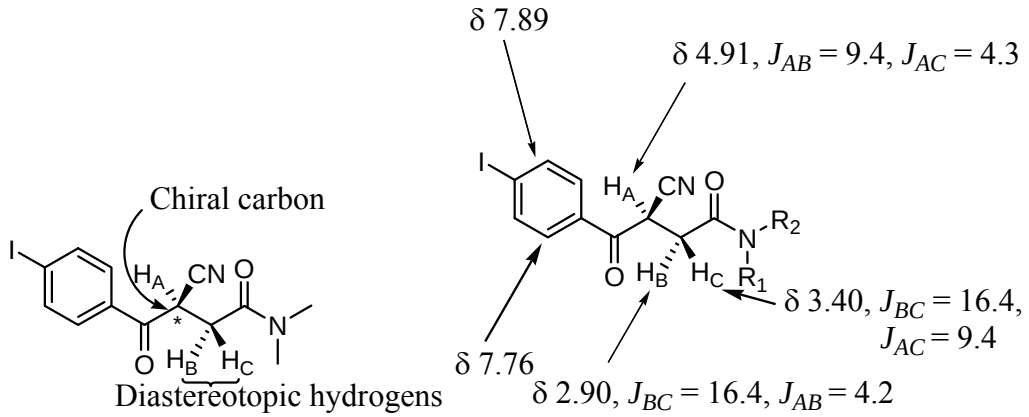

Figure 3.4 ^{1}H NMR spectra assignments of butanamide **[95]**, typical of butanamides **[96]-[98]**.

A minor side product **[99]** observed in 11% yield in these butanamide syntheses was a dialkylated product (Scheme 3.4). The desired reaction would occur, followed by proton abstraction from the activated methylene, leaving an electron which moved to form the alkene and an oxygen anion. O-Alkylation to another molecule of 2-chloro-*N*,*N*-dibutylacetamide gave the dialkylated product **[99]**. The ^{1}H NMR spectra of **[99]** revealed singlets at δ 3.57 and 4.37, each integrating to two protons, assigned to the two $COCH_2$ groups. The 36 protons of the two dibutylamide groups were observed, as well as the doublets at δ 7.27 and 7.78 of the *para*-substituted phenyl ring. In the ^{13}C NMR spectra, the peaks at δ 92.2 and 167.8 were assigned as the alkene carbons, peaks at δ 166.4 and 168.2 were assigned as the carbonyl carbons, and the peaks at δ 32.8 and 67.0 were assigned as the $CO\underline{C}H_2$ and $O\underline{C}H_2CO$ respectively.

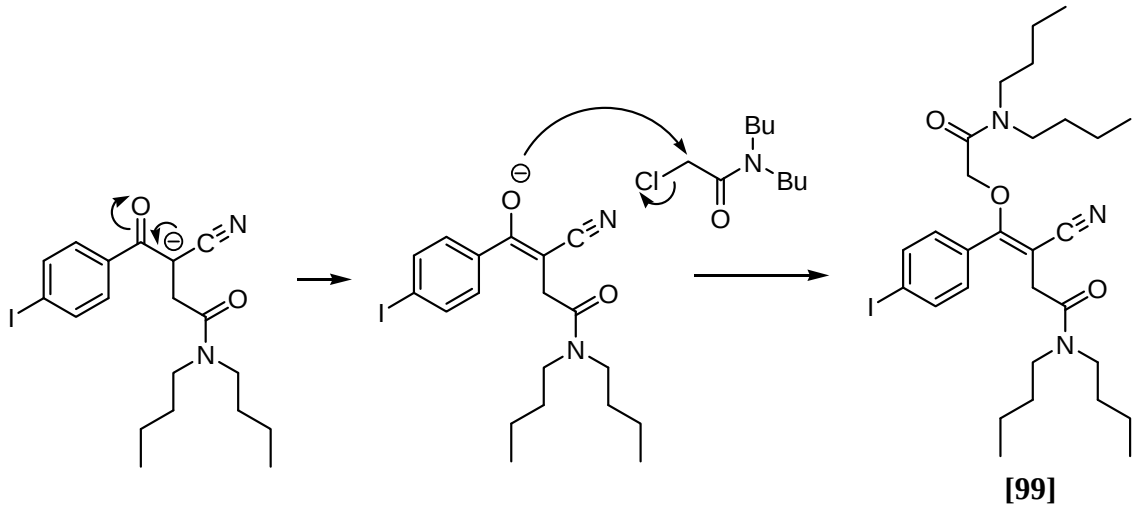

[99]

Scheme 3.4 Mechanism for the synthesis of dialkylated product **[99]**.

3.6 Synthesis of 3-Aminopyrazoles

The butanamide **[96]** was reacted with hydrazine hydrate in ethanol, along with a catalytic amount of AcOH to afford the desired aminopyrazole **[101]** in 26% yield. The diastereotopic CH_2 proton signals in the ^{1}H NMR spectra of **[96]** shifted to δ 3.47, observed as a singlet in the ^{1}H NMR spectra of **[101]**. A broad singlet appeared at δ 5.65, integrating for two protons, was assigned to the NH_2 group. Peaks corresponding to the carbonyl and the cyano carbons of **[96]** were not present in the ^{13}C NMR spectra, which also supported the addition of the hydrazine and cyclisation to form the pyrazole ring. Mass spectrometry revealed an M+1 peak at *m/z* 399, assigned to the molecular ion of **[101]**. A competing side reaction was observed with ethanol, giving an ethyl ester product **[103]** in 50% yield (Scheme 3.5). The ^{1}H NMR spectra of the side product **[103]** revealed the disappearance of the two NCH_2 and CH_3 peaks. One triplet at δ 1.27 integrating to three protons, and one quartet at δ 4.18 integrating to two protons was observed. ^{1}H NMR analysis showed the presence of the diastereotopic protons and the proton on the chiral carbon, indicating that the side product was similar to the starting

material **[96]** and had not formed the pyrazole ring. The ethanol probably acted as a nucleophile to displace the dialkylamine, forming the ethyl ester product **[103]**.

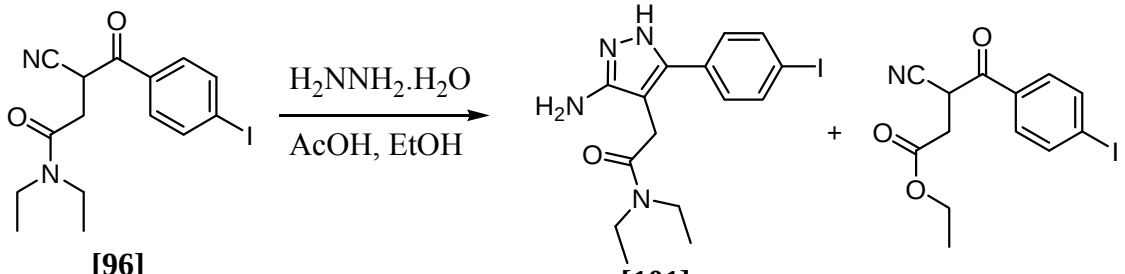

[96] **[101]** **26%** **[103]** **50%**

Scheme 3.5 Reaction of **[96]** with hydrazine hydrate in ethanol.

Optimisation of this reaction was attempted by using THF, a less nucleophilic solvent, resulting in a yield of 68% of **[101]**, with no ethyl ester side product observed. The 3-aminopyrazoles **[100]** and **[102]** were prepared in 50% and 68% yields using THF (Scheme 3.6).

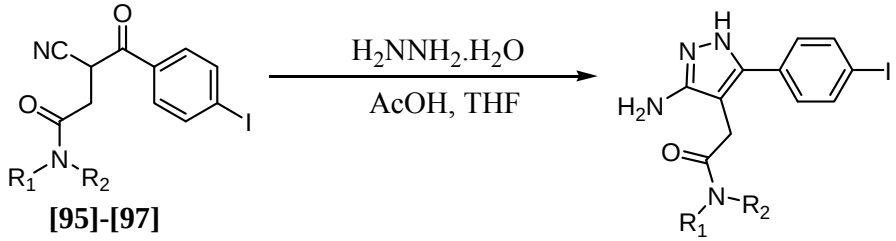

[95]-[97]

[100] R_1 and R_2 = Me, **50%**
[101] R_1 and R_2 = Et, **68%**
[102] R_1 and R_2 = Pr, **68%**

Scheme 3.6 Synthesis of pyrazoles **[100]-[102]**.

3.7 Synthesis of Pyrazolopyrimidines

The final step in the synthesis of the target compounds **[90]-[92]** was the condensation of the pyrazoles **[100]-[102]** with pentane-2,4-dione in ethanol at reflux (Scheme 3.7).

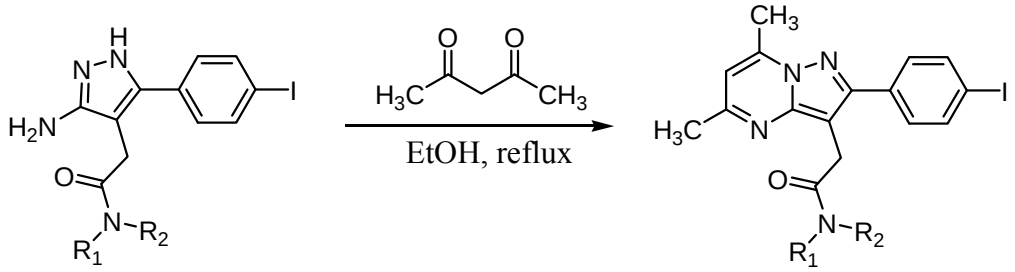

[100]-[102]

[90] R_1 and R_2 = Me, **39%**
[91] R_1 and R_2 = Et, **60%**
[92] R_1 and R_2 = Pr, **26%**

Scheme 3.7 Synthesis of 2-arylpyrazolo[1,5-*a*]pyrimidin-3-yl acetamides **[90]-[92]**.

^{1}H NMR spectra of **[91]** showed the addition of the aromatic CH at δ 6.53 of the newly formed pyrimidine ring, and singlets at δ 2.73 and 2.54 of the two methyl groups on the pyrimidine ring. The disappearance of the NH_2 peak of the pyrazole **[90]** was also observed. The ^{1}H NMR spectra assignments of **[91]** are summarised in Figure 3.5 and are typical of compounds **[90]** and **[92]**.

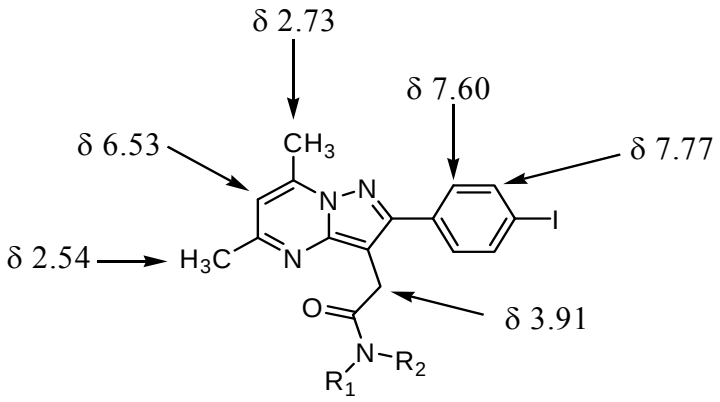

Figure 3.5 ^{1}H NMR assignment of **[91]**, typical of target compounds **[90]-[92]**.

3.8 *In Vitro* Binding of 2-Arylpyrazolo[1,5-*a*]pyrimidin-3-yl Acetamides

The three new iodinated compounds, *N*,*N*-dimethyl-[2-(4-iodophenyl)-5-7-dimethylpyrazolo[1,5-*a*]pyrimidin-3-yl]acetamide **[90]**, *N*,*N*-diethyl-[2-(4-iodophenyl)-5-7-dimethylpyrazolo[1,5-*a*]pyrimidin-3-yl]acetamide **[91]**, and *N*,*N*-dipropyl-[2-(4-iodophenyl)-5-7-dimethylpyrazolo[1,5-*a*]pyrimidin-3-yl]acetamide **[92]** were tested for their *in vitro* binding affinities for PBR and CBR. The binding affinities (IC_{50}) for the PBR were determined by measuring the displacement of [^{3}H]PK11195 bound to rat kidney mitochondrial membranes, as described in Chapter 2. To determine the selectivity of the compounds for PBR versus CBR, CBR binding affinities were determined using [^{3}H]flumazenil on rat cortical membranes, also described in Chapter 2. The binding affinity results along with the log *P* values determined by a HPLC method,[164] are shown in Figure 3.6.

The PBR binding affinities (IC_{50}) of **[90]-[92]** showed a small increase from 17.6 nM, 11.7 nM and 7.9 nM, respectively. All compounds were selective for PBR, showing CBR binding affinities of over 2000 nM. The chain length of the alkyl groups on the amide was important for binding affinity, with **[92]** bearing propyl groups having the highest affinity. The alkyl groups order of decreasing PBR affinity was propyl < ethyl < methyl. A similar literature result showed this same order with structures with a phenyl group instead of 4-iodophenyl group.[118] In that study, the compound with butyl groups **[82]** showed lower affinity than the compound with propyl groups **[81]**. By comparing literature compounds **[79]-[81]** shown in Table 3.1, with compounds **[90]-[92]**, it was observed that iodo substitution on the phenyl ring increased PBR binding for the

compounds with dimethyl and diethyl groups, but lowered PBR binding for the dipropyl compounds.

It would be interesting to investigate if butyl groups or even longer alkyl chains would improve the PBR binding affinity, but due to time constraints, this was not attempted. Determination of the log *P* values of **[90]-[92]** showed that the lipophilicity of the compounds increased with the length of the alkyl chains from methyl to ethyl to propyl with log *P* values of 2.86 in **[90]**, to 3.46 in **[91]**, to 4.22 in **[92]**.

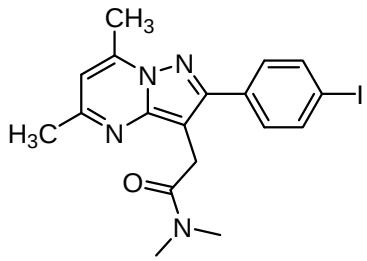

[90]

PBR IC_{50} = 17.6 ± 5.6 nM
CBR IC_{50} > 2000 nM
Log *P* = 2.86 ± 0.09

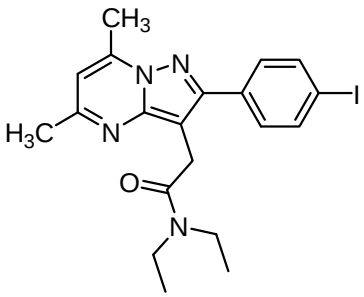

[91]

PBR IC_{50} = 11.7 ± 6.0 nM
CBR IC_{50} > 5000 nM
Log *P* = 3.46 ± 0.11

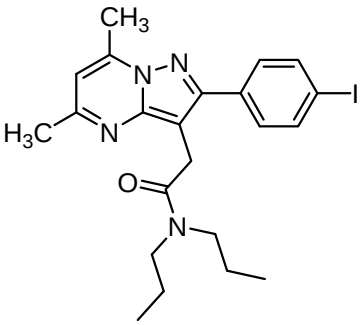

[92]

PBR IC_{50} = 7.9 ± 0.6 nM
CBR IC_{50} > 5000 nM
Log *P* = 4.22 ± 0.13

Figure 3.6 PBR and CBR binding affinities of **[90]-[92]**.

3.9 Conclusions and Future Directions

The general synthesis of 2-arylpyrazolo[1,5-*a*]pyrimidin-3-yl acetamides has been reported in the literature.[117] The literature method for the synthesis for similar butanamides using NaOH as the base resulted in low yields and the production of tars which required extensive purification.[117] The synthesis was improved by using a phase-transfer catalyst with K_2CO_3, giving the product in good yields. The literature method

for the synthesis of the pyrazole ring from the butanamide used hydrazine hydrate in EtOH and a catalytic amount of AcOH.[117] It was found that EtOH acted as a nucleophile and displaced the dialkylamine, creating an ethyl ester side product in 50% yield, and the pyrazole in 26% yield. In order to avoid this side reaction, use of THF as the solvent gave the pyrazole in 68% yield.

Three new iodinated 2-arylpyrazolo[1,5-*a*]pyrimidin-3-yl acetamides were synthesised and their PBR binding affinities were determined. All compounds were found to be potent and selective PBR ligands, with **[92]** having a higher binding affinity (7.9 ± 0.6 nM) than the best iodinated indol-3-ylglyoxylamide from Chapter 2 (**[50]** 8.2 ± 2.2 nM). Future directions would involve the synthesis of analogues with the butyl groups, or even pentyl or hexyl groups, or the synthesis of pyrazolopyrimidines with unsymmetrical amides (eg ethylmethyl or propylethyl). Modifying the position of the iodine to either *ortho* or *meta* substitution could also improve binding. In Chapter 5, the radioiodination of the compound **[91]** will be discussed, along with the *in vivo* evaluation of the radioiodinated compound in rats.[2]

[2] Although **[92]** had a higher PBR binding affinity than **[91]**, compound **[91]** was synthesised and tested before **[92],** and therefore was the best compound of that class at the time, and hence was radiolabelled. Compound **[92]** was not radiolabelled due to time constraints.

4 Synthesis of Pyridopyrrolooxazepines and Pyrrolobenzoxazepines

4.1 Pyrrolobenzothiazepines for the PBR

Extensive research has been conducted, synthesising and testing many pyrrolobenzothiazepines for the PBR (Figure 4.1).[120,122,123] Modifications were made on the substituents on the benzothiazepine ring, the phenyl group, and the groups attached to the oxygen. The compound with the best affinity for PBR (IC_{50} = 2.0 nM) was from structure **[104]** in Figure 4.1 with a chlorine substituent on R′ and a $CON(Et)_2$ group on R″.

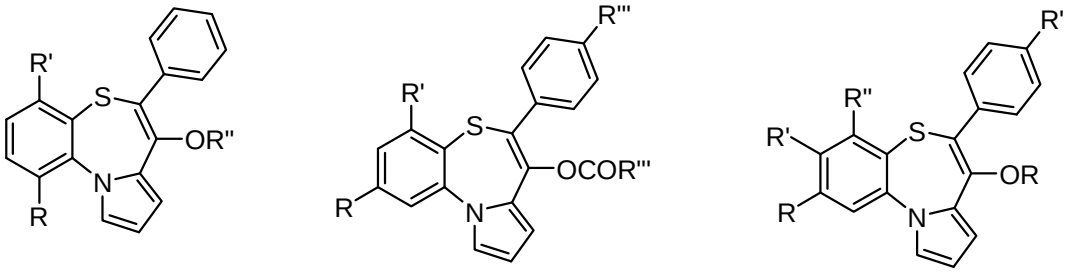

[104] **[105]** **[106]**

Figure 4.1 General structure of pyrrolobenzothiazepines for the PBR.

4.2 Pyridopyrrolo and Pyrrolobenzoxazepine Ligands for PBR

Other classes of compounds that have been shown to have high affinity for the PBR are pyridopyrrolooxazepines **[108]** and pyrrolobenzoxazepines **[107]**, **[109]**. The PBR binding affinities of selected compounds are shown in Figure 4.2. In the literature, the highest affinity compounds were the pyrrolobenzoxazepines with K_i values from 0.11 nM. Two pyrrolobenzoxazepine compounds with a chlorine atom had K_i values of 0.18

and 0.51 nM respectively for the PBR. The PBR binding affinity of pyridopyrrolooxazepines **[108]** reported ranged from 0.23 nM to 13.5 nM.

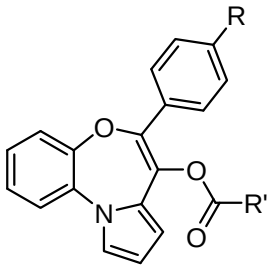

[107]

K_i = 0.11 nM (R = H, R' = NHEt)
K_i = 0.26 nM (R = H, R' = $N(Et)_2$)
K_i = 0.36 nM (R = CH_3, R' = $N(Et)_2$)
K_i = 0.52 nM (R = CH_3, R' = $N(Me)_2$)

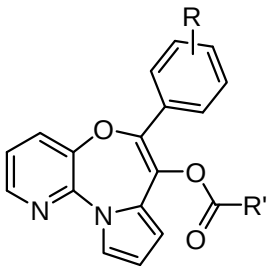

[108]

K_i = 0.44 nM (R = *p*-CH_3, R' = $N(Me)_2$)
K_i = 0.56 nM (R = *m*-CH_3, R' = $N(Et)_2$)
K_i = 1.77 nM (R = H, R' = $N(Et)_2$)

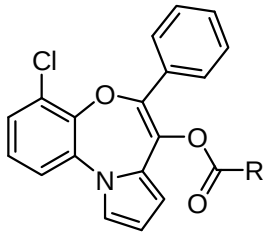

[109]

K_i = 0.18 nM (R = NHEt)
K_i = 0.51 nM (R = $N(Me)_2$)

Figure 4.2 Selected pyridopyrrolooxazepines and pyrrolobenzoxazepines and their binding affinities (K_i) for PBR.

Three pyrrolobenzoxazepines with PBR affinity were found to inhibit the proliferation of rat C6 glioma and human 1321N1 astrocytoma.[55] The inhibition occurred at micromolar concentrations, and was dose-dependent, however, the inhibition of proliferation did not appear to be mediated with the binding of these ligands to the PBR.

4.3 Rationale

The pyrrolobenzoxazepines and pyridopyrrolooxazepines reported have very high binding affinity for the PBR, most of which are more potent than PK11195. No iodinated compounds have been synthesised, and no analogues have been radiolabelled with any radioisotope for studying the PBR. The compounds have the potential to be radiolabelled with ^{123}I in several different positions. One position is on the benzoxazepine ring, and the other is on the phenyl group (Figure 4.3). Compounds in Figure 4.2 have chlorine on the benzoxazepine ring **[109]** or a methyl group on the phenyl ring. It was anticipated that replacing a chloro or methyl group with an iodine on the structure, would retain its potent PBR affinity.

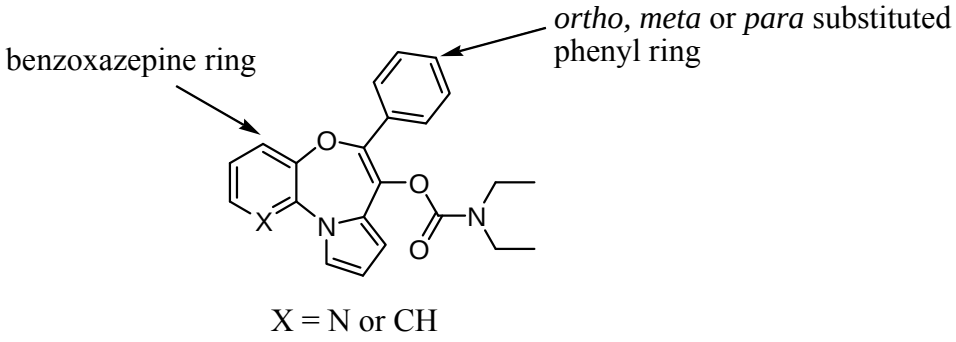

Figure 4.3 Compound showing possible positions for radiolabelling with ^{123}I.

4.4 General Synthetic Scheme

The synthesis of pyridopyrrolooxazepines and pyrrolobenzoxazepines have been previously reported in the literature.[121] The general synthetic scheme of these compounds is summarised in Scheme 4.1. The first step is pyrrole ring formation using 2,5-dimethoxytetrahydrofuran and the arylamine.

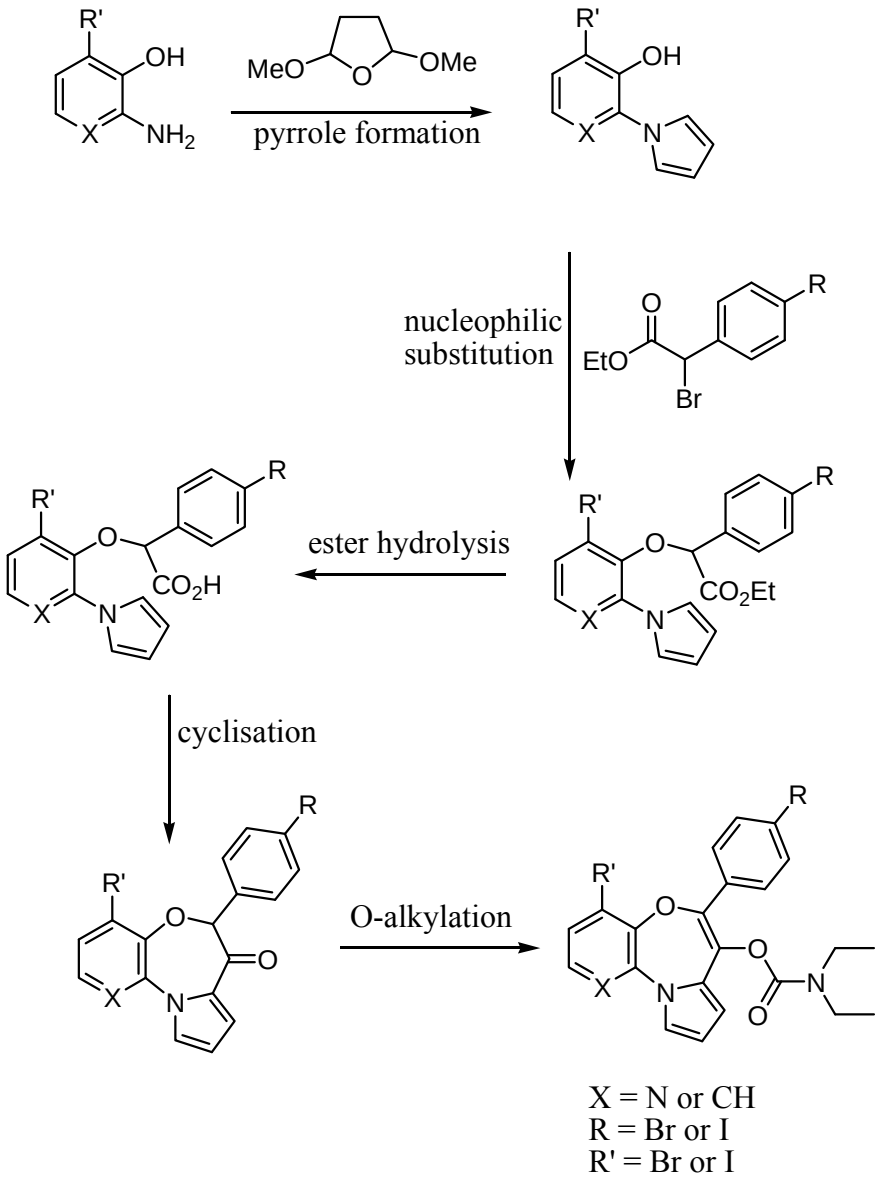

Scheme 4.1 General synthetic scheme for pyrrolobenzoxazepines and pyridopyrrolooxazepines.

The second step is a nucleophilic substitution reaction under basic conditions, with the ethyl (±)-α-bromoarylacetate which required prior synthesis. Ester hydrolysis and cyclisation follows, then O-alkylation using diethylcarbamoyl chloride, to give the final product for *in vitro* PBR binding studies.

4.5 Synthesis of Ethyl (±)-α-Bromoarylacetates

The esterification of 4-iodophenylacetic acid and 4-bromophenylacetic acid to give esters **[110]** and **[111]**, and the subsequent bromination to form the ethyl (±)-α-bromophenylacetates **[112]** and **[113]** have been previously reported.[172-174] Reaction of 4-iodophenylacetic acid or 4-bromophenylacetic acid with ethanol and a catalytic amount of sulphuric acid gave **[110]** and **[111]** in 97% and 93% yield, respectively (Scheme 4.2). The bromination of **[110]** and **[111]**, using *N*-bromosuccinimide (NBS) and a catalytic amount of benzoyl peroxide (a radical initiator) in carbon tetrachloride, gave **[112]** and **[113]** in 59% and 97% yield, respectively. All compounds were spectroscopically identical to that reported.[172-174]

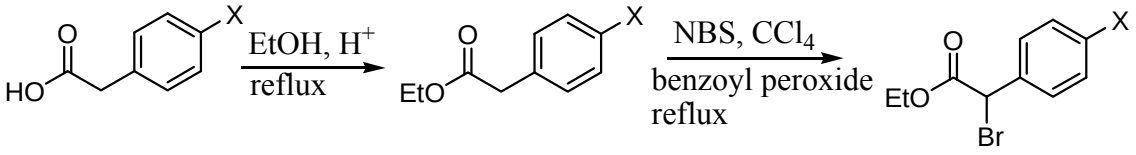

[110] X = I **97%**
[111] X = Br **93%**

[112] X = I **59%**
[113] X = Br **97%**

Scheme 4.2 Synthesis of ethyl (±)-α-bromophenylacetates **[112]** and **[113]**.

4.6 Synthesis of Pyridopyrrolooxazepines

The synthesis of the pyridopyrrolooxazepines is summarised in Scheme 4.3. The synthesis of 1-(3-hydroxy-2-pyridyl)pyrrole **[114]** via reaction of 2-amino-3-hydroxypyridine with 2,5-dimethoxytetrahydrofuran in glacial AcOH, has been previously reported in a yield of 43%.[175] Using this literature procedure a yield of only 16% was obtained, however this was not optimised as sufficient material was prepared. The following step was the nucleophilic substitution reaction of **[114]** with the α-

bromoaryl acetate **[112]**. Literature procedures for similar reactions have used sodium hydride resulting in yields of between 42-47%.[175] As discussed later in Section 4.7, with the brominated benzoxazepine analogue, this method resulted in several by-products and the desired product was difficult to purify. Alternatively, the use of a phase-transfer catalyst, tetrabutylammonium iodide, along with potassium iodide and potassium carbonate was employed. Using this method, the ester **[115]** was formed in an excellent yield of 94%. ^{1}H NMR analysis of **[115]** revealed downfield shifting of the methylene proton from δ 5.26 to 5.54. It also showed doublets at δ 7.25 and 7.71 assigned to the four protons of the *para*-substituted phenyl group, and doublet of doublets at δ 6.34 and 7.76 assigned to the four protons of the pyrrole group. Peaks at δ 7.01, 7.18, and 8.09, which showed characterstic pyridine coupling constants, were assigned to the three protons of the pyridine group. A triplet at δ 1.20 and a quartet at δ 4.19 were assigned to the ethyl ester group.

Base catalysed ester hydrolysis of **[115]** was achieved in 99% yield, with the loss of the peaks corresponding to the ethyl protons in the ^{1}H NMR spectrum of **[117]**. The carboxylic acid was then cyclised to form the oxazepinone **[119]** in 82% yield. This reaction used phosphorus pentachloride which formed the acid chloride *in situ* which then underwent intramolecular Friedel-Crafts cyclisation. ^{1}H NMR analysis of **[119]** revealed the disappearance of the doublet of doublets of the pyrrole group at δ 6.27 and 7.65 in **[117]**, and the addition of three separate peaks at δ 6.54, 7.49 and 8.08 assigned to the three protons of the pyrrole group. ^{13}C NMR spectra of **[119]** showed the downfield shifting of the carbonyl peak from δ 171.6 to 186.3 as it changed from a carboxylic acid to a ketone. Mass spectra showed a peak at *m/z* 402, assigned as the molecular peak.

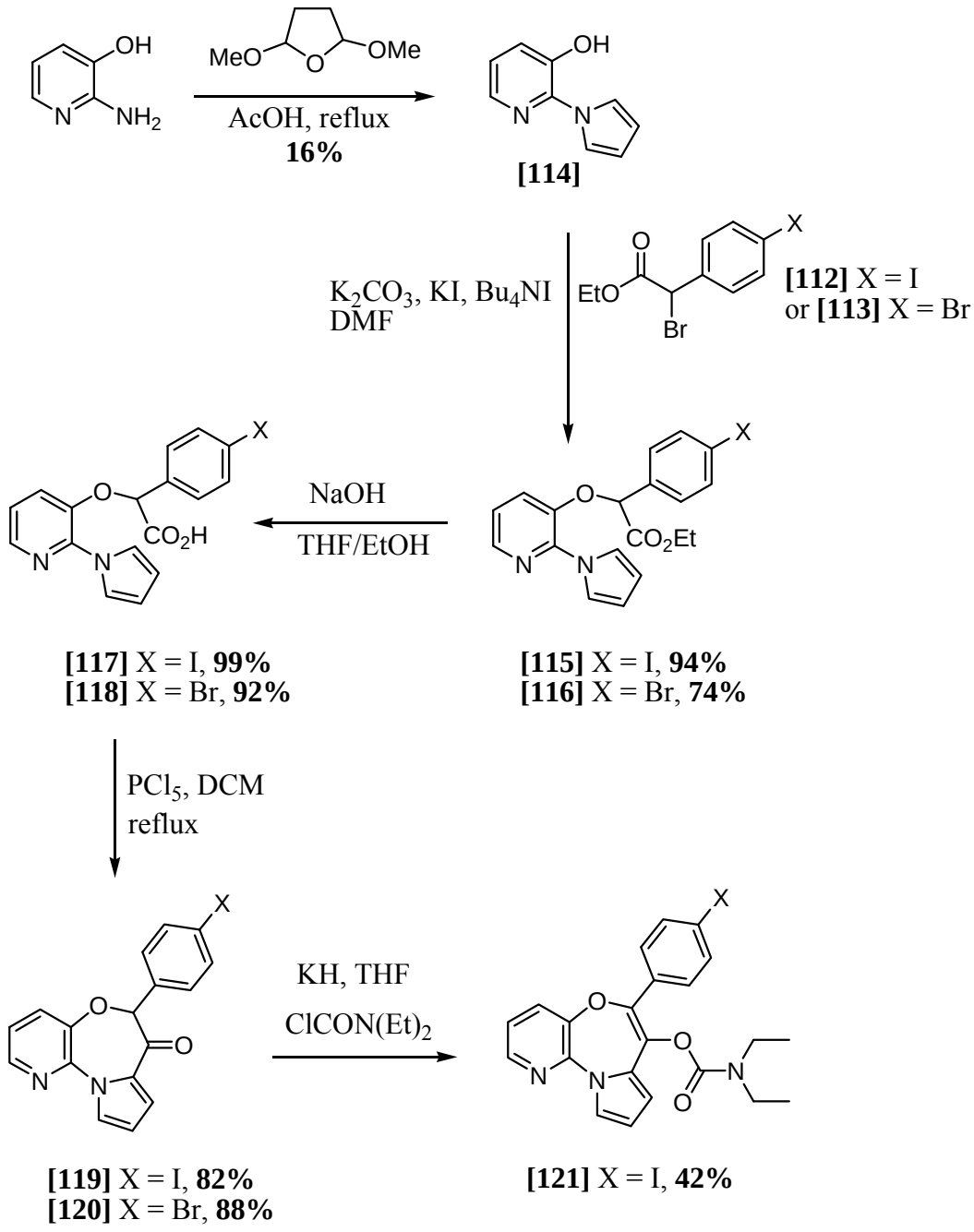

Scheme 4.3 General synthesis of 7-[(diethylcarbamoyl)oxy]-6-(4-iodophenyl)pyrido-[3,2-*b*]pyrrolo[1,2-*d*][1,4]oxazepine **[121]**.

The final step involved forming a potassium enolate from the ketone using potassium hydride, followed by O-alkylation using diethylcarbamoyl chloride. The first attempt involved stirring the ketone with potassium hydride for 2 hours before adding the

diethylcarbamoyl chloride, then stirring the reaction overnight. This reaction produced numerous side products, and none of the O-alkylated product was isolated. An unexpected product **[122]** was isolated in 16% yield by loss of the benzyl group and recyclisation, possibly caused by radical reaction caused by peroxide impurities in the THF (Scheme 4.4). ^{1}H NMR spectra of the by-product **[122]** revealed the loss of the two aromatic doublets, and the benzylic hydrogen of **[119]**. ^{13}C NMR spectra of showed the shifiting of the carbonyl peak from δ 186.3 in **[119]** to δ 153.0 in **[122]**. Mass spectra of **[122]** displayed a peak at *m/z* 187, assigned to the molecular peak.

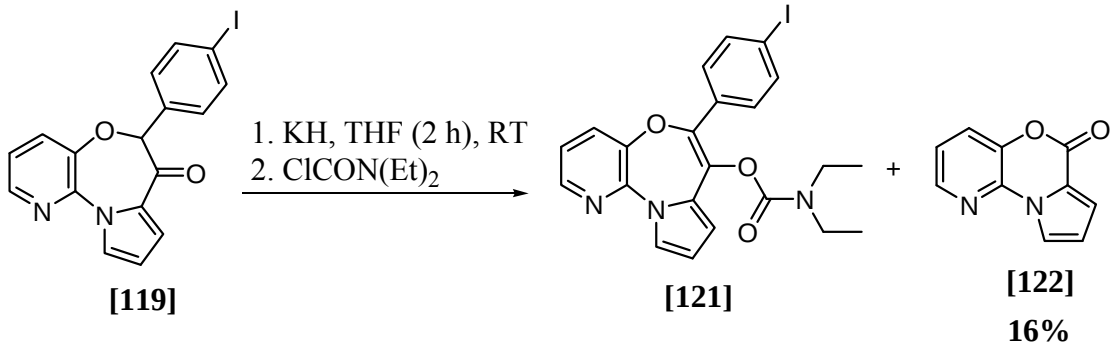

[119] **[121]** **[122]** **16%**

Scheme 4.4 An unexpected side-product from an O-alkylation reaction.

A proposed mechanism for the formation of this side-product is shown in Figure 4.4. Results of this study suggest that the carbanion formed while stirring the ketone with KH could have been oxidised by trace amounts of Cu^{2+} or Fe^{3+} in the reaction mixture, leaving a benzylic radical. This could then react with O_2 to form a hydroxyperoxide radical off the benzylic carbon. Homolytic cleavage of the peroxide bond could result in ring opening, leaving the radical electron on the adjacent oxygen. This radical could then attack the carbonyl group adjacent to the pyrrole ring and result in ring closure to give **[122]**, and loss of a phenoxy radical which would most likely become 4-iodobenzoic acid.

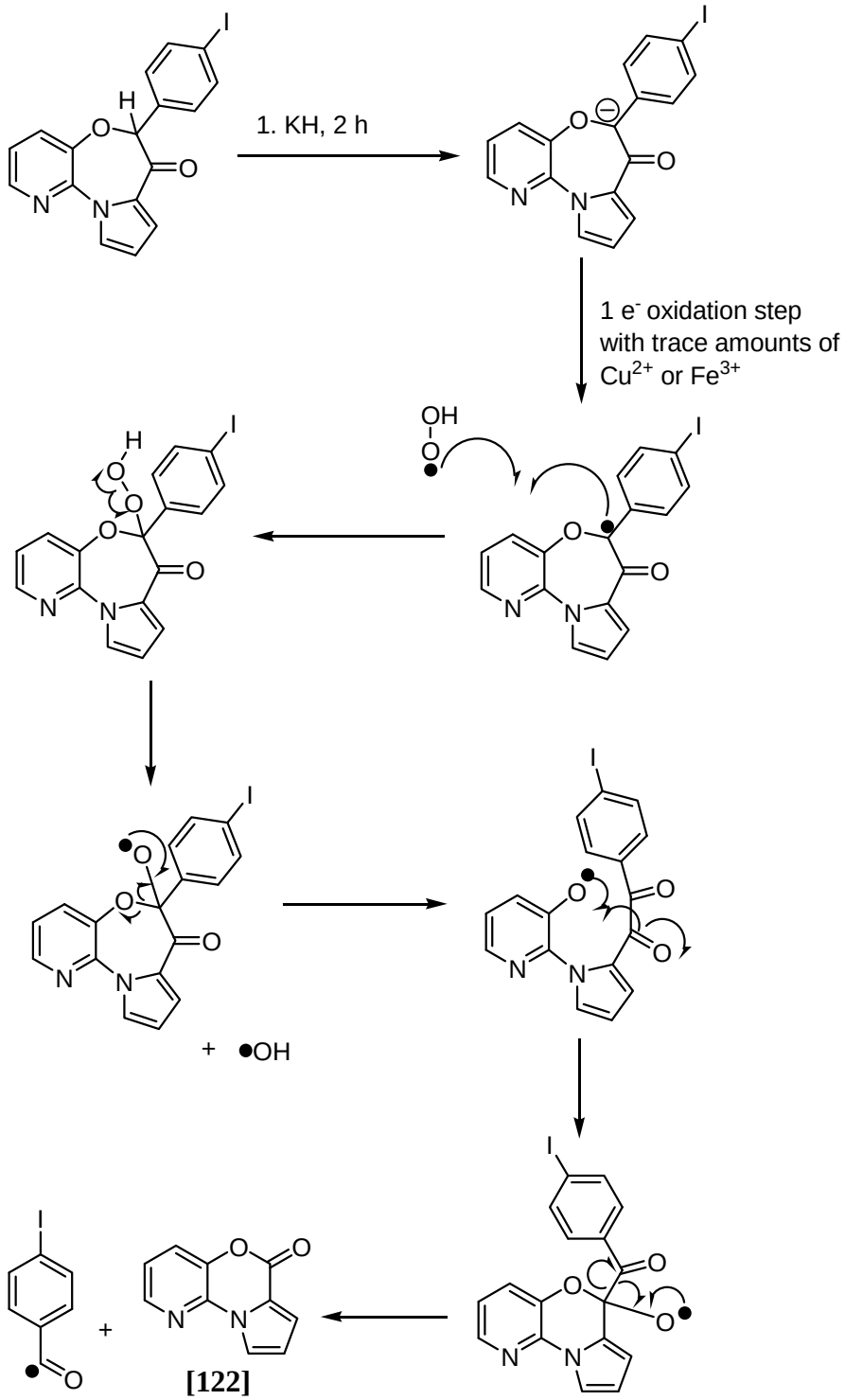

Figure 4.4 Proposed mechanism of radical reaction to form pyrido[3,2-*b*]pyrrolo[1,2-*d*][1,4]oxazine-6-one **[122]**.

The reaction was repeated with attention paid to the order of addition of reactants. Hence, the diethylcarbamoyl chloride was added to the ketone, followed by potassium hydride, and the mixture was allowed to stir overnight at room temperature. This method gave the product **[121]** in 42% yield. ^{1}H NMR spectra of **[121]** showed the loss of the methylene protons at δ 5.53, and the addition of two triplets and two quartets of the diethylamide group. The ^{13}C NMR of **[121]** showed the loss of the ketone carbonyl peak at δ 186.3 and the addition of an amide carbonyl peak at δ 153.0. Mass spectra displayed a peak at *m/z* 501 assigned as the molecular peak, and a peak at *m/z* 402, due to loss of $CON(Et)_2$.

Utilising the same general methods as above, the bromo analogues were synthesised. The O-alkylation of **[114]** with the α-bromoaryl acetate **[113]** gave **[116]** in 74% yield. Ester hydrolysis to afford **[118]** was achieved in 92% yield, followed by cyclisation to afford **[120]** in 88% yield. In an attempt to improve the yield of the general O-alkylation reaction, the reaction was performed in a mixture of DMF and THF. The desired product was not isolated, however, the carbon alkylated product **[123]** was isolated in 29% yield (Scheme 4.5). It is likely that the DMF complexed with the oxygen, preventing O-alkylation. Although this product was not the desired product, it was tested for PBR affinity (Section 4.9).

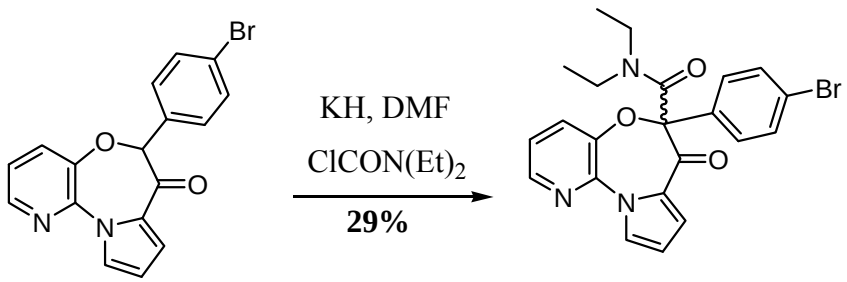

[120] **[123]**

Scheme 4.5 Carbon alkylation of **[120]** when using DMF as solvent.

4.7 Synthesis of Pyrrolobenzoxazepines

An alternative synthetic scheme was used for the synthesis of the target brominated and iodinated pyrrolobenzoxazepines (Scheme 4.6). 4-Bromophenylacetic acid was used as the starting material as it is less expensive than 4-iodophenylacetic acid, and both the bromine and iodine analogues can be synthesised in the same synthetic set. 1-(2-Hydroxyphenyl)pyrrole **[124]** was synthesised from *o*-aminophenol and 2,5-dimethoxytetrahydrofuran in 25% yield.[176] The nucleophilic addition of the ethyl α-bromoacetate **[113]** onto **[124]** was attempted twice. The first method used sodium hydride to form the anion, which could then attack the α-bromo compound **[113]** via nucleophilic attack. Utilising this method, the product **[125]** was isolated in 61% yield from a mixture of multiple products. The second method involved the use of a phase-transfer catalyst, resulting in an improved yield of 70%.

The base-catalysed ester hydrolysis of **[125]** gave the carboxylic acid **[126]** in 97% yield. The intramolecular Friedel-Crafts cyclisation of **[126]** with phosphorus pentachloride gave the oxazepinone **[127]** in 93% yield. ^{1}H NMR spectra of the cyclised product **[127]** revealed the disappearance of the peak corresponding to H2 of the pyrrole, and the large downfield shifting of the pyrrole H3 from δ 6.24 to 7.32. The mass spectra of **[127]** showed peaks at *m/z* 355 and 353, assigned to the ^{81}Br and ^{79}Br molecular peaks, a loss of 18 when compared to the carboxylic acid **[126]**.

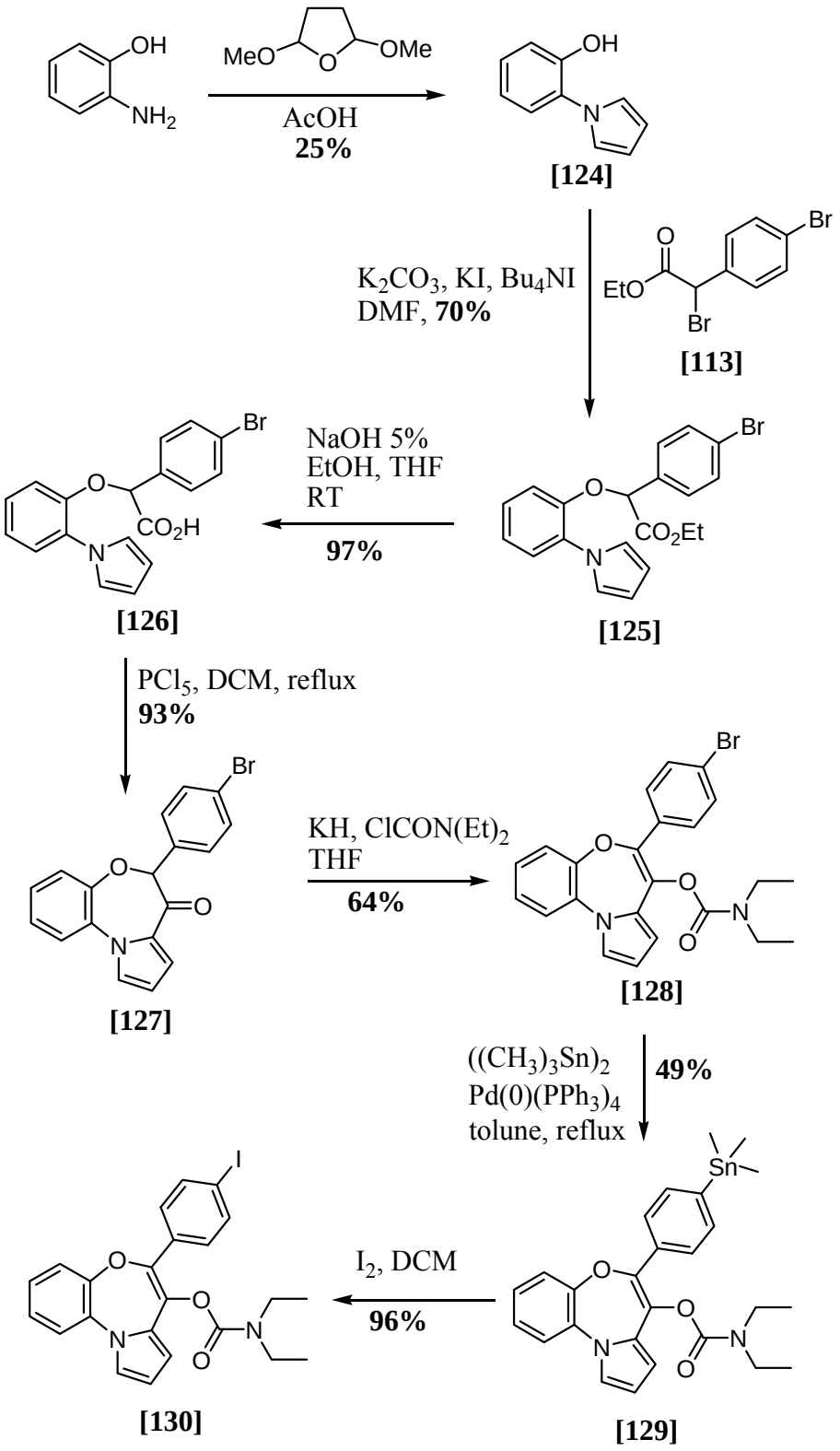

Scheme 4.6 Complete synthesis of target pyrrolobenzoxazepines **[128]** and **[130]**.

The next step was the O-alkylation of the oxazepinone **[127]** using potassium hydride to create the potassium enolate which subsequently reacted with diethylcarbamoyl chloride to give the target brominated pyrrolobenzoxazepine **[128]** in 64% yield. ^{1}H NMR of **[128]** showed a large upfield shift of pyrrole H3 from δ 7.32 to 6.41 due to the O-alkylation. Triplets at δ 1.10 and 1.22, and quartets at δ 3.31 and 3.43, were assigned as the two ethyl groups.

Stannylation of **[128]** was achieved in 49% yield by heating at reflux **[128]** in toluene, with hexamethylditin in the presence of $Pd(0)(PPh_3)_4$. The ^{1}H NMR spectra of the stannane **[129]** revealed a singlet at δ 0.30, assigned to the nine protons of the trimethyltin group. Iodination of the stannane **[129]** was achieved in 96% yield using iodine in DCM to give the target iodinated pyrrolobenzoxazepine **[130]**. The ^{1}H NMR of **[130]** showed loss of the trimethyltin peak in the ^{1}H NMR spectra, and the shifting of the doublets of the *para*-substituted aromatic ring.

The benzoxazepinone **[127]** was reacted with potassium hydride and dimethylcarbamoyl chloride in DMF, in an attempt to synthesise the O-alkylated product with a dimethylamide group. Instead, the product formed in 30% yield was the carbon alkylated product **[131]** (Scheme 4.7). This confirms that the use of DMF as the solvent for this type of reaction results in the favour of carbon alkylation over oxygen alkylation, which also occurred in the synthesis of **[123]**.

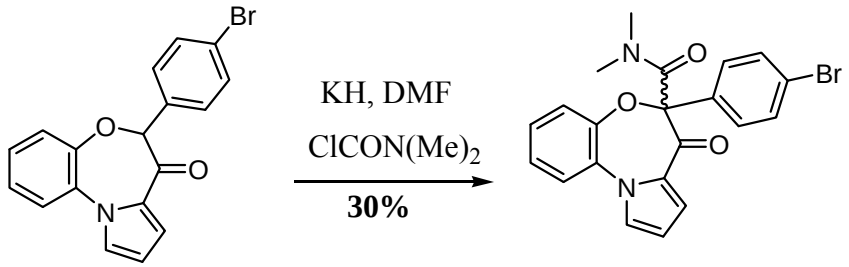

[127] **[131]**

Scheme 4.7 Carbon alkylation of **[127]** using DMF as solvent.

4.8 Synthesis of 4-Halogenated Pyrrolobenzoxazepines

In an attempt to find the optimum position for the iodine for potential radioiodinated ligands, compounds with the iodine atom being placed on the benzoxazepine ring were desired. By comparing compounds with different positions for the iodine, the optimum position for the iodine for PBR binding could be found.

The scheme for the synthesis of 4-halogenated pyrrolobenzoxazepines is summarised in Scheme 4.8. 1-(3-Bromo-2-hydroxyphenyl)pyrrole **[132]** was synthesised in two steps from 2-bromo-6-nitrophenol. The reduction of the nitro group was achieved using excess sodium dithionite in H_2O and EtOH. TLC analysis showed that all starting material had been consumed, however, all attempts to extract the product out of the water layer were unsuccessful. Instead, the reaction mixture was evaporated to dryness for direct use in the next reaction involving the synthesis of the pyrrole ring, using 2,5-dimethoxytetrahydrofuran in AcOH. The combined yield of **[132]** of the two steps was only 6%; however, yield optimisation was not attempted.

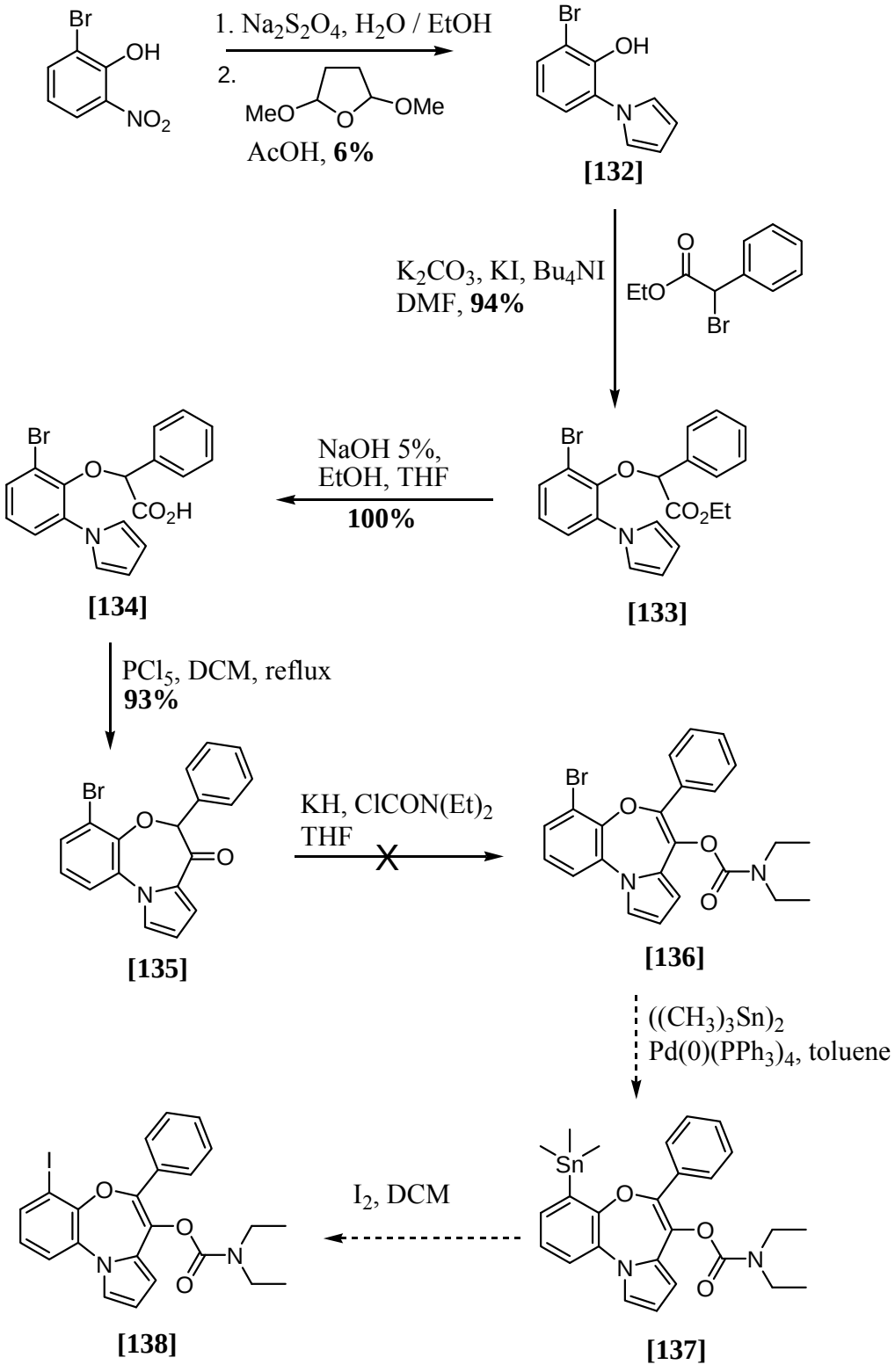

Scheme 4.8 Attempted synthesis of 7-[(diethylcarbamoyl)oxy]-4-iodo-6-phenyl-pyrrolo[2,1-*d*][1,5]benzoxazepine **[138]**.

1-(3-Bromo-2-hydroxyphenyl)pyrrole **[132]** was O-alkylated with ethyl α-bromophenyl acetate in 94% yield. ^{1}H NMR spectra of **[133]** showed the loss of the phenolic proton of **[132]** at δ 5.67 and the addition of peaks of the added phenyl group and ester. Hydrolysis of the ester **[133]** was achieved in quantitative yield. ^{1}H NMR spectra analysis of **[134]** showed the loss of the ethyl ester peaks. Mass spectrometry of **[134]** showed ^{79}Br and ^{81}Br molecular peaks at *m/z* 371 and 373, and a base peak at *m/z* 326 due to loss of the carboxylic acid (CO_2H). The cyclisation of **[134]** was achieved in 93% yield by reaction of the carboxylic acid with PCl_5 in DCM. ^{1}H NMR spectra analysis of **[135]** showed the loss of a proton on the pyrrole group. Mass spectrometry of **[135]** revealed ^{79}Br and ^{81}Br molecular peaks at *m/z* 353 and 355, a loss of 18 from the carboxylic acid **[134]** due to loss of the alcohol (OH) and a proton on the pyrrole. The ketone **[135]** was then reacted with KH, followed by 2-chloro-*N*,*N*-diethylacetamide, however, no desired product could be isolated **[136]**.

Due to difficulty in producing sufficient quantities of the starting material 1-(3-bromo-2-hydroxyphenyl)pyrrole **[132]**, and also due to failure of the O-alkylation reaction, the full synthetic scheme was not completed. The target compounds **[136]** and **[138]** were not synthesised and therefore were not tested for PBR binding affinity.

4.9 *In Vitro* Binding of Pyridopyrrolooxazepines and Pyrrolo-benzoxazepines

The PBR binding affinities of all four compounds were determined, and CBR binding affinities and log *P* values were determined for three compounds (Figure 4.5). Compounds **[121]**, **[128]** and **[130]** had moderate PBR binding affinities, ranging from 24-39 nM. These compounds were selective for PBR over CBR, with CBR IC_{50} values

of over 5000 nM. The brominated pyrrolobenzoxazepine **[128]** showed a higher binding affinity (IC_{50} = 24.0 nM) than its respective iodinated analogue **[130]** (IC_{50} = 39.4 nM), suggesting that a smaller halogen is preferred for PBR binding. Compared to literature K_i values of <2 nM for PBR ligands of this class (Figure 4.2),[56] it appears that a large bromine or iodine group on the phenyl ring largely decreases the binding affinity. The PBR binding affinities of the iodinated pyridopyrrolooxazepine **[121]** and pyrrolobenzoxazepine **[130]** were not significantly different (IC_{50} = 35.7 and 39.4 nM respectively), so it cannot be concluded that a pyridine or benzene is preferred for binding. The carbon alkylated product **[123]** did not show PBR affinity, suggesting the diethylamide group is not in the preferred conformation for binding to the PBR.

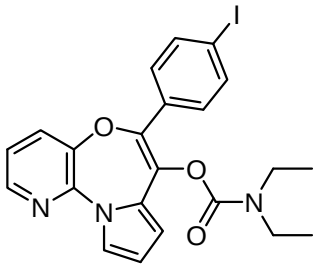

[121]

PBR IC_{50} = 35.7 nM
CBR IC_{50} > 5000 nM
log *P* = 4.60

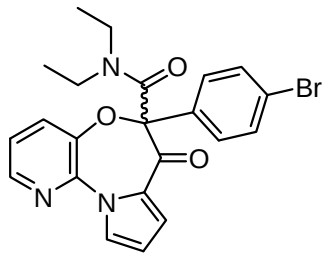

[123]

PBR IC_{50} > 1000 nM
CBR IC_{50} = not determined

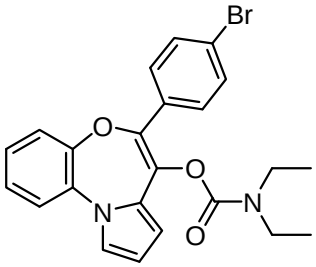

[128]

PBR IC_{50} = 24.0 nM
CBR IC_{50} > 5000 nM
log *P* = 4.78

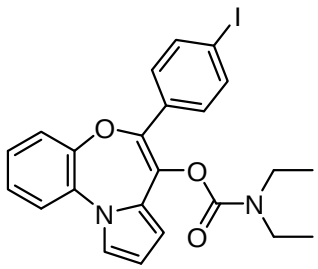

[130]

PBR IC_{50} = 39.4 nM
CBR IC_{50} > 5000 nM
log *P* = 4.98

Figure 4.5 PBR and CBR IC_{50} values for compounds **[121], [123], [128]**, **[130]**.

4.10 Conclusions and Future Directions

An improved method for the nucleophilic substitution reaction of the ethyl (±)-α-bromoarylacetates with the hydroxyarylpyrroles was developed, using a phase-transfer catalyst, instead of sodium hydride. These gave good yields of 70-94%, compared to yields of 40-50% of similar literature ester syntheses using sodium hydride.[56]

An interesting result was discovered when DMF was used as the solvent in the final alkylation step, leading to alkylation on the carbon, compared to O-alkylation when using THF.

The compounds synthesised and tested in this chapter had reasonably high affinity for PBR, however, none were radiolabelled with ^{123}I for *in vivo* evaluation because the binding affinity was not less than the target of approximately 10 nM. Further optimisation studies with this class of compounds could include the synthesis of compounds with different length alkyl groups on the amide, different positions of the iodine on the phenyl ring, and further derivatives with iodine on the benzoxazepine ring.

Future studies would involve developing an improved synthesis of 1-(3-bromo-2-hydroxyphenyl)pyrrole in order to efficiently prepare the target 4-halogenated pyrrolobenzoxazepines.

5 Radioiodination and *In Vivo* Studies

5.1 Radioiodination Methods

The main methods for radiolabelling with iodine are nucleophilic addition and electrophilic substitution.[177] Nucleophilic addition reactions include halogen exchange by either interhalogen exchange or isotopic exchange. An example of the first method is the replacement of a chlorine atom with the radioiodine, and the other method involves an iodine atom being replaced with an iodine radioisotope (Figure 5.1). These reactions require heating and longer reaction times than the electrophilic substitution method.

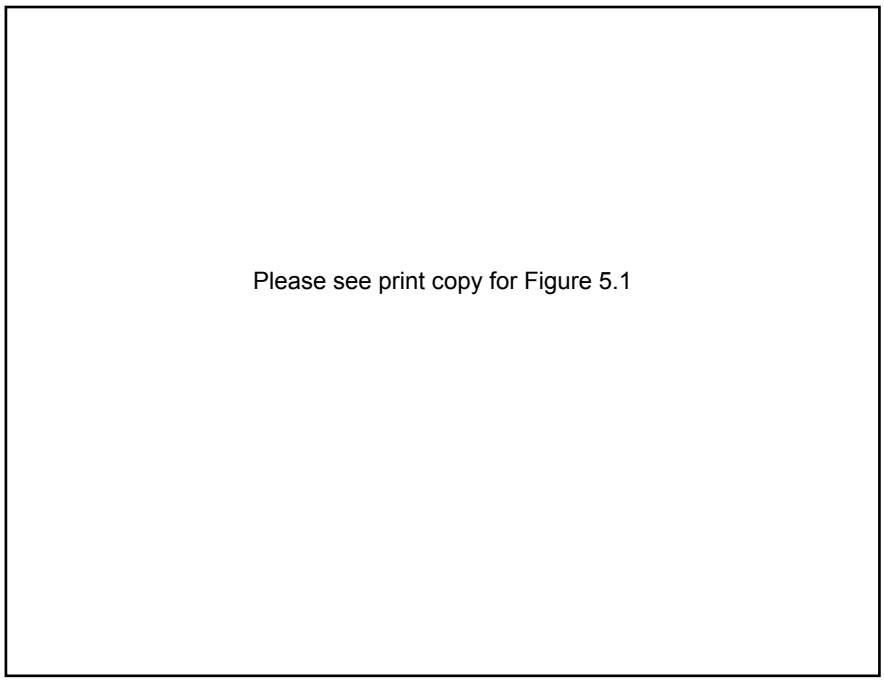

Figure 5.1 Radioiodination via nucleophilic addition to synthesise radioiodinated PK11195.[151]

Electrophilic substitution reactions include direct electrophilic iodination (radioiodo-deprotonation) or demetallation (radioiodo-demetallation). Electrophilic substitution is the attack of electrophilic iodine onto a double bond or an aromatic ring. In direct electrophilic iodination, the iodine replaces a proton (radioiodo-deprotonation). In this case, the desired position of the iodine must be activated by other groups on the aromatic ring. Direct radioiodination is often used to label proteins. In this case, the iodine is incorporated into tyrosine residues, and occasionally histidine residues. Figure 5.2 shows the direct radioiodination of the amino acid, tyrosine.

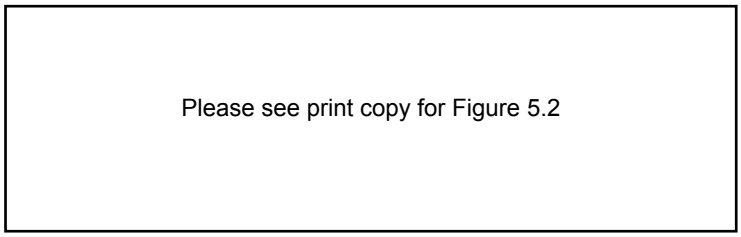

Figure 5.2 Direct radioiodination (radioiodo-deprotonation) of tyrosine.[178]

In other electrophilic iodinations, the iodine replaces an organometallic group. Organometallic intermediates used for radioiodo demetallation include boranes, silanes, germanes, stannanes, mercurials, and thallates.[179] The most suitable, however, are trialkylstannyl, trialkylsilyl, or boronic acid derivatives. An example of electrophilic radioiodination via demetallation is shown in Figure 5.3.

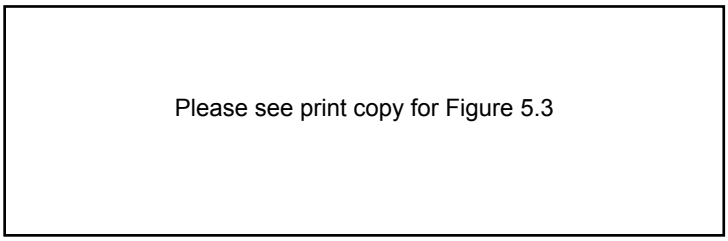

Figure 5.3 Electrophilic radioiodination of a tributylstannyl group.[113]

Some oxidising agents include iodine monohalide (ICl or IF), *N*-chloramides, iodogen, *N*-halosuccinimides, and peracids (Figure 5.4).[180] Sodium salts of *N*-chlorosulfonic acid amides such as chloramine-T **[139]** (CAT, *N*-chloro-*p*-toluenesulfonic acid) can be used as oxidants for electrophilic radioiodination. In aqueous solutions, these compounds release hypochlorous acid (HOCl) which oxidises iodide to the electrophilic I^+. Chloramine-T often produces chlorinated by-products, and because it is such a strong oxidising agent, can lead to over-oxidised by-products. To avoid the problems of chloramine-T, a water insoluble oxidant, iodogen **[140]** (1,3,4,6-tetrachloro-3α,6α-diphenylglycoluril) can be used. The tube is coated with a thin layer of iodogen so the compound to be radiolabelled does not come into contact with the oxidant.[180]

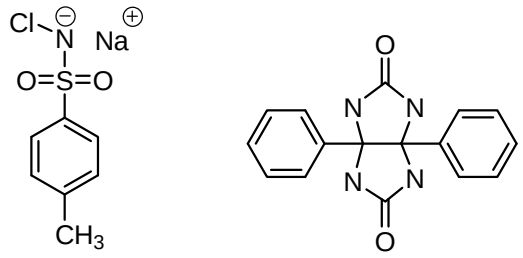

Chloramine-T **[139]** Iodogen **[140]**

Figure 5.4 Structure of two oxidants, chloramine-T and iodogen.

5.2 Synthesis of ^{123}I Compounds

5.2.1 Synthesis of [^{123}I]*N,N*-Diethyl-(5-chloro-2-(4-iodophenyl)indol-3-yl)glyoxylamide

The highest affinity iodinated compound from Chapter 2 was *N,N*-diethyl-(5-chloro-2-(4-iodophenyl)indol-3-yl)glyoxylamide **[50]** with a PBR IC_{50} of 8.23 nM. This compound radiolabelled with ^{123}I could provide a potential SPECT imaging agent for

cancer or neurodegenerative diseases, and would be the first radiolabelled PBR ligand of the phenylindolylglyxoxylamides. Therefore, the synthesis of [^{123}I]*N*,*N*-diethyl-(5-chloro-2-(4-iodophenyl)indol-3-yl)glyoxylamide (named [^{123}I]PBR200) was attempted.

Before the radiolabelling could be performed, it was necessary to prepare the radiolabelling precursor **[141]** for subsequent electrophilic radioiodination. The trimethylstannane precursor **[141]** was synthesised from the bromo analogue **[54]** in 32% yield by reaction with hexamethylditin in the presence of the catalyst, palladium tetrakistriphenylphosphine (Scheme 5.1).

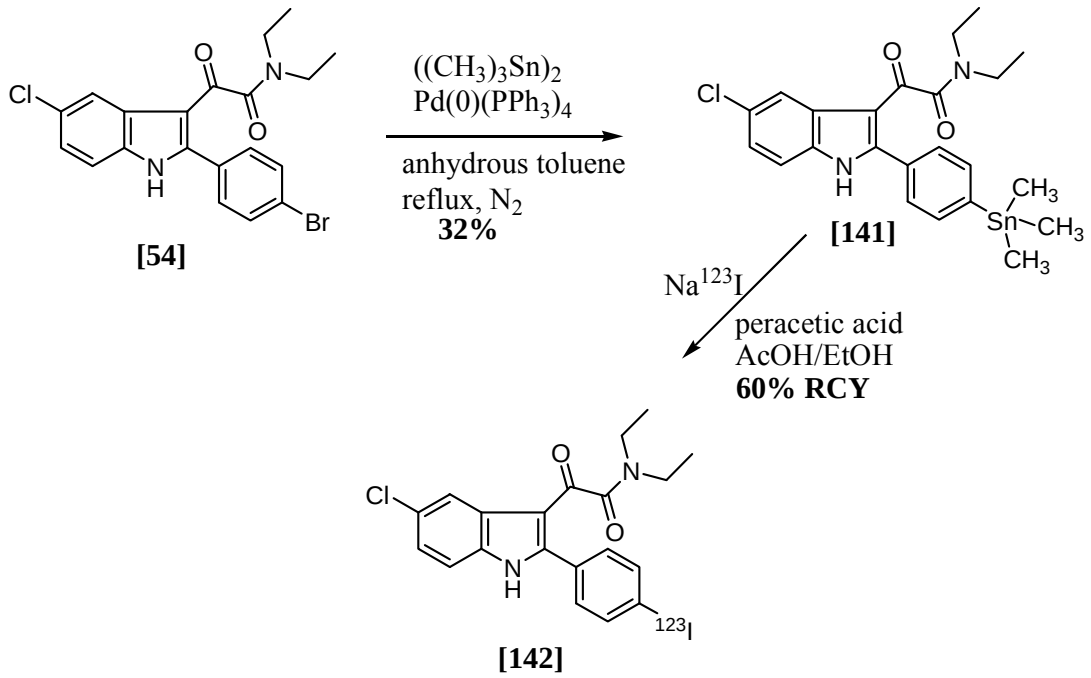

Scheme 5.1 Synthesis of [^{123}I]*N*,*N*-diethyl-(5-chloro-2-(4-iodophenyl)indol-3-yl)glyoxylamide **[142]**.

The ^{1}H NMR analysis of **[141]** revealed a singlet at δ 0.36 corresponding to the nine protons of the three methyl groups on the tin. Low resolution ES^{-} mass spectrometry showed molecular peaks (M-1) at *m/z* 519, 517, 516, 515, 513 corresponding to the

combination of the ^{35}Cl and ^{37}Cl isotopes, and the main tin isotopes ^{120}Sn, ^{119}Sn, ^{118}Sn, ^{117}Sn, ^{116}Sn. High resolution mass spectrometry gave a peak at 515.0903, confirming the molecular formula $C_{23}H_{28}N_2O_2Cl^{116}Sn$.

The ^{123}I radiolabelled compound was synthesised from the stannane precursor **[141]** via electrophilic iodination using $Na^{123}I$ in the presence of peracetic acid. The reaction was stirred at RT for 5 min, before being quenched and neutralised and passed through reverse phase HPLC to purify the radiolabelled product (Figure 5.5). The reaction resulted in three radioactive peaks of which the first smaller peak at 3 minutes was the un-reacted ^{123}I, and the peak at 14 minutes was an unwanted radiolabelled product. The largest peak at 16 minutes was collected, giving **[142]** in 60% radiochemical yield and 97% radiochemical purity. To confirm that the peak at 16 minutes was the desired product **[142]**, the collected fraction was coinjected with non-radioactive iodo standard **[50]** onto a HPLC column. The iodo standard (UV) and the radioactive peak co-eluted at 17 minutes, confirming the product **[142]** (Figure 5.6),

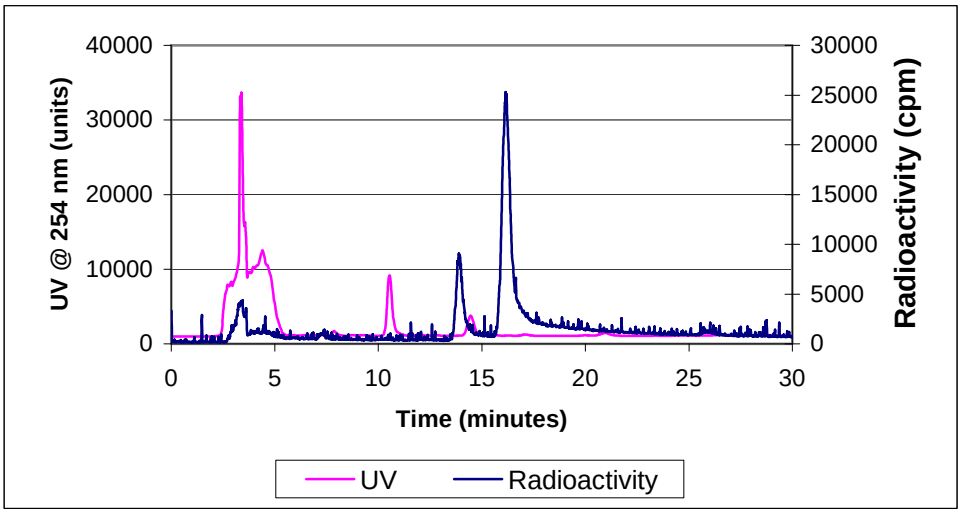

Figure 5.5 Purification of [^{123}I]PBR200 using a semipreparative RP HPLC column eluted with 60% acetonitrile: 40% ammonium acetate (0.01M) at 3 mL/min.

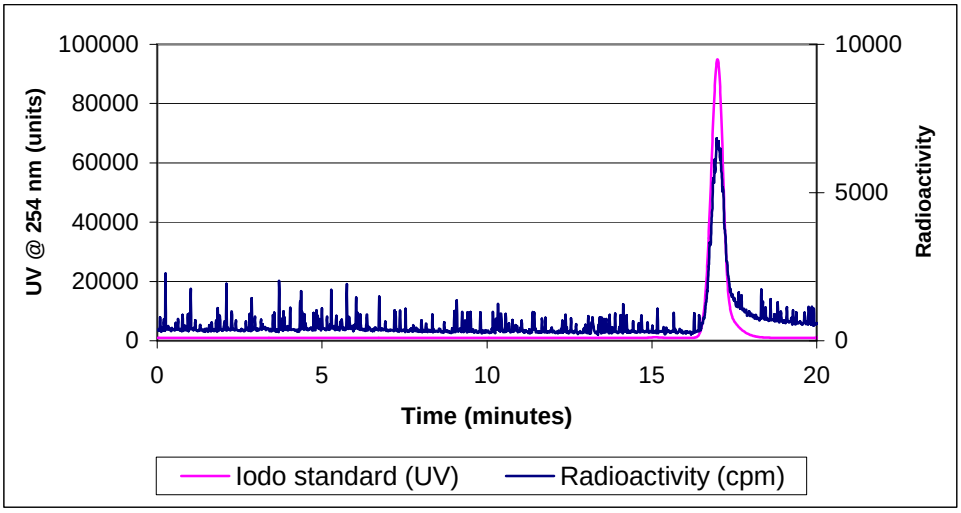

Figure 5.6 Coinjection of iodo standard **[50]** with [^{123}I]PBR200 **[142]** onto HPLC.

The radiolabelling was also attempted using chloramine-T as the oxidant for the reaction, which resulted in a large undesirable UV peak at 13 minutes, close to the radiolabelled product peak at 15 minutes (Figure 5.7). It also showed a radiolabelled peak with a retention time of 13 minutes, similar to that of Figure 5.5.

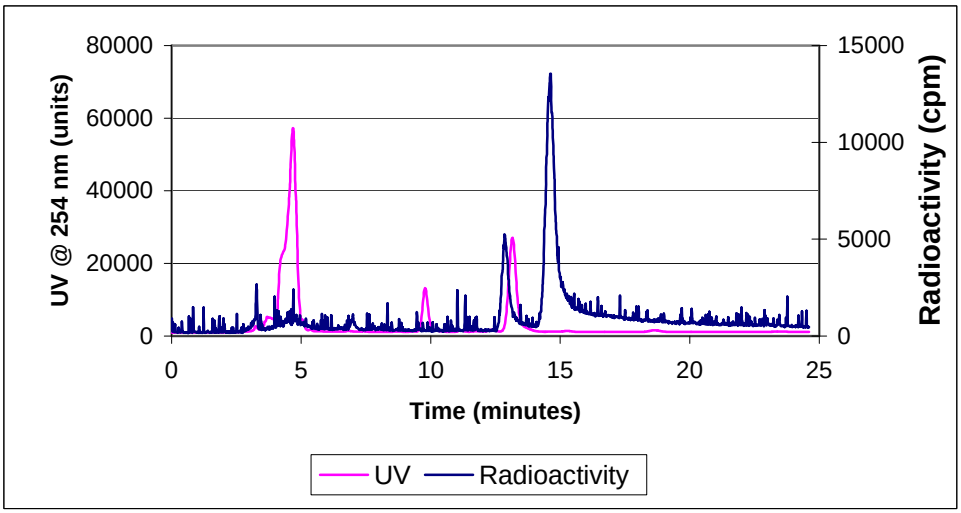

Figure 5.7 HPLC purification of [^{123}I]PBR200 when using chloramine-T.

The stability of [^{123}I]PBR200 in saline solution was determined by running the product through HPLC immediately after purification and formulation of the product in saline solution, and also after 5 hours in saline solution. By integrating the area under the peaks, it was determined that [^{123}I]PBR200 was 97.5% pure after formulation in saline solution, and 96.5% pure after 5 hours. This confirmed that the product is stable in saline and hence could be used in animal studies without degradation of the compound in the saline solution.

5.2.2 Synthesis of [^{123}I]*N*,*N*-Diethyl-[2-(4-iodophenyl)-5,7-dimethyl-pyrazolo[1,5-*a*]pyrimidin-3-yl]acetamide

The high affinity compound from Chapter 3, *N*,*N*-diethyl-[2-(4-iodophenyl)-5,7-dimethylpyrazolo[1,5-*a*]pyrimidin-3-yl]acetamide **[91]** had a PBR IC_{50} of 11.7 nM. The radiolabelling of this compound would provide the first radioiodinated compound of this class of PBR ligands.

The synthesis of [^{123}I]PBR200 **[142]** used a stannane precursor, made from the bromo analogue. For the synthesis of [^{123}I]*N*,*N*-diethyl-[2-(4-iodophenyl)-5,7-dimethylpyrazolo[1,5-*a*]pyrimidin-3-yl]acetamide (named [^{123}I]PBR215), the stannane precursor was prepared from the iodo compound **[91]**. The stannane was prepared in 35% yield by reaction of **[91]** with hexamethylditin in refluxing toluene, with palladium tetrakistriphenylphosphine catalyst (Scheme 5.2). The iodo and the stannane had the same Rf value as determined by TLC analysis using 10% MeOH: 90% DCM as the mobile phase. The reaction mixture was passed through Celite to remove any palladium, and was evaporated. The crude mixture was injected onto HPLC and the stannane **[143]**

was separated from the unreacted iodo starting material **[91]**. ^{1}H NMR analysis of **[143]** revealed a singlet at δ 0.30, integrating to the nine protons of the trimethylstannyl group. ^{13}C NMR spectra displayed a peak at δ -9.4, corresponding to the three methyl groups in the trimethylstannyl group.

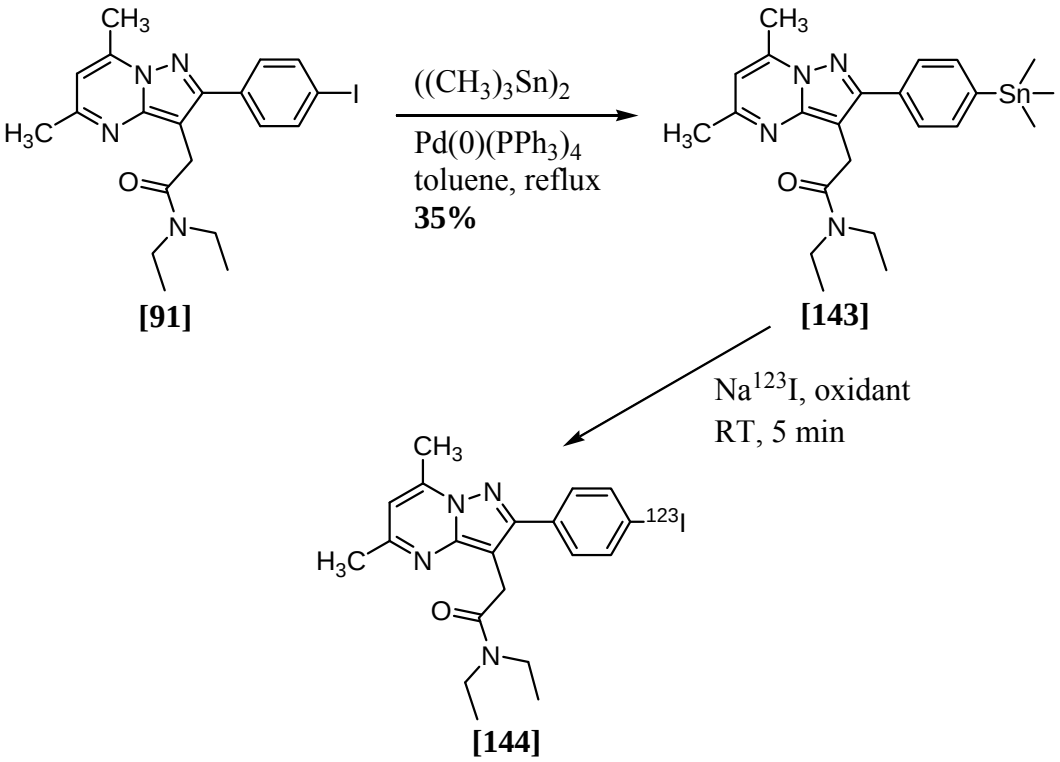

[91] **[143]** **[144]**

Using chloramine-T, HCl, EtOH, **83% RCY**
Using peracetic acid, AcOH, **68-95% RCY**

Scheme 5.2 Synthesis of [^{123}I]*N*,*N*-diethyl-[2-(4-iodophenyl)-5,7-dimethylpyrazolo[1,5-*a*]pyrimidin-3-yl]acetamide **[144]**.

[^{123}I]PBR215 **[144]** was prepared from the stannane **[143]** in 83% radiochemical yield using chloramine-T as the oxidant (Scheme 5.2). The HPLC trace of the reaction mixture showed at least two broad radioactive peaks at 10 minutes and 19 minutes using 60% ACN: 40% ammonium acetate (0.01M) as mobile phase at a flow rate of 2.5

mL/min (Figure 5.8). The problem with this method was the presence of UV activity at the same retention time as the larger radioactive peak corresponding to the desired labelled product. *In vivo* biological evaluation requires high specific activity to reduce pharmacological effects. An alternative method was used in an attempt to improve the radiolabelling to avoid low specific activity. The sharpness of the radiolabelled product peak was improved by using 65% ACN: 35% H_2O (0.1% TFA) as mobile phase at a flow rate of 3 mL/min. Per-acetic acid was used as the oxidant instead of chloramine-T, resulting in a much cleaner radioiodination, with undetectable UV activity in the radioactive peak at 12 minutes using the improved HPLC conditions (Figure 5.9). The peak at 12 minutes was confirmed to be **[144]** as it had the same retention time as the non-radioactive iodo standard **[91]**. The yield of this reaction ranged from 68-95% radiochemical yield with this reaction repeated 6 times (Scheme 5.2).

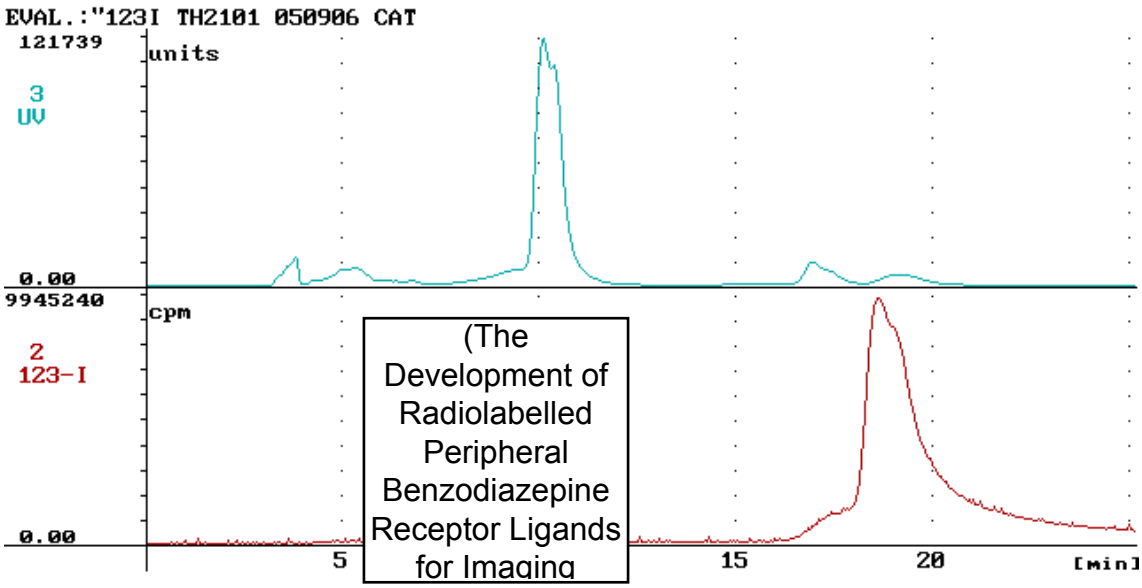

Figure 5.8 HPLC purification [^{123}I]PBR215 when used chloramine-T.

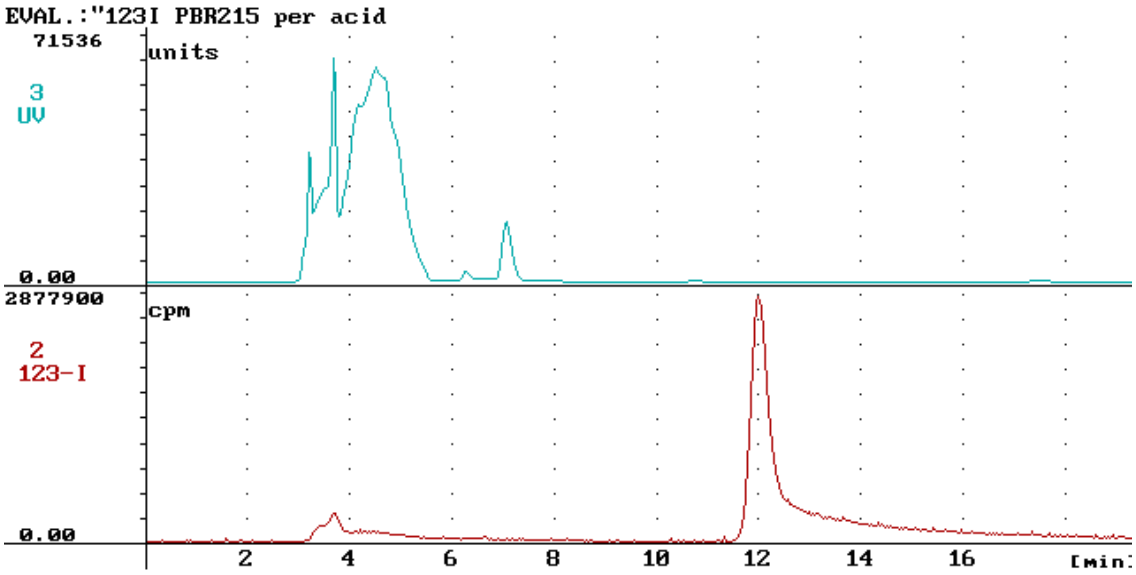

Figure 5.9 Purification of [^{123}I]PBR215 (at 12 min) using a semipreparative RP HPLC column eluted with 65% ACN: 35% H_2O (0.1% TFA) at 3 mL/min.

5.3 *In Vivo* Biodistribution Studies

Biodistribution studies are performed to determine how radiolabelled compounds are distributed throughout the body after being injected. A radiolabelled compound is injected into animals, and at certain time points, the animals are sacrificed and their organs removed and weighed. The amount of radioactivity in each organ is counted, and the percent of the injected dose per gram (% ID/g) of the organ is calculated.

5.3.1 *In Vivo* Biodistribution of [^{123}I]*N*,*N*-Diethyl-(5-chloro-2-(4-iodophenyl)indol-3-yl)glyoxylamide [142]

The radiolabelled compound **[142]** was injected into 28 male Sprague-Dawley rats, and the uptake into 17 organs was determined at 15 minutes, 30 minutes, 1, 3, 6 and 24 hours post injection of the radiotracer. Figure 5.10 shows the biodistribution of [^{123}I]PBR200 in organs at all time points.

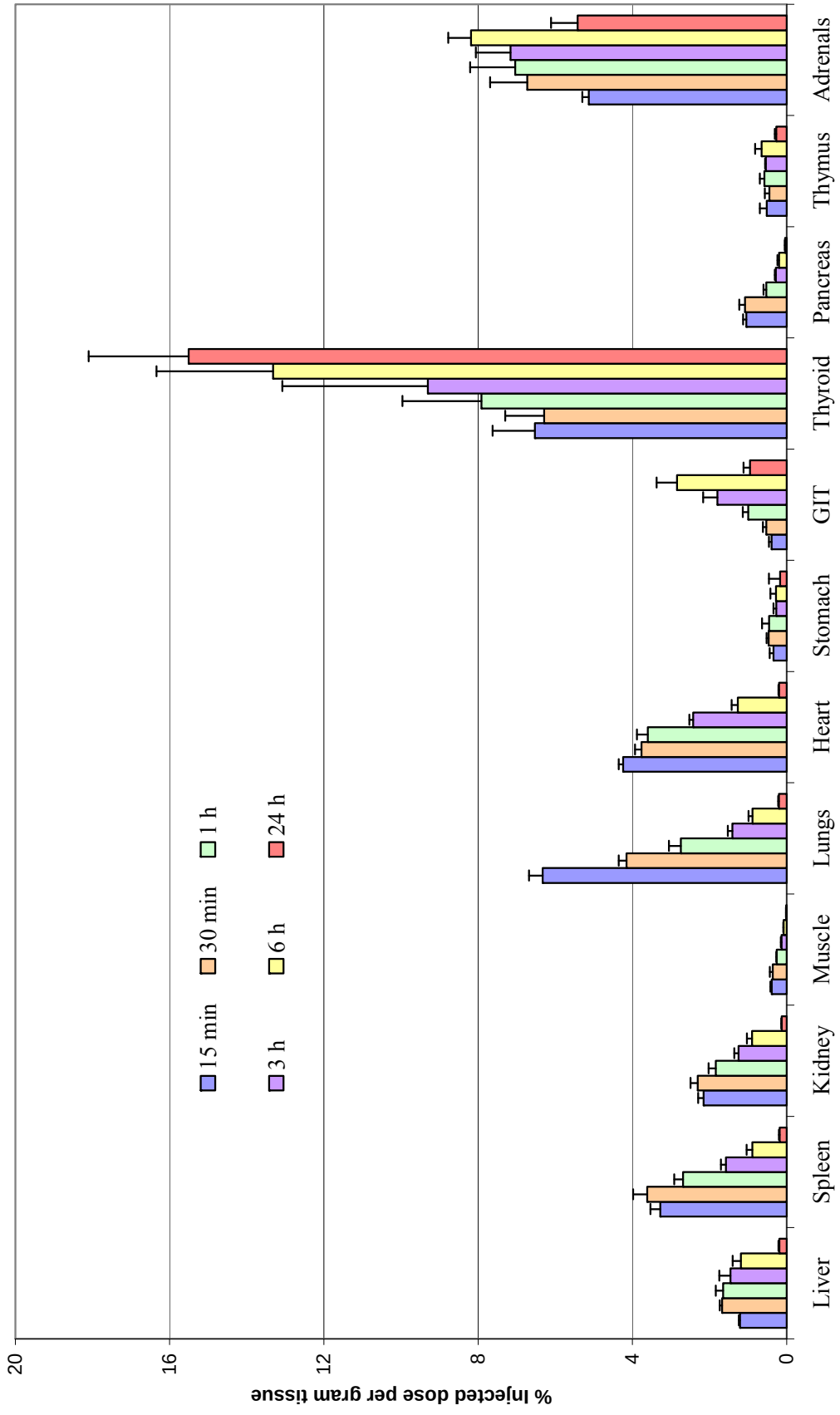

Figure 5.10 Biodistribution of [^{123}I]PBR200 in male Sprague-Dawley rats.

After 15 minutes, there was high uptake of radioactivity into organs known to have PBR sites, such as the kidneys (2.2%), adrenals (5.1%), heart (4.2%), liver (1.2%) and lungs (6.3%). There was also high uptake into the thyroid (6.5%), which naturally takes up free iodine, suggesting that the radiolabelled compound underwent some deiodination *in vivo*. Other than the thyroid, the uptake was the highest in the adrenals, showing an increase in uptake up to 6 hours (8.2% ID/g), then decreasing up to 24 hours. The uptake of radiotracer in the testes, brain, olfactory bulbs and blood was less than 0.17% ID/g at all time points, and is shown in Figure 5.11.

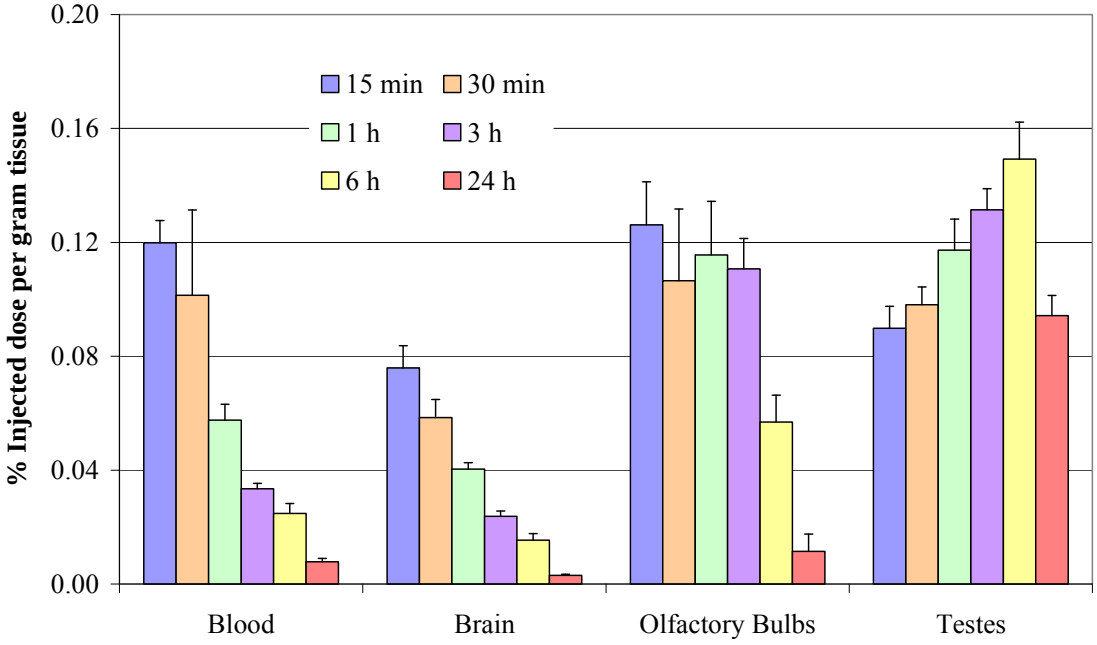

Figure 5.11 Biodistribution of [^{123}I]PBR200 in Sprague-Dawley rats in blood, brain, olfactory bulbs and testes.

The amount of radiotracer in the blood and brain decreased with time, with the uptake in the brain being lower than in the blood. The uptake into the testes and olfactory bulbs was higher than that of the blood, and was increasing as the amount in the blood decreased suggesting true uptake into these organs known to contain peripheral

benzodiazepine receptors. The uptake in the testes increased up 0.15% ID/g at 3 hours, followed by a decrease. The uptake in the olfactory bulbs remained between 0.11-0.13 % ID/g up to 3 h, followed by a decrease. The amount of radiotracer uptake in the gastrointestinal tract increased up to 2.4% ID/g at 6 hours, and decreased by 24 hours. The radioactivity in the stomach and gastrointestinal tract was probably due to the compound being excreted. Although not shown on the graph, at the timepoints 1, 3, 6 and 24 hours, the amount of radiotracer in the bladder was also determined, the highest being at 3 hours (4.8% ID/g), showing that the radiotracer was also being excreted in the urine.

5.3.2 *In Vivo* Biodistribution of [^{123}I]*N,N*-Diethyl-[2-(4-iodophenyl)-5,7-dimethylpyrazolo[1,5-*a*]pyrimidin-3-yl]acetamide [144]

[^{123}I]PBR215 was injected into 24 male Sprague-Dawley rats, and at 15 min, 30 min, 1, 3, 6, and 24 h, selected organs were removed, weighed, and the amount of radioactivity counted. The biodistribution of [^{123}I]PBR215 is summarised in Figure 5.12 and Figure 5.13. The uptake of activity observed after 15 min was highest in the lungs (17%), followed by the adrenals (5.2%), thyroid (5.0%), heart (4.0%), spleen (3.1%), and kidney (2.2%). Uptake in the lungs decreased from 15 min to 24 h, while the uptake in the heart remained around 4% ID/g from 15 min to 6 h, and then decreased to 2.4% at 24 h. The thyroid showed increasing uptake from 5-22% ID/g over the 24 h, suggesting *in vivo* deiodination. In the adrenals, uptake increased over time to around 9% ID/g at 24 h, and in the kidney remained around 2% ID/g up to 6 h. Figure 5.13 summarises the biodistribution in the blood, brain, olfactory bulbs and testes, which were all below 0.4% ID/g.

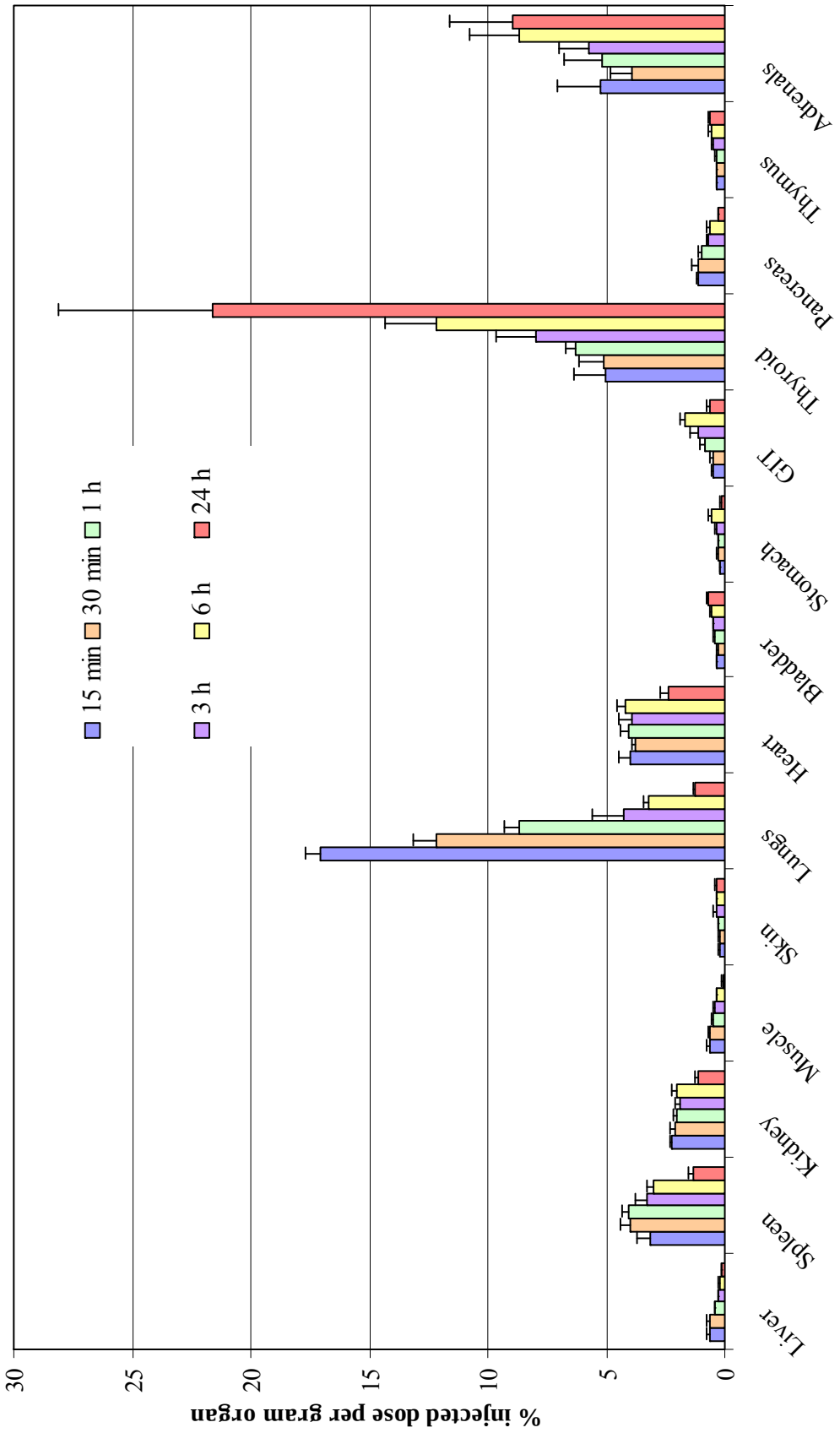

Figure 5.12 Biodistribution of [^{123}I]PBR215 in male Sprague-Dawley rats.

The amount of radiotracer in the blood, brain, and olfactory bulbs decreased with time, while the amount in the testes increased with time up to 0.2% ID/g at 24 h. The uptake in the olfactory bulbs decreased slower than that in the blood, displaying 0.20% ID/g in the olfactory bulbs at 24 h, compared to only 0.03% ID/g in the blood. In conclusion, [^{123}I]PBR215 exhibited high *in vivo* uptake of activity in tissues expressing the PBR.

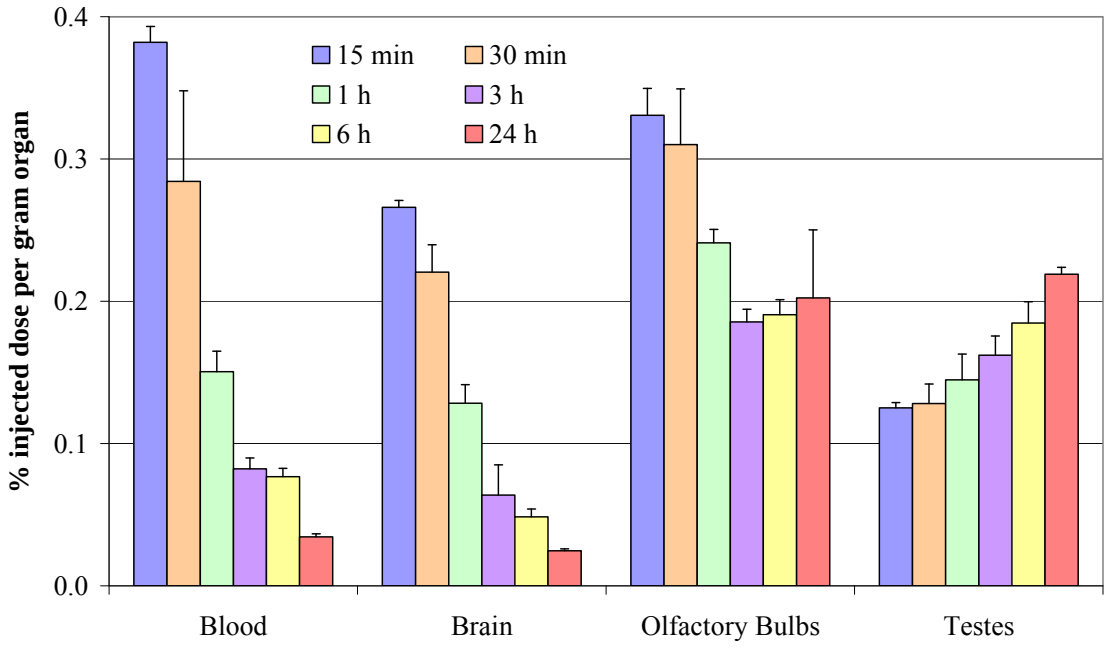

Figure 5.13 Biodistribution of [^{123}I]PBR215 in blood, brain, olfactory bulbs and testes.

5.4 *In Vivo* Competition Studies

5.4.1 *In Vivo* Competition Study of [^{123}I]*N*,*N*-Diethyl-(5-chloro-2-(4-iodophenyl)indol-3-yl)glyoxylamide [142]

To assess the specific binding of [^{123}I]PBR200 to PBR receptors *in vivo* in rats, the effect of pre-administration of PBR and CBR binding drugs on the distribution of the radioligand in various organs was examined. The competition drugs included non-radioactive PBR200, PK11195, Ro5-4864, flumazenil, and diazepam. PK11195 and

Ro5-4864 have affinity for peripheral benzodiazepine receptors; flumazenil has affinity for central benzodiazepine receptors; and diazepam has equal affinity for peripheral and central benzodiazepine receptors. For this experiment four rats for each competition drug, plus another four for a control (no competition drug, [^{123}I]PBR200 only) were used. Four rats per drug were injected with 1 mg/kg of the competition drug 5 min prior to injection of [^{123}I]PBR200. All rats were sacrificed 1 hour post injection of the [^{123}I]PBR200, and organs were removed. The organs used in this study include the liver, spleen, kidney, muscle, heart, blood, lungs, stomach, GIT, bladder, thyroid, pancreas, thymus, tail, adrenals, testes, brain, and olfactory bulb. The amount of radioactivity in each organ was measured using an automated gamma counter and the percent injected dose (% ID) for each organ as well as the percent injected dose per gram (% ID/g) of organ was calculated. The effects of the competition drugs on the uptake of [^{123}I]PBR200 into selected organs is summarised in Figure 5.14 and Figure 5.15.

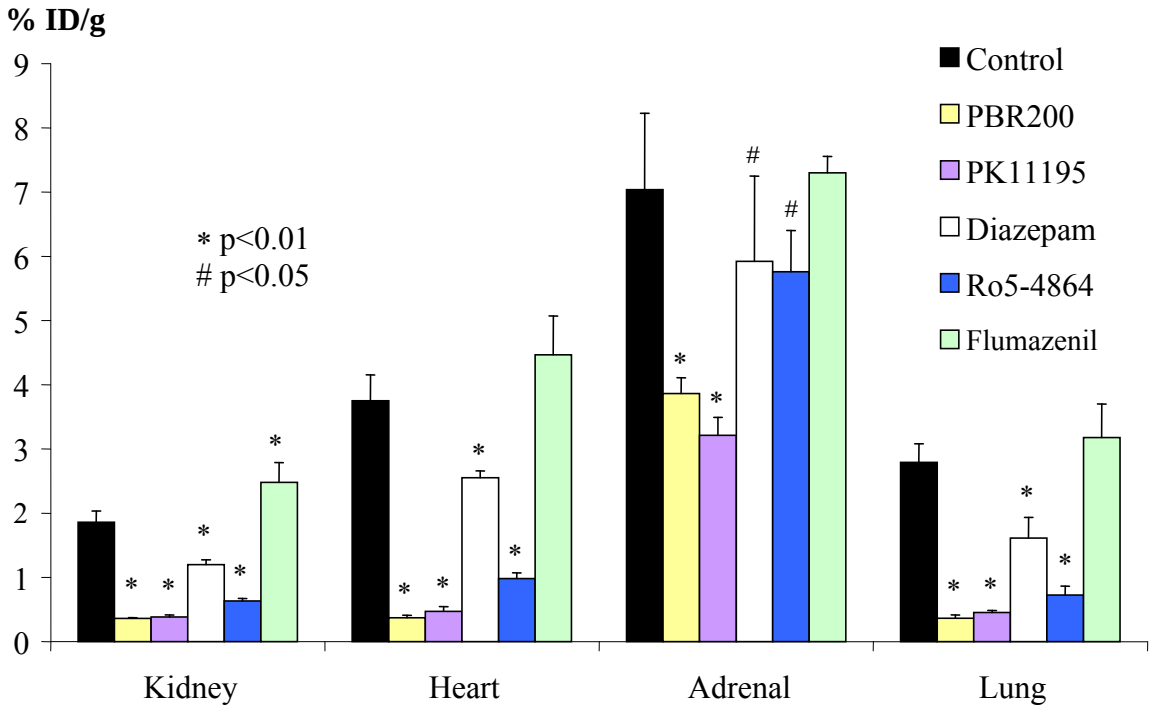

Figure 5.14 Effects of various drugs on [^{123}I]PBR200 uptake in rat organs.

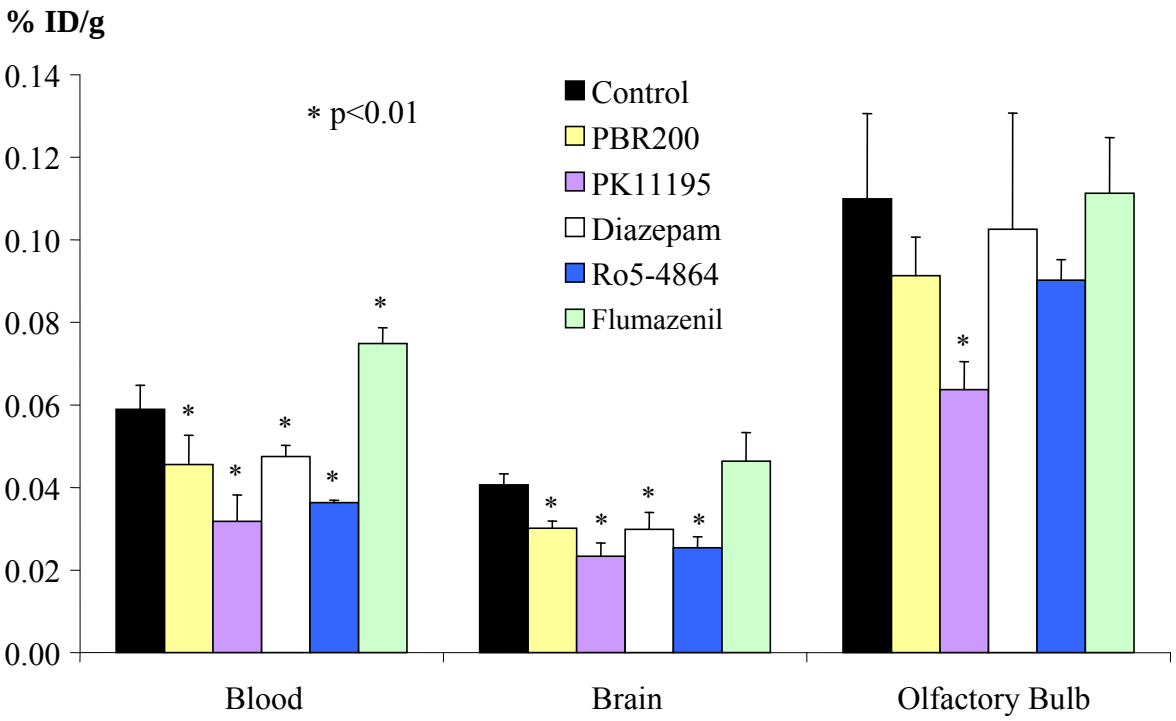

Figure 5.15 Effects of various drugs on [^{123}I]PBR200 uptake in rat blood, brain and olfactory bulbs.

The pre-administration of PBR binding drugs PK11195 and Ro5-4864 caused a significant reduction in the uptake of [^{123}I]PBR200 in the kidney, heart, and lungs ($p < 0.01$). There was over 80% reduction in uptake of [^{123}I]PBR200 in these organs due to PK11195 and over 65% reduction due to Ro5-4864. A 62% reduction of tracer uptake in the adrenals due to pre-administration with PK11195 was observed. There was no significant reduction of uptake in all organs with pre-administration with CBR binding drug, flumazenil, indicating there is negligible non-specific binding to CBR *in vivo*. Uptake of the tracer was prevented by both PK11195 and Ro5-4864 in most organs, however with a greater extent by PK11195 than Ro5-4864. Significant decrease in uptake of the radiotracer was observed in the blood and the brain with PBR200, PK11195, Ro5-4864 and diazepam, and in the olfactory bulbs with PK11195.

5.4.2 Competition Study of [^{123}I]*N*,*N*-Diethyl-[2-(4-iodophenyl)-5,7-dimethylpyrazolo[1,5-*a*]pyrimidin-3-yl]acetamide [144]

The competition study of [^{123}I]PBR215 included the drugs PK11195, Ro5-4864, and flumazenil, as well as the non-radioactive PBR215, and is summarised in Figure 5.16 and Figure 5.17. Results of the competition study showed that non-radioactive PBR215 significantly ($p<0.1$) decreased the uptake of [^{123}I]PBR215 in the spleen, kidney, heart, and lungs by 90%, 75%, 88% and 98% respectively. The PBR drug, PK11195, significantly ($p<0.1$) decreased the uptake in these organs by 64%, 41%, 44%, and 82% respectively. Interestingly, the other PBR drug, Ro5-4864, did not cause any significant decrease of uptake of radiotracer in the kidney or heart, but showed significant ($p<0.1$) 33% and 58% decrease in the spleen and lungs, respectively. A significant ($p<0.1$) increase of uptake of radiotracer in the adrenals was observed when pre-treated with PK11195 and Ro5-4864. This phenomenon has been observed in many similar studies at the injected concentration of 1 mg/kg and could be due to several factors including non-saturation of receptors due to the high number of binding sites. Figure 5.16 shows that PBR215, PK11195 and Ro5-4864 significantly ($p<0.1$) reduced the uptake of [^{123}I]PBR215 in the brain, and PBR215 and PK11195 significantly ($p<0.1$) reduced uptake in the olfactory bulbs.

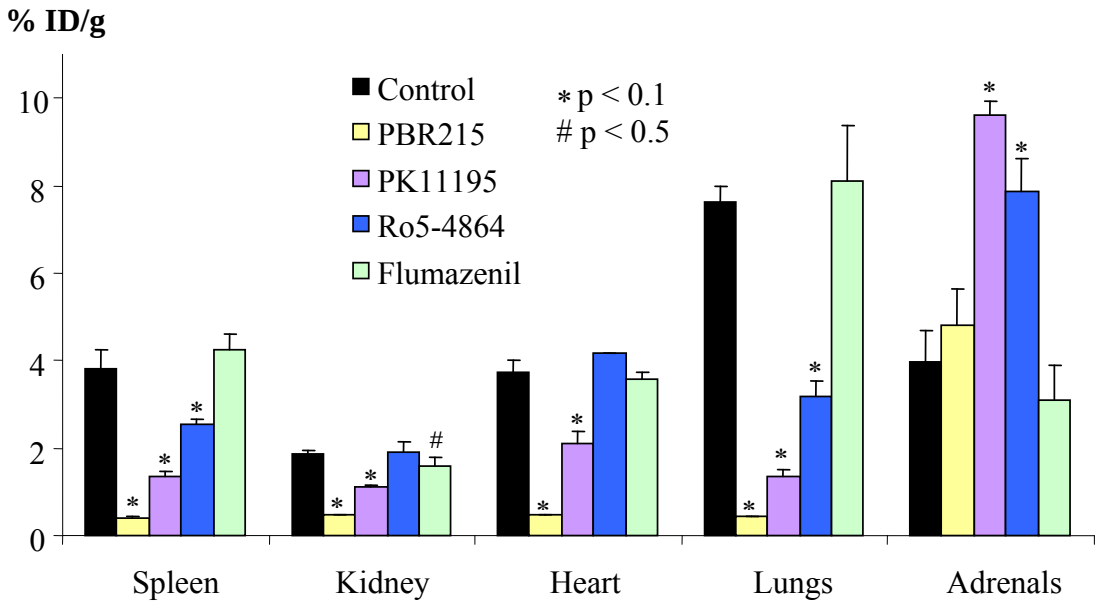

Figure 5.16 Effects of various drugs on [^{123}I]PBR215 uptake in rat organs.

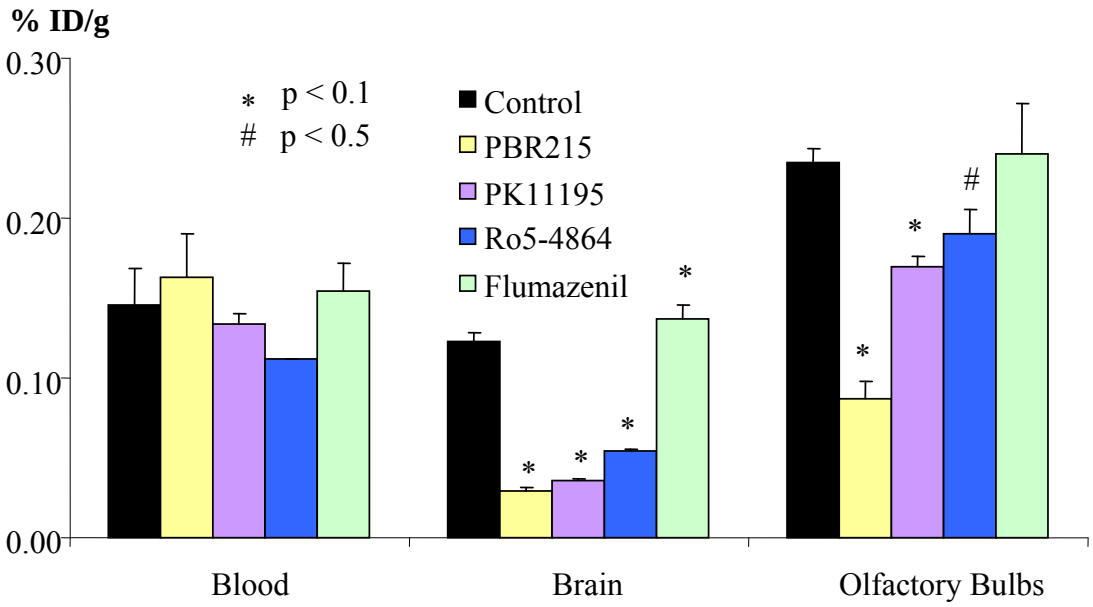

Figure 5.17 Effects of various drugs on [^{123}I]PBR215 uptake in rat organs.

These results are very interesting as they suggest that PK11195 blocks the binding of the [^{123}I]PBR215, but Ro5-4864 does not. It is thought by some groups that the PK11195 binding site and the Ro5-4864 binding site are in different locations on the

PBR protein.[58,59] It is also thought that these two binding sites overlap, and that a PBR ligand could bind to both parts at once.[59] The results of this competition study suggest that [^{123}I]PBR215 may bind to only the PK11195 binding site, and not the Ro5-4864 binding site.

The CBR drug flumazenil, did not significantly decrease the uptake of radiotracer in the spleen, heart, lungs, adrenals, blood, brain or olfactory bulbs.

5.5 *In Vivo* Stability Studies

Biodistribution studies are performed to determine the amount of radioactivity in organs after injection of a radiotracer into an animal. However, it is not known that the radioactivity measured is of intact (non-metabolised) radiotracer, or of some radioactive metabolite or free iodine. The purpose of an *in vivo* stability study is to determine the amount of intact tracer in organs at certain time points after injection of the radiotracer into an animal.

5.5.1 *In Vivo* Stability Study of [^{123}I]*N,N*-Diethyl-(5-chloro-2-(4-iodophenyl)indol-3-yl)glyoxylamide [142]

An *in vivo* stability study of [^{123}I]PBR200 was performed in three male Sprague-Dawley rats. [^{123}I]PBR200 (7 MBq in 100 μL per rat) was injected into the three rats and at 15 minutes, 1 hour, and 3 hours post injection, the rats were sacrificed and their organs and blood removed. The organs removed for this study included the adrenals, kidney, heart, brain and the plasma. The radioactivity in the tissues was extracted using acetonitrile

with sonication followed by centrifugation. The extractions were repeated at least twice to maximise extraction efficiency. The acetonitrile was evaporated to dryness and the radioactivity reconstituted in methanol. The methanol extract from each tissue as well as the standard radiotracer was analysed by radio-TLC.

More than 80% of the activity in each organ was extracted into the acetonitrile for the 15 min and 1 hour time points. More than 85% of the activity was extracted from the brain, heart, kidney and plasma for the 3 hour time point, however, only 76% from the adrenals.

The results of the study showed that in the adrenals, kidneys, heart, and brain, only [^{123}I]PBR200 was detected, with no evidence (<2%) of any radioactive metabolites, even at 3 hours post injection. In the plasma, 65% of the radioactivity was found to be intact [^{123}I]PBR200 at 3 hours post injection. These results show that it is indeed [^{123}I]PBR200 that is binding specifically to PBR in these organs, and that the compound is metabolically stable *in vivo*.

5.5.2 *In Vivo* Stability Study of [^{123}I]*N,N*-Diethyl-[2-(4-iodophenyl)-5,7-dimethylpyrazolo[1,5-*a*]pyrimidin-3-yl]acetamide [144]

An *in vivo* stability study of [^{123}I]PBR215 was performed as above. As the biodistribution of [^{123}I]PBR215 showed uptake of activity in the organs at 24 hours, a 24 hour time point was also added to the time points of 15 minutes, 1 hour, and 3 hours. The radiotracer was injected into four Sprague-Dawley rats. The extraction efficiencies for the brain, heart, kidney, and adrenals in all the timepoints ranged from 94% to 98% of the radioactivity extracted. The extraction efficiency for the plasma decreased from 75% at the 15 minute timepoint, to 67% at 1 hour, then 48% at the 3 hour timepoint. As

the extractions were performed exactly the same for all the organs, this low extraction efficiency could not be explained.

The percentage of intact radiotracer in the organs at the four timepoints is shown in Figure 5.18. The radiotracer was stable in the brain, heart, kidneys, and adrenals at 15 minutes, with 96% to >98% intact. The radiotracer remained stable in the brain, heart, and kidneys up to 1 hour, with 95% to > 98% intact. In the adrenals the radiotracer had started to metabolise, with 93% intact at 1 hour. At 3 hours, the radiotracer had metabolised a little in the brain, kidneys, heart and adrenals, with 81-88% still intact. At 24 hours, the radiotracer was between 71-81% intact. In the plasma the radiotracer metabolised immediately, and was 64% intact at 15 minutes, 62% at 1 hour, and 43% after 3 hours. The plasma at 24 hours did not contain sufficient radioactivity for a result at this timepoint. These results show that [^{123}I]PBR215 is metabolically stable in the brain, heart, and kidneys up to 1 hour, then after 1 hour, slowly starts to metabolise, with most of the radiotracer still intact after 24 hours. The radiotracer metabolised slightly faster in the adrenals.

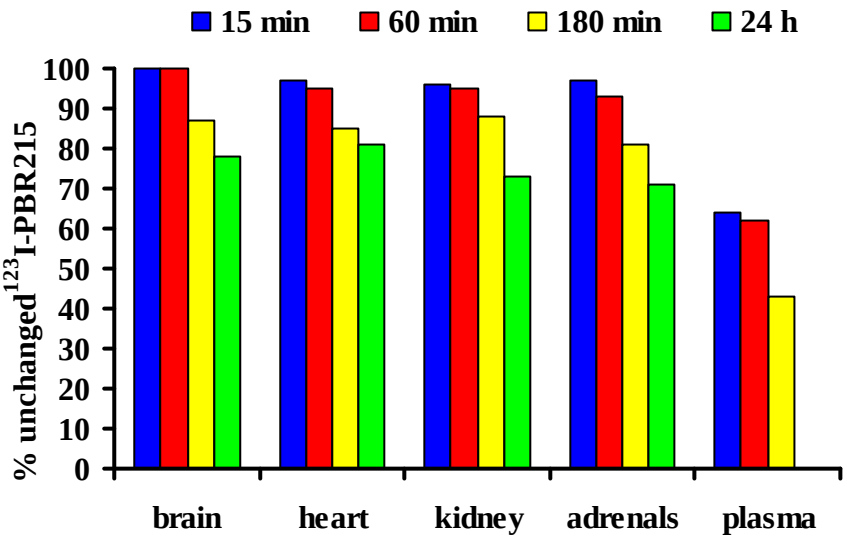

Figure 5.18 *In vivo* stability study of [^{123}I]PBR215 in Sprague-Dawley rats.

5.6 Conclusion and Future Directions

Two new high affinity PBR ligands were successfully radiolabelled with ^{123}I, which provides the first radioiodinated PBR ligands of these classes. *In vivo* biodistribution of [^{123}I]PBR200 and [^{123}I]PBR215 in male Sprague-Dawley rats indicated high activity uptake in organs expressing the PBR. Pre-treatment of PBR drugs, PK11195 and Ro5-4864 significantly reduced the uptake of [^{123}I]PBR200 in the kidneys, heart, adrenals, lungs, and brain. [^{123}I]PBR215 had higher uptake than [^{123}I]PBR200 in organs expressing PBR, however, pre-treatment with Ro5-4864 did not decrease the uptake of [^{123}I]PBR215 in the kidney, heart and adrenals. This suggests that PBR200 and PBR215 may bind to different areas of the binding site. Future studies would involve the *in vivo* evaluation of [^{123}I]PBR200 and [^{123}I]PBR215 in different tumour models using biodistribution studies and SPECT imaging.

6 Conclusions and Future Directions

The synthesis of fifteen new halogenated *N,N*-dialkyl-2-phenylindol-3-ylglyoxylamides was achieved. The synthetic strategy for these compounds included formation of a phenylhydrazone, from which the indole was prepared via Fischer indole synthesis. Acylation at position 3 of the indole with oxalyl chloride, followed by amination using various *N,N*-dialkylamines, gave the target compounds. The PBR and CBR binding affinities of the 15 compounds were determined by measuring the displacement of [^{3}H]PK11195 from rat kidney mitochondrial membranes or the displacement of [^{3}H]flumazenil from rat cortex membranes respectively. All compounds were selective for the PBR, displaying >2000 nM affinity for the CBR. Most of the compounds showed high nanomolar affinity for PBR, however, the presence of a bulky iodine atom on the phenyl ring decreased the PBR binding affinity, compared to the brominated compounds or literature compounds with a smaller chlorine or fluorine atom. The PBR affinity of the iodinated compounds was increased by placing shorter alkyl chains on the amide, and a chloro on position 5 of the indole, giving an iodinated compound with an IC_{50} value of 8.23 nM. This high affinity compound was radiolabelled with ^{123}I for *in vivo* pharmacological evaluation in Sprague-Dawley rats. Radiolabelling was achieved in 60% radiochemical yield, to give the first radiolabelled *N,N*-dialkyl-2-phenylindol-3-ylglyoxylamide. This radiolabelled product, named [^{123}I]PBR200, showed high uptake into all organs possessing PBR, and this uptake was shown to be specific as it was decreased by PBR drugs, PK11195 and Ro5-4864. [^{123}I]PBR200 was found to be metabolically stable in the heart, brain, adrenals, and kidneys up to 3 hours. Future studies would involve the further evaluation of [^{123}I]PBR200 in animals with various

tumours, or in animal models of neurodegeneration using SPECT imaging, biodistribution studies, and autoradiography.

The synthesis of three new iodinated 2-arylpyrazolo[1,5-*a*]pyrimidin-3-yl acetamides was achieved. The synthetic method reported in the literature was improved upon in this work. The alkylation of 4-iodobenzoylacetonitrile in the synthesis of *N*,*N*-dialkyl-[3-cyano-4-(4-iodophenyl)-4-oxo]butanamides was improved by using a phase transfer catalyst with K_2CO_3, although a dialkylated side-product was identified. The reaction to form the pyrazole ring was also optimised, using THF instead of EtOH as the solvent. It was found that ethanol was acting as a nucleophile to give an ethyl ester side-product. The iodinated 2-arylpyrazolo[1,5-*a*]pyrimidinyl-3-yl acetamides synthesised had different lengths of alkyl groups on the amide. The compound with propyl groups was found to have a higher binding affinity than compounds with ethyl or methyl groups. This compound, with an IC_{50} of 7.9 nM, had the highest binding affinity out of all compounds synthesised in this thesis. This was the last compound to be tested, and unfortunately there was insufficient time to radiolabel and perform *in vivo* studies. The compound with ethyl groups with a PBR IC_{50} of 11.7 nM was radiolabelled with ^{123}I in a 95% radiochemical yield. *In vivo* studies showed high uptake of radioactivity into PBR organs. The uptake of radioactivity in the kidney and heart was decreased by PBR drug PK11195, but not by Ro5-4864, suggesting that this radioligand binds to the same site on the receptor as PK11195, but a different site to Ro5-4864. Metabolite studies showed [^{123}I]PBR215 was not as metabolically stable as [^{123}I]PBR215, however was still relatively stable, with 80% of the radioactivity being intact [^{123}I]PBR215 after 3 hours. Future studies would involve the synthesis of a 2-arylpyrazolo[1,5-*a*]pyrimidinyl-3-yl acetamide with a dibutylacetamide group. Depending on whether the

dipropyl or dibutyl compound has the highest PBR binding affinity, one of these could be radiolabelled with ^{123}I and evaluated *in vivo*.

The synthesis of a brominated and an iodinated pyrrolobenzoxazepine for PBR testing was achieved in a synthetic scheme of seven steps. The brominated compound displayed a higher binding affinity than its iodinated analogue, with PBR IC_{50} values of 24.0 nM and 39.4 nM respectively. Only one pyridopyrrolooxazepine was synthesised, and it showed similar binding affinity (IC_{50} = 35.7 nM) as the pyrrolobenzoxazepines. These three compounds were selective for PBR, showing over 5000 nM affinity for the CBR. An unexpected side-product was also tested for PBR binding affinity but was shown to be inactive. None of these compounds were radiolabelled with ^{123}I for *in vivo* evaluation. The synthesis of a compound with the iodine placed on the benzoxazepine ring instead of the phenyl ring was attempted; however, the synthesis was not finished. Future directions would involve completion of this synthetic scheme and providing more compounds for PBR binding affinity testing and potential radioiodination and *in vivo* evaluation.

The results of this study have made significant progress towards the development of an imaging agent for the PBR. Potential candidate ligands have been identified by selecting suitable classes of compounds, and advanced schemes were used to synthesise a series of compounds which could be evaluated using SAR.

7 Experimental

7.1 General Experimental

All reagents were purchased from commercial sources and were used without further purification. Petroleum ether (PE) of boiling point range 40-60 °C was used. Melting points were carried out on a Gallenkamp melting point apparatus and are uncorrected. Elemental analyses were performed on a Carlo Erba 1106 Elemental Analyser at the Campbell Microanalytical Laboratory at the University of Otago (Dunedin, New Zealand) and results reported were within ±0.4% of the theoretical values.

Proton and carbon nuclear magnetic resonance (NMR) spectra were recorded using a Bruker 400 MHz spectrometer. Spectra were recorded in deuterated chloroform ($CDCl_3$) or deuterated dimethylsulfoxide (d_6-DMSO) unless otherwise specified, using tetramethylsilane (δ 0.00) or dimethylsulfoxide (δ 2.50) as the internal standard. Chemical shifts (δ) in ppm were measured relative to the internal standard. Signals are recorded as broad singlet (bs), singlet (s), doublet (d), doublet of doublets (dd), triplet (t), quartet (q) and multiplet (m). Coupling constants (*J*) are reported as Hertz.

Chemical ionization (CI), electron impact (EI) and electrospray (ES) mass spectra were obtained using either a Shimadzu QP-5000, VG Quattro triple quadrupole system, or an Autospec high-resolution mass spectrometer.

Analytical thin layer chromatography (TLC) was performed on Merck Kieselgel 60 F_{254} precoated polyester plates with a thickness of 250 μm. Column chromatography was

performed on Merck Keiselgel 60 (220-440 mesh). High performance liquid chromatography (HPLC) was performed on an Phenomenex bondclone semipreparative RP C-18 column using a Waters 510 pump, an Activon Linear UV detector set at 254 nm and an in-line NaI-Berthold radioactivity detector.

[^{3}H]PK11195 and [^{3}H]flumazenil were purchased from Perkin-Elmer Life Sciences (Boston, MA, USA). Carrier free Na^{123}I in 0.1M NaOH was obtained from Australian Radioisotopes and Industrials (ARI), Australia. Male Sprague-Dawley rats were purchased from Animal Resources Centre (Perth, WA, Australia). The rodents were housed in cages with access to standard rodent chow and water *ad libitum* in an animal house equipped with a high standard ventilation system and maintained at 22 ± 2 ^{o}C, 60% ± 10% humidity. Air changes were set at 15 changes/h and a 12 h/12 h light/dark cycle. All procedures were carried out in compliance with Australian laws governing animal experimentation.

The experimental data is divided into:

1. Experimental procedures for the synthesis of indole compounds
2. Experimental procedures for the synthesis of 2-arylpyrazolo[1,5-*a*]pyrimidin-3-yl acetamides
3. Experimental procedures for the synthesis of pyrrolobenzoxazepine and pyridopyrrolooxazepine compounds
4. Experimental procedures for the stannylation reactions and radioiodination reactions

Known literature compounds have their name written in *italics,* while new compounds have their names written in non-italics.

7.2 Experimental Procedures for the Synthesis of Indole Compounds

7.2.1 Experimental Procedures for the Synthesis of 5-Chlorosubstituted Indol-3-ylglyoxylamides

4-Iodoacetophenone 4-chlorophenylhydrazone [42]

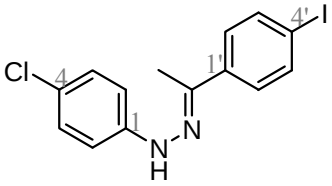

A mixture of 4-iodoacetophenone (4.15 g, 16.9 mmol), 4-chlorophenylhydrazine hydrochloride (3.00 g, 16.8 mmol) and 10 drops of glacial AcOH in EtOH (40 mL) was heated at reflux for 45 min. The precipitate which formed on cooling was filtered and the solid washed with dilute HCl (10 mL) followed by cold 95% EtOH (10 mL). The crude product was recrystallised from EtOH to yield **[42]** (3.34 g, 54%) as yellow crystals, mp. 130-132 °C. ^{1}H NMR ($CDCl_3$) δ 2.21 (s, 3H, CH_3), 7.11 (d, 2H, *J* = 8.9, ArH2 and ArH6), 7.24 (d, 2H, *J* = 8.9, ArH3 and ArH5), 7.34 (bs, 1H, NH), 7.51 (d, 2H, *J* = 8.6, ArH2' and ArH6'), 7.71 (d, 2H, *J* = 8.6, ArH3' and ArH5'). ^{13}C NMR ($CDCl_3$) δ 12.0 (CH_3), 94.2 (ArC4'), 114.8 (ArC2 and ArC6), 125.4 (ArC4), 127.7 (ArC2' and ArC6'), 129.6 (ArC3 and ArC5), 137.8 (ArC3' and ArC5'), 138.8 (ArC1'), 141.0 (CN), 144.0 (ArC1). MS-EI *m/z* 372 (^{37}Cl M^+, 6), 370 (^{35}Cl M^+, 33), 149 (100%). HRMS-EI calculated for $C_{14}H_{12}N_2{}^{37}ClI$: 371.9704, found 371.9704. Anal. calculated for $C_{14}H_{12}ClIN_2$: C, 45.37; H, 3.26; N, 7.56. Found: C, 45.67; H, 3.37; N, 7.47.

4-Bromoacetophenone 4-chlorophenylhydrazone [43]

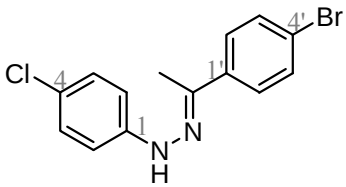

A mixture of 4-bromoacetophenone (6.89 g, 34.6 mmol) and 4-chlorophenylhydrazine hydrochloride (6.20 g, 34.6

mmol) in EtOH (60 mL) and 10 drops of glacial AcOH was heated at reflux for 5 h. Crystals appeared as the solution cooled, which were collected by filtration and washed with distilled water, then cold 95% EtOH (10 mL). The resulting pale yellow crystals were dried in a 110 °C oven to yield **[43]** (8.38 g, 75%), mp. 132-134 °C. ^{1}H NMR ($CDCl_3$) δ 2.20 (s, 3H, CH_3), 7.09 (d, 2H, *J* = 8.9, ArH2 and ArH6), 7.23 (d, 2H, *J* = 8.9, ArH3 and ArH5), 7.33 (bs, 1H, NH), 7.49 (d, 2H, *J* = 8.7, ArH2' and ArH6'), 7.64 (d, 2H, *J* = 8.7, ArH3' and ArH5'). ^{13}C NMR (DMSO) δ 13.4 (CH_3), 115.0 (ArC2 and ArC6), 121.6 (ArC4'), 123.1 (ArC4), 127.9 (ArC2' and ArC6'), 129.4 (ArC3 and ArC5), 131.8 (ArC3' and ArC5'), 138.9 (ArC1'), 140.9 (CN), 145.5 (ArC1). MS-EI *m/z* 326 ($^{81}Br^{37}Cl$ M^+, 17), 324 ($^{79}Br^{37}Cl$ and $^{81}Br^{35}Cl$ M^+, 74), 322 ($^{79}Br^{35}Cl$ M^+, 57), 126 (100%). HRMS-EI calculated for $C_{14}H_{12}N_2{}^{35}Cl^{79}Br$: 321.9872, found 321.9873. Anal. calculated for $C_{14}H_{12}BrClN_2$: C, 51.96; H, 3.74; N, 8.66. Found: C, 52.07; H, 3.59; N, 8.88.

5-Chloro-2-(4-iodophenyl)indole [44]

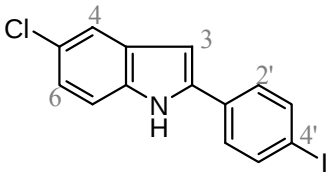

A mixture of hydrazone **[42]** (3.10 g, 8.4 mmol) and polyphosphoric acid (20 g) was stirred for 30 min at 110 °C. Ice water (250 mL) was added and the mixture was manually stirred until a precipitate formed. The precipitate was filtered, washed with water, and recrystallised from 95% EtOH, to yield **[44]** (1.66 g, 56%) as a white solid, mp. 210-211 °C. ^{1}H NMR (DMSO) δ 6.92 (s, 1H, H3), 7.10 (dd, 1H, $J_{6,7}$ = 8.6, $J_{6,4}$ = 2.0, H6), 7.39 (d, 1H, $J_{7,6}$ = 8.6, H7), 7.57 (d, 1H, $J_{4,6}$ = 1.9, H4), 7.66 (d, 2H, *J* = 8.4, ArH2' and ArH6'), 7.83 (d, 2H, *J* = 8.4, ArH3' and ArH5'), 11.77 (s, 1H, NH). ^{13}C NMR (DMSO) δ 95.4 (ArC4'), 100.6 (C3), 114.5 (C7), 120.9 (C4), 123.5 (C6), 125.7 (C5), 128.8 (ArC2' and ArC6'), 131.3 (C3a), 132.9 (ArC1'), 137.3 (C7a), 139.4 (ArC3'

and ArC5'), 139.9 (C2). MS-CI *m/z* 356 (^{37}Cl M+1, 14), 354 (^{35}Cl M+1, 34), 230 (^{37}Cl M+1 - I, 39), 228 (^{35}Cl M+1 - I, 100%). HRMS-EI calculated for $C_{14}H_9N^{35}ClI$: 352.9468, found 352.9473. Anal. calculated for $C_{14}H_9ClIN$: C, 47.56; H, 2.57; N, 3.96. Found: C, 47.56; H, 2.36; N, 4.18.

2-(4-Bromophenyl)-5-chloroindole [45]

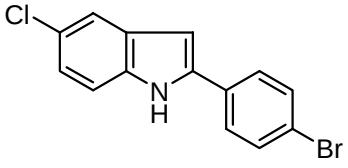

A mixture of 4-bromoacetophenone 4-chlorophenylhydrazone **[43]** (5.12 g, 15.8 mmol) and polyphosphoric acid (30 g) was heated at 100-110 °C until the yellow mixture turned reddish brown. The mixture was then added to ice water (250 mL) and stirred until a precipitate formed. The resulting solid was filtered, washed with water, and recrystallised from 95% EtOH to produce **[45]** (3.35 g, 69%) as a pale yellow solid, mp. 206–207 °C. ^{1}H NMR (DMSO) δ 6.91 (s, 1H, H3), 7.11 (dd, 1H, $J_{6,7}$ = 8.6, $J_{6,4}$ = 2.0, H6), 7.40 (d, 1H, $J_{7,6}$ = 8.6, H7), 7.57 (d, 1H, $J_{4,6}$ = 1.9, H4), 7.66 (d, 2H, J = 8.5, ArH2' and ArH6'), 7.80 (d, 2H, J = 8.5, ArH3' and ArH5'), 11.79 (s, 1H, NH). ^{13}C NMR (DMSO) δ 99.0 (C3), 112.8 (C7), 119.2 (C4), 120.8 (ArC4'), 121.8 (C6), 124.1 (C5), 127.1 (ArC2' and ArC6'), 129.7 (C3a), 130.9 (ArC1'), 131.9 (ArC3' and ArC5'), 135.7 (C7a), 138.1 (C2). MS-CI *m/z* 310 (^{81}Br^{37}Cl M+1, 22), 308 (^{81}Br^{35}Cl and ^{79}Br^{37}Cl M+1, 79), 306 (^{79}Br^{35}Cl M+1, 69), 230 (^{37}Cl M+1 - Br, 38), 228 (^{35}Cl M+1 - Br, 100%). HRMS-EI calculated for $C_{14}H_9N^{35}Cl^{81}Br$: 306.9586, found 306.9598. Anal. calculated for $C_{14}H_9BrClN$: C, 54.85; H, 2.96; N, 4.57. Found: C, 54.93; H, 3.11; N, 4.50.

[5-Chloro-2-(4-iodophenyl)indol-3-yl]glyoxylyl chloride [46]

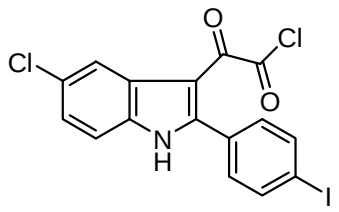

Acylation Method: Oxalyl chloride (0.22 mL, 2.57 mmol) was added dropwise to a solution of 5-chloro-2-(4-iodophenyl)indole **[44]** (0.65 g, 1.84 mmol) at 0 °C in anhydrous diethyl ether (10 mL), and the reaction was stirred at RT for 1 h. The solution was cooled, and the precipitate which formed was collected by filtration and washed with anhydrous diethyl ether (2 x 5 mL) to give the acid chloride **[46]** (0.72 g, 88%) as a yellow solid, which was used without further purification for subsequent reactions. ^{1}H NMR (DMSO) δ 7.33 (d, 1H, $J_{6,7}$ = 8.6, H6), 7.38 (d, 2H, J = 8.1, ArH2' and ArH6'), 7.54 (d, 1H, $J_{7,6}$ = 8.6, H7), 7.89 (d, 2H, J = 8.1, ArH3' and ArH5'), 8.08 (s, 1H, H4), 12.83 (bs, 1H, NH).

[2-(4-Bromophenyl)-5-chloroindol-3-yl]glyoxylyl chloride [47]

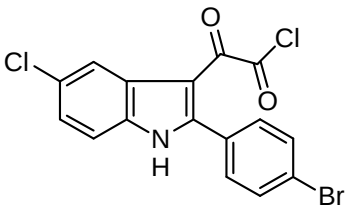

The title compound was prepared as a yellow solid (1.96 g, 98%) from oxalyl chloride (0.62 mL, 7.08 mmol) and **[45]** (1.55 g, 5.06 mmol) in anhydrous diethyl ether (14 mL) using the *acylation method*, and was used without further purification for subsequent amination reactions. ^{1}H NMR (DMSO) δ 7.34 (dd, 1H, $J_{6,7}$ = 8.6, $J_{6,4}$ = 2.1, H6), 7.38 (d, 2H, J = 8.3, ArH2' and ArH6'), 7.54 (d, 1H, $J_{7,6}$ = 8.6, H7), 7.90 (d, 2H, J = 8.3, ArH3' and ArH5'), 8.08 (d, 1H, $J_{4,6}$ = 2.0, H4), 12.84 (s, 1H, NH).

***N,N*-Dihexyl-[5-chloro-2-(4-iodophenyl)indol-3-yl]glyoxylamide [48]**

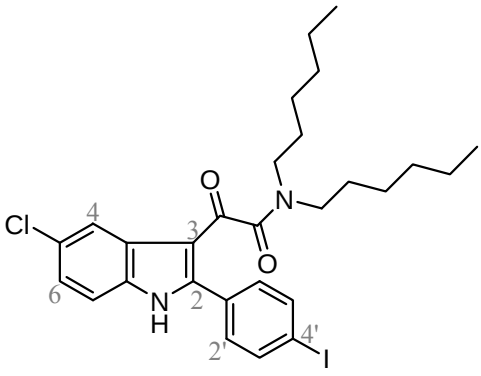

Amination Method: To a solution of **[46]** (0.30 g, 0.67 mmol) and NEt_3 (0.11 mL, 0.81 mmol) in anhydrous toluene (30 mL) at 0 °C was added dropwise a solution of dihexylamine (0.17 mL, 0.74 mmol) in anhydrous toluene (20 mL). The solution was stirred at RT for 24 h. The solution was filtered and the filtrate was washed sequentially with 0.5M HCl (25 mL), saturated $NaHCO_3$ (25 mL) and water (25 mL). The combined organic extracts were dried ($MgSO_4$) and the solvent evaporated. The crude product was subjected to silica gel column chromatography using MeOH:$CHCl_3$ (1:19), and the appropriate fractions were concentrated. The residue was recrystallised from EtOAc:PE (1:9) to afford **[48]** (0.12 g, 30%) as a white solid, mp. 108–110 °C. ^{1}H NMR (DMSO) δ 0.75 (t, 3H, *J* = 6.9, CH_3), 0.88 (t, 3H, *J* = 6.8, CH_3), 1.00-1.20 (m, 10H, 5 x CH_2), 1.21-1.35 (m, 4H, 2 x CH_2), 1.36-1.46 (m, 2H, CH_2), 2.94-3.08 (m, 4H, 2 x NCH_2), 7.32 (dd, 1H, *J* = 8.7, 1.8, H6), 7.37 (d, 2H, *J* = 8.1, ArH2' and ArH6'), 7.50 (d, 1H, *J* = 8.7, H7), 7.88 (d, 2H, *J* = 8.1, ArH3' and ArH5'), 8.04 (s, 1H, H4), 12.68 (bs, 1H, NH). ^{13}C NMR (DMSO) δ 15.4 (CH_3), 15.6 (CH_3), 23.5 (CH_2), 23.7 (CH_2), 27.2 (CH_2), 27.9 (CH_2), 28.1 (CH_2), 29.3 (CH_2), 32.3 (CH_2), 32.8 (CH_2), 45.4 (NCH_2), 48.9 (NCH_2), 98.7 (ArC4'), 111.0 (C3), 115.5 (C7), 121.7 (C4), 125.3 (C6), 128.9 (C3a), 129.5 (C5), 131.4 (ArC1'), 133.5 (ArC2' and ArC6'), 136.0 (C7a), 138.6 (ArC3' and ArC5'), 148.9 (C2), 168.6 (NC=O), 188.6 (C=O). MS-EI *m/z* 592 (^{35}Cl M^+, 3), 382 (^{37}Cl M^+ - $CON(Hex)_2$, 34), 380 (^{35}Cl M^+ - $CON(Hex)_2$, 100%). HRMS-ES calculated for $C_{28}H_{35}N_2O_2{}^{35}ClI$: 593.1432, found 593.1470. Anal. calculated for $C_{28}H_{34}ClIN_2O_2$: C, 56.72; H, 5.78; N, 4.72. Found: C, 56.49; H, 5.75; N, 4.72.

_N,N_-Di-_n_-propyl-[5-chloro-2-(4-iodophenyl)indol-3-yl]glyoxylamide [49]

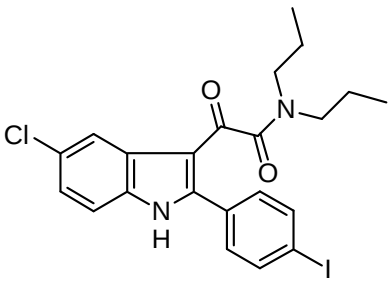

The title compound was prepared as an off-white solid (0.47 g 57%) from **[46]** (0.72 g, 1.78 mmol) and NEt_3 (0.27 mL, 1.95 mmol) in anhydrous toluene (55 mL) and di-*n*-propylamine (0.25 mL, 1.78 mmol) in anhydrous toluene (35 mL) using the *amination method*. The product was triturated in PE. mp. 148-150 °C. ^{1}H NMR (DMSO) δ 0.69 (t, 3H, J = 7.4, CH_3), 0.78 (t, 3H, J = 7.4, CH_3), 1.12-1.28 (m, 2H, CH_2), 1.40-1.50 (m, 2H, CH_2), 2.95 (t, 2H, J = 7.8, NCH_2), 3.01 (t, 2H, J = 7.7, NCH_2), 7.31 (dd, 1H, $J_{6,7}$ = 8.6, $J_{6,4}$ = 2.1, H6), 7.35 (d, 2H, J = 8.3, ArH2' and ArH6'), 7.51 (d, 1H, $J_{7,6}$ = 8.6, H7), 7.87 (d, 2H, J = 8.3, ArH3' and ArH5'), 8.02 (d, 1H, $J_{4,6}$ = 1.9, H4). ^{13}C NMR (DMSO) δ 12.5 (CH_3), 13.1 (CH_3), 21.6 (CH_2), 22.8 (CH_2), 47.2 (NCH_2), 50.8 (NCH_2), 98.6 (ArC4'), 111.05 (C3), 115.5 (C7), 121.6 (C4), 125.3 (C6), 128.9 (C3a), 129.5 (C5), 131.4 (ArC1'), 133.4 (ArC2' and ArC6'), 136.0 (C7a), 138.6 (ArC3' and ArC5'), 149.0 (C2), 168.8 (NC=O), 188.5 (C=O). MS-ES *m/z* 511 (^{37}Cl M+1, 26), 509 (^{35}Cl M+1, 88), 106 (100%). HRMS-ES calculated for $C_{22}H_{23}N_2O_2{}^{35}ClI$: 509.0493, found 509.0524. Anal. calculated for $C_{22}H_{22}ClIN_2O_2$: C, 51.94; H, 4.36; N, 5.51. Found: C, 52.14; H, 4.58; N, 5.53.

_N,N_-Diethyl-[5-chloro-2-(4-iodophenyl)indol-3-yl]glyoxylamide [50]

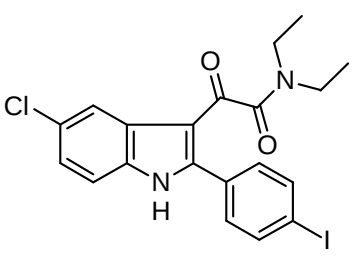

The title compound was prepared as clear crystals (0.14 g, 36%) from **[46]** (0.39 g, 0.80 mmol) and NEt_3 (0.13 mL, 0.96 mmol) in anhydrous toluene (45 mL) and diethylamine (0.09 mL, 0.88 mmol) in anhydrous toluene (20 mL) using the *amination method*. The product was subjected to silica gel column

chromatography using EtOAc:PE (1:1). Clear crystals formed in several fractions, which were collected by filtration to afford **[50]** (0.14 g, 36%), mp. 221-222 °C. ^{1}H NMR (DMSO) δ 0.83 (t, 3H, J = 7.1, CH_3), 1.02 (t, 3H, J = 7.0, CH_3), 3.07 (q, 2H, J = 7.1, CH_2), 3.15 (q, 2H, J = 7.0, CH_2), 7.32 (dd, 1H, $J_{6,7}$ = 8.6, $J_{6,4}$ = 2.1, H6), 7.37 (d, 2H, J = 8.3, ArH2' and ArH6), 7.51 (d, 1H, $J_{7,6}$ = 8.6, H7), 7.88 (d, 2H, J = 8.3, ArH3' and ArH5'), 8.05 (d, 1H, $J_{4,6}$ = 2.0, H4). ^{13}C NMR (DMSO) δ 12.5 (CH_3), 14.1 (CH_3), 38.4 (NCH_2), 42.2 (NCH_2), 97.4 (ArC4'), 109.8 (C3), 114.3 (C7), 120.5 (C4), 124.1 (C6), 127.7 (C3a), 128.4 (C5), 130.3 (ArC1'), 132.3 (ArC2' and ArC6'), 134.8 (C7a), 137.3 (ArC3' and ArC5'), 147.9 (C2), 167.1 (NC=O), 187.4 (C=O). MS-ES *m/z* 480 (^{37}Cl M-1, 37), 478 (^{35}Cl M-1, 100%). HRMS-ES calculated for $C_{20}H_{19}N_2O_2{}^{35}ClI$: 481.0180, found 481.0180. Anal. calculated for $C_{20}H_{18}ClIN_2O_2$: C, 49.97; H, 3.77; N, 5.83. Found: C, 50.27; H, 4.05; N, 5.85.

***N,N*-Dimethyl-[5-chloro-2-(4-iodophenyl)indol-3-yl]glyoxylamide [51]**

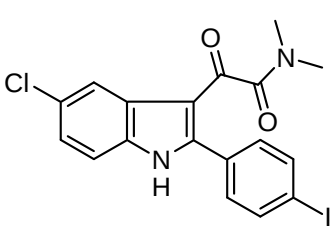

Dimethylamine (30 mL, 40% wt/vol in water) was gently heated and under constant N_2 pressure passed through NaOH pellets and bubbled into a solution of **[46]** (0.65 g, 1.46 mmol) and NEt_3 (0.27 mL, 1.90 mmol) in anhydrous toluene (50 mL). After 15 min, dimethylamine (4 mL, 40% wt/vol in water) was added to the toluene solution, and this was stirred for 30 min. The toluene solution was washed with saturated $NaHCO_3$ (25 mL), dilute HCl (25 mL), then water (25 mL). The organic extracts were dried ($MgSO_4$), filtered, and evaporated to dryness. The reddish solid was triturated in EtOAc:PE (3:7) to form **[51]** (65 mg, 10%) as an off-white solid, mp. 238 °C (d). ^{1}H NMR (DMSO) δ 2.45 (s, 3H, NCH_3), 2.79 (s, 3H, NCH_3), 7.32 (d, 2H, J = 8.3, ArH2' and ArH6'), 7.33 (dd, 1H, J = 8.6, 2.2, H6), 7.52 (d, 1H, J = 8.6, H7), 7.91

(d, 2H, J = 8.3, ArH3' and ArH5'), 8.11 (d, 1H, J = 2.0, H4). ^{13}C NMR (DMSO) δ 33.7 (NCH_3), 37.4 (NCH_3), 97.9 (ArC4'), 110.6 (C3), 114.8 (C7), 121.1 (C4), 124.7 (C6), 128.3 (C3a), 128.8 (C5), 130.6 (ArC1'), 132.5 (ArC2' and ArC6'), 135.3 (C7a), 137.7 (ArC3' and ArC5'), 148.8 (C2), 167.5 (NC=O), 188.1 (C=O). MS-ES *m/z* 455 (^{37}Cl M+1, 4), 453 (^{35}Cl M+1, 21), 338 (100%). HRMS-ES calculated for $C_{18}H_{15}N_2O_2{}^{35}ClI$: 452.9867, found 452.9872. Anal. calculated for $C_{18}H_{14}ClIN_2O_2$: C, 47.76; H, 3.12; N, 6.19. Found: C, 47.54; H, 3.39; N, 5.89.

***N,N*-Dihexyl-[2-(4-bromophenyl)-5-chloroindol-3-yl]glyoxylamide [52]**

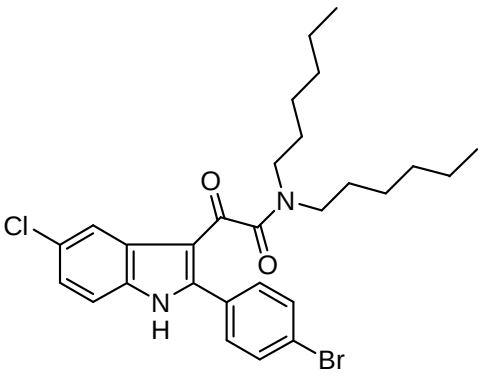

The title compound was prepared as a white solid (0.20 g, 32%) from **[47]** (0.46 g, 1.16 mmol) and NEt_3 (0.19 mL, 1.39 mmol) in anhydrous toluene (30 mL) and dihexylamine (0.30 mL, 1.27 mmol) in anhydrous toluene (20 mL) using the *amination method*. The product was subjected to silica gel column chromatography using EtOAc:PE (2:3), and the isolated product was recrystallised from EtOAc:PE (1:9), mp. 103–105 °C. ^{1}H NMR (DMSO) δ 0.77 (t, 3H, J = 7.0, CH_3), 0.87 (t, 3H, J = 6.8, CH_3), 1.00–1.34 (m, 14H, 7 x CH_2), 1.35–1.46 (m, 2H, CH_2), 2.95–3.09 (m, 4H, 2 x NCH_2), 7.32 (dd, 1H, $J_{6,7}$ = 8.6, $J_{6,4}$ = 2.0, H6), 7.51 (d, 1H, $J_{7,6}$ = 8.7, H7), 7.54 (d, 2H, J = 8.4, ArH2' and ArH6') 7.72 (d, 2H, J = 8.4, ArH3' and ArH5'), 8.03 (s, 1H, H4). ^{13}C NMR (DMSO) δ 14.7 (CH_3), 14.9 (CH_3), 22.8 (CH_2), 23.0 (CH_2), 26.5 (CH_2), 27.1 (CH_2), 27.4 (CH_2), 28.6 (CH_2), 31.6 (CH_2), 32.0 (CH_2), 44.7 (NCH_2), 48.2 (NCH_2), 110.4 (C3), 114.8 (C7), 121.0 (C4), 124.5 (ArC4'), 124.6 (C6), 128.1 (C3a), 128.7 (C5), 130.4 (ArC1'), 132.0 (ArC2' and ArC6'), 132.9 (ArC3' and ArC5'), 135.3 (C7a), 148.0 (C2), 167.9 (NC=O), 187.8 (C=O). MS-EI *m/z* 546

($^{79}Br^{37}Cl$ and $^{81}Br^{35}Cl$ M^+, 1), 336 ($^{81}Br^{37}Cl$ M^+ - $CON(Hex)_2$, 24), 334 ($^{79}Br^{37}Cl$ and $^{81}Br^{35}Cl$ M^+ - $CON(Hex)_2$, 100%), 332 ($^{79}Br^{35}Cl$ M^+ - $CON(Hex)_2$, 72). HRMS-EI calculated for $C_{28}H_{34}N_2O_2{}^{37}Cl^{81}Br$: 548.1442, found 548.1442. Anal. calculated for $C_{28}H_{34}BrClN_2O_2$: C, 61.60; H, 6.28; N, 5.13. Found: C, 61.35; H, 6.02; N, 5.06.

_N,N_-Di-_n_-propyl-[2-(4-bromophenyl)-5-chloroindol-3-yl]glyoxylamide [53]

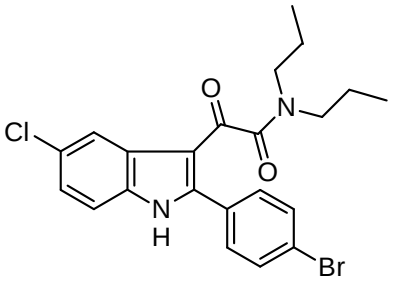

The title compound was prepared as a pale pink solid (0.25 g, 53%) from **[47]** (0.41 g, 1.03 mmol) and NEt_3 (0.17 mL, 1.24 mmol) in anhydrous toluene (40 mL) and di-*n*-propylamine (0.16 mL, 1.13 mmol) in anhydrous toluene (30 mL) using the *amination method*. The product was subjected to silica gel column chromatography using EtOAc:PE (1:1) and the isolated product recrystallised from diethyl ether:PE, mp. 128-129 °C. ^{1}H NMR (DMSO) δ 0.69 (t, 3H, J = 7.4, CH_3), 0.77 (t, 3H, J = 7.4, CH_3), 1.15-1.25 (m, 2H, CH_2), 1.40-1.50 (m, 2H, CH_2), 2.96 (m, 2H, NCH_2), 3.02 (m, 2H, NCH_2), 7.31 (dd, 1H, $J_{6,7}$ = 8.6, $J_{6,4}$ = 2.1, H6), 7.51 (d, 1H, $J_{7,6}$ = 8.7, H7), 7.52 (d, 2H, J = 8.5, ArH2' and ArH6'), 7.70 (d, 2H, J = 8.5, ArH3' and ArH5'), 8.00 (d, 1H, $J_{4,6}$ = 1.7, H4). ^{13}C NMR (DMSO) δ 11.5 (CH_3), 12.0 (CH_3), 20.6 (CH_2), 21.8 (CH_2), 46.2 (NCH_2), 49.9 (NCH_2), 110.1 (C3), 114.6 (C7), 120.6 (C4), 124.2 (C6), 124.3 (ArC4'), 127.9 (C3a), 128.4 (C5), 130.2 (ArC1'), 131.7 (ArC2' and ArC6'), 132.5 (ArC3' and ArC5'), 135.0 (C7a), 147.8 (C2), 167.8 (NC=O), 187.4 (C=O). MS-ES *m/z* 465 ($^{81}Br^{37}Cl$ M+1, 13), 463 ($^{79}Br^{37}Cl$ and $^{81}Br^{35}Cl$ M+1, 61), 461 ($^{79}Br^{35}Cl$ M+1, 50), 106 (100%). HRMS-ES calculated for $C_{22}H_{23}N_2O_2{}^{35}Cl^{79}Br$: 461.0631, found 461.0649. Anal. calculated for $C_{22}H_{22}BrClN_2O_2$: C, 57.22; H, 4.80; N, 6.07. Found: C, 57.33; H, 4.89; N, 6.01.

***N,N*-Diethyl-[2-(4-bromophenyl)-5-chloroindol-3-yl]glyoxylamide [54]**

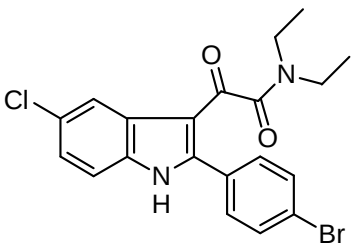

The title compound was prepared as a white solid (0.46 g, 59%) from **[47]** (0.72 g, 1.81 mmol) and NEt_3 (0.30 mL, 2.18 mmol) in anhydrous toluene (40 mL) and diethylamine (0.21 mL, 1.99 mmol) in anhydrous toluene (10 mL) using the *amination method*. The product was recrystallised from EtOAc:PE (1:1), mp. 216-217 °C. ^{1}H NMR (DMSO) δ 0.84 (t, 3H, *J* = 7.1, CH_3), 1.02 (t, 3H, *J* = 7.0, CH_3), 3.07 (q, 2H, *J* = 7.1, NCH_2), 3.15 (q, 2H, *J* = 7.0, NCH_2), 7.32 (dd, 1H, *J* = 8.7, 2.1, H6), 7.47-7.56 (m, 3H, ArH2' and ArH6' and H7), 7.72 (d, 2H, *J* = 8.4, ArH3' and ArH5'), 8.05 (d, 1H, *J* = 2.0, H4). ^{13}C NMR (DMSO) δ 13.0 (CH_3), 14.6 (CH_3), 38.9 (NCH_2), 42.7 (NCH_2), 110.4 (C3), 114.9 (C7), 121.0 (C4), 124.5 (ArC4'), 124.6 (C6), 128.1 (C3a), 128.9 (C5), 130.1 (ArC1'), 132.0 (ArC2' and ArC6'), 132.9 (ArC3' and ArC5'), 135.3 (C7a) 148.5 (C2), 167.7 (NC=O), 188.0 (C=O). MS-EI *m/z* 434 ($^{79}Br^{37}Cl$ and $^{81}Br^{35}Cl$ M^+, 4), 336 ($^{81}Br^{37}Cl$ M^+ - $CON(Et)_2$, 79), 334 ($^{79}Br^{37}Cl$ and $^{81}Br^{35}Cl$ M^+ - $CON(Et)_2$, 100%), 332 ($^{79}Br^{35}Cl$ M^+ - $CON(Et)_2$, 25). HRMS-EI calculated for $C_{20}H_{18}N_2O_2{}^{37}Cl^{79}Br$: 434.0211, found 434.0207. Anal. calculated for $C_{20}H_{18}BrClN_2O_2$: C, 55.38; H, 4.18; N, 6.46. Found: C, 55.37; H, 4.36; N, 6.40.

7.2.2 Experimental Procedures for the Synthesis of Indol-3-ylglyoxylamides

4-Iodoacetophenone phenylhydrazone [57]

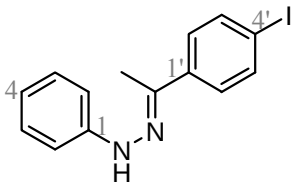

A mixture of 4-iodoacetophenone (5.0 g, 20.3 mmol), phenylhydrazine (2.0 mL, 20.3 mmol), and 10 drops of glacial AcOH in EtOH (30 mL) was warmed for 15 min. The mixture was then cooled in an ice bath and the pale yellow precipitate was filtered and washed with dilute HCl (10 mL), followed by 95% EtOH (10 mL). The solid was dried *in vacuo*, and recrystallised from EtOH to give **[57]** (4.38 g, 64%) as orange crystals, mp. 108-110 °C. ^{1}H NMR ($CDCl_3$) δ 2.19 (s, 3H, CH_3), 6.89 (dd, 1H, *J* = 7.2, 7.2, ArH4), 7.16 (d, 2H, *J* = 7.7, ArH2 and ArH6), 7.28 (d, 2H, *J* = 7.9, ArH3 and ArH5), 7.52 (d, 2H, *J* = 8.6, ArH2' and ArH6'), 7.68 (d, 2H, *J* = 8.6, ArH3' and ArH5'). ^{13}C NMR ($CDCl_3$) δ 11.6 (CH_3), 94.0 (ArC4'), 113.4 (ArC2 and ArC6), 120.6 (ArC4), 127.4 (ArC2' and ArC6'), 129.3 (ArC3 and ArC5), 137.5 (ArC3' and ArC5'), 138.0 (ArC1'), 140.1 (CN), 145.2 (ArC1). MS-EI *m/z* 336 (M^+, 100%). HRMS-EI calculated for $C_{14}H_{13}N_2I$: 336.0124, found 336.0112.

4-Bromoacetophenone phenylhydrazone **[58]** [160]

Please see print copy for image

A mixture of 4-bromoacetophenone (10.0 g, 50.2 mmol), phenylhydrazine (5.4 g, 50.2 mmol), and 10 drops of glacial AcOH in EtOH (60 mL) was warmed for 15 min. The mixture was then cooled in an ice bath and the precipitate which formed was filtered off and washed with dilute HCl (2 x 5 mL), followed by a small amount of 95% EtOH (5 mL).

Recrystallisation from EtOH gave **[58]** (10.6 g, 73%) as white crystals, mp. 115-117 °C (Lit mp. 124-126 °C).[160] ^{1}H NMR ($CDCl_3$) δ 2.20 (s, 3H, CH_3), 6.89 (dd, 1H, *J* = 7.3, 7.3, ArH4), 7.16 (d, 2H, *J* = 7.8, ArH2 and ArH6), 7.28 (dd, 2H, *J* = 7.9, 7.9, ArH3 and ArH5), 7.35 (bs, 1H, NH), 7.48 (d, 2H, *J* = 8.7, ArH2' and ArH6'), 7.65 (d, 2H, *J* = 8.7, ArH3' and ArH5'). ^{13}C NMR ($CDCl_3$) δ 11.7 (CH_3), 113.4 (ArC2 and ArC6), 120.6 (ArC4), 122.1 (ArC4'), 127.1 (ArC2' and ArC6'), 129.4 (ArC3 and ArC5), 131.5 (ArC3' and ArC5'), 138.2 (ArC1'), 139.9 (CN), 145.1 (ArC1). MS-EI *m/z* 290 (^{81}Br M^+, 33), 288 (^{79}Br M^+, 34), 183 (100%). HRMS-EI calculated for $C_{14}H_{13}N_2{}^{79}Br$: 288.0262, found 288.0261.

2-(4-Iodophenyl)indole **[59]** [159]

Please see print copy for image

A mixture of 4-iodoacetophenone phenylhydrazone **[57]** (3.09 g, 9.19 mmol) and polyphosphoric acid (15 g) was heated at 60-70 °C for 30 min, stirring every few min. The mixture was added to ice water (200 mL), stirred, and the brown solid was filtered off and recrystallised from 95% EtOH to produce **[59]** (1.70 g, 58%) as a white solid, mp. 230 °C (Lit mp. 240 °C)[3].[159] ^{1}H NMR ($CDCl_3$) δ 6.82 (d, 1H, *J* = 1.4, H3), 7.12 (ddd, 1H, *J* = 7.6, 7.1, 1.1, H5), 7.21 (ddd, 1H, *J* = 7.5, 7.0, 0.9, H6), 7.38 (d, 3H, *J* = 8.5, ArH2' and ArH6' and H7), 7.62 (d, 2H, *J* = 7.7, H4), 7.76 (d, 2H, *J* = 8.5, ArH3' and ArH5'), 8.27 (bs, 1H, NH). ^{13}C NMR (DMSO) δ 94.1 (ArC4'), 100.5 (C3), 112.5 (C7), 120.7 (C4), 121.4 (C5), 123.1 (C6), 128.1 (ArC2' and ArC6'), 129.7 (C3a), 132.9 (ArC1'), 137.7 (C7a), 138.4 (C2), 138.8 (ArC3' and ArC5'). MS-EI *m/z* 319 (M^+, 100%). HRMS-EI calculated for $C_{14}H_{10}NI$: 318.9858, found 318.9866.

---

[3] Ref 159 only included mp. No NMR data was recorded.

***2-(4-Bromophenyl)indole* [60]** [161]

Please see print copy for image

Method 1: A mixture of 4-bromoacetophenone phenylhydrazone **[58]** (5.0 g, 17.3 mmol) and polyphosphoric acid (32 g) was stirred for 10 min at 100 °C. Water (250 mL) was added and the mixture was stirred manually until the viscous product formed a precipitate. The brown solid was filtered, washed with water, and recrystallised from 95% EtOH producing **[60]** (1.90 g, 40%) as a white solid, spectroscopically identical to that reported in literature. mp. 208-209 °C (Lit mp. 208-212 °C).[181] ^{1}H NMR ($CDCl_3$) δ 6.82 (d, 1H, *J* = 1.3, H3), 7.13 (ddd, *J* = 7.9, 7.0, 0.9, 1H, H5), 7.21 (ddd, 1H, *J* = 8.1, 7.1, 1.1, H6), 7.39 (d, *J* = 8.0, 1H, H7), 7.51 (d, 2H, *J* = 8.7, ArH2' and ArH6'), 7.56 (d, 2H, *J* = 8.7, ArH3' and ArH5'), 7.62 (d, 1H, *J* = 8.0, H4), 8.27 (bs, 1H, NH). ^{13}C NMR (DMSO) δ 99.4 (C3), 111.4 (C7), 119.5 (C4), 120.2 (C5), 120.3 (ArC4'), 121.9 (C6), 126.9 (ArC2' and ArC6'), 128.5 (C3a), 131.5 (ArC1'), 131.8 (ArC3' and ArC5'), 136.4 (C7a), 137.2 (C2). MS-EI *m/z* 273 (^{81}Br M^+, 98), 271 (^{79}Br M^+, 100%). HRMS-EI calculated for $C_{14}H_{10}N^{79}Br$: 270.9997, found 270.9995.

Method 2: A mixture of 4-bromoacetophenone (6.89 g, 34.6 mmol) and phenylhydrazine (3.40 mL, 34.6 mmol) was added to polyphosphoric acid (40 g). The reaction mixture was stirred at 110 °C until the mixture turned a deep reddish brown colour. The reaction mixture was then added to ice water (300 mL) and stirred until a precipitate was formed. The precipitate was collected by filtration and washed with water. Recrystallisation from 95% EtOH gave **[60]** as a white solid (5.41 g, 58%).

[2-(4-Iodophenyl)indol-3-yl]glyoxylyl chloride [61]

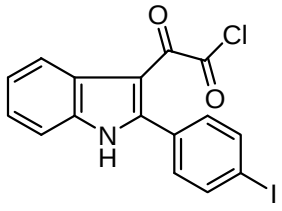

The title compound was prepared as a yellow solid (0.34 g, 68%) from oxalyl chloride (0.15 mL, 1.70 mmol) and **[59]** (0.39 g, 1.22 mmol) in anhydrous diethyl ether (6.5 mL) according to the *acylation method* and used without further purification in subsequent amination reactions. ^{1}H NMR (DMSO) δ 7.25–7.35 (m, 2H, H5 and H6), 7.39 (d, 2H, *J* = 8.3, ArH2' and ArH6'), 7.52 (d, 1H, $J_{7,6}$ = 7.6, H7), 7.89 (d, 2H, *J* = 8.2, ArH3' and ArH5'), 8.09 (d, 1H, $J_{4,5}$ = 7.4, H4), 12.83 (s, 1H, NH). ^{13}C NMR (DMSO) δ 98.0 (ArC4'), 109.6 (C3), 113.2 (C7), 121.7 (C4), 123.7 (C5), 124.8 (C6), 127.9 (C3a), 131.2 (ArC1'), 132.7 (ArC2' and ArC6'), 136.8 (C7a), 138.1 (ArC3' and ArC5'), 147.8 (C2), 167.7 (ClC=O), 185.2 (C=O).

[2-(4-Bromophenyl)indol-3-yl]glyoxylyl chloride [62]

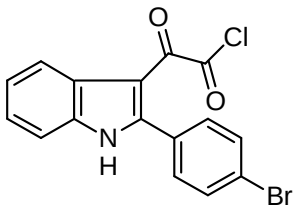

The title compound was prepared as a yellow solid (1.75 g, 66%) from oxalyl chloride (0.90 mL, 10.29 mmol) and **[60]** (2.00 g, 7.35 mmol) in anhydrous diethyl ether (20 mL) according to the *acylation method*, and was used without further purification in the next amination reactions. ^{1}H NMR ($CDCl_3$) δ 7.37-7.41 (m, 2H, H5 and H6), 7.42 (d, 2H, *J* = 8.5, ArH2' and ArH6'), 7.44-7.49 (m, 1H, H7), 7.66 (d, 2H, *J* = 8.5, ArH3' and ArH5'), 8.24-8.29 (m, 1H, H4), 8.92 (bs, 1H, NH).

***N,N*-Dihexyl-[2-(4-iodophenyl)indol-3-yl]glyoxylamide [63]**

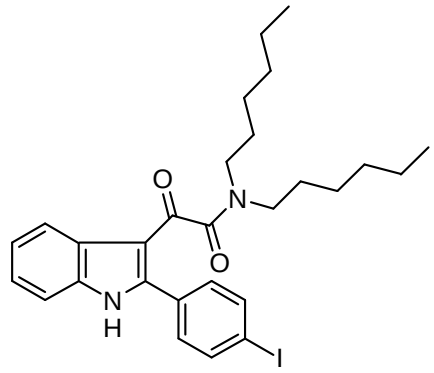

The title compound was prepared as a white solid (0.10 g, 32%) from **[61]** (0.23 g, 0.56 mmol) and NEt_3 (90 μL, 0.67 mmol) in anhydrous toluene (20 mL) and dihexylamine (0.15 mL, 0.62 mmol) in anhydrous toluene (10 mL) using the *amination method*. The crude product was subjected to silica gel column chromatography using EtOAc:PE (2:3), and the appropriate fractions concentrated and the residue recrystallised from EtOH:H_2O, mp. 120-122 °C. ^{1}H NMR (DMSO) δ 0.74 (t, 3H, *J* = 7.0, CH_3), 0.84 (t, 3H, *J* = 6.9, CH_3), 1.00-1.45 (m, 16H, 8 x CH_2), 2.95-3.07 (m, 4H, 2 x NCH_2), 7.21-7.31 (m, 2H, H5 and H6), 7.37 (d, 2H, *J* = 8.3, ArH2' and ArH6'), 7.48 (d, 1H, *J* = 7.7, H7), 7.87 (d, 2H, *J* = 8.3, ArH3' and ArH5'), 8.04 (d, 1H, *J* = 7.7, H4). ^{13}C NMR (DMSO) δ 13.8 (CH_3), 14.0 (CH_3), 21.8 (CH_2), 22.1 (CH_2), 25.6 (CH_2), 26.2 (CH_2), 26.4 (CH_2), 27.5 (CH_2), 30.6 (CH_2), 31.1 (CH_2), 43.7 (NCH_2), 47.3 (NCH_2), 96.7 (ArC4'), 109.8 (C3), 112.1 (C7), 120.9 (C4), 122.5 (C5), 123.6 (C6), 126.7 (C3a), 130.2 (ArC1'), 131.9 (ArC2' and ArC6'), 135.8 (C7a), 136.8 (ArC3' and ArC5'), 146.0 (C2), 167.3 (NC=O), 187.1 (C=O). MS-EI *m/z* 558 (M^+, 4), 346 (M^+ - $CON(Hex)_2$, 100%). HRMS-EI calculated for $C_{28}H_{35}N_2O_2I$: 558.1743, found 558.1747.

***N,N*-Di-*n*-propyl-[2-(4-iodophenyl)indol-3-yl]glyoxylamide [64]**

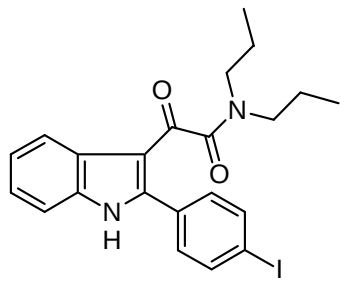

The title compound was prepared as an off-white solid (58.2 mg, 22%) from **[61]** (0.23 g, 0.56 mmol) and NEt_3 (90 μL, 0.67 mmol) in anhydrous toluene (30 mL) and di-*n*-propylamine (85 μL, 0.62 mmol) in anhydrous toluene (20 mL) using the *amination method*. The product was subjected to silica gel column chromatography using EtOAc:PE (1:1), with the isolated product triturated in EtOAc:PE (3:7), mp. 159-161 °C. ^{1}H NMR (DMSO) δ 0.69 (t, 3H, *J* = 7.4, CH_3), 0.79 (t, 3H, *J* = 7.4, CH_3), 1.13-1.25 (m, 2H, CH_2), 1.41-1.52 (m, 2H, CH_2), 2.96 (t, 2H, *J* = 7.9, NCH_2), 3.03 (t, 2H, *J* = 7.7, NCH_2), 7.21-7.33 (m, 2H, H5 and H6), 7.37 (d, 2H, *J* = 8.4, ArH2' and ArH6'), 7.48 (d, 1H, *J* = 7.3, H7), 7.88 (d, 2H, *J* = 8.4, ArH3' and ArH5'), 8.03 (d, 1H, *J* = 7.3, H4). ^{13}C NMR (DMSO) δ 11.9 (CH_3), 12.4 (CH_3), 20.9 (CH_2), 22.2 (CH_2), 46.5 (NCH_2), 50.2 (NCH_2), 97.6 (ArC4'), 110.8 (C3), 113.1 (C7), 121.8 (C4), 123.5 (C5), 124.5 (C6), 127.6 (C3a), 131.3 (ArC1'), 132.9 (ArC2' and ArC6'), 136.8 (C7a), 137.8 (ArC3' and ArC5'), 147.0 (C2), 168.4 (NC=O), 188.0 (C=O). MS-EI *m/z* 474 (M^+, 6), 346 (M^+ - CON(propyl)$_2$, 100%). HRMS-EI calculated for $C_{22}H_{23}N_2O_2I$: 474.0804, found 474.0795.

***N,N*-Diethyl-[2-(4-iodophenyl)indol-3-yl]glyoxylamide [65]**

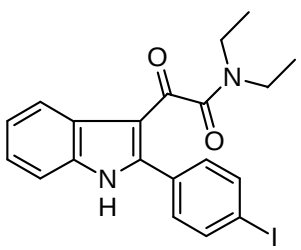

The title compound was prepared as off-white crystals (60 mg, 40%) from **[61]** (0.14 g, 0.34 mmol) and NEt_3 (0.10 mL, 0.75 mmol) in anhydrous toluene (40 mL) and diethylamine (0.05 mL, 0.47 mmol) in anhydrous toluene (20 mL) using the *amination method*. The product was recrystallised from EtOAc:PE (1:1), mp. 169-171 °C. ^{1}H NMR (DMSO) δ 0.85 (t, 3H, *J* = 7.1, CH_3), 1.02 (t, 3H, *J* = 7.0, CH_3), 3.07 (q,

2H, *J* = 7.1, NCH_2), 3.15 (q, 2H, *J* = 7.0, NCH_2), 7.22-7.32 (m, 2H, H5 and H6), 7.37 (d, 2H, *J* = 8.3, ArH2' and ArH6'), 7.49 (d, 1H, *J* = 7.3, H7), 7.87 (d, 2H, *J* = 8.3, ArH3' and ArH5'), 8.06 (d, 1H, *J* = 7.2, H4). ^{13}C NMR (DMSO) δ 13.8 (CH_3), 15.3 (CH_3), 39.5 (NCH_2), 43.5 (NCH_2), 98.3 (ArC4'), 111.5 (C3), 113.8 (C7), 122.5 (C4), 124.2 (C5), 125.3 (C6), 128.4 (C3a), 131.9 (ArC1'), 133.6 (ArC2' and ArC6'), 137.3 (C7a), 138.4 (ArC3' and ArC5'), 147.7 (C2), 168.7 (NC=O), 188.8 (C=O). MS-ES *m/z* 445 (M-1, 100%). HRMS-EI calculated for $C_{20}H_{19}N_2O_2I$: 446.0491, found 446.0489. Anal. calculated for $C_{20}H_{19}IN_2O_2$: C, 53.83; H, 4.29; N, 6.28. Found: C, 53.50; H, 4.41; N, 6.11.

***N,N*-Dimethyl-[2-(4-iodophenyl)indol-3-yl]glyoxylamide [66]**

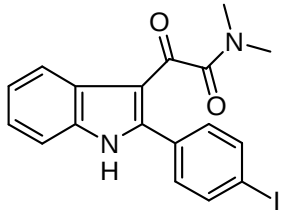

Dimethylamine (30 mL, 40% wt/vol in water) was gently heated and under constant N_2 pressure that was passed through NaOH pellets and bubbled into a solution of **[61]** (0.30 g 0.73 mmol) and NEt_3 (0.12 mL, 0.88 mmol) in anhydrous toluene (50 mL). The product was subjected to silica gel column chromatography using EtOAc:PE (1:1) to afford **[66]** (14 mg, 5%) as an off-white solid, mp. 231-232 °C. ^{1}H NMR (DMSO) δ 2.49 (s, 3H, NCH_3), 2.79 (s, 3H, NCH_3), 7.20-7.30 (m, 2H, H5 and H6), 7.34 (d, 2H, *J* = 8.1, ArH2' and ArH6'), 7.48 (d, 1H, *J* = 7.0, H7), 7.89 (d, 2H, *J* = 8.3, ArH3' and ArH5'), 8.07 (d, 1H, *J* = 7.3, H4). ^{13}C NMR (DMSO) δ 34.4 (NCH_3), 38.1 (NCH_3), 98.0 (ArC4'), 111.3 (C3), 114.0 (C7), 122.5 (C4), 124.3 (C5), 125.2 (C6), 128.2 (C3a), 130.5 (ArC1'), 133.3 (ArC2' and ArC6'), 137.5 (C7a), 138.2 (ArC3' and ArC5'), 148.7 (C2), 168.8 (NC=O), 187.2 (C=O). MS-EI *m/z* 418 (M^+, 6), 346 (M^+ - $CON(CH_3)_2$, 100%). HRMS-EI calculated for $C_{18}H_{15}N_2O_2I$: 418.0178, found 418.0161.

***N,N*-Dihexyl-[2-(4-bromophenyl)indol-3-yl]glyoxylamide [67]**

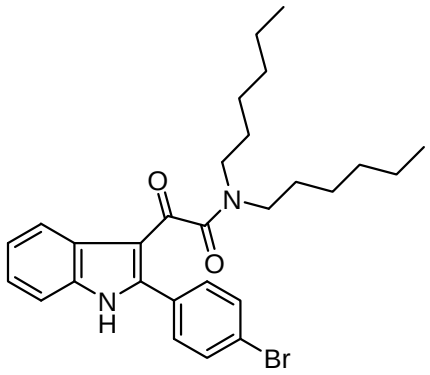

The title compound was prepared as a white solid (0.62 g, 46%) from **[62]** (0.96 g, 2.65 mmol) and NEt_3 (0.44 mL, 3.18 mmol) in anhydrous toluene (60 mL) and dihexylamine (0.68 mL, 2.91 mmol) in anhydrous toluene (40 mL) using the *amination method*. The crude product was subjected to silica gel column chromatography using MeOH:DCM (1:19), and the appropriate fractions were concentrated. The residue was recrystallised from EtOH:H_2O, mp. 106–110 °C. ^{1}H NMR (DMSO) δ 0.74 (t, 3H, *J* = 7.0, CH_3), 0.88 (t, 3H, *J* = 6.9, CH_3), 1.00-1.20 (m, 10H, 5 x CH_2), 1.20-1.30 (m, 4H, 2 x CH_2), 1.35-1.47 (m, 2H, CH_2), 2.95-3.08 (m, 4H, 2 x NCH_2), 7.21-7.32 (m, 2H, H5 and H6), 7.48 (d, 1H, *J* = 7.6, H7), 7.53 (d, 2H, *J* = 8.4, ArH2' and ArH6'), 7.70 (d, 2H, *J* = 8.4, ArH3' and ArH5'), 8.05 (d, 1H, *J* = 7.8, H4), 12.49 (s, 1H, NH). ^{13}C NMR (DMSO) δ 15.4 (CH_3), 15.6 (CH_3), 23.5 (CH_2), 23.7, (CH_2) 27.2 (CH_2), 27.8 (CH_2), 28.1 (CH_2), 29.4 (CH_2), 32.3 (CH_2), 32.7 (CH_2), 45.4 (NCH_2), 49.0 (NCH_2), 111.5 (C3), 113.8 (C7), 122.6 (C4), 124.2 (C5), 124.9 (ArC4'), 125.3 (C6), 128.3 (C3a), 131.6 (ArC1'), 132.6 (ArC2' and ArC6'), 133.7 (ArC3' and ArC5'), 137.4 (C7a), 147.4 (C2), 168.9 (NC=O), 188.8 (C=O). MS-CI *m/z* 513 (^{81}Br M+1, 3), 511 (^{79}Br M+1, 4), 300 (^{81}Br M+1 - $CON(Hex)_2$, 98), 298 (^{79}Br M+1 - $CON(Hex)_2$, 100%). HRMS-EI calculated for $C_{28}H_{35}N_2O_2{}^{79}Br$: 510.1882, found 510.1874. Anal. calculated for $C_{28}H_{35}BrN_2O_2$: C, 65.75; H, 6.90; N, 5.48. Found: C, 65.64; H, 6.78; N, 5.49.

7.2.3 Experimental Procedures for the Synthesis of *meta*-Substituted Phenylindol-3-ylglyoxylamides

3-Bromoacetophenone 4-chlorophenylhydrazone [68]

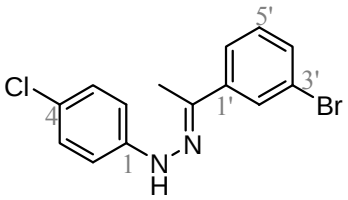

A solution of 4-chlorophenylhydrazine hydrochloride (2.00 g, 11.2 mmol), 3-bromoacetophenone (2.22 g, 11.2 mmol), and 10 drops of glacial AcOH in EtOH (40 mL) was heated at reflux for 1 h. The mixture was cooled and the resulting precipitate was collected by filtration and washed with 0.5M HCl (10 mL) and cold 95% EtOH (10 mL). The crude product was recrystallised from EtOH to yield **[68]** (2.21 g, 61%) as pale yellow needle crystals, mp. 117-120 °C. ^{1}H NMR (DMSO) δ 2.24 (s, 3H, CH_3), 7.20-7.28 (m, 4H, ArH2 and ArH6, ArH3 and ArH5), 7.34 (dd, 1H, *J* = 7.9, 7.9, ArH5'), 7.48 (d, 1H, *J* = 7.9, ArH6'), 7.66 (d, 1H, *J* = 7.8, ArH4'), 7.92 (s, 1H, ArH2'), 9.51 (s, 1H, NH). ^{13}C NMR (DMSO) δ 13.8 (CH_3), 115.3 (ArC2 and ArC6), 122.9 (ArC3'), 123.5 (ArC4), 125.2 (ArC6'), 128.6 (ArC5'), 129.7 (ArC3 and ArC5), 131.2 (ArC2'), 131.4 (ArC4'), 140.8 (ArC1'), 142.4 (CN), 145.7 (ArC1). MS-EI *m/z* 328 ($^{81}Br^{37}Cl$ M^+, 17), 326 ($^{81}Br^{35}Cl$ and $^{79}Br^{37}Cl$ M^+, 63), 324 ($^{79}Br^{35}Cl$ M^+, 53), 230 (100%). HRMS-EI calculated for $C_{14}H_{12}N_2{}^{35}Cl^{79}Br$: 321.9872, found 321.9850. Anal. calculated for $C_{14}H_{12}BrClN_2$: C, 51.96; H, 3.74; N, 8.66. Found: C, 51.83; H, 3.72; N, 8.35.

2-(3-Bromophenyl)-5-chloroindole [69]

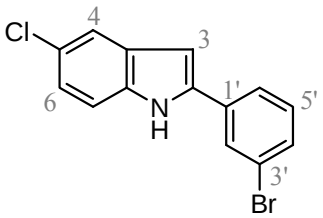

A mixture of phenylhydrazone **[68]** (2.00 g, 6.18 mmol) and polyphosphoric acid (20 g) was heated at 100 – 110 °C for 30 min with occasional stirring. The mixture changed colour from yellow to orange to red and eventually green. The mixture was poured into ice water (250 mL) and stirred. The precipitate was collected by filtration, washed with water, then recrystallised from EtOH to afford **[69]** (1.03 g, 55%) as a white solid, mp. 149-150 °C. ^{1}H NMR (DMSO) δ 6.98 (s, 1H, H3), 7.11 (dd, 1H, $J_{6,5}$ = 8.6, $J_{6,4}$ = 1.9, H6), 7.39-7.45 (m, 2H, H7 and ArH5'), 7.51 (d, 1H, *J* = 7.9, ArH4'), 7.58 (s, 1H, H4), 7.86 (d, 1H, *J* = 7.8, ArH6'), 8.08 (s, 1H, ArH2'). ^{13}C NMR (DMSO) δ 100.5 (C3), 113.9 (C7), 120.3 (C4), 123.0 (C6), 123.4 (ArC3'), 125.1 (C5), 125.2 (ArC6'), 128.4 (ArC2'), 130.5 (C3a), 131.3 (ArC4'), 132.1 (ArC5'), 135.0 (ArC1'), 136.7 (C7a), 138.5 (C2). MS-EI *m/z* 309 ($^{81}Br^{37}Cl$ M^+, 26), 307 ($^{81}Br^{35}Cl$ and $^{79}Br^{37}Cl$ M^+, 100%), 305 ($^{79}Br^{35}Cl$ M^+, 81). HRMS-EI calculated for $C_{14}H_9N^{81}Br^{35}Cl$: 306.9586, found 306.9597.

[2-(3-Bromophenyl)-5-chloroindol-3-yl]glyoxylyl chloride [70]

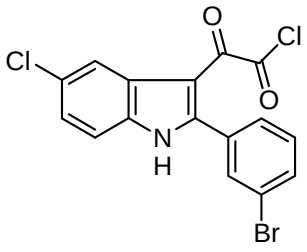

The title compound was prepared as a green solid (0.53 g, 93%) from oxalyl chloride (0.18 mL, 2.02 mmol) and **[69]** (0.44 g, 1.44 mmol) in anhydrous diethyl ether (7 mL) using the *acylation method*, and used without further purification for the subsequent amination reaction. ^{1}H NMR (DMSO) δ 7.35 (dd, 1H, *J* = 8.6, 2.1, H6), 7.48 (dd, 1H, *J* = 7.9, 7.9, ArH5'), 7.55 (d, 1H, *J* = 8.6, H7), 7.58-7.62 (m, 1H, ArH4'), 7.74-7.78 (m, 1H, ArH6'), 7.82 (dd, 1H, *J* = 1.7, 1.7, ArH2'), 8.08 (d, 1H, *J* = 2.1, H4).

***N,N*-Diethyl-[2-(3-bromophenyl)-5-chloroindol-3-yl]glyoxylamide [71]**

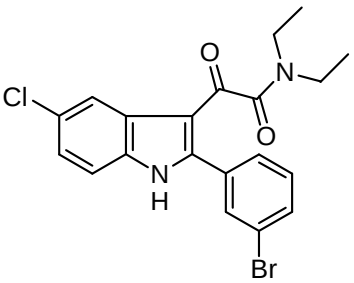

To a solution of the acid chloride **[70]** (0.53 g, 1.33 mmol) in anhydrous toluene (30 mL) at 0 °C was added diethylamine (0.15 mL, 1.49 mmol) and NEt_3 (0.20 mL, 2.80 mmol) in toluene (10 mL). The reaction mixture was stirred for 3 h. The white precipitate which formed was filtered, washed with water, and dried *in vacuo* to give **[71]** (0.21 g, 37%) as a white solid, mp. 230-231 °C. ^{1}H NMR (DMSO) δ 0.84 (t, 3H, J = 7.1, CH_3), 1.04 (t, 3H, J = 7.0, CH_3), 3.07 (q, 2H, J = 7.1, NCH_2), 3.19 (q, 2H, J = 7.0, NCH_2), 7.32 (dd, 1H, $J_{6,7}$ = 8.6, $J_{6,4}$ = 2.1, H6), 7.46 (dd, 1H, J = 7.9, 7.9, ArH5'), 7.52 (d, 1H, $J_{7,6}$ = 8.6, H7), 7.59 (d, 1H, J = 7.7, ArH6'), 7.73 (d, 1H, J = 7.7, ArH4'), 7.80 (s, 1H, ArH2'), 8.07 (d, 1H, $J_{4,6}$ = 2.0, H4). ^{13}C NMR (DMSO) δ 13.2 (CH_3), 14.7 (CH_3), 39.1 (NCH_2), 42.9 (NCH_2), 110.5 (C3), 115.0 (C7), 121.1 (C4), 122.1, (ArC3'), 124.7 (C6), 128.2 (C3a), 128.9 (C5), 130.0 (ArC6'), 131.1 (ArC1'), 133.3, 133.5, 133.7 (ArC2', ArC4', ArC5'), 135.5 (C7a), 147.7 (C2), 167.6 (NC=O), 187.8 (C=O). MS-ES *m/z* 435 ($^{81}Br^{37}Cl$ M-1, 23), 433 ($^{79}Br^{37}Cl$ and $^{81}Br^{35}Cl$ M-1, 100%), 431 ($^{79}Br^{35}Cl$ M-1, 69). HRMS-EI calculated for $C_{20}H_{18}N_2O_2{}^{79}Br^{37}Cl$: 434.0211, found 434.0205. Anal. calculated for $C_{20}H_{18}BrClN_2O_2$: C, 55.38; H, 4.18; N, 6.46. Found: C, 55.62; H, 4.41; N, 6.45.

***N,N*-Diethyl-[5-chloro-2-(3-trimethylstannylphenyl)indol-3-yl]glyoxylamide [72]**

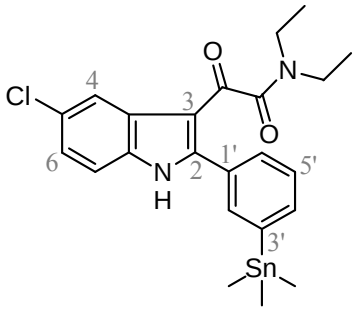

To a solution of bromo indole **[71]** (100 mg, 0.23 mmol) in anhydrous toluene (8 mL) under a N_2 gas atmosphere, was added hexamethylditin (195 mg, 0.69 mmol), and a catalytic amount of $Pd(0)(PPh_3)_4$ (2-5 mg). The solution was heated at reflux for 4.5 h, adding catalyst (2-5 mg) and hexamethylditin every hour. The mixture was allowed to cool and was passed through Celite. The solvent was evaporated *in vacuo* leaving a crude yellow oil which was subjected to silica gel column chromatography using EtOAc:PE (1:1) to yield the stannane **[72]** (49 mg, 42%) as a clear oil. ^{1}H NMR (CD_3OD) δ 0.36 (s, 9H, $Sn(CH_3)_3$), 0.81 (t, 3H, *J* = 7.2, CH_3), 1.10 (t, 3H, *J* = 7.1, CH_3), 3.04 (q, 2H, *J* = 7.2, NCH_2), 3.16 (q, 2H, *J* = 7.1, NCH_2), 7.31 (dd, 1H, *J* = 8.6, 2.1, H6), 7.44 (d, 1H, *J* = 8.6, H7), 7.42-7.51 (m, 2H, ArH5', ArH6'), 7.67 (d, 1H, *J* = 7.1, ArH4') 7.73 (s, 1H, ArH2'), 8.28 (d, 1H, *J* = 1.5, H4). ^{13}C NMR (DMSO) δ -9.3 ($Sn(CH_3)_3$), 12.1 (CH_3), 13.6 (CH_3), 37.7 (NCH_2), 41.6 (NCH_2), 109.8 (C3), 113.7 (C7), 120.1 (C4), 123.5 (C6), 127.1 (ArC6'), 127.4 (C3a), 127.9 (C5), 129.7 (ArC5'), 129.8 (ArC1'), 134.3 (C7a), 136.8 (ArC2'), 137.2 (ArC3'), 141.9 (ArC4'), 149.0 (C2), 166.7 (NC=O), 187.2 (C=O). MS-ES *m/z* 521 ($^{122}Sn^{37}Cl$ M-1, 18), 519 ($^{120}Sn^{37}Cl$ M-1, 39), 518 ($^{119}Sn^{37}Cl$ M-1, 27), 517 ($^{120}Sn^{35}Cl$ M-1, 100%), 516 ($^{119}Sn^{35}Cl$ M-1, 40), 515 ($^{118}Sn^{35}Cl$ M-1, 71), 514 ($^{117}Sn^{35}Cl$ M-1, 24), 513 ($^{116}Sn^{35}Cl$ M-1, 32). HRMS-ES calculated for $C_{23}H_{28}N_2O_2{}^{35}Cl^{120}Sn$: 519.0861, found 519.0876.

***N,N*-Diethyl-[5-chloro-2-(3-iodophenyl)indol-3-yl]glyoxylamide [73]**

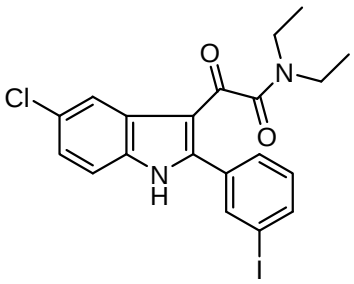

To a solution of the stannane **[72]** (45 mg, 0.087 mmol) in DCM (2 mL) was added dropwise a solution of I_2 (26 mg, 0.104 mmol) in DCM (3 mL). The reaction mixture was stirred at RT for 30 min, then washed once with $Na_2S_2O_5$ (240 mg in 7 mL water), and the organic layer was dried ($MgSO_4$), filtered, and the solvent evaporated *in vacuo* to yield the iodinated product **[73]** (41 mg, 98%) as a white solid, mp. 234-236 °C. ^{1}H NMR (DMSO) δ 0.83 (t, 3H, *J* = 7.1, CH_3), 1.05 (t, 3H, *J* = 7.0, CH_3), 3.06 (q, 2H, *J* = 7.1, NCH_2), 3.19 (q, 2H, *J* = 7.0, NCH_2), 7.31 (dd, 1H, *J* = 7.8, 7.8, ArC5'), 7.32 (dd, 1H, *J* = 8.6, 2.1, H6), 7.51 (d, 1H, *J* = 8.6, H7), 7.59 (d, 1H, *J* = 7.9, ArH6'), 7.89 (d, 1H, *J* = 7.9, ArH4'), 7.94 (dd, 1H, *J* = 1.5, 1.5, ArH2'), 8.08 (d, 1H, *J* = 2.0, H4). ^{13}C NMR (DMSO) δ 12.2 (CH_3), 13.7 (CH_3), 38.2 (NCH_2), 42.0 (NCH_2), 94.2 (ArC3'), 109.5 (C3), 113.8 (C7), 120.1 (C4), 123.7 (C6), 127.2 (C3a), 127.8 (C5), 129.4 (ArC6'), 130.0 (ArC5'), 132.5 (ArC1'), 134.3 (C7a), 137.9 (ArC2'), 138.4 (ArC4'), 146.7 (C2), 166.6 (NC=O), 187.0 (C=O). MS-ES *m/z* 481 (^{37}Cl M-1, 36), 479 (^{35}Cl M-1, 100%). HRMS-ES calculated for $C_{20}H_{19}N_2O_2{}^{35}ClI$: 481.0180, found 481.0181. Anal. calculated for $C_{20}H_{18}ClIN_2O_2$: C, 49.97; H, 3.77; N, 5.83. Found: C, 50.18; H, 3.97; N, 5.81.

7.2.4 Experimental Procedures for the Synthesis of Fluorinated Indol-3-ylglyoxylamides

2-(4-Fluorophenyl)indole **[74]**

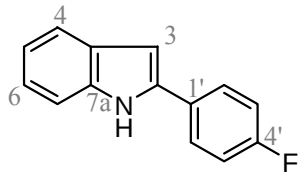

A mixture of 4-fluoroacetophenone (6.0 g, 43 mmol), phenylhydrazine (4.3 mL, 43 mmol) and polyphosphoric acid (40 g) was heated to 100-110 °C and stirred every few min for 30 min. The mixture was poured into ice water (250 mL) and stirred. The precipitate was filtered, then recrystallised from EtOH to give **[74]** (5.10 g, 56%) as a white solid which was spectroscopically identical to that reported in literature,[162] mp. 181-182 °C (Lit mp. 190 °C). ^{1}H NMR (DMSO) δ 6.86 (s, 1H, H3), 7.00 (dd, 1H, *J* = 7.4, 7.4, H5 or H6), 7.10 (dd, 1H, *J* = 7.4, 7.4, H6 or H5), 7.30 (dd, 2H, *J* = 8.8, 8.8, ArH3' and ArH5'), 7.40 (d, 1H, *J* = 8.0, H7), 7.52 (d, 1H, *J* = 7.8, H4), 7.89 (dd, 2H, *J* = 8.6, 5.5, ArH2' and ArH6'). ^{13}C NMR (DMSO) δ 98.7 (C3), 111.3 (C7), 115.8 (d, $^{2}J_{CF}$ = 21.5, ArC3' and ArC5'), 119.4 (C4), 120.0 (C5), 121.6 (C6), 127.0 (d, $^{3}J_{CF}$ = 8.4, ArC2' and ArC6'), 128.7 (C3a), 128.9 (d, $^{4}J_{CF}$ = 3.1, ArC1'), 136.7 (C7a), 137.1 (C2), 161.6 (d, $^{1}J_{CF}$ = 245, ArC4'). MS-EI *m/z* 211 (M^{+}, 100%). HRMS-EI calculated for $C_{14}H_{10}NF$: 211.0797, found 211.0795.

[2-(4-Fluorophenyl)indol-3-yl]glyoxylyl chloride **[75]** [162]

Please see print copy for image

To a mixture of the indole **[74]** (2.00 g, 9.5 mmol) in anhydrous diethyl ether (19 mL), was added dropwise oxalyl chloride (1.16 mL, 13.3 mmol) at 0 °C. After 1 h at RT, the resulting green

precipitate was filtered and washed with diethyl ether (10 mL) to give **[75]** (1.72 g, 60%) as a pale green product, which was used without further purification in the subsequent reaction. ^{1}H NMR (DMSO) δ 7.24-7.33 (m, 2H, H5 and H6), 7.36 (dd, 2H, *J* = 8.9, 8.9, ArH3' and ArH5'), 7.52 (d, 1H, *J* = 6.7, H7), 7.65 (dd, 2H, *J* = 8.8, 5.5, ArH2' and ArH6'), 8.10 (d, 1H, *J* = 6.9, H4).

_N_-Methyl-_N_-propargyl-[2-(4-fluorophenyl)indol-3-yl]glyoxylamide [76]

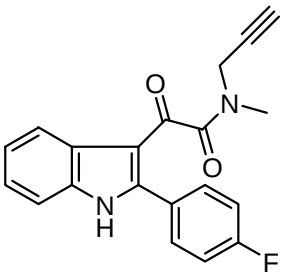

To a solution of *N*-methylpropargylamine (0.30 mL, 3.6 mmol) in anhydrous DCM (30 mL) at 0 °C was added **[75]** (1.00 g, 3.3 mmol) and NEt_3 (0.5 mL, 3.7 mmol). The reaction mixture was stirred overnight at RT. The mixture was poured into 1M HCl (50 mL) and extracted into DCM (2 x 30 mL). The combined organic extracts were washed with saturated brine (25 mL), dried ($MgSO_4$), and evaporated to dryness. The product was subjected to silica gel column chromatography using EtOAc:PE (1:1) to afford **[76]** (0.615 g, 56%) as off-white crystals, mp. 72-74 °C. [4] ^{1}H NMR (DMSO) δ 2.56 and 2.87 (2 x s, 3H, NCH_3), 3.26 and 3.36 (2 x dd, 1H, *J* = 2.4, 2.4, C≡C-H), 3.87 and 4.08 (2 x d, 2H, *J* = 2.4, NCH_2), 7.21-7.38 (m, 4H, H5, H6, ArH3' and ArH5'), 7.46-7.51 (m, 1H, H7), 7.60-7.64 (m, 2H, ArH2' and ArH6'), 8.05-8.15 (m, 1H, H4). ^{13}C NMR (DMSO) δ 31.4 (NCH_3), 34.8 (NCH_2), 35.1 (NCH_2), 75.9 (C<u>C</u>H), 76.8 (C<u>C</u>H), 78.91 (<u>C</u>CH), 78.94 (<u>C</u>CH), 80.1 (<u>C</u>CH), 110.6 (C3), 113.05 (C7), 113.12 (C7), 115.9 (t, $^{2}J_{CF}$ = 21.0, ArC3' and ArC5'), 121.8 (C4), 122.0 (C4), 123.7 (C5), 124.6 (C6), 127.5 (C3a), 127.6 (C3a), 127.9 (d, $^{4}J_{CF}$ = 3.1, ArC1'), 133.1 (dd, $^{2}J_{CF}$

[4] Rotamers were present in the ^{1}H and ^{13}C NMR of **[76]**. Rotamers and $^{13}C^{19}F$ couplings in made the ^{13}C NMR assignments difficult.

= 21.4, $^{3}J_{CF}$ = 8.5, ArC2' and ArC6'), 136.6 (C7a), 136.7 (C7a), 147.7 (C2), 147.9 (C2), 166.3 (d, $^{1}J_{CF}$ = 240, ArC4'), 167.5 (NC=O), 187.2 (C=O). MS-ES *m/z* 335 (M+1, 30), 238 (100%). HRMS-ES calculated for $C_{20}H_{16}N_2O_2F$: 335.1196, found 335.1183.

7.3 Experimental Procedures for the Synthesis of 2-Arylpyrazolo[1,5-*a*]pyrimidin-3-yl Acetamides

2-Bromo-1-(4-iodophenyl)-1-ethanone **[88]** [116]

Please see print copy for image

To a solution of 4-iodoacetophenone (26.8 g, 0.109 mol) in dry $CHCl_3$ (150 mL) at 0 °C was added $AlCl_3$ (50 mg) and then dropwise Br_2 (17.4 g, 0.109 mol). After the addition, the solvent was evaporated and the product recrystallised from heptane, giving **[88]** (28.9 g, 82%) as pale brown crystals, which was spectroscopically identical to that reported in literature[5],[116] mp. 102-104 °C. (Lit mp. 110.5–111.0 °C).[168] ^{1}H NMR (DMSO) δ 4.90 (s, 2H, CH_2) 7.75 (d, 2H, *J* = 8.5, ArH2 and ArH6) 7.95 (d, 2H, *J* = 8.6, ArH3 and ArH5). ^{13}C NMR (DMSO) δ 33.9 (CH_2), 102.7 (ArC4), 130.3 (ArC2 and ArC6), 133.3 (ArC1), 137.8 (ArC3 and ArC5), 191.3 (C=O). MS-EI *m/z* 326 (^{81}Br M^+, 19), 324 (^{79}Br M^+, 20), 231 (M^+ - CH_2Br, 100%). HRMS-EI calculated for $C_8H_6O^{79}BrI$: 323.8647, found 323.8642.

4-Iodobenzoylacetonitrile **[89]** [167]

Please see print copy for image

To a solution of KCN (4.2 g, 65 mmol) in water (12.6 mL), was added a solution of **[88]** (7.0 g, 22 mmol) in EtOH (12.6 mL), and the

[5] ^{13}C NMR was not reported in ref. 116

mixture was heated for 3 h at 50 °C. Water (50 mL) and concentrated HCl (50 mL) were added, the solution was cooled, and the precipitate filtered, giving **[89]** in quantitative yield as an off-white solid which was spectroscopically identical to that reported in literature, mp. 178-180 °C.[167] ^{1}H NMR (DMSO) δ 4.72 (s, 2H, CH_2), 7.68 (d, 2H, *J* = 8.4, ArH2 and ArH6), 7.97 (d, 2H, *J* = 8.4, ArH3 and ArH5). ^{13}C NMR (DMSO) δ 29.9 (CH_2), 103.1 (ArC4), 115.7 (CN), 130.0 (ArC2 and ArC6), 133.9 (ArC1), 137.8 (ArC3 and ArC5), 189.3 (C=O). MS-EI *m/z* 271 (M^+, 24), 231 (M^+ - CH_2CN, 100%). HRMS-EI calculated for C_9H_6NOI: 270.9494, found 270.9496.

2-Chloro-N,N-di-n-propylacetamide **[93]** [169]

Please see print copy for image

To a mixture of di-*n*-propylamine (4.05 g, 40 mmol) and NaOH (20%, 10 mL) in 1,2-dichloroethane (15 mL) at -5 °C was added drop-wise chloroacetyl chloride (3.97 mL, 50 mmol). The temperature was allowed to increase to 10 °C then the aqueous layer was separated and washed with 1,2-dichloroethane (2 x 10 mL). The organic layers were combined and were washed successively with 5% HCl (10 mL), 5% $NaHCO_3$ (10 mL) and water (10 mL), and dried ($MgSO_4$). The solvent was removed *in vacuo* and the crude product distilled under reduced pressure to afford **[93]** (4.89 g, 69%) as a colourless liquid.[6] ^{1}H NMR ($CDCl_3$) δ 0.80-1.00 (m, 6H, 2 x CH_3), 1.50-1.66 (m, 4H, 2 x CH_2), 3.21-3.31 (m, 4H, 2 x NCH_2), 4.05 (s, 2H, CH_2Cl). ^{13}C NMR ($CDCl_3$) δ 11.3 (CH_3), 11.4 (CH_3), 20.7 (CH_2), 22.4 (CH_2), 41.4 (CH_2Cl), 47.9 (NCH_2), 50.0 (NCH_2), 166.3 (C=O). MS-ES *m/z* 180 (^{37}Cl M+1, 9), 178 (^{35}Cl M+1, 24), 102 (100%). HRMS-ES calculated for $C_8H_{17}NO^{35}Cl$: 178.0999, found 178.1002.

---

[6] Ref. 169 did not include NMR data

***2-Chloro-N,N-di-n-butylacetamide* [94]** [182]

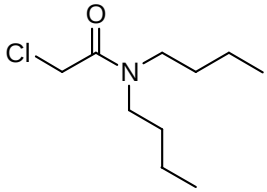

Using the same method for the synthesis of **[93]**, the title compound was prepared as a yellow oil (3.25 g, 39%) from di-*n*-butylamine (5.17 g, 40 mmol), NaOH (20%, 10 mL), and chloroacetyl chloride (3.97 mL, 50 mmol) in 1,2-dichloroethane (15 mL).[7] ^{1}H NMR ($CDCl_3$) δ 0.89-0.97 (m, 6H, 2 x CH_3), 1.30-1.34 (m, 4H, 2 x $C\underline{H_2}CH_3$), 1.50-1.58 (m, 4H, 2 x $NCH_2C\underline{H_2}$), 3.24-3.34 (m, 4H, 2 x NCH_2), 4.04 (s, 2H, CH_2Cl). ^{13}C NMR ($CDCl_3$) δ 13.8 (CH_3), 14.0 (CH_3), 20.19 ($\underline{C}H_2CH_3$), 20.25 ($\underline{C}H_2CH_3$), 29.6 ($NCH_2\underline{C}H_2$), 31.3 ($NCH_2\underline{C}H_2$), 41.4 (CH_2Cl), 46.1 (NCH_2), 48.2 (NCH_2), 166.3 (C=O). MS-EI *m/z* 207 (^{37}Cl M^+, 4), 178 (^{35}Cl M^+, 4), 120 (100%).

***N,N*-Dimethyl-[3-cyano-4-(4-iodophenyl)-4-oxo]butanamide [95]**

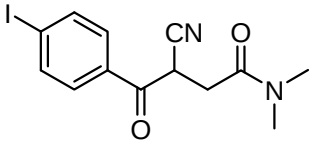

A mixture of 4-iodobenzoylacetonitrile **[89]** (2.71 g, 10 mmol), 2-chloro-*N,N*-dimethylacetamide (1.08 mL, 10.5 mmol), K_2CO_3 (1.52 g, 11 mmol), KI (0.25 g, 1.5 mmol), Bu_4NI (0.5 g) and anhydrous DMF (15 mL) was stirred at RT for 24 h. The mixture was partitioned between EtOAc (100 mL) and dilute brine (50 mL) containing AcOH (1.5 mL). The organic layer was washed with dilute brine (2 x 25 mL), dried (Na_2SO_4), and evaporated. The resulting brown oil was subjected to silica gel column chromatography using EtOAc:PE (1:1) to afford **[95]** (2.13 g, 60%) as a yellow oil. ^{1}H NMR ($CDCl_3$) δ 2.90 (dd, 1H, ^{2}J = 16.4, ^{3}J = 4.2, C$\underline{H}$HCO), 2.92 (s, 3H, NCH_3), 3.07 (s, 3H, NCH_3),

[7] Ref. 182 did not include NMR data

3.40 (dd, 1H, ^{3}J = 9.4, ^{2}J = 16.4, CH<u>H</u>CO), 4.91 (dd, 1H, ^{3}J = 9.4, ^{3}J = 4.3, CH), 7.76 (d, 2H, J = 8.6, ArH2 and ArH6), 7.89 (d, 2H, J = 8.6, ArH3 and ArH5). ^{13}C NMR ($CDCl_3$) δ 33.0 (CH), 33.9 (CH_2), 35.8 (NCH_3), 37.1 (NCH_3), 103.0 (ArC4), 116.9 (CN), 130.3 (ArC2 and ArC6), 133.7 (ArC1), 138.5 (ArC3 and ArC5), 168.0 (NC=O), 189.3 (C=O). MS-EI *m/z* 356 (M^+, 35), 231 (100%). HRMS-EI calculated for $C_{13}H_{13}O_2N_2I$: 356.0022, found 356.0025.

***N,N*-Diethyl-[3-cyano-4-(4-iodophenyl)-4-oxo]butanamide [96]**

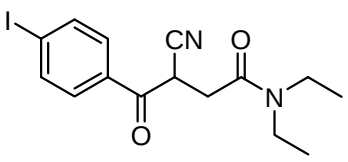

A mixture of **[89]** (1.10 g, 4.06 mmol), 2-chloro-*N,N*-diethylacetamide (0.59 mL, 4.26 mmol), K_2CO_3 (0.62 g, 4.5 mmol), KI (125 mg, 1.5 mmol), Bu_4NI (0.25 g), and anhydrous DMF (6 mL) was stirred at RT for 24 h. The mixture was partitioned between EtOAc (100 mL) and water (50 mL) containing AcOH (1.5 mL) and some NaCl. The EtOAc layer was washed with dilute brine (2 x 25 mL), dried (Na_2SO_4), and evaporated. The brown oil was subjected to silica gel column chromatography using EtOAc:heptane (1:1), and the isolated product was recrystallised from EtOAc:PE to afford **[96]** (0.89 g, 57%) as white crystals, mp. 114-115 °C. ^{1}H NMR ($CDCl_3$) δ 1.08 (t, 3H, J = 7.2, CH_3) 1.27 (t, 3H, J = 7.2, CH_3), 2.89 (dd, 1H, ^{2}J = 16.2, ^{3}J = 4.3, C<u>H</u>HCO), 3.24-3.45 (m, 5H, 2 x NCH_2, CH<u>H</u>CO), 4.95 (dd, 1H, ^{3}J = 9.6 ^{3}J = 4.3, CH), 7.76 (d, 2H, J = 8.4, ArH2 and ArH6), 7.90 (d, 2H, J = 8.8, ArH3 and ArH5). ^{13}C NMR ($CDCl_3$) δ 13.3 (CH_3), 14.4 (CH_3), 33.1 (CH), 34.1 (CH_2), 41.0 (NCH_2), 42.4 (NCH_2), 103.2 (ArC4), 117.1 (CN), 130.5 (ArC2 and ArC6), 133.8 (ArC1), 138.7 (ArC3 and ArC5), 167.2 (NC=O), 189.5 (C=O). MS-ES *m/z* 385 (M+1, 100%). HRMS-ES calculated for $C_{15}H_{18}N_2O_2I$: 385.0413, found 385.0395.

***N,N*-Di-*n*-propyl-[3-cyano-4-(4-iodophenyl)-4-oxo]butanamide [97]**

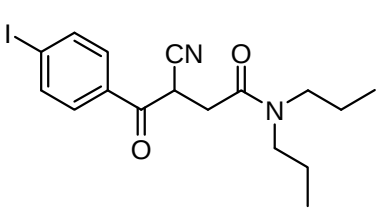

A mixture of **[89]** (1.50 g, 5.5 mmol), 2-chloro-*N,N*-di-*n*-propylacetamide **[93]** (1.03 g, 5.8 mmol), K_2CO_3 (0.84 g, 6.1 mmol), KI (0.1 g), Bu_4NI (0.2 g), and anhydrous DMF (6 mL) was stirred at RT for 24 h. The mixture was partitioned between EtOAc (100 mL) and dilute brine (50 mL) containing AcOH (1.5 mL). The organic layer was washed with dilute NaCl solution (2 x 25 mL), dried (Na_2SO_4), and evaporated. The crude product was subjected to silica gel column chromatography using EtOAc:heptane (35:65) to give **[97]** (1.57 g, 69%) as a yellow oil. ^{1}H NMR ($CDCl_3$) δ 0.84 (t, 3H, J = 7.4, CH_3), 0.99 (t, 3H, J = 7.4, CH_3), 1.46-1.71 (m, 4H, 2 x CH_2), 2.88 (dd, 1H, ^2J = 16.2, ^3J = 4.1, C<u>H</u>HCO), 3.15-3.41 (m, 4H, 2 x NCH_2), 3.41 (dd, 1H, ^3J = 9.7, ^2J = 16.2, CH<u>H</u>CO), 4.95 (dd, 1H, ^3J = 9.6, ^3J = 4.1, CH), 7.74 (d, 2H, J = 8.5, ArH2 and ArH6), 7.89 (d, 2H, J = 8.5, ArH3 and ArH5). ^{13}C NMR ($CDCl_3$) δ 11.4 (2 x CH_3), 20.9 (<u>C</u>H_2CH_3), 22.2 (<u>C</u>H_2CH_3), 33.0 (CH), 34.0 (<u>C</u>H_2CO), 48.1 (NCH_2), 49.8 (NCH_2), 103.0 (ArC4), 117.0 (CN), 130.3 (ArC2 and ArC6), 133.8 (ArC1), 138.5 (ArC3 and ArC5), 167.5 (NC=O), 189.3 (C=O). MS-ES *m/z* 413 (M+1, 8), 186 (100%). HRMS-ES calculated for $C_{17}H_{22}N_2O_2I$: 413.0726, found 413.0733.

_N,N_-Di-_n_-butyl-[3-cyano-4-(4-iodophenyl)-4-oxo]butanamide [98] and _N,N_-Di-_n_-butyl-[3-cyano-4-(4-iodophenyl)-4-(_N,N_-di-_n_-butylacetamidyl)oxy]-3-butenamide [99]

A mixture of **[89]** (256 mg, 0.94 mmol), 2-chloro-*N,N*-di-*n*-butylacetamide **[94]** (200 mg, 0.99 mmol), K_2CO_3 (0.14 g, 1.03 mmol), KI (25 mg), Bu_4NI (50 mg), and anhydrous DMF (6 mL) was stirred at RT for 24 h. The mixture was partitioned between EtOAc (25 mL) and dilute NaCl solution (10 mL) containing AcOH (0.5 mL).

The organic layer was washed with dilute NaCl solution (2 x 10 mL), dried (Na_2SO_4), and evaporated. The crude product was subjected to silica gel column chromatography using EtOAc:heptane (50:50) to give **[98]** (245 mg, 59%) as a yellow oil, and **[99]** (61 mg, 11%) as a yellow oil.

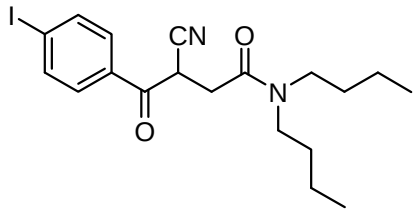

[98] ^{1}H NMR ($CDCl_3$) δ 0.84-1.00 (m, 6H, 2 x CH_3), 1.20-1.70 (m, 8H, 4 x CH_2), 2.87 (dd, 1H, ^2J = 16.2, ^3J = 4.1, C<u>H</u>HCO), 3.20-3.38 (m, 4H, 2 x NCH_2), 3.40 (dd, 1H, ^2J = 16.2, ^3J = 9.7, CH<u>H</u>CO), 4.95 (dd, 1H, ^3J = 9.6, ^3J = 4.1, CH), 7.75 (d, 2H, J = 8.5, ArH2 and ArH6), 7.90 (d, 2H, J = 8.5, ArH3 and ArH5). ^{13}C NMR ($CDCl_3$) δ 14.0 (2 x CH_3), 20.3 (2 x <u>C</u>H_2CH_3), 29.9 (NCH_2<u>C</u>H_2), 31.1 (NCH_2<u>C</u>H_2), 33.0 (CH), 34.0 (<u>C</u>H_2CO), 46.3 (NCH_2), 47.9 (NCH_2), 103.0 (ArC4), 117.0 (CN), 130.3 (ArC2 and ArC6), 133.7 (ArC1), 138.6 (ArC3 and ArC5), 167.4 (NC=O), 189.2 (C=O). MS-EI *m/z* 440 (M^+, 24), 312 (M^+ - $N(Bu)_2$, 47), 231 (100%). HRMS-EI calculated for $C_{19}H_{25}N_2O_2I$: 440.0961, found 440.0950.

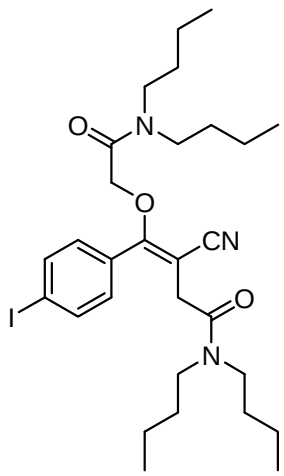

[99] ^{1}H NMR ($CDCl_3$) δ 0.84 (t, 3H, J = 7.2, CH_3), 0.85-1.00 (m, 9H, 3 x CH_3), 1.02-1.13 (m, 2H, CH_2), 1.20-1.36 (m, 10H, 5 x CH_2), 1.50-1.60 (m, 4H, 2 x CH_2), 2.83 (t, 2H, J = 7.6, NCH_2), 3.21 (t, 2H, J = 7.6, NCH_2), 3.26-3.35 (m, 4H, 2 x NCH_2), 3.57 (s, 2H, $COCH_2$), 4.37 (s, 2H, $COCH_2$), 7.27 (d, 2H, J = 8.3, ArH2 and ArH6), 7.78 (d, 2H, J = 8.3, ArH3 and ArH5). ^{13}C NMR ($CDCl_3$) δ 13.91, 13.96, 14.00 (double intensity) (4 x CH_3), 19.9, 20.3 (double intensity), 20.4 (4 x CH_2), 29.7, 30.0, 30.8, 31.3 (4 x CH_2), 32.8 (CO<u>C</u>H_2), 45.9, 46.35, 46.39, 48.1 (4 x NCH_2), 67.0 (OCH_2), 92.2 (OC=<u>C</u>), 97.5 (ArC4), 119.6 (CN), 130.5 (ArC1), 131.3 (ArC2 and ArC6), 138.2 (ArC3

and ArC5), 166.4 (C=O), 167.8 (OC=C), 168.2 (C=O). MS-ES *m/z* 611 (M+1, 20), 265 (100%).

_N,N_-Dimethyl-[3-amino-5-(4-iodophenyl)pyrazol-4-yl]acetamide [100]

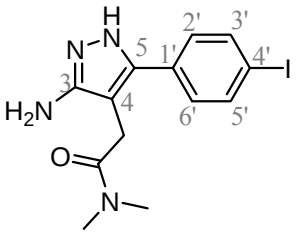

To a solution of the amide **[95]** (140 mg, 0.393 mmol) in THF (5 mL) was added hydrazine hydrate (157 μL, 0.786 mmol, 24-26% in H_2O), followed by AcOH (50 μL). The mixture was heated at reflux for 24 h. The mixture was evaporated and 10% Na_2CO_3 (20 mL) was added. The mixture was extracted into $CHCl_3$ (2 x 25 mL), dried ($MgSO_4$), and evaporated, leaving **[100]** (73 mg, 50%) as a brown solid. ^{1}H NMR (DMSO) δ 2.79 (s, 3H, NCH_3), 2.92 (s, 3H, NCH_3), 3.42 (s, 2H, CH_2), 4.58 (bs, 2H, NH_2), 7.24 (d, 2H, *J* = 8.3, ArH2' and ArH6'), 7.75 (d, 2H, *J* = 8.3, ArH3' and ArH5'). ^{13}C NMR (DMSO) δ 27.8 (CH_2), 35.2 (NCH_3), 36.9 (NCH_3), 93.3 (ArC4'), 129.0 (ArC2' and ArC6'), 129.3 (ArC1'), 137.3 (ArC3' and ArC5'), 170.5 (C=O).[8] MS-EI *m/z* 370 (M^+, 53), 298 (M^+ - $CON(Me)_2$, 100%). HRMS-EI calculated for $C_{13}H_{15}ON_4I$: 370.0291, found 370.0281.

_N,N_-Diethyl-[3-amino-5-(4-iodophenyl)pyrazol-4-yl]acetamide [101]

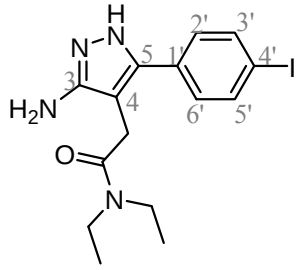

To a solution of the butanamide **[96]** (1.17 g, 3.04 mmol) in THF (20 mL) was added hydrazine hydrate (0.55 mL, 6.08 mmol, 35% in H_2O) and AcOH (0.2 mL) and the reaction

[8] Some quaternary carbons in the ^{13}C NMR were too weak to distinguish and assign, even after 14000 scans. See compounds **[101]** and **[102]** for quaternary peaks (which were also very weak and broad, but distinguishable).

mixture was heated at reflux for 20 h. The solvent was evaporated, and Na_2CO_3 solution (20% w/v, 40 mL) and DCM (50 mL) were added. The DCM layer was separated, dried ($MgSO_4$), and evaporated to afford **[101]** (0.82 g, 68%) as a yellow solid, mp. 46-48 °C. ^{1}H NMR ($CDCl_3$) δ 0.95 (t, 3H, *J* = 7.1, CH_3), 1.08 (t, 3H, *J* = 7.1, CH_3), 3.08 (q, 2H, *J* = 7.1, NCH_2), 3.32 (q, 2H, *J* = 7.1, NCH_2), 3.47 (s, 2H, CH_2), 5.65 (bs, 2H, NH_2), 7.10 (d, 2H, *J* = 8.3, ArH2' and ArH6'), 7.71 (d, 2H, *J* = 8.3, ArH3' and ArH5'). ^{13}C NMR ($CDCl_3$) δ 13.0 (CH_3), 14.1 (CH_3), 28.4 (CH_2), 40.6 (NCH_2), 42.4 (NCH_2), 93.9 (ArC4'), 96.8 (C4), 129.4 (ArC2' and ArC6'), 130.9 (ArC1'), 137.8 (ArC3' and ArC5'), 143.2 (C5), 152.7 (C3), 170.2 (NC=O). MS-ES *m/z* 399 (M+1, 100%). HRMS-ES calculated for $C_{15}H_{20}N_4OI$: 399.0682, found 399.0688.

_N,N_-Di-_n_-propyl-[3-amino-5-(4-iodophenyl)pyrazol-4-yl]acetamide [102]

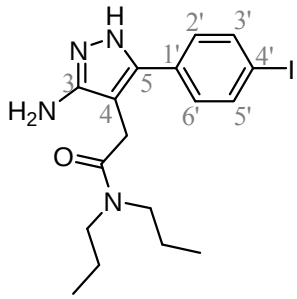

To a solution of the amide **[97]** (0.98 g, 2.4 mmol) in THF (10 mL) was added hydrazine hydrate (950 μL, 4.8 mmol, 24-26% in H_2O), followed by AcOH (50 μL). The mixture was heated at reflux for 20 h. The solvent was evaporated, and Na_2CO_3 solution (20% w/v, 40 mL) and DCM (50 mL) were added. The DCM layer was separated, dried ($MgSO_4$), and evaporated. The crude product was subjected to silica gel column chromatography using MeOH:DCM (1:19) to give the product **[102]** (0.693 g, 68%) as a yellow oil. ^{1}H NMR ($CDCl_3$) δ 0.60 (t, 3H, *J* = 7.4, CH_3), 0.84 (t, 3H, *J* = 7.4, CH_3), 1.34-1.38 (m, 2H, CH_2), 1.46-1.52 (m, 2H, CH_2), 2.88-2.94 (m, 2H, NCH_2), 3.19-3.24 (m, 2H, NCH_2), 3.47 (s, 2H, $COCH_2$), 4.90 (bs, 2H, NH_2), 7.10 (d, 2H, *J* = 8.3, ArH2' and ArH6'), 7.73 (d, 2H, *J* = 8.3, ArH3' and ArH5'). ^{13}C NMR ($CDCl_3$) δ 10.9 (CH_3), 11.4 (CH_3), 20.9 (CH_2), 22.2 (CH_2), 28.5 ($CO\underline{C}H_2$), 48.1 (NCH_2), 50.0 (NCH_2), 94.1 (ArC4'), 97.0 (C4), 129.8 (ArC2' and

ArC6'), 130.8 (ArC1'), 138.1 (ArC3' and ArC5'), 143.2 (C5), 153.0 (C3), 170.7 (NC=O) MS-ES *m/z* 427 (M+1, 75), 324 (100%). HRMS-ES calculated for $C_{17}H_{24}N_4OI$: 427.0995, found 427.0974.

Ethyl [3-cyano-4-(4-iodophenyl)-4-oxo]butanoate [103]

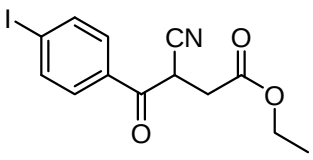

To a solution of butanamide **[96]** (1.03 g, 2.67 mmol) in EtOH (20 mL) was added hydrazine hydrate (0.26 mL, 5.35 mmol) followed by AcOH (0.3 mL), and the mixture was heated at reflux for 8 h. The mixture was evaporated, leaving a crude yellow oil. To this was added Na_2CO_3 solution (20% w/v, 40 mL), followed by $CHCl_3$ (25 mL). The organic layer was separated and the aqueous layer was extracted with $CHCl_3$ (2 x 25 mL). The organic layers were combined, dried ($MgSO_4$), and the solvent evaporated. The crude product was subjected to silica gel column chromatography using MeOH:DCM (1:9), to give **[103]** (0.53 g, 50%), and **[102]** (0.28 g, 26%). **[103]** ^{1}H NMR ($CDCl_3$) δ 1.27 (t, 3H, J = 7.1, CH_3), 2.93 (dd, 1H, ^2J = 17.3, ^3J = 5.2, CHC<u>H</u>H), 3.26 (dd, 1H, ^2J = 17.3, ^3J = 8.6, CHCH<u>H</u>), 4.18 (q, 2H, J = 7.1, OCH_2), 4.68 (dd, 1H, ^3J = 8.6, ^3J = 5.2, C<u>H</u>CH_2), 7.74 (d, 2H, J = 8.5, ArH2 and ArH6), 7.92 (d, 2H, J = 8.6, ArH3 and ArH5). ^{13}C NMR ($CDCl_3$) δ 15.3 (CH_3), 34.1 (CH<u>C</u>H_2), 35.4 (CH), 63.0 (OCH_2), 104.5 (ArC4), 117.2 (CN), 131.3 (ArC2 and ArC6), 134.3 (ArC1), 139.7 (ArC3 and ArC5), 170.6 (OC=O), 189.3 (C=O).

***N,N*-Dimethyl-[2-(4-iodophenyl)-5,7-dimethylpyrazolo[1,5-*a*]pyrimidin-3-yl]acetamide [90]**

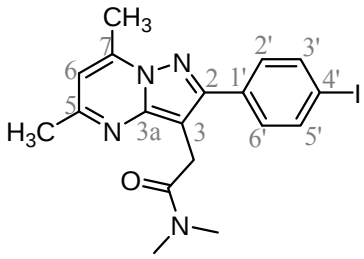

Pentane-2,4-dione (64 μL, 0.627 mmol) was added to a stirred solution of **[100]** (232 mg, 0.627 mmol) in EtOH (8 mL) and the mixture was heated at reflux for 7 h. The solvent was evaporated, leaving a yellow oil which was subjected to silica gel column chromatography using MeOH:DCM (1:19), with the isolated product recrystallised from EtOH to afford **[90]** (106 mg, 39%) as white crystals, mp. 189-191 °C. ^{1}H NMR ($CDCl_3$) δ 2.54 (s, 3H, $ArCH_3$), 2.73 (s, 3H, $ArCH_3$), 2.98 (s, 3H, NCH_3), 3.19 (s, 3H, NCH_3), 3.91 (s, 2H, CH_2), 6.54 (s, 1H, ArH6), 7.59 (d, 2H, *J* = 8.4, ArH2' and ArH6'), 7.78 (d, 2H, *J* = 8.3, ArH3' and ArH5'). ^{13}C NMR ($CDCl_3$) δ 17.0 ($ArCH_3$), 24.9 ($ArCH_3$), 28.3 (CH_2), 36.1 (NCH_3), 37.8 (NCH_3), 94.6 (ArC4'), 101.1 (C3), 108.8 (C6), 130.6 (ArC2' and ArC6'), 133.5 (ArC1'), 137.8 (ArC3' and ArC5'), 145.0 (C7), 147.8 (C3a), 154.3 (C2), 158.0 (C5), 170.9 (NC=O). MS-EI *m/z* 434 (M^+, 25), 362 (M^+ - $CON(Me)_2$, 100%). HRMS-EI calculated for $C_{18}H_{19}N_4OI$: 434.0604, found 434.0602.

***N,N*-Diethyl-[2-(4-iodophenyl)-5,7-dimethylpyrazolo[1,5-*a*]pyrimidin-3-yl]-acetamide [91]**

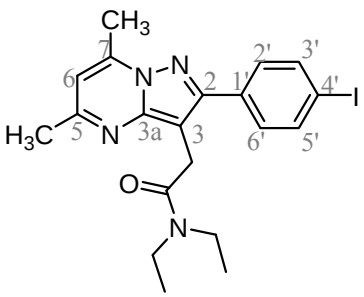

Pentane-2,4-dione (65 μL, 0.63 mmol) was added to a stirred solution of **[101]** (0.25 g, 0.63 mmol) and absolute EtOH (6 mL) and the mixture was heated at reflux for 4 h. The solvent was evaporated, leaving a yellow oil which was subjected to silica gel column chromatography using MeOH:DCM (1:19). The appropriate fractions were concentrated, and the residue was

recrystallised from EtOAc:PE to give **[91]** (0.136 g, 47%) as white crystals, mp. 171-172 °C. ^{1}H NMR ($CDCl_3$) δ 1.11 (t, 3H, *J* = 7.1, CH_3), 1.23 (t, 3H, *J* = 7.1, CH_3), 2.54 (s, 3H, $ArCH_3$), 2.73 (s, 3H, $ArCH_3$), 3.40 (q, 2H, *J* = 7.1, NCH_2), 3.52 (q, 2H, *J* = 7.1, NCH_2), 3.91 (s, 2H, $COCH_2$), 6.53 (s, 1H, ArH6), 7.60 (d, 2H, *J* = 8.4, ArH2' and ArH6'), 7.77 (d, 2H, *J* = 8.4, ArH3' and ArH5'). ^{13}C NMR ($CDCl_3$) δ 13.0 (CH_3), 14.3 (CH_3), 16.9 ($ArCH_3$), 24.3 ($ArCH_3$), 27.9 ($CO\underline{C}H_2$), 40.6 (NCH_2), 42.3 (NCH_2), 94.5 (ArC4'), 101.3 (C3), 108.5 (C6), 130.4 (ArC2' and ArC6'), 133.2 (ArC1'), 137.6 (ArC3' and ArC5'), 145.2 (C7), 147.1 (C3a), 154.3 (C2), 157.7 (C5), 169.7 (NC=O). MS-ES *m/z* 463 (M+1, 100%). HRMS-ES calculated for $C_{20}H_{24}N_4OI$: 463.0995, found 463.0987.

_N,N_-Di-_n_-propyl-[2-(4-iodophenyl)-5,7-dimethylpyrazolo[1,5-_a_]pyrimidin-3-yl]acetamide [92]

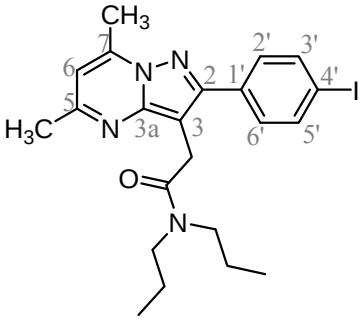

Pentane-2,4-dione (70 μL, 0.678 mmol) was added to a stirred solution of **[102]** (289 mg, 0.678 mmol) in EtOH (7.0 mL) and the mixture was heated at reflux for 4 h. The solvent was evaporated, leaving a yellow oil which was subjected to silica gel column chromatography using $CHCl_3$ to afford **[92]** (85.1 mg, 26%) as a yellow solid, mp. 123-125 °C. ^{1}H NMR ($CDCl_3$) δ 0.85 (t, 3H, *J* = 7.4, CH_3), 0.92 (t, 3H, *J* = 7.4, CH_3), 1.50-1.55 (m, 2H, CH_2), 1.62-1.70 (m, 2H, CH_2), 2.54 (s, 3H, $ArCH_3$), 2.73 (s, 3H, $ArCH_3$), 3.28-3.33 (m, 2H, NCH_2), 3.37-3.42 (m, 2H, NCH_2), 3.91 (s, 2H, $COCH_2$), 6.53 (s, 1H, ArH6), 7.60 (d, 2H, *J* = 8.4, ArH2' and ArH6'), 7.77 (d, 2H, *J* = 8.4, ArH3' and ArH5'). ^{13}C NMR ($CDCl_3$) δ 11.4 (CH_3), 11.5 (CH_3), 17.0 ($ArCH_3$), 21.1 (CH_2), 22.5 (CH_2), 24.8 ($ArCH_3$), 28.2 ($CO\underline{C}H_2$), 48.3 (NCH_2), 50.2 (NCH_2), 94.6 (ArC4'), 101.1 (C3), 108.7

(C6), 130.6 (ArC2' and ArC6'), 133.5 (ArC1'), 137.7 (ArC3' and ArC5'), 144.9 (C7), 147.7 (C3a), 154.2 (C2), 157.9 (C5), 170.5 (NC=O). MS-ES *m/z* 491 (M+1, 100%). HRMS-ES calculated for $C_{22}H_{28}N_4OI$: 491.1308, found 491.1310.

7.4 Experimental Procedure for the Synthesis of Pyrrolobenzoxazepine and pyridopyrrolooxazepine compounds

7.4.1 Synthesis of Ethyl (±)-α-bromophenylacetates

Ethyl 4-iodophenylacetate **[110]** [172]

Please see print copy for image

To a solution of 4-iodophenylacetic acid (5.10 g, 19.5 mmol) in EtOH (15 mL) was added a catalytic amount of conc. H_2SO_4 (30 μL). The reaction mixture was heated at reflux for 3.5 h and then concentrated. The residue was taken up in DCM (40 mL) and the organic phase was washed with 10% Na_2CO_3 (30 mL), brine (30 mL), dried ($MgSO_4$) and evaporated, leaving **[110]** (5.50 g, 97%) as a yellow oil, which was spectroscopically identical to that reported[9].[172] ^{1}H NMR ($CDCl_3$) δ 1.25 (t, 3H, *J* = 7.1, CH_3), 3.54 (s, 2H, CH_2), 4.15 (q, 2H, *J* = 7.1, OCH_2), 7.03 (d, 2H, *J* = 8.3, ArH2 and ArH6), 7.65 (d, 2H, *J* = 8.3, ArH3 and ArH5). ^{13}C NMR ($CDCl_3$) δ 14.3 (CH_3), 41.0 (CH_2), 61.2 (OCH_2), 92.7 (ArC4), 131.4 (ArC2 and ArC6), 133.9 (ArC1), 137.8 (ArC3 and ArC5), 171.2 (C=O). MS-EI *m/z* 290 (M^+, 76), 217 (M^+ - CO_2Et, 100%). HRMS-EI calculated for $C_{10}H_{11}O_2I$: 289.9804, found 289.9793.

[9] Only ^{1}H NMR was recorded in ref 172

***Ethyl 4-bromophenylacetate* [111]** [173]

Please see print copy for image

To a solution of 4-bromophenylacetic acid (4.30 g, 20 mmol) in dry EtOH (10 mL) was added a catalytic amount of conc. H_2SO_4 (30 μL). The reaction mixture was heated at reflux for 4 h and then concentrated. The residue was taken up in DCM (40 mL) and the organic phase was washed with 10% Na_2CO_3 (25 mL) and brine, dried ($MgSO_4$) and evaporated, leaving **[111]** (4.53 g, 93%) as a clear liquid, which was spectroscopically identical to that reported.[173] ^{1}H NMR ($CDCl_3$) δ 1.25 (t, 3H, *J* = 7.1, CH_3), 3.56 (s, 2H, CH_2), 4.15 (q, 2H, *J* = 7.1, OCH_2), 7.16 (d, 2H, *J* = 8.5, ArH2 and ArH6), 7.44 (d, 2H, *J* = 8.4, ArH3 and ArH5). ^{13}C NMR ($CDCl_3$) δ 14.5 (CH_3), 41.1 (CH_2), 61.4 (OCH_2), 121.5 (ArC4), 131.4 (ArC2 and ArC6), 132.0 (ArC3 and ArC5), 133.5 (ArC1), 171.4 (C=O). MS-EI *m/z* 244 (^{81}Br M^+, 17), 242 (^{79}Br M^+, 18), 169 (^{79}Br M^+ - CO_2Et, 100%). HRMS-EI calculated for $C_{10}H_{11}O_2{}^{79}Br$: 241.9942, found 241.9936.

***Ethyl (±)-α-bromo-4-iodophenylacetate* [112]** [172]

Please see print copy for image

To the ester **[110]** (3.54 g, 12.2 mmol) in CCl_4 (50 mL) was added *N*-bromosuccinimide (2.49 g, 14 mmol) and a catalytic amount of benzoyl peroxide. The mixture was heated at reflux for 17 h, then the succinimide was filtered and the solvent evaporated, leaving a red oil. The crude product was subjected to silica gel column chromatography using DCM:PE (3:7) to yield **[112]** (2.68 g, 59%) as a yellow oil, which was spectroscopically identical to that reported[10].[172] ^{1}H NMR ($CDCl_3$) δ 1.28 (t, 3H, *J* = 7.1, CH_3), 4.24 (m, 2H,

[10] Only ^{1}H NMR was recorded in ref 172

OCH_2), 5.26 (s, 1H, CH), 7.29 (d, 2H, *J* = 8.4, ArH2 and ArH6), 7.70 (d, 2H, *J* = 8.3, ArH3 and ArH5). ^{13}C NMR ($CDCl_3$) δ 14.1 (CH_3), 46.0 (CH), 62.8 (OCH_2), 95.5 (ArC4), 130.6 (ArC2 and ArC6), 135.7 (ArC1), 138.1 (ArC3 and ArC5), 168.0 (C=O). MS-EI *m/z* 370 (^{81}Br M^+, 33), 368 (^{79}Br M^+, 36), 289 (M^+ - Br, 100%). HRMS-EI calculated for $C_{10}H_{10}O_2{}^{79}BrI$: 367.8909, found 367.8911.

Ethyl (±)-α-bromo-4-bromophenylacetate **[113]** [174]

Please see print copy for image

A mixture of the ester **[111]** (3.70 g, 16.5 mmol), *N*-bromosuccinimide (3.00 g, 16.9 mmol), and a catalytic amount of benzoyl peroxide in CCl_4 (50 mL) was heated at reflux for 24 h. The succinimide was filtered off, and the filtrate concentrated, leaving **[113]** (4.75 g, 97%) as a clear liquid, which was spectroscopically identical to that reported.[174] ^1H NMR ($CDCl_3$) δ 1.28 (t, 3H, *J* = 7.1, CH_3), 4.24 (m, 2H, OCH_2), 5.28 (s, 1H, CH), 7.43 (d, 2H, *J* = 8.6, ArH2 and ArH6), 7.50 (d, 2H, *J* = 8.6, ArH3 and ArH5). ^{13}C NMR ($CDCl_3$) δ 15.1 (CH_3), 46.9 (CH), 63.9 (OCH_2), 124.7 (ArC4), 131.5 (ArC2 and ArC6), 133.2 (ArC3 and ArC5), 136.1 (ArC1), 169.1 (C=O). MS-EI *m/z* 323, ($^{81}Br^{81}Br$ M^+, 42), 321 ($^{81}Br^{79}Br$ M^+, 82), 319 ($^{79}Br^{79}Br$, 42), 249 (100%). HRMS-EI calculated for $C_{10}H_{10}O_2{}^{79}Br^{81}Br$: 321.9027, found 321.9018.

7.4.2 Experimental Procedures for the Synthesis of Pyridopyrrolooxazepines

***1-(3-Hydroxy-2-pyridyl)pyrrole* [114]** [175]

Please see print copy for image

This was synthesised as reported,[175] using 2-amino-3-hydroxypyridine (7.5 g, 68 mmol) and 2,5-dimethoxytetrahydrofuran (9.0 g, 68 mmol) in AcOH (250 mL). The product **[114]** (1.7 g, 16%, white solid) was spectroscopically identical to that reported.[11] mp. 188-190 °C. ^{1}H NMR (CD_3OD) δ 6.22 (dd, 2H, *J* = 2.2, 2.2, ArH3 and ArH4), 7.09 (dd, 1H, *J* = 8.1, 4.7, ArH5'), 7.34 (dt, 1H, *J* = 8.1, 1.5, ArH4'), 7.56 (dd, 2H, *J* = 2.2, 2.2, ArH2 and ArH5), 7.88 (dd, 1H, *J* = 4.7, 1.5 ArH6'). ^{13}C NMR (CD_3OD) δ 110.2 (ArC3 and ArC4), 121.6 (ArC2 and ArC5), 122.7 (ArC5'), 126.2 (ArC4'), 139.5 (ArC6'), 146.1 (ArC3'). MS-EI *m/z* 160 (M^+, 100%). HRMS-EI calculated for $C_9H_8ON_2$: 160.0637, found 160.0639.

Ethyl (±)-α-[3[2-(1*H*-pyrrol-1-yl)pyridyl]oxy]-4-iodophenylacetate [115]

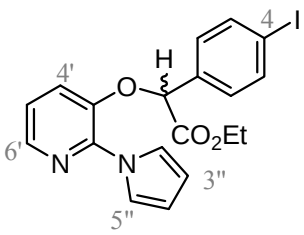

To a solution of the ester **[112]** (1.47 g, 3.98 mmol) and **[114]** (0.64 g, 3.98 mmol) in anhydrous DMF (10 mL) was added K_2CO_3 (0.55 g, 4.0 mmol), KI (0.25 g), and Bu_4NI (0.13 g). The mixture was stirred at RT for 2 h. EtOAc (60 mL) was then added to the mixture and the organic layer was washed with water (50 mL) and dilute brine (2 x 25 mL), dried (Na_2SO_4), and the solvent evaporated, leaving a yellow

[11] Ref 175 did not include mp. or ^{13}C NMR.

oil which was subjected to silica gel column chromatography using EtOAc:PE (1:1) to give **[115]** (1.68 g, 94%) as a pale yellow oil. ^{1}H NMR ($CDCl_3$) δ 1.20 (t, 3H, *J* = 7.13, CH_3), 4.19 (m, 2H, OCH_2), 5.54 (s, 1H, OCH), 6.34 (dd, 2H, *J* = 2.3, ArH3" and ArH4"), 7.01 (dd, 1H, *J* = 8.2, 4.7, ArH5'), 7.18 (dd, 1H, *J* = 8.2, 1.2, ArH4'), 7.25 (d, 2H, *J* = 8.4, ArH2 and ArH6), 7.71 (d, 2H, *J* = 8.4, ArH3 and ArH5), 7.76 (dd, 2H, *J* = 2.3, 2.3, ArH2" and ArH5"), 8.09 (dd, 1H, *J* = 4.7, 1.3, ArH6'). ^{13}C NMR ($CDCl_3$) δ 14.1 (CH_3), 62.3 (OCH_2), 79.1 (OCH), 95.5 (ArC4), 110.1 (ArC3" and ArC4"), 120.8 (ArC5' or ArC4'), 121.2 (ArC2" and ArC5"), 123.2 (ArC4' or ArC5'), 128.9 (ArC2 and ArC6), 134.1 (ArC1), 138.2 (ArC3 and ArC5), 141.4 (ArC6'), 142.6 (ArC3' or ArC2'), 143.6 (ArC2' or ArC3'), 168.4 (C=O). MS-EI *m/z* 448 (M^+, 50), 375 (M^+ - CO_2Et, 100%). HRMS-EI calculated for $C_{19}H_{17}N_2O_3I$: 448.0284, found 448.0277.

Ethyl (±)-α-[3[2-(1*H*-pyrrol-1-yl)pyridyl]oxy]-4-bromophenylacetate [116]

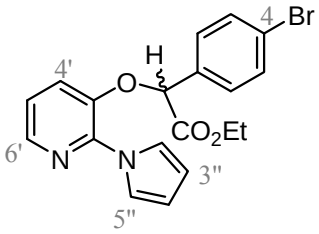

To a solution of the ester **[113]** (0.84 g, 2.57 mmol) and **[114]** (0.42 g, 2.57 mmol) in anhydrous DMF (10 mL) was added K_2CO_3 (0.42 g, 3.00 mmol), KI (0.1 g), and Bu_4NI (0.1 g). The mixture was stirred at RT for 3 h, then EtOAc (60 mL) was added. The organic layer was washed with water (50 mL), dilute brine (2 x 25 mL), dried (Na_2SO_4), and the solvent evaporated, leaving a yellow oil. The crude product was subjected to silica gel column chromatography using DCM:PE (2:3) to afford **[116]** (0.76 g, 74%) as a yellow oil. ^{1}H NMR ($CDCl_3$) δ 1.21 (t, 3H, *J* = 7.1, CH_3), 4.20 (q, 2H, *J* = 7.1, OCH_2), 5.56 (s, 1H, OCH), 6.34 (m, 2H, ArH3" and ArH4"), 7.03 (dd, 1H, *J* = 8.1, 4.7, ArH5'), 7.19 (d, 1H, *J* = 8.1, ArH4'), 7.39 (d, 2H, *J* = 8.4, ArH2 and ArH6), 7.52 (d, 2H, *J* = 8.4, ArH3 and ArH5), 7.76 (m, 2H, ArH2" and ArH5"), 8.11 (d, 1H, *J* = 4.7, ArH6'). ^{13}C NMR ($CDCl_3$) δ 14.1 (CH_3), 62.4 (OCH_2), 79.1 (OCH), 110.2

(ArC3" and ArC4"), 120.9 (ArC5' or ArC4'), 121.2 (ArC2" and ArC5"), 123.3 (ArC4' or ArC5'), 123.7 (ArC4), 128.9 (ArC2 and ArC6), 132.3 (ArC3 and ArC5), 133.5 (ArC1), 141.5 (ArC6'), 142.8 (ArC3' or ArC2'), 143.7 (ArC2' or ArC3'), 168.5 (C=O). MS-EI *m/z* 402 (^{81}Br M^+, 46), 400 (^{79}Br M^+, 48), 327 (100%). HRMS-EI calculated for $C_{19}H_{17}N_2O_3{}^{81}Br$: 402.0402, found 402.0394.

(±)-α-[3[2-(1*H*-Pyrrol-1-yl)pyridyl]oxy]-4-iodophenylacetic acid [117]

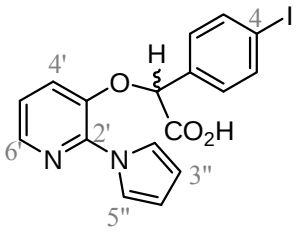

To a solution of the ester **[115]** (1.60 g, 3.8 mmol) in THF:EtOH (1:1, 50 mL) was added 5% aqueous NaOH (15 mL) and the reaction mixture was stirred at RT for 1 h. The mixture was then concentrated, acidified with 1M HCl, then extracted into EtOAc. The organic layers were combined, dried ($MgSO_4$), filtered, and the solvent evaporated, to afford **[117]** (1.49 g, 99%) as an off-white solid. ^{1}H NMR (CD_3OD) δ 5.89 (s, 1H, OCH), 6.27 (dd, 2H, *J* = 2.2, 2.2, ArH3" and ArH4"), 7.19 (dd, 1H, *J* = 8.2, 4.8, ArH5'), 7.30 (d, 2H, *J* = 8.3, ArH2 and ArH6), 7.52 (d, 1H, *J* = 7.9, ArH4'), 7.65 (dd, 2H, *J* = 2.2, 2.2, ArH2" and ArH5"), 7.74 (d, 2H, *J* = 8.3, ArH3 and ArH5), 8.03 (d, 1H, *J* = 4.7, ArH6'). ^{13}C NMR (CD_3OD) δ 79.5 (OCH), 95.3 (ArC4), 110.5 (ArC3" and ArC4"), 122.0 (ArC2" and ArC5"), 122.4 (ArC5'), 124.6 (ArC4'), 130.2 (ArC2 and ArC6), 132.7 (ArC3' or ArC2'), 136.3 (ArC1), 138.8 (ArC3 and ArC5), 141.5 (ArC6'), 145.6 (ArC2' or ArC3'), 171.6 (C=O). MS-EI *m/z* 420 (M^+, 29), 375 (M^+ - CO_2H, 39), 159 (M^+ - $IArCHCO_2H$, 100%). HRMS-EI calculated for $C_{17}H_{13}N_2O_3I$: 419.9971, found 419.9955.

(±)-α-[3[2-(1*H*-Pyrrol-1-yl)pyridyl]oxy]-4-bromophenylacetic acid [118]

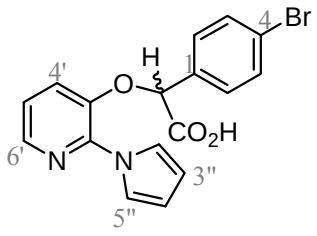

To a solution of the ester **[116]** (0.63 g, 1.56 mmol) in a mixture of THF:EtOH (1:1, 25 mL) was added 5% aqueous NaOH (8 mL). The reaction mixture was stirred at RT for 3 h, concentrated, acidified with 1M HCl, and extracted into EtOAc. The organic layers were combined, dried ($MgSO_4$), filtered, and the solvent evaporated to give **[118]** (0.53 g, 92%) as an off-white solid, mp. 86-88 °C. ^{1}H NMR (CD_3OD) δ 5.91 (s, 1H, OCH), 6.27 (m, 2H, ArH3" and ArH4"), 7.20 (dd, 1H, *J* = 8.1, 4.8, ArH5'), 7.45 (d, 2H, *J* = 8.2, ArH2 and ArH6), 7.51-7.60 (m, 3H, ArH3 and ArH5, ArH4'), 7.65 (m, 2H, ArH2" and ArH5"), 8.04 (d, 1H, *J* = 4.8, ArH6'). ^{13}C NMR (CD_3OD) δ 79.5 (CH), 110.7 (ArC3" and ArC4"), 122.2 (ArC2" and ArC5"), 122.6 (ArC5'), 124.1 (ArC4), 124.8 (ArC4'), 130.3 (ArC2 and ArC6), 132.9 (ArC3 and ArC5), 135.9 (ArC1), 141.7 (ArC6'), 143.8 (ArC3' or ArC2'), 145.8 (ArC2' or ArC3'), 171.8 (C=O). MS-EI *m/z* 374 (^{81}Br M^+, 20), 372 (^{79}Br M^+, 21), 159 (100%). HRMS-EI calculated for $C_{17}H_{13}N_2O_3{}^{79}Br$: 372.0110, found 372.0098.

(±)-6-(4-Iodophenyl)pyrido[3,2-*b*]pyrrolo[1,2-*d*][1,4]oxazepin-7(6*H*)one [119]

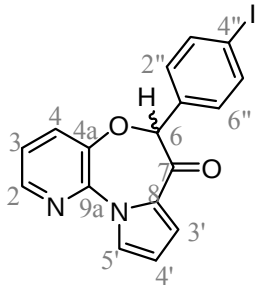

To a stirring mixture of the acid **[117]** (82.6 mg, 0.197 mmol) in dry DCM (20 mL) was added PCl_5 (53 mg, 0.217 mmol). The mixture was then heated at reflux for 20 h before the solution was poured into water and neutralised with 5% NaOH solution. The solution was extracted into DCM, dried ($MgSO_4$), filtered, and evaporated, leaving **[119]** (64.9 mg, 82%) as a yellow solid. ^{1}H NMR ($CDCl_3$) δ 5.53 (s, 1H, CH), 6.54 (m, 1H, ArH4'), 7.06 (d, 2H, *J* = 8.1, ArH2" and ArH6"), 7.15 (dd, 1H, *J* = 7.9, 4.6, ArH3), 7.41 (d, 1H, *J* = 8.1, ArH4), 7.49 (m, 1H, ArH3'), 7.69 (d, 2H, *J* =

8.3, ArH3" and ArH5"), 8.08 (d, 1H, *J* = 2.7, ArH5'), 8.27 (d, 1H, *J* = 4.6, ArH2). ^{13}C NMR ($CDCl_3$) δ 88.3 (CH), 95.3 (ArC4"), 112.2 (ArC4'), 122.8 (ArC3), 123.4 (ArC3'), 127.5 (ArC5'), 130.4 (ArC2" and ArC6"), 131.9 (qC), 132.0 (qC), 132.6 (ArC4), 134.6 (qC), 137.9 (ArC3" and ArC5"), 143.2 (qC), 144.8 (ArC2), 186.3 (C=O).[12] MS-EI *m/z* 402 (M^+, 25), 170 (M^+ - OCPhI, 100%). HRMS-EI calculated for $C_{17}H_{11}N_2O_2I$: 401.9865, found 401.9857.

(±)-6-(4-Bromophenyl)pyrido[3,2-*b*]pyrrolo[1,2-*d*][1,4]oxazepin-7(6*H*)-one [120]

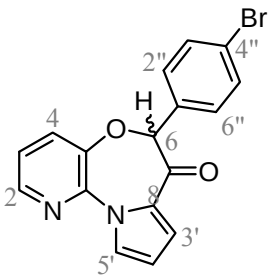

To a solution of the acid **[118]** (88 mg, 0.24 mmol) in dry DCM (15 mL) was added PCl_5 (69 mg, 0.28 mmol). The reaction mixture was heated at reflux for 25 h, then poured into icy water, neutralised with 5% NaOH solution, and the organic layer separated. The organic layer was washed with brine (2 x 10 mL), dried ($MgSO_4$), and evaporated to afford **[120]** (75 mg, 88%) as a red solid. ^{1}H NMR ($CDCl_3$) δ 5.55 (s, 1H, CH), 6.55 (m, 1H, ArH4'), 7.18 (dd, 1H, *J* = 7.9, 4.7, ArH3), 7.19 (d, 2H, *J* = 8.3, ArH2" and ArH6"), 7.42 (d, 1H, *J* = 7.8, ArH4), 7.47-7.50 (m, 3H, ArH3" and ArH3", ArH4'), 8.08 (m, 1H, ArH5'), 8.27 (d, 1H, *J* = 4.6, ArH2). ^{13}C NMR ($CDCl_3$) δ 88.2 (CH), 112.3 (ArC4'), 122.8 (ArC3), 123.4 (ArC3'), 123.5 (ArC4"), 127.6 (ArC5'), 130.3 (ArC2" and ArC6" or ArC3" and ArC5"), 131.9 (ArC3" and ArC5" or ArC2" and ArC6"), 132.1 (qC), 132.3 (qC), 132.7 (ArC4), 133.9 (qC), 143.2 (qC), 144.7 (ArC2), 186.2 (C=O). MS-EI *m/z* 356 (^{81}Br M^+, 34), 354 (^{79}Br M^+, 28), 170 (100%). HRMS-EI calculated for $C_{17}H_{11}N_2O_2{}^{79}Br$: 354.0004, found 354.0001.

---

[12] Carbons labelled as qC are quaternary carbons which could not be assigned with confidence as they did not show distinctive cross coupling in 2D NMR experiments.

7-[(Diethylcarbamoyl)oxy]-6-(4-iodophenyl)pyrido[3,2-*b*]pyrrolo[1,2-*d*][1,4]-oxazepine [121]

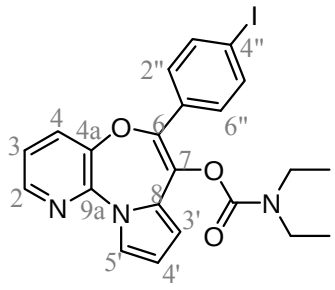

To a solution of the ketone **[119]** (55 mg, 0.137 mmol) in dry THF (4 mL) was added *N*,*N*-diethylcarbamyl chloride (21 μL, 0.164 mmol) and a suspension of KH (30-35% in oil, 25 mg, 0.219 mmol) in dry THF (2 mL). The reaction mixture was stirred overnight at RT. The solvent was evaporated and the residue taken up in DCM (20 mL). The organic layer was washed with NH_4Cl (10 mL), brine (10 mL), dried ($MgSO_4$) and concentrated. The residue was subjected to silica gel column chromatography using EtOAc:PE (1:1) to give **[121]** (28.6 mg, 42%) as a off-white solid. ^{1}H NMR ($CDCl_3$) δ 1.12 (t, 3H, *J* = 7.1, CH_3), 1.22 (t, 3H, *J* = 7.1, CH_3), 3.30 (q, 2H, *J* = 7.1, NCH_2), 3.43 (q, 2H, *J* = 7.1, NCH_2), 6.40 (m, 1H, ArH4'), 6.44 (m, 1H, ArH3'), 7.13 (dd, 1H, *J* = 7.9, 4.7, ArH3), 7.45-7.50 (m, 3H, ArH2" and ArH6", ArH4), 7.70-7.73 (m, 3H, ArH3" and ArH5", ArH5'), 8.23 (dd, 1H, *J* = 4.7, 1.5, ArH2). ^{13}C NMR ($CDCl_3$) δ 13.4 (CH_3), 14.6 (CH_3), 42.0 (NCH_2), 42.5 (NCH_2), 94.3 (ArC4"), 111.1 (ArC4'), 112.2 (ArC3'), 122.4 (ArC3), 122.7 (ArC5'), 127.4 (qC), 128.6 (ArC2" and ArC6"), 130.2 (ArC4), 132.8 (qC), 134.0 (qC), 137.6 (ArC3" and ArC5"), 143.1 (qC), 144.9 (ArC2), 145.4 (qC), 146.0 (qC), 153.0 (C=O). MS-EI *m/z* 501 (M^+, 60), 402 (M^+ - $CON(Et)_2$, 21), 100 (100%). HRMS-EI calculated for $C_{22}H_{20}N_3O_3I$: 501.0549, found 501.0549.

Pyrido[3,2-*b*]pyrrolo[1,2-*d*][1,4]oxazine-6-one [122]

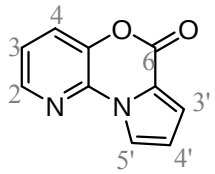

To a suspension of KH (30-35% in oil, 25 mg, 0.219 mmol) in dry THF (1.5 mL) was added a solution of the ketone **[119]** (80 mg, 0.199 mmol) in dry THF (3.5 mL). The solution was stirred at room temperature for 2 h, then *N*,*N*-diethylcarbamyl chloride (30 μL, 0.239 mmol) was added. The reaction mixture was stirred for 24 h, the solvent was evaporated, and the residue taken up in DCM (20 mL). The organic layer was washed with NH_4Cl (10 mL), brine (10 mL), dried ($MgSO_4$) and concentrated. The residue was subjected to silica gel column chromatography using EtOAc:PE (3:7) to give **[122]** (5.9 mg, 16%) as a white solid. ^{1}H NMR ($CDCl_3$) δ 6.72 (dd, 1H, *J* = 3.6, 2.6, H4'), 7.29 (dd, 1H, *J* = 8.2, 4.8, H3), 7.42 (dd, 1H, *J* = 3.9, 1.3, H3'), 7.67 (dd, 1H, *J* = 8.2, 1.3, H4), 8.08 (dd, 1H, *J* = 2.6, 1.4, H5'), 8.29 (dd, 1H, *J* = 4.8, 1.3, H2). ^{13}C NMR ($CDCl_3$) δ 114.7 (ArC4'), 117.8 (qC), 119.4 (ArC3'), 119.9 (ArC5'), 122.2 (ArC3), 125.8 (ArC4), 135.7 (qC), 139.0 (qC), 144.0 (ArC2), 153.0 (C=O). MS-ES *m/z* 187 (M+1, 65), 129 (100%).

(±)-6-(4-Bromophenyl)-6-(*N*,*N*-diethylcarbamoyl)pyrido[3,2-*b*]pyrrolo[1,2-*d*][1,4]oxazepin-7-one [123]

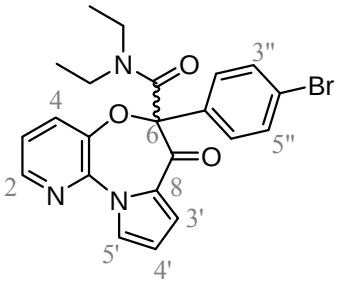

To a suspension of KH (30-35% in oil, 43 mg, 0.325 mmol) in THF (2 mL) was added the ketone **[120]** (105 mg, 0.295 mmol) in DMF (2 mL). The reaction mixture was stirred at RT for 2 h, then *N*,*N*-diethylcarbamoyl chloride (49.4 μL, 0.390 mmol) was added. The reaction mixture was stirred at RT overnight, then the solvent was evaporated. The mixture was taken up in DCM and washed with NH_4Cl then brine, dried ($MgSO_4$), and evaporated, leaving a crude oil. The crude oil was subjected to silica gel column chromatography using EtOAc:PE (3:2) to

give **[123]** (43.1 mg, 29%) as a sticky yellow oil. ^{1}H NMR ($CDCl_3$) δ 1.00 (t, 3H, *J* = 7.0, CH_3), 1.07 (t, 3H, *J* = 7.1, CH_3), 3.21 (m, 4H, 2 x NCH_2), 6.41 (m, 1H, ArH4'), 7.08 (dd, 1H, *J* = 4.0, 1.3, ArH3'), 7.31 (m, 1H, ArH5'), 7.46 (dd, 1H, *J* = 8.1, 4.8, ArH3), 7.59 (d, 2H, *J* = 8.6, ArH2" and ArH6"), 7.79 (dd, 1H, *J* = 8.1, 1.3, ArH4), 7.82 (d, 2H, *J* = 8.5, ArH3" and ArH5"), 8.39 (dd, 1H, *J* = 4.7, 1.3, ArH2). ^{13}C NMR ($CDCl_3$) δ 13.1 (CH_3), 14.0 (CH_3), 42.1 (NCH_2), 42.4 (NCH_2), 111.6 (ArC4'), 122.2 (ArC4"), 125.0 and 125.1 (ArC3' and ArC3), 129.0 (ArC4), 130.0 (qC), 131.7 (ArC2" and ArC6"), 132.0 (ArC1"), 132.2 (ArC3" and ArC5"), 133.1 (ArC5'), 143.6 (qC), 145.0 (ArC2), 145.3 (qC), 152.5 (qC), 181.1 (NC=O), 191.2 (C=O).

7.4.3 Experimental Procedures for the Synthesis of Pyrrolobenzoxazepines

1-(2-Hydroxyphenyl)pyrrole **[124]**

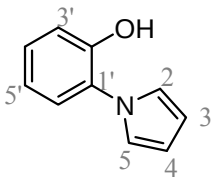

A mixture of 2,5-dimethoxytetrahydrofuran (13.2 g, 0.1 mol), *o*-aminophenol (12.0 g, 0.11 mol) and AcOH (35 mL) was heated at reflux for 4 h, then poured into ice water. The oil which precipitated was taken up into EtOAc, the organic solution was then washed with 5% $NaHCO_3$, then water. The organic extracts were dried (Na_2SO_4) and evaporated. The residual black oil was treated with benzene and filtered through Celite. The product was subjected to silica gel column chromatography using EtOAc:heptane (3:7) to give **[124]** (3.96 g, 25%) as a white solid which was spectroscopically identical to that reported in literature[176], mp. 39-41 °C. (Lit mp. 45-47 °C). ^{1}H NMR ($CDCl_3$) δ 5.27 (bs, 1H, OH), 6.39 (dd, 2H, *J* = 2.1, 2.1, ArH3 and ArH4), 6.86 (dd, 2H, *J* = 2.1, 2.1, ArH2 and ArH5), 6.96 (ddd, 1H, *J* = 7.6, 7.6, 1.3, ArH5'), 7.03 (dd, 1H, *J* = 8.1, 1.3, ArH3'), 7.20-7.30 (m, 2H, ArH6' and ArH4'). ^{13}C NMR ($CDCl_3$) δ 110.5 (ArC3 and ArC4), 116.8 (ArC3'), 121.0 (ArC2 and ArC5), 121.9 (ArC5'), 126.7 (ArC6'), 128.3 (ArC1'), 129.0 (ArC4'), 150.4 (ArC2'). MS-EI *m/z* 159 (M^+, 100%). HRMS-EI calculated for $C_{10}H_9ON$: 159.0684, found 159.0679.

Ethyl (±)-α-[2[1-(1*H*-pyrrol-1-yl)phenyl]oxy]-4-bromophenylacetate [125]

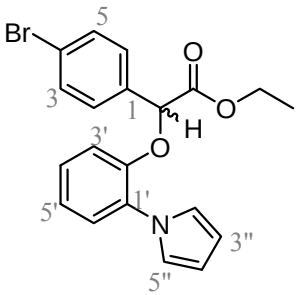

To a solution of the ester **[113]** (1.56 g, 4.84 mmol) and **[124]** (0.77 g, 4.84 mmol) in anhydrous DMF (15 mL) was added K_2CO_3 (0.69 g, 5.00 mmol), KI (0.3 g), and Bu_4NI (0.2 g). The

mixture was stirred at RT for 24 h. EtOAc (60 mL) was added to the mixture and the organic layer was washed with water (50 mL) and dilute brine (2 x 25 mL), dried (Na_2SO_4), and the solvent evaporated, leaving a yellow oil which was subjected to silica gel column chromatography using DCM:PE (2:3) to afford **[125]** (1.36 g, 70%) as a clear oil. ^{1}H NMR ($CDCl_3$) δ 1.17 (t, 3H, *J* = 7.1, CH_3), 4.14 (q, 2H, *J* = 7.1, OCH_2), 5.45 (s, 1H, OCH), 6.32 (dd, 2H, *J* = 2.1, 2.1, ArH3" and ArH4"), 6.97 (d, 1H, ArH6'), 7.04-7.10 (m, 3H, ArH2" and ArH5", ArH4'), 7.20 (dd, 1H, *J* = 7.2, 7.2, ArH5'), 7.29-7.35 (m, 3H, ArH3', ArH2 and ArH6), 7.46 (d, 2H, *J* = 8.5, ArH3 and ArH5). ^{13}C NMR ($CDCl_3$) δ 14.0 (CH_3), 61.8 (OCH_2), 78.7 (OCH), 109.1 (ArC3" and ArC4"), 115.4 (ArC3'), 122.1 (ArC2" and ArC5"), 122.8 (ArC5'), 123.1 (ArC4), 126.1 (ArC6'), 127.3 (ArC4'), 128.7 (ArC2 and ArC6), 131.5 (ArC1'), 131.8 (ArC3 and ArC5), 134.0 (ArC1), 149.9 (ArC2'), 169.0 (C=O). MS-EI *m/z* 401 (^{81}Br M^+, 34), 399 (^{79}Br M^+, 34), 328 (^{81}Br M^+ - CO_2Et, 90), 326 (^{79}Br M^+ - CO_2Et, 100%). HRMS-EI calculated for $C_{20}H_{18}NO_3{}^{81}Br$: 401.0450, found 401.0440.

(±)-α-[2[1-(1*H*-Pyrrol-1-yl)phenyl]oxy]-4-bromophenylacetic acid [126]

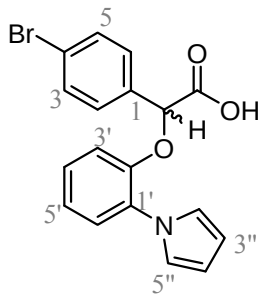

To a solution of the ester **[125]** (1.21 g, 3.02 mmol) in THF:EtOH (1:1, 40 mL) was added 5% aqueous NaOH (12 mL). The reaction mixture was stirred at RT for 2 h, concentrated, acidified with 1M HCl, and extracted into EtOAc. The organic layers were combined, dried ($MgSO_4$), filtered, and the solvent evaporated to give **[126]** (1.09, 97%) as an off-white solid, mp. 45-47 °C. ^{1}H NMR (CD_3OD) δ 5.56 (s, 1H, CH), 6.24 (dd, 2H, *J* = 2.1, ArH3" and ArH4"), 7.01 (dd, 1H, *J* = 7.8, ArH4'), 7.08 (d, 1H, *J* = 7.8, ArH3'), 7.10 (t, 2H, *J* = 2.1, ArH2" and ArH5"), 7.18 (dd, 1H, *J* = 7.8, 7.8, ArH5'), 7.27 (dd, 1H, *J* = 7.8, ArH6'), 7.36 (d, 2H, *J* = 8.6, ArH2 and ArH6 or

ArH3 and ArH5), 7.41 (d, 2H, *J* = 8.6, ArH2 and ArH6 or ArH3 and ArH5). ^{13}C NMR (CD_3OD) δ 80.1 (CH), 109.8 (ArC3" and ArC4"), 116.3 (ArC3'), 123.1 (ArC2" and ArC5"), 123.30 (ArC5'), 123.35 (ArC4), 126.8 (ArC6'), 128.3 (ArC4'), 130.0 (ArC2 and ArC6), 132.4 (ArC3 and ArC5), 132.5 (ArC1'), 136.8 (ArC1), 151.5 (ArC2'), 173.7 (C=O). MS-EI *m/z* 373 (^{81}Br M^+, 13), 371 (^{79}Br M^+, 13), 328 (^{81}Br M^+ - CO_2H, 21), 326 (^{79}Br M^+ - CO_2H, 24), 158 (M^+ - $BrArCHCO_2H$, 100%). HRMS-EI calculated for $C_{18}H_{14}NO_3{}^{79}Br$: 371.0157, found 371.0162.

(±)-6-(4-Bromophenyl)pyrrolo[2,1-*d*][1,5]benzoxazepin-7(6*H*)-one [127]

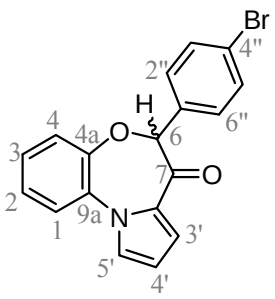

To a solution of the acid **[126]** (0.78 g, 2.10 mmol) in dry DCM (25 mL) was added PCl_5 (0.61 g, 2.93 mmol). The reaction mixture was heated at reflux for 20 h, then poured into icy water and neutralised with 5% NaOH solution. The organic layer was separated and washed with brine (2 x 25 mL), dried ($MgSO_4$), and evaporated to afford **[127]** (0.69 g, 93%) as a red viscous oil. ^{1}H NMR ($CDCl_3$) δ 5.46 (s, 1H, CH), 6.51 (dd, 1H, *J* = 3.2, 3.2, ArH4'), 7.11 (dd, 1H, *J* = 7.7, 1.5, ArH4), 7.19–7.29 (m, 4H, ArH2" and ArH6", ArH2, ArH3), 7.31–7.33 (m, 2H, ArH3' and ArH5'), 7.42 (dd, 1H, *J* = 7.8, 1.5, ArH1), 7.49 (d, 2H, *J* = 8.4, ArH3" and ArH5"). ^{13}C NMR ($CDCl_3$) δ 91.0 (CH), 113.3 (ArC4'), 122.3 (ArC3'), 123.5 (ArC4), 124.2 (ArC4"), 125.2 (ArC2), 127.4 (ArC3), 127.7 (ArC1), 129.0 (ArC5'), 131.1 (ArC2" and ArC6"), 132.8 (ArC3" and ArC5"), 134.3 (qC), 134.9 (qC), 136.3 (qC), 149.9 (ArC4a), 190.2 (C=O). MS-EI *m/z* 355 (^{81}Br M^+, 25) 353 (^{79}Br M^+, 25), 170 (100%). HRMS-EI calculated for $C_{18}H_{12}NO_2{}^{79}Br$: 353.0051, found 353.0040.

7-[(Diethylcarbamoyl)oxy]-6-(4-bromophenyl)pyrrolo[2,1-*d*][1,5]benzoxazepine [128]

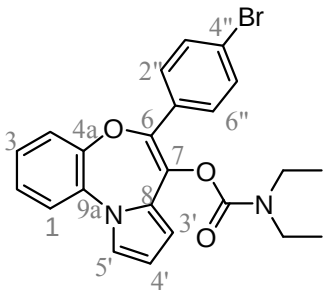

To a solution of the ketone **[127]** (0.96 g, 2.71 mmol) in anhydrous THF (7 mL) was added a suspension of KH (30-35% in oil, 0.41 g, 3.1 mmol) in dry THF (2 mL), and then *N*,*N*-diethylcarbamoyl chloride (0.43 mL, 3.36 mmol). After stirring overnight at RT, the solvent was evaporated and the residue taken up in EtOAc (25 mL). The organic layer was washed with NH_4Cl (25 mL), brine (25 mL), dried ($MgSO_4$) and concentrated. The residue was subjected to silica gel column chromatography using EtOAc:heptane (3:7) to afford **[128]** (0.78 g, 64%) as a white solid, mp. 58-60 °C. ^{1}H NMR ($CDCl_3$) δ 1.10 (t, 3H, *J* = 7.1, CH_3), 1.22 (t, 3H, *J* = 7.0, CH_3), 3.31 (q, 2H, *J* = 7.1, NCH_2), 3.43 (q, 2H, *J* = 7.1, NCH_2), 6.41 (m, 2H, ArH3' and ArH4'), 7.15-7.17 (m, 1H, ArH5') 7.17-7.22 (m, 3H, ArH2, ArH3, ArH4), 7.37 (d, 1H, *J* = 7.3, ArH1), 7.50 (d, 2H, *J* = 8.4, ArH3" and ArH5"), 7.63 (d, 2H, *J* = 8.7, ArH2" and ArH6"). ^{13}C NMR ($CDCl_3$) δ 13.5 (CH_3), 14.6 (CH_3), 42.0 (NCH_2), 42.4 (NCH_2), 110.3 (ArC4'), 111.0 (ArC3'), 121.7 (ArC5'), 122.1 (ArC4), 122.4 (ArC4"), 122.8 (ArC1), 126.1 (ArC3), 127.2 (ArC2), 128.51 (ArC1"), 128.54 (ArC2" and ArC6"), 131.5 (ArC3" and ArC5"), 132.5, 133.5, 134.2 (ArC4a, ArC7, ArC8), 144.1 (ArC6), 151.9 (ArC9a), 153.2 (C=O). MS-EI *m/z* 454 (^{81}Br M^+, 7), 452 (^{79}Br M^+, 7), 100 (100%). HRMS-EI calculated for $C_{23}H_{21}N_2O_3{}^{81}Br$: 454.0715, found 454.0708.

7-[(Diethylcarbamoyl)oxy]-6-(4-trimethylstannylphenyl)pyrrolo[2,1-*d*][1,5]benzoxazepine [129]

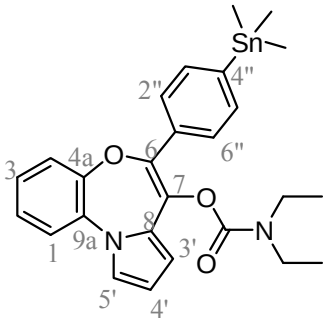

To a solution of the bromo derivative **[128]** (384 mg, 0.85 mmol) in anhydrous toluene (6 mL) was added hexamethylditin (830 mg, 2.54 mmol) and a catalytic amount of $Pd(0)(PPh_3)_4$ (~5 mg). The reaction mixture was heated at reflux for 7 h under N_2 gas, adding 2-5 mg of catalyst and hexamethylditin 4 times throughout the day. The reaction mixture was then cooled to RT, filtered and washed through Celite with EtOAc (25 mL) to remove the palladium, and the solvent evaporated. The crude oil was subjected to silica gel column chromatography using EtOAc:heptane (3:7) to yield stannane **[129]** (226 mg, 49%) as a white foam, mp. 53-55 °C . ^{1}H NMR ($CDCl_3$) δ 0.30 (s, 9H, $Sn(CH_3)_3$), 1.12 (t, 3H, *J* = 7.0, CH_3), 1.24 (t, 3H, *J* = 7.1, CH_3), 3.31 (q, 2H, *J* = 7.1, NCH_2), 3.42 (q, 2H, *J* = 7.1, NCH_2), 6.40 (m, 2H, ArH3' and ArH4'), 7.14-7.23 (m, 4H, ArH2, ArH3, ArH4, ArH5'), 7.37 (dd, 1H, *J* = 7.8, 1.8, ArH1), 7.50 (d, 2H, *J* = 8.1, ArH3" and ArH5"), 7.73 (d, 2H, *J* = 8.1, ArH2" and ArH6"). ^{13}C NMR ($CDCl_3$) δ -9.4 ($Sn(CH_3)_3$), 13.5 (CH_3), 14.6 (CH_3), 41.9 (NCH_2), 42.3 (NCH_2), 110.0 (ArC4'), 110.9 (ArC3'), 121.4 (ArC5'), 122.3 (ArC4), 122.6 (ArC1), 125.9 (ArC3), 126.2 (^{117}Sn-^{13}C *J* = 23, ArC3" and ArC5"), 127.0 (ArC2), 128.9 (ArC1"), 133.2, 133.6, 133.8 (ArC4a, ArC7, ArC8), 135.8 (^{117}Sn-^{13}C *J* = 18, ArC2" and ArC6"), 143.3 (ArC4"), 145.2 (ArC6), 152.0 (ArC9a), 153.4 (C=O). MS-EI *m/z* 538 (^{120}Sn M^+, 57), 537 (^{119}Sn M^+, 25), 536 (^{118}Sn M^+, 43), 535 (^{117}Sn M^+, 20), 534 (^{116}Sn M^+, 23), 100 (100%). HRMS-EI calculated for $C_{26}H_{30}N_2O_3{}^{120}Sn$: 538.1278, found 538.1271.

7-[(Diethylcarbamoyl)oxy]-6-(4-iodophenyl)pyrrolo[2,1-*d*][1,5]benzoxazepine [130]

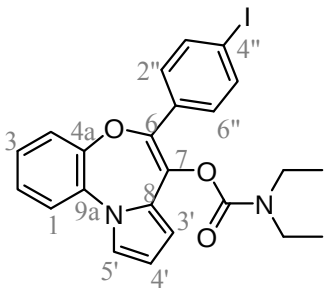

To a solution of the stannane **[129]** (88 mg, 0.16 mmol) in DCM (2.5 mL) was added dropwise a solution of I_2 (52 mg, 0.21 mmol) in DCM (2.5 mL). The solution was stirred at RT for 30 min, then was washed with $Na_2S_2O_5$ (240 mg in 7 mL water), then water (5 mL). The organic layers were dried ($MgSO_4$) and evaporated to give **[130]** (79 mg, 96%) as a white foam, mp. 56-58 °C. ^{1}H NMR ($CDCl_3$) δ 1.12 (t, 3H, *J* = 7.1, CH_3), 1.23 (t, 3H, *J* = 7.1, CH_3) 3.31 (q, 2H, *J* = 7.1, NCH_2), 3.43 (q, 2H, *J* = 7.1, NCH_2), 6.38-6.42 (m, 2H, ArH3' and ArH4'), 7.12-7.21 (m, 4H, 3 x ArH and ArH5'), 7.37 (d, 1H, *J* = 7.4, ArH), 7.49 (d, 2H, *J* = 8.6, ArH2" and ArH6"), 7.71 (d, 2H, *J* = 8.6, ArH3" and ArH5"). ^{13}C NMR ($CDCl_3$) δ 13.5 (CH_3), 14.6 (CH_3), 42.0 (NCH_2), 42.4 (NCH_2), 94.1 (ArC4"), 110.4 (ArC4'), 111.0 (ArC3'), 121.7 (ArC5'), 122.1 (ArC4), 122.8 (ArC1), 126.1 (ArC3), 127.2 (ArC2), 128.5 (ArC1"), 128.6 (ArC2" and ArC6"), 133.1, 133.5, 134.3 (ArC4a, ArC7, ArC8), 137.5 (ArC3" and ArC5"), 144.0 (ArC6), 151.9 (ArC9a), 153.2 (C=O). MS-EI *m/z* 500 (M^+, 11), 100 (100%). HRMS-EI calculated for $C_{23}H_{21}N_2O_3I$: 500.0597, found 500.0605.

6-(4-Bromophenyl)-6-dimethylcarbamoyl-7-oxypyrrolo[2,1-*d*][1,5]benzoxazepine [131]

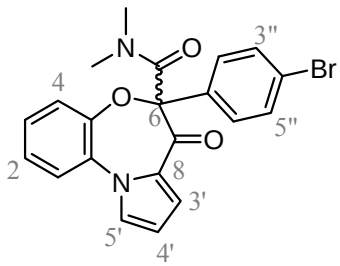

To a solution of **[127]** (0.47g, 1.33 mmol) in anhydrous DMF (5.0 mL), was added *N*,*N*-dimethylcarbamoyl chloride (147 μL, 1.60 mmol) and KH (195 mg, 1.46 mmol) in THF (2.0 mL). The mixture was stirred at RT for 20 h and the solvent was evaporated. The residue was taken up into DCM (40 mL) and

washed with NH_4Cl (25 mL), then brine (25 mL). The organic layer was evaporated and dried ($MgSO_4$), and the crude oil was subjected to silica gel column chromatography using EtOAc:heptane (4:6) to give **[131]** (0.172 g, 30%) as a sticky yellow oil. ^{1}H NMR ($CDCl_3$) δ 2.82 (s, 3H, NCH_3), 2.83 (s, 3H, NCH_3), 6.37 (dd, 1H, *J* = 4.0, 2.6, ArH4'), 7.05 (dd, 1H, *J* = 4.1, 1.5, ArH3'), 7.08-7.11 (m, 1H, ArH5'), 7.30-7.35 (m, 2H, ArH2 or ArH3, ArH4), 7.41 (d, 1H, *J* = 8.3, ArH1), 7.48 (dd, 1H, *J* = 8.3, 8.3, ArH2 or ArH3), 7.59 (d, 2H, *J* = 8.6, ArH2" and ArH6"), 7.84 (d, 2H, *J* = 8.6, ArH3" and ArH5"). ^{13}C NMR ($CDCl_3$) δ 36.5 (NCH_3), 36.8 (NCH_3), 111.0 (ArC4'), 123.7 (ArC4), 124.6 (ArC2), 125.9 (ArC1), 127.9 (ArC3), 129.0 (qC), 129.9 (ArC3'), 130.0 (qC), 131.7 (ArC2" and ArC6"), 132.1 (qC), 132.2 (ArC3" and ArC5"), 133.1 (qC), 134.3 (ArC5'), 147.3 (qC), 154.0 (qC), 181.2 (NC=O), 191.5 (C=O). HRMS-EI calculated for $C_{21}H_{17}N_2O_3{}^{79}Br$: 424.0423, found 424.0404.

1-(3-Bromo-2-hydroxyphenyl)pyrrole [132]

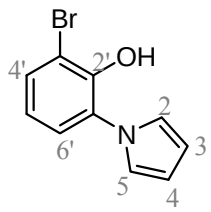

To a suspension of 6-bromo-2-nitrophenol (4.36 g, 20 mmol) in EtOH (150 mL) was added dropwise a solution of sodium dithionite (20.2 g, 116.3 mmol) in H_2O (90 mL) within 1 h. The resulting mixture was heated at reflux for 2 h, then stirred overnight at RT, then concentrated. AcOH (100 mL) and 2,5-dimethoxytetrahydrofuran (2.2 mL) were added and the mixture was heated at reflux for 5 h. The mixture was filtered, and the filtrate evaporated. Ethyl acetate (150 mL) and the mixture was washed with 5% $NaHCO_3$ solution (100 mL), then dilute brine (100 mL), dried ($MgSO_4$), and evaporated. The crude product was subjected to silica gel column chromatography using EtOAc:heptane (2:8), to give **[132]** (0.309 g, 6% overall) as a yellow oil. ^{1}H NMR ($CDCl_3$) δ 5.67 (s, 1H, OH), 6.36 (dd, 2H, *J* = 2.1, 2.1, ArH3 and ArH4), 6.87 (dd, 1H,

J = 8.0, 8.0, ArH5'), 6.97 (dd, 2H, *J* = 2.1, 2.1, ArH2 and ArH5), 7.24 (dd, 1H, *J* = 8.0, 1.5, ArH4'), 7.45 (dd, 1H, *J* = 8.1, 1.5, ArH6'). ^{13}C NMR ($CDCl_3$) δ 110.1 (ArC3 and ArC4), 111.4 (ArC3'), 121.7 (ArC6'), 121.9 (ArC2 and ArC5), 125.6 (ArC5'), 130.8 (ArC4'), 132.0 (ArC1'), 146.7 (ArC2'). MS-EI *m/z* 239 (^{79}Br M^+, 91), 237 (^{81}Br M^+, 95), 130 (100%). HRMS-EI calculated for $C_{10}H_8NO^{79}Br$: 236.9789, found 236.9784.

Ethyl (±)-α-[2[3-bromo-1-(1*H*-pyrrol-1-yl)phenyl]oxy]phenylacetate [133]

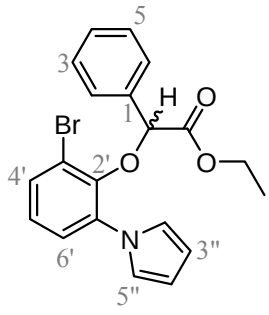

To a solution of 1-(3-bromo-2-hydroxyphenyl)pyrrole **[132]** (0.30 g, 1.26 mmol) and ethyl α-bromophenylacetate (0.23 mL, 1.26 mmol) in anhydrous DMF (3.0 mL) was added K_2CO_3 (0.21 g, 1.51 mmol), KI (0.10 g), and Bu_4NI (0.10 g). The reaction mixture was stirred at RT overnight, then EtOAc (25 mL) and water (25 mL) was added. The organic layer was separated and washed with dilute brine, dried ($MgSO_4$), and evaporated, leaving the crude product. The product was subjected to silica gel column chromatography using EtOAc:heptane (1:4) to yield **[133]** (0.47 g, 94%) as a pale yellow oil. ^{1}H NMR ($CDCl_3$) δ 1.05 (t, 3H, *J* = 7.1, CH_3), 4.00 (m, 2H, OCH_2), 4.73 (s, 1H, OCH), 6.25 (dd, 2H, *J* = 2.1, 2.1, ArH3" and ArH4"), 6.81 (dd, 2H, *J* = 2.1, 2.1, ArH2" and ArH5"), 6.90 (dd, 1H, *J* = 8.0, 8.0, ArH5'), 7.09 (dd, 1H, $^3J_{4,5}$ = 8.0, $^4J_{4,6}$ = 1.5, ArH4'), 7.13-7.20 (m, 5H, phenyl group), 7.39 (dd, 1H, $^3J_{6,5}$ = 8.0, $^4J_{6,4}$ = 1.5, ArH6'). ^{13}C NMR ($CDCl_3$) δ 13.9 (CH_3), 61.3 (OCH_2), 81.5 (CH), 110.2 (ArC3" and ArC4"), 118.9 (ArC3'), 121.8 (ArC2" and ArC5"), 125.2 (ArC6'), 125.6 (ArC5'), 128.27 (ArC2 and ArC6, or ArC3 and ArC5), 128.33 (ArC3 and ArC5, or ArC2 and ArC6), 129.0 (ArC4), 131.7 (ArC4'), 134.6 (ArC1'), 135.0 (ArC1), 147.7 (ArC2'), 169.0 (C=O). MS-EI *m/z* 401 (^{81}Br M^+, 24), 399 (^{79}Br M^+, 24), 328 (^{81}Br M^+ -

CO_2Et, 98), 326 (^{79}Br M^+ - CO_2Et, 100%). HRMS-EI calculated for $C_{20}H_{18}NO_3{}^{79}Br$: 399.0470, found 399.0458.

(±)-α-[2[3-Bromo-1-(1*H*-pyrrol-1-yl)phenyl]oxy]phenylacetic acid [134]

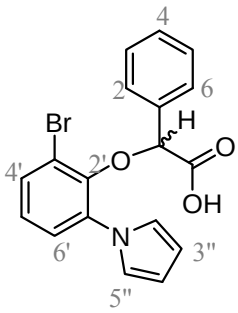

To a solution of **[133]** (0.45 g, 1.12 mmol) in THF/EtOH (1:1, 3 mL), was added 5% NaOH (1 mL). The reaction mixture was stirred at RT for 2 h, concentrated, and acidified to pH 4 with 1M HCl. The suspension was extracted into ethyl acetate (20 mL), and washed with dilute brine (2 x 10 mL). The organic layers were dried ($MgSO_4$) and evaporated, leaving **[134]** (0.42 g, 100%) as a pale yellow oil. ^1H NMR (CD_3OD) δ 4.80 (s, 1H, CH), 6.30 (dd, 2H, *J* = 2.1, 2.1, ArH3" and ArH4"), 6.91 (dd, 2H, *J* = 2.1, 2.1, ArH2" and ArH5"), 7.03 (dd, 1H, *J* = 8.0, ArH5'), 7.15 – 7.25 (m, 6H, 5 x ArH and ArH4'), 7.47 (dd, 1H, *J* = 8.0, 1.5, ArH6'). ^{13}C NMR (CD_3OD) δ 82.5 (CH), 111.2 (ArC3" and ArC4"), 119.8 (ArC3'), 122.8 (ArC2" and ArC5"), 126.6 (ArC6'), 126.8 (ArC5'), 129.2 (ArC2 and ArC6, or ArC3 and ArC5), 129.7 (ArC3 and ArC5, or ArC2 and ArC6), 130.1 (ArC4), 132.8 (ArC4'), 136.3 (ArC1'), 136.7 (ArC1), 148.5 (ArC2'), 172.4 (C=O). MS-EI *m/z* 373 (^{81}Br M^+, 45), 371 (^{79}Br M^+, 44), 328 (^{81}Br M^+ - CO_2H, 96), 326 (^{79}Br M^+ - CO_2H, 100%). HRMS-EI calculated for $C_{18}H_{14}NO_3{}^{81}Br$: 373.0137, found 373.0139.

(±)-4-Bromo-6-phenylpyrrolo[2,1-*d*][1,5]benzoxazepin-7(6*H*)-one [135]

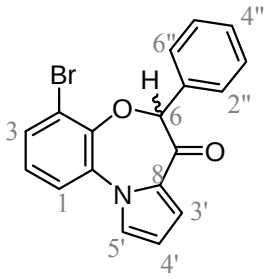

To a solution of **[134]** (255 mg, 0.69 mmol) in dry DCM (5 mL) was added PCl_5 (173 mg, 0.83 mmol) and the reaction was heated at reflux for 6 h. Water was added, and the solution was basified with 5% NaOH and extracted with DCM (2 x 10 mL). The solution was washed with dilute brine, dried ($MgSO_4$), and evaporated, leaving **[135]** (226 mg, 93%) as a pink solid. ^{1}H NMR ($CDCl_3$) δ 5.05 (s, 1H, CH), 6.50 (dd, 1H, *J* = 3.8, 2.9, ArH4'), 7.11 (dd, 1H, *J* = 8.1, 8.1, ArH2), 7.26-7.30 (m, 2H, ArH3' and ArH5'), 7.32-7.43 (m, 6H, 5 x ArH", ArH3), 7.48 (dd, 1H, *J* = 8.1, 1.3, ArH1). ^{13}C NMR ($CDCl_3$) δ 90.7 (CH), 112.4 (ArC4'), 119.1 (ArC4), 121.2 (ArC3'), 121.6 (ArC2), 126.4 (ArC4"), 126.7 (ArC5'), 128.5 (ArC2" and ArC6", or ArC3" and ArC5"), 128.7 (ArC3" and ArC5", or ArC2" and ArC6"), 129.1 (ArC2), 131.3 (ArC3), 133.7 (qC), 135.4 (qC), 135.8 (qC), 146.6 (qC), 189.7 (C=O). MS-EI *m/z* 355 (^{81}Br M^+, 61), 353 (^{79}Br M^+, 60), 250 (^{81}Br M^+ - ArCO, 99), 248 (^{79}Br M^+ - ArCO, 100%). HRMS-EI calculated for $C_{18}H_{12}NO_2{}^{79}Br$: 353.0051, found 353.0048.

7.5 Experimental Procedures for the Stannylation Reactions and Radioiodination Reactions

***N*,*N*-Diethyl-[5-chloro-2-(4-trimethylstannylphenyl)indol-3-yl]glyoxylamide [141]**

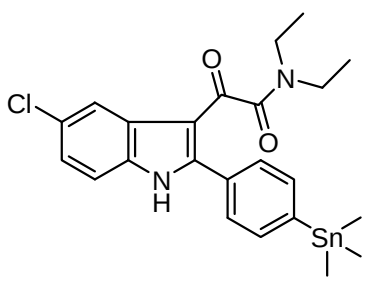

To a solution of the bromo derivative **[54]** (112 mg, 0.26 mmol) in anhydrous toluene (8 mL) was added hexamethylditin (230 mg, 0.70 mmol) and a catalytic amount of $Pd(0)(PPh_3)_4$ (2-5 mg). The reaction mixture was heated at reflux under N_2 for 8 h. During the 8 h, catalyst (2-5 mg) and

hexamethylditin (2-5 mg) were added every 2 h. The reaction mixture was washed through Celite with EtOAc (25 mL) and the solvent evaporated. The product was subjected to silica gel column chromatography using EtOAc:PE (1:1) to yield **[141]** (43 mg, 32%) as a white solid, mp. 160–162 °C. ^{1}H NMR (CD_3OD) δ 0.36 (s, 9H, $Sn(CH_3)_3$), 0.79 (t, 3H, *J* = 7.2, CH_3), 1.15 (t, 3H, *J* = 7.2, CH_3), 3.07 (q, 2H, *J* = 7.2, NCH_2), 3.24 (q, 2H, *J* = 7.2, NCH_2), 7.32 (dd, 1H, *J* = 8.4, 2.0, H6), 7.47 (d, 1H, *J* = 8.4, H7), 7.54 (d, 2H, *J* = 8.0, ArH2' and ArH6'), 7.65 (d, 2H, *J* = 8.0, ArH3' and ArH5'), 8.27 (d, 1H, *J* = 2.0, H4). ^{13}C NMR (DMSO) δ -9.4 ($Sn(CH_3)_3$), 12.0 (CH_3), 13.5 (CH_3), 37.6 (NCH_2), 41.6 (NCH_2), 109.3 (C3), 113.7 (C7), 120.0 (C4), 123.5 (C6), 127.1 (C5), 128.0 (C3a), 129.1 (ArC2' and ArC6'), 130.1 (ArC1'), 134.3 (C7a), 135.2 (ArC3' and ArC5'), 144.8 (ArC4'), 148.8 (C2), 166.7 (NC=O), 187.2 (C=O). MS-ES *m/z* 519 ($^{120}Sn^{37}Cl$ M-1, 25), 517 ($^{120}Sn^{35}Cl$ and $^{118}Sn^{37}Cl$ M-1, 67), 516 ($^{119}Sn^{35}Cl$ M-1, 25), 515 ($^{118}Sn^{35}Cl$ M-1, 45), 513 ($^{116}Sn^{35}Cl$ M-1, 24), 115 (100%). HRMS-ES calculated for $C_{23}H_{28}N_2O_2{}^{35}Cl^{116}Sn$: 515.0857, found 515.0903.

[^{123}I]*N*,*N*-Diethyl-[5-chloro-2-(4-iodophenyl)indol-3-yl]glyoxylamide [142]

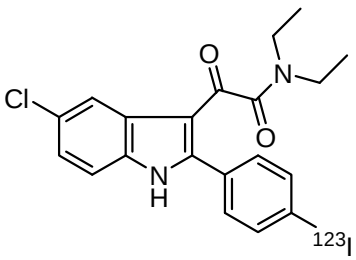

To a solution of stannane **[141]** (125 μg) in EtOH (50 μL) and AcOH (200 μL), was added $Na^{123}I$ (311 – 544 MBq) and peracetic acid (30%, 25 μL). After 5 min at RT, the reaction was quenched with $Na_2S_2O_5$ (50 mg/mL, 100 μL) and $NaHCO_3$ (50 mg/mL, 100 μL). Mobile phase (ACN:0.01M ammonium acetate, 3:2 v/v, 350 μL) was added and the solution was injected onto a semipreparative C-18 RP HPLC column. The peak with a retention time of 16 min at a flow rate of 3 mL/min was collected and the radiochemical yield (R.C.Y) was 55-60% (n=3). The radiochemical purity was > 96% after formulation in saline.

***N,N*-Diethyl-[2-(4-trimethylstannylphenyl)-5,7-dimethylpyrazolo[1,5-*a*]pyrimidin-3-yl]acetamide [143]**

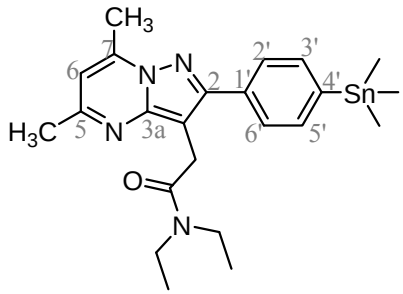

To the iodo derivative **[91]** (187 mg, 0.404 mmol) in anhydrous toluene (8 mL) was added hexamethylditin (396 mg, 1.21 mmol) and a catalytic amount of $Pd(0)(PPh_3)_4$. The reaction mixture was heated at reflux for 4 h, then the mixture was filtered through Celite, and the solvent evaporated. ACN was added, and the dissolved compound was subjected to HPLC using ACN:H_2O:ammonium bicarbonate (90:8:2, 200 mM) at a flow rate of 10 mL/min on an Altima C18 250 x 22 mm column. A peak at 21 min was collected and evaporated, leaving **[143]** (70 mg, 35%) as a white solid, mp. 150-151 °C. ^{1}H NMR ($CDCl_3$) δ 0.30 (s, 9H, $Sn(CH_3)_3$), 1.11 (t, 3H, J = 7.1, CH_3), 1.21 (t, 3H, J = 7.1, CH_3), 2.54 (s, 3H, $ArCH_3$), 2.74 (s, 3H, $ArCH_3$), 3.42 (q, 2H, J = 7.1, NCH_2), 3.50 (q, 2H, J = 7.1, NCH_2), 3.93 (s, 2H, CH_2), 6.51 (s, 1H, H6), 7.56 (d, 2H, J = 7.9, ArH3' and ArH5'), 7.78 (d, 2H, J = 7.9, ArH2' and ArH6'). ^{13}C NMR ($CDCl_3$) δ -9.4 ($Sn(CH_3)_3$), 13.2 (CH_3), 14.4 (CH_3), 17.0 ($ArCH_3$), 24.8 ($ArCH_3$), 28.2 (CH_2), 40.7 (NCH_2), 42.4 (NCH_2), 101.3 (C3), 108.4 (C6), 128.2 (ArC3' and ArC5'), 133.8 (ArC1'), 136.0 (ArC2' and ArC6'), 142.6 (ArC4'), 144.9 (C7), 147.8 (C3a), 155.3 (C2), 157.6 (C5), 170.1 (C=O). MS-ES *m/z* 503 (^{124}Sn M+1, 31), 502 (^{122}Sn M+1, 44), 501 (^{120}Sn M+1, 100%), 500 (^{119}Sn M+1, 39), 499 (^{118}Sn M+1, 63), 498 (^{117}Sn M+1, 29), 497 (^{116}Sn M+1, 49). HRMS-ES calculated for $C_{23}H_{33}N_4O^{120}Sn$: 501.1676, found 501.1679.

[^{123}I]*N*,*N*-Diethyl-[2-(4-iodophenyl)-5,7-dimethylpyrazolo[1,5-*a*]pyrimidin-3-yl]acetamide [144]

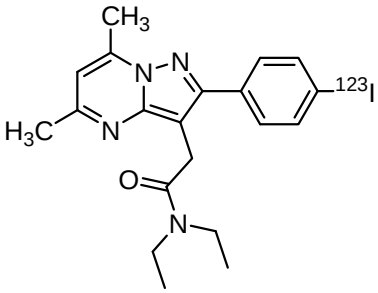

To a solution of the stannane **[143]** (200 μg) in AcOH (300 μL) was added Na^{123}I (259 MBq) and peracetic acid (30%, 25 μL). After 5 min at RT, the reaction was quenched with $Na_2S_2O_5$ (50 mg/mL, 100 μL) and $NaHCO_3$ (50 mg/mL, 100 μL). Mobile phase (ACN:H_2O (0.1% TFA), 65:35 v/v, 350 μL) was added and the solution was injected onto a semipreparative C-18 RP HPLC column. The peak at a retention time of 12 min at a flow rate of 3 mL/min was collected to give **[144]** (245 MBq, 95% R.C.Y).

7.6 Pharmacology Methods

7.6.1 *In Vitro* Binding Assays for Peripheral Benzodiazepine Receptors

Membrane Preparation [163]

Male Sprague-Dawley rats were sacrificed by CO_2 administration followed by cervical dislocation. Kidneys were removed and placed in 20 volumes of ice-cold buffer (50 mM Tris-HCl, pH 7.4) and minced finely with scissors. After homogenising the preparation with a polytron (PCU-Kinematica, Bioblock, Switzerland) with one 10 second burst at a setting of 10, the suspension was then centrifuged at 49000 g for 15 min at 4 °C. The pellets were resuspended in buffer with a dounce (manual homogeniser) to yield a protein concentration of 4 mg/mL. Membranes were stored at -80 °C until required. Protein measurements were made by Lowry's method using bovine serum albumin as standard.[183]

***In Vitro* Binding Assay** [163]

The test compounds were dissolved in DMSO to make up a stock solution of 500 or 1000 μM. Six concentrations of test compound were made up with buffer in 6 test tubes by serial dilution of the stock solution. A drop of Tween 80 was used in the first solution to help dissolve the compound. The inhibition constant of the test compound (IC_{50}) was determined by incubating aliquots (0.1 mL), in triplicate, of diluted kidney membrane preparation at 4 °C for 1 h with 6 or more concentrations of test compound (usually 10^{-5} to 10^{-10} M), together with a trace amount (2 nM) of [^{3}H]PK11195 in a final volume of 0.5 mL. Non-specific binding was determined by competition with non-radioactive PK11195 (10 μM). Incubation was terminated by rapid filtration through a Whatman GF/B glass fibre filter pre-soaked in 50 mM Tris-HCl. Each sample tube and filter was immediately washed with 3 aliquots of 5 mL ice-cold 50 mM Tris-HCl at pH 7.4. The filters were placed in scintillation vials along with scintillation fluid (2 mL) and counted with a β-scintillation counter (Packard) to measure the amount of bound radioactivity. IC_{50} values were calculated by an iterative non-linear least squares curve fitting computer program called Kell Radioligand. The whole method was performed in triplicate to obtain the average and standard deviation of at least three IC_{50} determinations.

7.6.2 *In Vitro* Binding Assays for Central Benzodiazepine Receptors

Membrane Preparation

Male Sprague-Dawley rats were sacrificed by CO_2 administration followed by cervical dislocation. Cortex were removed and placed in 20 volumes of ice-cold buffer (50 mM

Tris-HCl, pH 7.4) and minced finely with scissors. After homogenising the preparation with a polytron (PCU-Kinematica, Bioblock, Switzerland) with one 10 second burst at a setting of 6, the suspension was then centrifuged at 20000 g for 20 min at 4 °C. The pellets were resuspended in the previous buffer with a dounce (manual homogeniser). After the second centrifugation, the pellet was suspended in a final buffer (50 mM Tris-HCl, 0.32M sucrose, pH 7.4) to achieve a protein concentration of 4 mg/mL, and the membranes were stored at -80 °C until required. Protein measurements were made by Lowry's method using bovine serum albumin as standard.[183]

In Vitro Binding Assay

The inhibition constant of the test compound (IC_{50}) was determined by incubating aliquots (0.1 mL), in triplicate, of diluted cortex membrane preparation at 25 °C for 45 min with 6 concentrations of test compound (10^{-5} to 10^{-10} M), together with a trace amount (2 nM) of [^{3}H]flumazenil in a final volume of 0.5 mL. Non-specific binding was determined by competition with non-radioactive flumazenil (20 μM). Incubation was terminated by rapid filtration through a Whatman GF/B glass filter. Each sample tube and filter was immediately washed with 3 aliquots of 5 mL ice-cold 50 mM Tris-HCl at pH 7.4. Filters were counted with a β-scintillation counter (Packard) to measure the amount of bound radioactivity. IC_{50} values were calculated by Kell Radioligand. The whole method was performed in triplicate to obtain the average and standard deviation of at least three IC_{50} determinations.

7.6.3 *In Vivo* Biodistribution Studies for [^{123}I]PBR200 [142] and [^{123}I]PBR215 [144]

Directly after radiolabelling, [^{123}I]PBR200 was dissolved in 100 μL of EtOH and 200 μL saline solution. This solution was diluted with saline, to achieve a concentration of 15 μCi/ 100 μL. The biodistribution of [^{123}I]PBR200 was studied in normal male Sprague-Dawley rats, weighing between 230 g and 280 g. Twenty-five rats were injected with the radiolabelled compound (15 μCi in 100 μL) via the tail vein (after warming the tail in warm water). After 15 min, 30 min, 1, 3, 6 and 24 h post injection, 4 rats per time-point were sacrificed by CO_2 administration. The rats were weighed, and 17 organs were removed from each rat and weighed. The organs in the study include the liver, spleen, kidney, muscle, heart, blood, lungs, stomach, GIT, thyroid, pancreas, thymus, tail, adrenals, testes, brain, and olfactory bulb. The amount of radioactivity in each organ was measured using an automated gamma counter and the percent injected dose (% ID) for each organ was calculated by comparison with a diluted standard solution of the initial injected dose. The density of radioactivity of each organ (% ID/g) was found by dividing the % ID for each tissue by the weight of the tissue.

The *in vivo* biodistribution of [^{123}I]PBR215 was performed using the same procedure as for [^{123}I]PBR200.

7.6.4 *In Vivo* Competition Studies for [^{123}I]PBR200 [142] and [^{123}I]PBR215 [144]

[^{123}I]PBR200 was synthesised and formulated to 15.2 μCi / 100 μL of saline. The competition drugs used for this study were unlabelled PBR200, diazepam, PK11195, Ro5-4864, and flumazenil. Male Sprague-Dawley rats were grouped into 6 groups of 4 (4 rats per competition drug plus 4 rats for control), with each group having similar weights. Competition drugs were dissolved in saline (with 20% DMSO) to a concentration of 1 mg drug / kg rat. Rats in each group were injected via the tail vein with drugs (as listed below) and sacrificed 1 h later by CO_2 administration and cervical dislocation. Rats were injected with the competition drug 5 min prior to the injection of [^{123}I]PBR200.

Group 1 [^{123}I]PBR200 (control)

Group 2 non-radioactive PBR200 and [^{123}I]PBR200

Group 3 PK11195 and [^{123}I]PBR200

Group 4 Ro5-4864 and [^{123}I]PBR200

Group 5 Flumazenil and [^{123}I]PBR200

Group 6 Diazepam and [^{123}I]PBR200

Blood was collected immediately after sacrifice from the heart cavity. Organs dissected were liver, spleen, kidney, muscle, heart, blood, bladder, lungs, stomach, GIT, thyroid, pancreas, thymus, tail, adrenals, testes, brain, and olfactory bulb. Organs were put in pre-weighed tubes and weighed and counted using a Wallac Gamma Counter 1470 (program 90/91 for weighing, and program 70 for counting). From weights and counts

acquired, a percent injected dose per gram (% ID/g) was calculated against standards of the injected solution.

Statistical analysis

Results for the competition study were analysed by one-way analysis of variance (ANOVA) for comparing the tissue radioactivity concentrations in the treated animals (n = 3-4) and in the controls (n = 4). The criteria for significance were $p < 0.01$ and $p < 0.05$.

The competition study for [^{123}I]PBR215 was performed the same as for [^{123}I]PBR200, but the competition drugs used were PBR215, PK11195, Ro5-4864, and flumazenil.

7.6.5 *In Vivo* Stability Studies for [^{123}I]PBR200 [142] and [^{123}I]PBR215 [144]

Three Sprague-Dawley rats were injected with [^{123}I]PBR200 (200 μCi in 100 μL saline per rat) into the tail vein. A rat each was sacrificed at 15 min, 1 h, and 3 h post injection. The liver, heart, brain, kidneys, adrenals (~100-200 mg for each organ) and blood were collected. The blood was added to a heparinised tube and centrifuged at 2000 g for 5 min to collect the plasma (200-300 μL). The samples were weighed and the activity was counted. The organs were minced with scissors, ACN (1 mL) was added, and the tissues were sonicated using an ultrasonic probe for 2 min. The sample was then centrifuged at 2000 rpm for 5 min and the supernatant was collected. A second extraction was performed and the combined ACN fractions were evaporated to dryness. The activity was reconstituted in MeOH (50 μL) and applied onto an aluminium backed silica TLC plate (20 x 20 cm), along with the radioactive and non-radioactive standards. After the

TLC was run in EtOAc:PE (2:3), the radioactivity on the plate was counted using a Berthold radio-TLC scanner using the Berthold TLABE software. The radioactivity in the remaining tissue was counted by the Wallac counter and compared with the counted activity before the extraction to calculate the extraction efficiency.

The radioactive CPM (counts per minute) after extraction is corrected for decay (13 h half life of ^{123}I) using the following formula:

Corrected CPM = CPM before extraction x $e^{(\ln 2 / 780 \text{ min x min between counts})}$

The extraction efficiency formula is:

Extraction efficiency = 100 – (corrected CPM after extraction x 100 / CPM before extraction).

Using the Berthold TLABE software, the radioactive peaks were integrated.

The *in vivo* stability study for [^{123}I]PBR215 was performed the same as for [^{123}I]PBR200, but a 24 h time point was added. The TLC was run in MeOH:DCM (5:95).

7.7 Lipophilicity Estimations

The lipophilicity of each ligand was examined by determination of the log $P_{7.5}$ value using a HPLC method.[164] Samples were analysed using a C18 column (X-Terra, 5 μ, 4.6 x 250 mm) and a mobile phase of MeOH and 0.1M phosphate buffer (65:35 v/v, pH 7.5) with a flow rate of 1 mL/min. The log *P* values were estimated by comparing HPLC retention times of test compounds with retention times of standards having known log *P* values. The standards used were aniline, benzene, bromobenzene, ethylbenzene and trimethylbenzene. A calibration curve of log *P* versus ln retention time was generated. The equation was linear with an r^2 of 0.9969.

8 References

1. Rang, H.P.; Dale, M.M.; Ritter, J.M. *Pharmacology* (4th Ed.), Churchill Livingstone: Edinburgh, **2000**
2. Braestrup, C.; Squires, R.F. *Proc. Natl. Acad. Sci. U.S.A.* **1977**, *74*, 3805
3. Schoemaker, H.; Morelli, M.; Deshmukh, P.; Yamamura, H.I. *Brain Res.* **1982**, *248*, 396
4. Beurdeley-Thomas, A.; Miccoli, L.; Oudard, S.; Dutrillaux, B.; Poupon, M.F. *J. Neuro-Oncol.* **2000**, *46*, 45
5. Papadopoulos, V.; Baraldi, M.; Guilarte, T.R.; Knudsen, T.B.; Lacapère, J-J.; Lindemann, P.; Norenberg, M.D.; Nutt, D.; Weizman, A.; Zhang, M-R.; Gavish, M. *Trends Pharmacol. Sci.* **2006**, *27*, 402
6. McEnery, M.W.; Snowman, A.M.; Trifiletti, R.R.; Snyder, S.H. *Proc. Natl. Acad. Sci. U.S.A.* **1992**, *89*, 3170
7. Sprengel, R.; Werner, P.; Seeburg, P.H.; Mukhin, A.G.; Santi, M.R.; Grayson, D.R.; Guidotti, A.; Krueger, K.E. *J. Biol. Chem.* **1989**, *264*, 20415
8. Riond, J.; Mattei, M.G.; Kaghad, M.; Dumont, X.; Guillemot, J.C.; Le Fur, G.; Caput, D.; Ferrara, P. *Eur. J. Biochem.* **1991**, *195*, 305
9. Parola, A.L.; Stump, D.G.; Pepper, D.J.; Krueger, K.E.; Regan, J.W.; Laird II, H.E. *J. Biol. Chem.* **1991**, *266*, 14082
10. Taketani, S.; Kohno, H.; Okuda, M.; Furukawa, T.; Tokunaga, R. *J. Biol. Chem.* **1994**, *269*, 7527
11. Gavish, M.; Bachman, I.; Shoukrun, R.; Katz, Y.; Veenman, L.; Weisinger, G.; Weizman, A. *Pharmacol. Rev.* **1999**, *51*, 629

12. Casalotti, S.O.; Pelaia, G.; Yakovlev, A.G.; Csikós, T.; Grayson, D.R.; Krueger, K.E. *Gene* **1992**, *121*, 377

13. Lin, D.; Chang, Y.J.; Strauss, J.F. III.; Miller, W.L. *Genomics* **1993**, *18*, 643

14. Joseph-Liauzun, E.; Delmas, P.; Shire, D.; Ferrara, P. *J. Biol. Chem.* **1998**, *273*, 2146

15. Bernassau, J.M.; Reversat, J.L.; Ferrara, P.; Caput, D.; Lefur, G. *J. Mol. Graph.* **1993**, *11*, 236

16. Lacapère, J-J.; Papadopoulos, V. *Steroids* **2003**, *68*, 569

17. Lacapère, J-J.; Delavoie, F.; Li, H.; Péranzi, G.; Maccario, J.; Papadopoulos, V.; Vidic, B. *Biochem. Biophys. Res. Commun.* **2001**, *284*, 536

18. Delavoie, F.; Li, H.; Hardwick, M.; Robert, J.C.; Giatzakis, C.; Péranzi, G.; Yao, Z-X.; Maccario, J.; Lacapère, J-J.; Papadopoulos, V. *Biochemistry* **2003**, *42*, 4506

19. Blahos, J.; Whalin, M.E.; Krueger, K.E. *J. Biol. Chem.* **1995**, *270*, 20285

20. Galiègue, S.; Jbilo, O.; Combes, T.; Bribes, E.; Carayon, P.; Le Fur, G.; Casellas, P. *J. Biol. Chem.* **1999**, *274*, 2938

21. Liu, J.; Cavalli, L.R.; Haddad, B.R.; Papadopoulos, V. *Gene* **2003**, *308*, 1

22. Liu, J.; Li, H.; Papadopoulos, V. *J. Steroid Biochem. Mol. Biol.* **2003**, *85*, 275

23. De Souza, E.B.; Anholt, R.R.; Murphy, K.M.; Snyder, S.H.; Kuhar, M.J. *Endocrinology* **1985**, *116*, 567

24. Doble, A.; Benavides, J.; Ferris, O.; Bertrand, P.; Menager, J.; Vaucher, N.; Burgevin, M-C.; Uzan, A.; Guérémy, C.; Le Fur, G. *Eur. J. Pharmacol.* **1985**, *119*, 153

25. O'Beirne, G.B.; Woods, M.J.; Williams, D.C. *Eur. J. Biochem.* **1990**, *188*, 131

26. O'Beirne, G.B.; Williams, D.C. *Eur. J. Biochem.* **1988**, *175*, 413

27. Gehlert, D.R.; Yamamura, H.I.; Wamsley, J.K. *Naunyn-Schmiedeberg's Arch. Pharmacol.* **1985**, *328*, 454

28. Gallager, D.W.; Mallorga, P.; Oertel, W.; Henneberry, R.; Tallman, J. *J. Neurosci.* **1981**, *1*, 218

29. Canat, X.; Carayon, P.; Bouaboula, M.; Cahard, D.; Shire, D.; Roque, C.; Le Fur, G.; Casellas, P. *Life Sci*. **1992**, *52*, 107

30. Carayon, P.; Portier, M.; Dussossoy, D.; Bord, A.; Petitprêtre, G.; Canat, X.; Le Fur, G.; Casellas, P. *Blood* **1996**, *87*, 3170

31. Anholt, R.R.H.; Pedersen, P.L.; De Souza, E.B.; Snyder, S.H. *J. Biol. Chem.* **1986**, *261*, 576

32. Olson, J.M.M.; Ciliax, B.J.; Mancini, W.R.; Young, A.B. *Eur. J. Pharmacol*. **1988**, *152*, 47

33. Woods, M.J.; Williams, D.C. *Biochem. Pharmacol*. **1996**, *52*, 1805

34. Woods, M.J.; Zisterer, D.M.; Williams, D.C. *Biochem. Pharmacol*. **1996**, *51*, 1283

35. Garnier, M.; Boujrad, N.; Oke, B.O.; Brown, A.S.; Riond, J.; Ferrara, P.; Shoyab, M.; Suarez-Quian, C.A.; Papadopoulos, V. *Endocrinology* **1993**, *132*, 444

36. Mestre, M.; Carriot, T.; Belin, C.; Uzan, A.; Renault, C.; Dubroeucq, M.C.; Guérémy, C.; Doble, A.; Le Fur, G. *Life Sci*. **1985**, *36*, 391

37. Oke, B.O.; Suarez-Quian, C.A.; Riond, J.; Ferrara, P.; Papadopoulos, V. *Mol. Cell. Endocrinol*. **1992**, *87*, R1

38. Venturini, I.; Zeneroli, M.L.; Corsi, L.; Avallone, R.; Farina, F.; Alho, H.; Baraldi, C.; Ferrarese, C.; Pecora, N.; Frigo, M.; Ardizzone, G.; Arrigo, A.; Pellicci, R.; Baraldi, M. *Life Sci*. **1998**, *63*, 1269

39. Casellas, P.; Galiègue, S.; Basile, A.S. *Neurochem. Int*. **2002**, *40*, 475

40. Corsi, L.; Avallone, R.; Geminiani, E.; Cosenza, F.; Venturini, I.; Baraldi, M. *Biochem. Biophys. Res. Commun*. **2004**, *313*, 62

41. Lindemann, P.; Koch, A.; Degenhardt, B.; Hause, G.; Grimm, B.; Papadopoulos, V. *Plant Cell Physiol*. **2004**, *45*, 723

42. Snyder, M.J.; Antwerpen, R.V. *Cell Tissue Res*. **1998**, *294*, 161

43. Papadopoulos, V.; Amri, H.; Boujrad, N.; Cascio, C.; Culty, M.; Garnier, M.; Hardwick, M.; Li, H.; Vidic, B.; Brown, A.S.; Reversa, J.L.; Bernassau, J.M.; Drieu, K. *Steroids* **1997**, *62*, 21

44. Papadopoulos, V.; Brown, A.S. *J. Steroid. Molec. Biol*. **1995**, *53*, 103

45. Berkovich, A.; McPhie, P.; Campagnone, M.; Guidotti, A.; Hensley, P. *Mol. Pharmacol*. **1990**, *37*, 164

46. Papadopoulos, V.; Guarneri, P.; Krueger, K.E.; Guidotti, A.; Costa, E. *Proc. Natl. Acad. Sci. U.S.A*. **1992**, *89*, 5113

47. Costa, E.; Guidotti, A. *Life Sci*. **1991**, *49*, 325

48. Snyder, S.H.; Verma, A.; Trifiletti, R.R. *FASEB J*. **1987**, *1*, 282

49. Mantione, C.R.; Goldman, M.E.; Martin, B.; Bolger, G.T.; Lueddens, H.W.M.; Paul, S.M.; Skolnick, P. *Biochem. Pharmacol*. **1988**, *37*, 339

50. Le Fur, G.; Perrier, M.L.; Vaucher, N.; Imbault, F.; Flamier, A.; Benavides, J.; Uzan, A.; Renault, C.; Dubroeucq, M.C.; Guérémy, C. *Life Sci*. **1983**, *32*, 1839

51. Doble, A.; Ferris, O.; Burgevin, M.C.; Menager, J.; Uzan, A.; Dubroeucq, M.C.; Renault, C.; Guérémy, C.; Le Fur, G. *Mol. Pharmacol*. **1987**, *31*, 42

52. Wang, J.K.T.; Taniguchi, T.; Spector, S. *Mol. Phamacol*. **1984**, *25*, 349

53. Langer, S.Z.; Arbilla, S. *Pharmacol. Biochem. Behav*. **1988**, *29*, 763

54. Skowronski-Lutz, E.M.; Bitran, D. *Neurosteroid Effects in the Central Nervous System*. (Smith, S.S. (ed.)), pp. 197-218, CRC Press: London, **2004**

55. Zisterer, D.M.; Hance, N.; Campiani, G.; Garafolo, A.; Nacci, V.; Williams, D.C. *Biochem. Pharmacol*. **1998**, *55*, 397

56. Campiani, G.; Nacci, V.; Fiorini, I.; De Filippis, M.P.; Garofalo, A.; Ciani, S.M.; Greco, G.; Novellino, E.; Williams, D.C.; Zisterer, D.M.; Woods, M.J.; Mihai, C.; Manzoni, C.; Mennini, T. *J. Med. Chem*. **1996**, *39*, 3435

57. Ferzaz, B.; Brault, E.; Bourliaud, G.; Robert, J-P.; Poughon, G.; Claustre, Y.; Marguet, F.; Liere, P.; Schumacher, M.; Nowicki, J-P.; Fournier, J.; Marabout, B.; Sevrin, M.; George, P.; Soubrie, P.; Benavides, J.; Scatton, B. *J. Pharmacol. Exp. Ther*. **2002**, *310*, 1067

58. Garnier, M.; Dimchev, A.B.; Boujrad, N.; Price, J.M.; Musto, N.A.; Papadopoulos, V. *Mol. Pharmacol*. **1994**, *45*, 201

59. Joseph-Liauzun, E.; Farges, R.; Delmas, P.; Ferrara, P.; Loison, G. *J. Biol. Chem*. **1997**, *272*, 28102

60. Larcher, J-P.; Vayssiere, J-L.; Lemarquer, F.J.; Cordeau, L.R.; Keane, P.E.; Bachy, A.; Gros, F.; Crazat, B.P. *Eur. J. Pharmacol*. **1989**, *161*, 197

61. Hirsch, J.D.; Beyer, C.F.; Malkowitz, L.; Beer, B.; Blume, A.J. *Mol. Pharmacol*. **1989**, *35*, 157

62. Zisterer, D.M.; Gorman, A.M.C.; Williams, D.C.; Murphy, M.P. *Meth. Find. Exp. Clin. Pharmacol*. **1992**, *14*, 85

63. Kinnaly, K.W.; Zorov, D.; Antonenkoy, N.; Snyder, S.H.; McEnery, M.W.; Todeschi, H. *Proc. Natl. Acad. Sci. U.S.A*. **1993**, *90*, 1374

64. Mukhin, A.G.; Papadopoulos, V.; Costa, E.; Krueger, K.E. *Proc. Natl. Acad. Sci. U.S.A*. **1989**, *86*, 9813

65. Papadopoulos, V.; Amri, H.; Li, H.; Boujrad, N.; Vidic, B.; Garnier, M. *J. Biol. Chem*. **1997**, *272*, 32129

66. Pandak, W.M.; Ren, S.; Marques, D.; Hall, E.; Redford, K.; Mallonee, D.; Bohdan, P.; Heuman, D.; Gil, G.; Hylemon, P. *J. Biol. Chem*. **2002**, *277*, 48158

67. Tsankova, V.; Magistrelli, A.; Cantoni, L.; Tacconi, M.T. *Eur. J. Pharmacol*. **1995**, *294*, 601

68. Tsankova, V.; Visentin, M.; Cantoni, L.; Carelli, M.; Tacconi, M.T. *Eur. J. Phamacol*. **1996**, *299*, 197

69. Hauet, T.; Yao, Z-X.; Bose, H.S.; Wall, C.T.; Han, Z.; Li, W.; Hales, D.B.; Miller, W.L.; Culty, M.; Papadopoulos, V. *Mol. Endocrinol*. **2005**, *19*, 540

70. Wang, J.K.T.; Morgan, J.I.; Spector, S. *Proc. Natl. Acad. Sci. U.S.A.* **1984**, *81*, 753

71. Landau, M.; Weizman, A.; Zoref-Shani, E.; Beery, E.; Wasseman, L.; Landau, O.; Gavish, M.; Brenner S.; Nordenberg. J. *Biochem. Pharmacol*. **1998**, *56*, 1029

72. Carmel, I.; Fares, F.A.; Leschiner, S.; Scherubl, H.; Weisinger, G.; Gavish, M. *Biochem. Pharmacol*. **1999**, *58*, 273

73. Gorman, A.M.C.; O'Beirne, G.B.; Regan, C.M.; Williams, D.C. *J. Neurochem*. **1989**, *53*, 849

74. Camins, A.; Diez-Fernandez, C.; Pujadas, E.; Camarasa, J.; Escubedo, E. *Eur. J. Pharmacol*. **1995**, *272*, 289

75. Cleary, J.; Johnson, K.M.; Opipari, A.W. Jr.; Glick, G.D. *Bioorg. Med. Chem. Lett*. **2007**, *17*, 1667

76. Ikezaki, K.; Black, K.L. *Cancer Lett*. **1990**, *49*, 115

77. Clarke, G.D.; Ryan, P.J. *Nature* **1980**, *287*, 160

78. Strittmatter, W.J.; Hirata, F.; Axelrod, J.; Mallorga, P.; Tallman, J.F.; Henneberry, R.C. *Nature* **1979**, *282*, 857

79. Morgan, J.I.; Johnson, M.D.; Wang, J.K.T.; Sonnenfeld, K.H.; Spector, S. *Proc. Natl. Acad. Sci. U.S.A.* **1985**, *82*, 5223

80. Curran, T.; Morgan, J.I. *Science* **1985**, *229*, 1265

81. Shiraishi, T.; Black, K.L.; Ikezaki, K.; Becker, D.P. *J. Neurosci. Res*. **1991**, *30*, 463

82. Matthew, E.; Laskin, J.D.; Zimmerman, E.A.; Weinstein, I.B.; Hsu, K.C.; Engelhardt, D.L. *Proc. Natl. Acad. Sci. U.S.A.* **1981**, *78*, 3935

83. Ruff, M.R.; Pert, C.B.; Weber, R.J.; Wahl, L.M.; Wahl, S.M.; Paul, S.M. *Science* **1985**, *229*, 1281

84. Sacerdote, P.; Panerai, A.E.; Frattola, L.; Ferrarese, C. *Psychoneuroendocrinology* **1999**, *24*, 243

85. Zavala, F.; Taupin, V.; Descamps-Latscha, B. *J. Pharmacol. Exp. Ther*. **1990**, *255*, 442

86. Zavala, F.; Lenfant, M. *Int. J. Immunophamac*. **1988**, *10*, 531

87. Anholt, R.R.H.; Murphy, K.M.M.; Mack, G.E.; Snyder, S.H. *J. Neurosci*. **1984**, *4*, 593

88. Meßmer, K.; Reynolds, G.P. *Neurosci. Lett*. **1998**, *241*, 53

89. Vowinckel, E.; Reutens, D.; Becher, B.; Verge, G.; Evans, A.; Owens, T.; Antel, J.P. *J. Neurosci. Res*. **1997**, *50*, 345

90. Cagnin, A.; Brooks, D.J.; Kennedy, A.M.; Gunn, R.N.; Myers, R.; Turkheimer, F.E.; Jones, T.; Banati, R.B. *Lancet* **2001**, *358*, 461

91. Bonuccelli, U.; Nuti, A.; Del Dotto, P.; Piccini, P.; Martini, C.; Giannaccini, G.; Lucacchini, A.; Muratoria, A. *Life Sci*. **1991**, *48*, 1185

92. Bongioanni, P.; Castagna, M.; Mondino, C.; Boccardi, B.; Borgna, M. *Exp. Neurol*. **1997**, *146*, 560

93. Bongioanni, P.; Gemignani, F.; Ronato, M.; Castagna, M.; Mondino, C. *Parkinsonism Relat. Disord*. **1997**, *3*, 37

94. Cagnin, A.; Gerhard, A.; Banati, R.B. *Eur. Neuropsychopharmacol*. **2002**, *12*, 581

95. Bribes, E.; Galiègue, S.; Bourrie, B.; Casellas, P. *Immunol. Lett*. **2003**, *85*, 13

96. Bribes, E.; Bourrie, B.; Casellas, P. *Immunol. Lett*. **2003**, *88*, 241

97. Galiègue, S.; Tinel, N.; Casellas, P. *Curr. Med. Chem*. **2003**, *10*, 1563

98. Katz, Y.; Eitan, A.; Amiri, Z.; Gavish, M. *Eur. J. Pharmacol*. **1988**, *148*, 483

99. Katz, Y.; Ben-Baruch, G.; Kloog, Y.; Menczer, J.; Gavish, M. *Clin. Sci*. **1990**, *78*, 155

100. Black, K.L.; Ikezaki, K.; Santori, E.; Becker, D.P.; Vinters, H.V. *Cancer* **1990**, *65*, 93

101. Hardwick, M.; Fertikh, D.; Culty, M.; Li, H.; Vidic, B.; Papadopoulos, V. *Cancer Res*. **1999**, *59*, 831

102. Beinlich, A.; Strohmeier, R.; Kaufmann, M.; Kuhl, H. *Biochem. Pharmacol*. **2000**, *60*, 397

103. Li, W.; Hardwick, M.J.; Rosenthal, D.; Culty, M.; Papadopoulos, V. *Biochem. Pharmacol*. **2007**, *73*, 491

104. Han, Z.; Slack, R.S.; Li, W.; Papadopoulos, V. *J. Recept. Sig. Transd*. **2003**, *23*, 225

105. Maaser, K.; Grabowski, P.; Sutter, A.P.; Höpfner, M.; Foss, H-D.; Stein, H.; Berger, G.; Gavish, M.; Zeitz, M.; Scherübl, H. *Clin. Cancer Res*. **2002**, *8*, 3205

106. Maaser, K.; Sutter, A.P.; Scherübl, H. *Biochem. Biophys. Res. Commun*. **2005**, *332*, 646

107. Krueger, K.E. *Biochim. Biophys. Acta*. **1995**, *1241*, 453

108. Cappelli, A.; Anzini, M.; Vomero, S.; De Benedetti, P.G.; Menziani, M.C.; Giorgi, G.; Manzoni, C. *J. Med. Chem*. **1997**, *40*, 2910

109. Anzini, M.; Cappelli, A.; Vomero, S.; Seeber, M.; Menziani, M.C.; Langer, T.; Hagen, B.; Manzoni, C.; Bourguignon, J-J. *J. Med. Chem*. **2001**, *44*, 1134

110. Almirante, L.; Mugnaini, A.; Rugarli, P.; Gamba, A.; Zefelippo, E.; De Toma, N.; Murmann, W. *J. Med. Chem*. **1969**, *12*, 122

111. Bourguignon, J-J. (Geisen-Crouse, E. (ed.)) *Peripheral Benzodiazepine Receptors*. pp. 59-85, Academic Press: London, **1993**

112. Trapani, G.; Franco, M.; Ricciardi, L.; Latrofa, A.; Genchi, G.; Sanna, E.; Tuveri, F.; Cagetti, E.; Biggio, G.; Liso, G. *J. Med. Chem*. **1997**, *40*, 3109

113. Katsifis, A.; Mattner, F.; Dikic, B.; Papazian, V. *Radiochim. Acta*. **2000**, *88*, 229

114. Serra, M.; Madau, P.; Chessa, M.F.; Caddeo, M.; Sanna, E.; Trapani, G.; Franco, M.; Liso, G.; Purdy, R.H.; Barbaccia, M.L.; Biggio, G. *Br. J. Pharmacol*. **1999**, *127*, 177

115. Davies, L.P.; Barlin, G.B.; Selley, M.L. *Pharmacol. Lett*. **1995**, *57*, PL 381

116. Barlin, G.P.; Davies, L.P.; Harrison, P.W. *Aust. J. Chem*. **1997**, *50*, 61

117. Selleri, S.; Bruni, F.; Costagli, C.; Costanzo, A.; Guerrini, G.; Ciciani, G.; Costa, B.; Martini, C. *Bioorg. Med. Chem*. **2001**, *9*, 2661

118. Selleri, S.; Gratteri, P.; Costagli, C.; Bonaccini, C.; Costanzo, A.; Melani, F.; Guerrini, G.; Ciciani, G.; Costa, B.; Spinetti, F.; Martini, C.; Bruni, F. *Bioorg. Med. Chem*. **2005**, *13*, 4821

119. Nacci, V.; Fiorini, I.; Garofalo, A.; Cagnotto, A. *Farmaco. Ed. Sci*. **1990**, *45*, 545

120. Fiorini, I.; Nacci, V.; Ciani, S.M.; Garofalo, A.; Campiani, G.; Savini, L.; Novellino, E.; Greco, G.; Bernasconi, P.; Mennini, T. *J. Med. Chem*. **1994**, *37*, 1427

121. Campiani, G.; Ramunno, A.; Fiorini, I.; Nacci, V.; Morelli, E.; Novellino, E.; Goegan, M.; Mennini, T.; Sullivan, S.; Zisterer, D.M.; Williams, C.D. *J. Med. Chem*. **2002**, *45*, 4276

122. Campiani, G.; Fiorini, I.; De Filippis, M.P.; Ciani, S.M.; Garofalo, A.; Nacci, V.; Giorgi, G.; Sega, A.; Botta, M.; Chiarini, A.; Budriesi, R.; Bruni, G.; Romeo, M.R.; Manzoni, C.; Mennini, T. *J. Med. Chem*. **1996**, *39*, 2922

123. Campiani, G.; Nacci, V.; Fiorini, I.; De Filippis, M.P.; Garofalo, A.; Ciani, S.M.; Greco, G.; Novellino, E.; Manzoni, C.; Mennini, T. *Eur. J. Med. Chem*. **1997**, *32*, 241

124. Okubo, T.; Yoshikawa, R.; Chaki, S.; Okuyama, S.; Nakazato, A. *Bioorg. Med. Chem*. **2004**, *12*, 423

125. Okuyama, S.; Chaki, S.; Yoshikawa, R.; Ogawa, S.; Suzuki, Y.; Okubo, T.; Nakazato, A.; Nagamine, M.; Tomisawa, K. *Life Sci*. **1999**, *64*, 1455

126. Romeo, E.; Auta, J.; Kozikowski, A.P.; Ma, D.; Papadopoulos, V.; Puia, G.; Costa, E.; Guidotti, A. *J. Pharmacol. Exp. Ther*. **1992**, *262*, 971

127. Kozikowski, A.P.; Ma, D.; Brewer, J.; Sun, S.; Costa, E.; Romeo, E.; Guidotti, A. *J. Med. Chem*. **1993**, *36*, 2908

128. Romeo, E.; Cavallaro, S.; Korneyev, A.; Kozikowski, A.P.; Ma, D.; Polo, A.; Costa, E.; Guidotti, A. *J. Pharmacol. Exp. Ther*. **1993**, *267*, 462

129. Liao, Y.; Kozikowski, A.P.; Guidotti, A.; Costa, E. *Bioorg. Med. Chem. Lett*. **1998**, *8*, 2099

130. Guillon, J.; Boulouard, M.; Lelong, V.; Dallemagne, P.; Rault, S.; Jarry, C. *J. Pharm. Pharmacol*. **2001**, *53*, 1561

131. Primofiore, G.; Da Settimo, F.; Taliani, S.; Simorini, F.; Patrizi, M.P.; Novellino, E.; Greco, G.; Abignente, E.; Costa, B.; Chelli, B.; Martini, C. *J. Med. Chem*. **2004**, *47*, 1852

132. Murray, I.P.C.; Ill, P.J.; Strauss, W. *Nuclear Medicine in clinical diagnosis and treatment*. Churchill Livingstone: London, **1995**

133. Alazraki, N.P.; Mishkin, F.S. *Fundamentals of Nuclear Medicine*. The Society of Nuclear Medicine: New York, **1988**

134. Kowalsky, R.J.; Falen, S.W. *Radiopharmaceuticals in Nuclear Pharmacy and Nuclear Medicine*. American Pharmacists Association: Washington, **2004**

135. Blahd, W.H. *Nuclear Medicine*. McGraw-Hill: New York, **1971**

136. Theobald, A.E. *Radiopharmacy and Radiopharmaceuticals*. Taylor and Francis: London, **1985**

137. Jager, P.L.; Vaalburg, W.; Pruim, J.; de Vries, E.G.E.; Langen, K-J.; Piers, D.A. *J. Nucl. Med*. **2001**, *42*, 432

138. Sharkey, R.M.; Goldenberg, D.M. *J. Nucl. Med*. **2005**, *46*, 115S

139. Zhang, M-R.; Maeda, J.; Ogawa, M.; Noguchi, J.; Ito, T.; Yoshida, Y.; Okauchi, T.; Obayashi, S.; Suhara, T.; Suzuki, K. *J. Med. Chem*. **2004**, *47*, 2228

140. Zhang, M-R.; Maeda, J.; Ito, T.; Okauchi, T.; Ogawa, M.; Noguchi, J.; Suhara, T.; Halldin, C.; Suzuki, K. *Bioorg. Med. Chem*. **2005**, *13*, 1811

141. Zhang, M-R.; Kida, T.; Noguchi, J.; Furutsuka, K.; Maeda, J.; Suhara, T.; Suzuki, K. *Nucl. Med. Biol*. **2003**, *30*, 513

142. Zhang, M-R.; Maeda, J.; Furutsuka, K.; Yoshida, Y.; Ogawa, M.; Suhara, T.; Suzuki, K. *Bioorg. Med. Chem. Lett*. **2003**, *13*, 201

143. Chaki, S.; Funakoshi, T.; Yoshikawa, R.; Okuyama, S.; Okubo, T.; Nakazato, A.; Nagamine, M.; Tomisawa, K. *Eur. J. Pharmacol*. **1999**, *371*, 197

144. Fujimura, Y.; Ikoma, Y.; Yasuno, F.; Suhara, T.; Ota, M.; Matsumoto, R.; Nozaki, S.; Takano, A.; Kosaka, J.; Zhang, M-R.; Nakao, R.; Suzuki, K.; Kato, N.; Ito, H. *J. Nucl. Med*. **2006**, *47*, 43

145. Belloli, S.; Moresco, R.M.; Matarrese, M.; Biella, G.; Sanvito, F.; Simonelli, P.; Turolla, E.; Olivieri, S.; Cappelli, A.; Vomero, S.; Galli-Kienle, M.; Fazio, F. *Neurochem. Int*. **2004**, *44*, 433

146. James, M.L.; Fulton, R.R.; Henderson, D.J.; Eberl, S.; Meikle, S.R.; Thomson, S.; Allan, R.D.; Dolle, F.; Fulham, M.J.; Kassiou, M. *Bioorg. Med. Chem*. **2005**, *13*, 6188

147. Thominiaux, C.; Dollé, F.; James, M.L.; Bramoullé, Y.; Boutin, H.; Besret, L.; Grégoire, M.-C.; Valette, H.; Bottlaender, M.; Tavitian, B.; Hantraye, Ph.; Selleri, S.; Kassiou, M. *Appl. Radiat. Isot*. **2006**, *64*, 570

148. Banati, R.B. *Glia* **2002**, *40*, 206

149. Banati, R.B.; Newcombe, J.; Gunn, R.N.; Cagnin, A.; Turkheimer, F.; Heppner, F.; Price, G.; Wegner, F.; Giovannoni, G.; Miller, D.H.; Perkin, G.D.; Smith, T.; Hewson, A.K.; Bydder, G.; Kreutzberg, G.W.; Jones, T.; Cuzner, M.L.; Myers, R. *Brain* **2000**, *123*, 2321

150. Cagnin, A.; Myers, R.; Gunn, R.N.; Lawrence, A.D.; Stevens, T.; Kreutzberg, G.W.; Jones, T.; Banati, R.B. *Brain* **2001**, *124*, 2014

151. Gildersleeve, D.L.; Van Dort, M.E.; Johnson, J.W.; Sherman, P.S.; Wieland, D.M. *Nucl. Med. Biol*. **1996**, *23*, 23

152. Versijpt, J.J.; Dumont, F.; Van Laere, K.J.; Decoo, D.; Santens, P.; Audenaert, K.; Achten, E.; Slegers, G.; Dierckx, R.A.; Korf, J. *Eur. Neurol*. **2003**, *50*, 39

153. Katsifis, A.; Mattner, F.; Zhang, Z.; Dikic, B.; Papazian, V. *J. Label. Compd. Radiopharm*. **2000**, *43*, 385

154. Katsifis, A.; Barlin, G.; Mattner, F.; Dikic, B. *Radiochim. Acta*. **2004**, *92*, 305

155. Katsifis, A.; Mattner, F.; Papazian, V.; Chapman, J. *J. Label. Compd. Radiopharm*. **2003**, *46*, S9

156. Mattner, F.; Katsifis, A.; Staykova, M.; Ballantyne, P.; Willenborg, D.O. *Eur. J. Nucl. Med. Mol. Imaging* **2005**, *32*, 557

157. Kissman, H.M.; Farnsworth, D.W.; Witkop, B. *J. Am. Chem. Soc*. **1952**, *74*, 3948

158. Pavia, D.L.; Lampman, G.M.; Kriz, G.S. *Introduction to Spectroscopy*, 3rd Ed, Harcourt: Orlando, **2001**

159. Calvaire, A.; Pallaud, R. *Ecole Natl. Super. Chim*. **1960**, *250*, 3194

160. Asiri, A.M.; Bahajaj, A.A.; Ismail, I.M.I.; Fatani, N.A. *Dyes Pigment*. **2006**, *71*, 103

161. Al-Azawe, S.; Sarkis, G.Y. *J. Chem. Eng. Data* **1973**, *18*, 109

162. Joshi, K.C.; Pathak, V.N.; Singh, R.P. *Mon. Chem*. **1980**, *111*, 1343

163. Fonia, O.; Weizman, R.; Zisman, E.; Ashkenazi, R.; Gavish, M. *Eur. J. Pharmacol*. **1995**, *293*, 335

164. Dumont, F.; Waterhouse, R.N.; Montoya, J.A.; Mattner, F.; Katsifis, A.; Kegeles, L.S.; Laruelle, M. *Nucl. Med. Biol*. **2003**, *30*, 435

165. Homes, T.P.; Mattner, F.; Keller, P.A.; Katsifis, A. *Bioorg. Med. Chem*. **2006**, *14*, 3938

166. Bennacef, I.; Haile, C.N.; Schmidt, A.; Koren, A.O.; Seibyl, J.P.; Staley, J.K.; Bois, F.; Baldwin, R.M.; Tamagnan, G. *Bioorg. Med. Chem*. **2006**, *14*, 7582

167. Van der Klein, P.A.M.; Kourounakis, A.P.; IJzerman, A. P. *J. Med. Chem.* **1999**, *42*, 3629

168. Mason, P.; Greer, V.P.; Kirby, A.J.; Simons, C.; Nicholls, P.J.; Smith, H.J. *J. Enzym. Inhib. Med. Chem*. **2003**, *18*, 511

169. Speziale, A.J.; Hamm, P.C. *J. Am. Chem. Soc*. **1956**, *78*, 2556

170. Fedorynski, M.; Wojciechowski, K.; Matacz, Z.; Makosza, M. *J. Org. Chem*. **1978**, *43*, 4682

171. Sasson, Y.; Newman, R. (Eds) *Handbook of phase transfer catalysts*. Blackie Academic and Professional: London, **1997**

172. Fattorusso, C.; Gemma, S.; Butini, S.; Huleatt, P.; Catalanotti, B.; Persico, M.; De Angelis, M.; Fiorini, I.; Nacci, V.; Ramunno, A.; Rodriquez, M.; Greco, G.; Novellino, E.; Bergamini, A.; Marini, S.; Coletta, M.; Maga, G.; Spadari, S.; Campiani, G. *J. Med. Chem*. **2005**, *48*, 7153

173. Katz, C.E.; Aube, J. *J. Am. Chem. Soc*. **2003**, *125*, 13948

174. De Luca, C.; Achille, I.; Rampazzo, L. *J. Chem. Soc. Perkin Trans. II* **1987**, *7*, 847

175. Campiani, G.; Morelli, E.; Fabbrini, M.; Nacci, V.; Greco, G.; Novellino, E.; Ramunno, A.; Maga, G.; Spadari, S.; Caliendo, G.; Bergamini, A.; Faggioli, E.; Uccella, I.; Bolacchi, F.; Marini, S.; Coletta, M.; Nacca, A.; Caccia, S. *J. Med. Chem*. **1999**, *42*, 4462

176. Artico, M.; Porretta, G.C.; De Martino, G. *J. Heterocycl. Chem*. **1971**, *8*, 283

177. Coenen, H.H.; Mertens, J.; Maziére, B. *Radioiodination reactions for pharmaceuticals: Compendium for effective synthesis strategies.* Springer: Netherlands, **2006**

178. El-Mohty, A.A.; El-Wetery, A.S.; El-Kolaly, M.T.; Raieh, M. *J. Radioanal. Nucl. Chem. Lett*. **1996**, *214*, 133

179. Kabalka, G.W.; Varma, R.S. *Tetrahedron* **1989**, *45*, 6601

180. Jones, J.R. (Ed). *Isotopes: Essential Chemistry and Applications II*. Royal Society of Chemistry: London, **1988**

181. Deprez, N.R.; Kalyani, D.; Krause, A.; Sanford, M.S. *J. Am. Chem. Soc*. **2006**, *128*, 4972

182. Kern, K.M.; Nguyen, N.V.; Cross, D.J. *J. Org. Chem*. **1981**, *46*, 5188

183. Lowry, O.H.; Rosebrough, N.J.; Farr, A.L.; Randall, R.J. *J. Biol. Chem*. **1951**, *193*, 265